

Statistical assessment of the consequences caused by deviations in the cross-sectional geometry of hot-rolled I-sections

Master thesis

Michael Lisser

Zürich, 03.07.2023

Supervisor:

Prof. Dr. Andreas Taras

Advisor:

Robin Steinmetz

ETH Zürich

Institute of Structural Engineering – IBK

Chair of Steel and Composite Structures

Abstract

The structural resistance given by a steel structure depends heavily on the cross-sectional dimensions of the used steel profiles. Obviously, the dimensions of the produced cross-sections will undergo some spreading due to equipment limitations, process variables or other reasons. Therefore, there is quite some interest in observing the effective dimensions of produced steel profiles and their effect on the structural resistance. This thesis strongly focuses on the cross-section geometry of hot-rolled I- and H-sections. As unfortunately steel producers don't give out specific measurement data, but only directly some statistical values, an extensive measurement campaign investigating 561 cross-sections has been carried out making use of the measuring concept developed by Ackermann & Reinhardt [5] with slight adjustments. As a preliminary investigation, it is shown that it is sufficient to measure the cross-sectional dimensions at the ends of the steel beams as the measured dimensions remain approximately constant along the length. Additionally, the accuracy of the measuring concept is demonstrated. Finally, statistical approaches are used in order to evaluate the data of this measurement campaign. Among other things, the results are compared with existing literature such as the new Annex E of the draft standard prEN 1993-1-1 [9].

It is observed that the flange thicknesses can vary relatively strongly within the cross-sectional plane of the same steel beam. There can be a large discrepancy especially between the inner (towards the web) and the outer flange thicknesses. Furthermore, it is figured out that there can also be some web eccentricity compared to the standardized cross-section. Therefore, in a second step, the effects of this non-idealized cross-section geometry on the cross-sectional resistance are studied using on the one hand simplified sectional properties and on the other hand the finite element program Abaqus. Thereby, three load cases are investigated: Pure compression, bending around the strong axis and bending around the weak axis. It is identified that there are considerable discrepancies between the cross-sectional resistance of the real geometry and the one of the standardized nominal geometry especially for bending around the weak axis, as the flanges exhibit a pronounced role for this loading situation. Moreover, it is observed that there are some differences between the cross-sectional resistances obtained by applying the pure sectional properties compared to the resistances derived from the more advanced numerical investigation.

As an additional study, the influence of neglecting the variability of the flange thickness within the cross-sectional plane is checked. This is done by introducing an idealized cross-section with a constant flange thickness which is determined in consideration of the measurement results. It is shown that one would overestimate the bending resistance around the weak axis considerably when neglecting the variability of the flange thickness within the cross-sectional plane. For the other two load cases, no significant influence is observed.

Table of contents:

Abstract.....	1
1. Introduction & background.....	4
1.1. Motivation	4
1.2. Standardized nominal dimensions.....	5
1.3. Geometrical Tolerances.....	5
1.4. Annex E in prEN 1993-1-1	6
1.5. Already carried out investigations.....	7
2. Measuring concept	12
2.1. Measured quantities.....	12
2.2. Measurement devices.....	14
2.3. Longitudinal measurements	15
2.4. Repetitive measurements – Uncertainty in measurement	15
2.5. Possible measurement errors	16
3. Measurement results & statistical evaluation	18
3.1. Statistical post-processing of the data.....	18
3.2. Longitudinal measurements	20
3.3. Uncertainty in measurement	24
3.4. Investigation of the measured flange thicknesses	25
3.5. General statistical evaluation.....	28
4. Investigation of the sectional properties.....	41
4.1. Nominal cross-section.....	41
4.2. Real cross-section.....	43
4.3. Idealized cross-section.....	45
4.4. Evaluation of the sectional properties	47
5. Numerical investigation of the cross-sectional resistance.....	51
5.1. Methodology.....	51
5.2. Abaqus model.....	51
5.3. Python script.....	67
5.4. Evaluation of the Abaqus results.....	73
6. Summary & Conclusion	77
7. Bibliography.....	79
8. List of figures and tables.....	81
Appendix A – Cross-sectional dimensions	83
A.1 Nominal values of the sectional dimensions and properties.....	83

A.2	Measurement results.....	85
A.3	Investigation of the flange thicknesses.....	96
A.4	Statistical evaluation of the general measurements.....	101
Appendix B - Sectional properties		118
B.1	Real cross-sections.....	118
B.2	Idealized cross-sections.....	133
Appendix C - Abaqus investigation		141
C.1	Model verification GMNIA.....	141
C.2	Abaqus results – Nominal cross-sections.....	143
C.3	Abaqus results – Real cross-sections.....	144
C.4	Abaqus results – Idealized cross-sections.....	155
C.5	Further Abaqus investigations.....	163

1. Introduction & background

1.1. Motivation

There is a large field of application for hot-rolled steel I- and H-sections in the construction industry. One will find several reasons why these profiles are widely used, primarily because of their simple production process, their excellent strength to weight ratio and their cost-effectiveness. For these steel profiles, the structural design codes rely on some specified geometrical dimensions of the cross-sections. However, despite advanced developments in manufacturing processes, variations in the cross-sectional geometry of hot-rolled I-sections are inevitable and remain a serious challenge. Obviously, the design codes cannot be considered as valid if the discrepancy between the assumed nominal cross-sectional dimensions and the real non-idealized dimensions is too large. Even relatively small deviations from the nominal values can already induce some drawbacks regarding the structural resistance. In the extreme case, the structural safety is not given anymore. Therefore, it's essential to ensure that the geometrical dimensions of these steel profiles meet the required specifications to guarantee a safe use.

This thesis focuses on the statistical evaluation of measurements of cross-sectional dimensions of 561 rolled profiles. Among other things, a goal is to verify the recommendations given in the Annex E of the new draft standard prEN 1993-1-1 [9], see section 1.4 for more details. Furthermore, the structural behaviour regarding the cross-sectional resistance of the measured profiles is investigated and compared to the behaviour of the nominal cross-sections. There is a strong interest in the influence of the imperfect cross-section geometry on the load-carrying capacity, as Melcher et al. (2004) [4] already studied the quantities influencing the structural response of an IPE 180 profile within the scope of a sensitivity analysis. They evaluated the sensitivity analysis in the form of Spearman rank-order correlation coefficients between the input quantities f_y , h , b , t_1 , t_2 (yield strength, profile height, profile width, web thickness and flange thickness respectively) and the tensile and bending load-carrying capacity. The results are illustrated in the following figure:

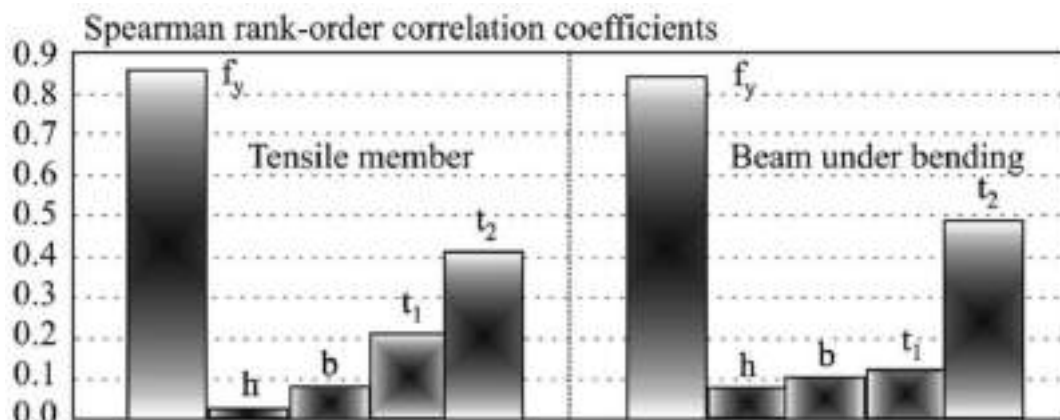


Figure 1: Sensitivity analysis between input quantities and load-carrying capacity according to Melcher et al. [4]

Although being still below the importance of the yield strength, they observed that the flange thicknesses t_2 have quite a large impact on the load-carrying capacity for both load cases. Therefore, the structural behaviour responses quite heavily to the variability of the flange thicknesses. It is pointed out that Melcher et al. examined an IPE 180 profile for this sensitivity study. However, it is expected that the results would be similar for other hot-rolled profiles, being even more pronounced for HEA and HEB sections as the percentage contribution of the flange to the total cross-sectional area is larger than for IPE sections.

Based on this observation, this thesis will investigate the influence of the imperfect cross-sectional geometry on the structural behaviour even further, particularly focusing on the flange thicknesses. It is emphasized that this thesis will only examine the cross-sectional geometry and will not study the influence of the yield strength.

In the following sections, the standardized geometrical dimensions of hot-rolled profiles are described. Afterwards, the geometrical tolerances specified in the codes are presented. Then, some developments regarding the second generation of

Eurocode 3 are pointed out. Finally, there will be a description of some investigations on this application field which have already been carried out. These investigations will serve as comparative values later.

1.2. Standardized nominal dimensions

As already indicated above, it's important to prescribe the nominal cross-sectional dimensions of hot-rolled I- and H-sections in order to form a basis for the design codes. In Europe, these dimensions are defined in the standard EN 10365 [11]. The following figure illustrates the prescribed dimensions:

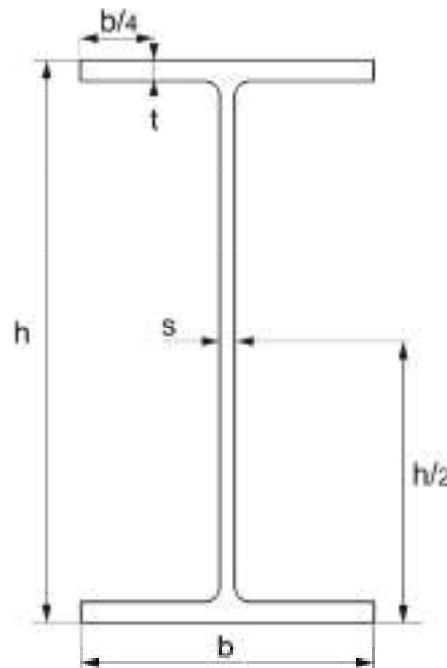


Figure 2: Prescribed dimensions of hot-rolled I- and H-sections according to EN 10365 [11]

The specified dimensions are the profile height, the profile width, the web thickness and the flange thickness. It is emphasized that the root fillet radius is not standardized in this code and is allowed to deviate depending on the producer.

In Switzerland, there are the SZS C5/18 tables [7] which are based on the European standard EN 10365 and represent the same nominal cross-sectional dimensions. However, they give some additional information, including some guiding value of the root fillet radius among other things. These tables also summarize some important quantities for the structural design, as for example the moments of inertia or the section moduli. As these tables contain all dimensions given in the standard EN 10365 plus some further specifications, they will be used in the course of this thesis. More specifically, the used quantities are summarized in Appendix A.1. It is pointed out that the sectional properties of the SZS C5/18 tables, such as the area or the section moduli for example, may contain some rounding errors. Therefore, it is decided to recalculate them in order to get the maximum accuracy. The used equations will be introduced in section 4.1.

1.3. Geometrical Tolerances

Due to the rolling manufacturing process, the cross-sectional dimensions of hot-rolled profiles cannot be produced to be exactly the same for each profile of the same profile type. There will always be some deviations from one production to the other due to equipment limitations, wear of the shaping rollers or process variables for example. Therefore, it's important to prescribe the geometrical tolerances which need to be complied with. In Europe, these tolerances of the geometrical dimensions of I- and H-sections are listed in the tolerance standard EN 10034 [2]. The following figure gives an example of the content of this standard:

Section height h		Flange width b		Web thickness s		Flange thickness t	
height mm	tolerance mm	width mm	tolerance mm	thickness mm	tolerance mm	thickness mm	tolerance mm
$h \leq 180$	+3,0 -2,0	$b \leq 110$	+4,0 -1,0	$s < 7$	$\pm 0,7$	$t < 6,5$	+1,5 -0,5
$180 < h \leq 400$	+4,0 -2,0	$110 < b \leq 210$	+4,0 -2,0	$7 \leq s < 10$	$\pm 1,0$	$6,5 \leq t < 10$	+2,0 -1,0
$400 < h \leq 700$	+5,0 -3,0	$210 < b \leq 325$	+4,0 -4,0	$10 \leq s < 20$	$\pm 1,5$	$10 \leq t < 20$	+2,5 -1,5
$h > 700$	+5,0 -5,0	$b > 325$	+6,0 -5,0	$20 \leq s < 40$	$\pm 2,0$	$20 \leq t < 30$	+2,5 -2,0
				$40 \leq s < 60$	$\pm 2,5$	$30 \leq t < 40$	+2,5 -2,5
				$s \geq 60$	$\pm 3,0$	$40 \leq t < 60$	+3,0 -3,0
						$t \geq 60$	+4,0 -4,0

Figure 3: Excerpt of the standard EN 10034 [2]

It is noted that in this standard, there are no reference statistical distributions of the geometrical dimensions that need to be satisfied. Therefore, according to this standard, it would be possible to produce all the profiles at the very lowest end of the tolerance range which would still be complying with the standard.

In Switzerland, the geometrical tolerances are defined a bit differently. There is the standard SIA 263/1 [12] which also contains tables with tolerances. These values slightly deviate from the tolerances defined in the European standard. However, this thesis focuses on the European standards.

1.4. Annex E in prEN 1993-1-1

Within the revision and development of the second generation of Eurocode 3, there are a lot of extensions, improvements and simplifications made. Especially the part 1-1 has experienced some major developments leading to the new draft standard prEN 1993-1-1 [9], see also Kuhlmann et al. (2020) [1]. One of these new developments is the integration of the Annex E within the new draft standard. The informative Annex E helps to build a clear connection between the nominal minimum values of the yield strength, the ultimate strength or the geometrical dimensions and the application of the recommended partial safety factors γ_{Mi} used to calculate the design resistances by giving some information about the assumed statistical distribution of the geometrical and mechanical properties underlying the usage of the partial safety factors according to Eurocode 3. Practically speaking, the tables E.1 and E.2 of the Annex E contain some information about the mean, the coefficient of variation and the upper and lower reference value of the statistical distribution of a specific mechanical or geometrical property. For this thesis, the table E.2 including the geometrical properties is of major interest, therefore being shown here:

Table E.2 — Assumed variability of dimensional parameters

Dimension type	Parameter	Mean value X_m	Coefficient of variation	Upper reference value $X_{5\%}$	Lower reference value $X_{0,12\%}$
Outer dimensions of cross-section	Depth h	$1,0 h_{nom}^a$	0,9 %	$0,98 h_{nom}^a$	$0,97 h_{nom}^a$
	Width b	$1,0 b_{nom}^a$	0,9 %	$0,98 b_{nom}^a$	$0,97 b_{nom}^a$
	Outer diameter d of circular hollow section	$1,0 d_{nom}^a$	0,5 %	$0,99 d_{nom}^a$	$0,98 d_{nom}^a$
Thickness	Rolled and welded I- and H-sections: flange thickness t_f	$0,98 t_{f,nom}^a$	2,5 %	$0,95 t_{f,nom}^a$	$0,91 t_{f,nom}^a$
	Rolled and welded I- and H-sections: web thickness t_w	$1,0 t_{w,nom}^a$	2,5 %	$0,96 t_{w,nom}^a$	$0,93 t_{w,nom}^a$
	Hot rolled (seamless) or welded structural hollow sections (acc. to EN 10210): wall thickness t	$0,99 t_{nom}^a$	2,5 %	$0,95 t_{nom}^a$	$0,92 t_{nom}^a$
	Cold-formed sections made from coils or plates (acc. to EN 10219): wall thickness t	$0,99 t_{nom}^a$	2,5 %	$0,95 t_{nom}^a$	$0,92 t_{nom}^a$
	All other welded sections made from heavy plates: thickness t	$0,99 t_{nom}^a$	2,5 %	$0,95 t_{nom}^a$	$0,92 t_{nom}^a$
^a Nominal dimensions according to the applicable product standard or specification.					

Figure 4: Excerpt of the Annex E of the standard prEN 1993-1-1 [9].

It can be seen in Figure 4 that some values of the dimensional parameters must be assumed to fall below the nominal values of the applicable product standard quite frequently. For example, the tabular values for the flange thickness of rolled and welded I- and H-sections show that the assumed mean value of the flange thickness is only 98 % of the nominal thickness. Furthermore, it is observed that the assumed variation of the web and flange thicknesses is larger than the one of the profile height and width.

Among other things, this thesis aims to collect and evaluate the geometrical measurement data of 561 hot-rolled steel sections enabling a verification of the corresponding values in the table E.2 in Annex E.

1.5. Already carried out investigations

In the past, there were already some relevant research investigations made about similar topics as the one of this thesis. Four of them are described in the following.

SAFEBRIC TILE:

One research example is the SAFEBRIC TILE project where a lot of geometrical and mechanical data of steel profiles were collected systematically [3]. The main objective of this project was to describe the variability of the material and geometrical properties for the European steel production. Steel profiles with flange thicknesses up to 140 mm were investigated. Among other things, an outcome of this project was the recommendation of the statistical distributions of the geometrical properties for hot-rolled I- and H-sections described in Table 1. Thereby, the expression mean/nom represents the normalized mean

value, meaning that each measurement result was normalized by the standardized nominal value of the corresponding dimension and the mean value was calculated based on these normalized values. The c.o.v. represents the coefficient of variation which is the ratio between the observed standard deviation and the mean value.

Table 1: Recommended distributions of geometrical properties according to SAFEBRICKTILE [3]

	b	h	t_w	t_f
mean/nom [-]	1.00	1.00	1.00	0.975
c.o.v. [%]	0.9	0.9	2.5	2.5

The similarity of these values to the ones stated in Annex E of prEN 1993-1-1 (see Figure 4) is not a coincidence, as the values of the Annex E were developed primarily based on the results of the SAFEBRICKTILE project.

Melcher et al. (2004):

A further experimental research project of geometrical and material properties of steel profiles was conducted by Melcher et al. (2004) [4] as already introduced in section 1.1. Beneath the mentioned sensitivity analysis, they investigated the geometrical characteristics of 371 hot-rolled IPE sections in the size range 160 – 240 which were produced in the Czech Republic. The following figure shows an excerpt of the obtained statistical results:

Relative statistic characteristics of IPE profiles—valid observations: 371

Quantity	<i>m</i>	<i>S</i>	Minimum value	Maximum value	<1 (%)	Skewness	Kurtosis
<i>h</i>	1.001	0.00443	0.989	1.013	34	-0.4063	3.015
<i>b₁</i>	1.012	0.01026	0.975	1.049	8	-0.3939	4.239
<i>b₂</i>	1.015	0.00961	0.975	1.037	5	-0.5448	3.887
<i>t₁</i>	1.055	0.04182	0.949	1.300	4	1.0545	7.473
<i>t₂₁</i>	0.988	0.04357	0.880	1.094	55	-0.2991	2.663
<i>t₂₂</i>	0.998	0.04803	0.858	1.129	47	0.3303	2.766
<i>A</i>	1.025	0.03245	0.931	1.127	21	-0.2152	3.076
<i>W_{pl}</i>	1.019	0.03347	0.926	1.107	31	-0.2583	2.650

Figure 5: Excerpt of the results of Melcher et al. [4]

The web thickness is denoted by t_1 , while t_{21} and t_{22} stand for the upper and lower flange thicknesses respectively. The width of the profiles was measured at the level of both flanges, therefore resulting in the quantities b_1 and b_2 . Furthermore, it is noted that W_{pl} describes the plastic section modulus around the strong axis, while A depicts the cross-sectional area. These two quantities were calculated based on the measurement data of the geometrical dimensions. The column marked with “<1” shows the percentage of cases where the measured or calculated value was lower than the nominal one. The column marked with “m” shows the mean value of the normalized measurements, the latter being the ratio between the measured and the standardized nominal quantity. It is observed that apart from the flange thicknesses, all the measured quantities resulted in a mean value which is above the nominal value. There is a pronounced large mean value for the web thickness.

The column marked with “S” in Figure 5 displays the obtained standard deviations. Based on these results, the coefficients of variation can be calculated as the ratio between the standard deviation and the mean value. The results are summarized in Table 2. These coefficients of variation will be used later for comparative studies.

Table 2: Calculated coefficients of variation according to the results of Melcher et al. [4]

	h	b₁	b₂	t₁	t₂₁	t₂₂	A	W_{pl}
c.o.v. [%]	0.44	1.01	0.95	3.96	4.41	4.81	3.17	3.28

Additionally, the Pearson correlation coefficients between the cross-sectional dimensions and properties were investigated, as can be seen in the following correlation matrix which contains the Pearson correlation coefficients between two properties each time in a tabular form:

$$K \approx \begin{bmatrix} h & b_1 & b_2 & t_1 & t_{21} & t_{22} & A & W_{pl} \\ 1 & -0.0068 & 0.0534 & 0.0399 & -0.0686 & -0.0989 & 0.0901 & 0.1092 \\ -0.0068 & 1 & \mathbf{0.6227} & -0.2142 & -0.2681 & -0.1456 & -0.1196 & -0.0694 \\ 0.0534 & \mathbf{0.6227} & 1 & -0.2132 & -0.1596 & -0.0423 & -0.0296 & 0.0394 \\ 0.0399 & -0.2142 & -0.2132 & 1 & 0.2368 & 0.2451 & \mathbf{0.6482} & 0.4712 \\ 0.0686 & -0.2681 & -0.1596 & 0.2368 & 1 & \mathbf{0.7634} & \mathbf{0.8103} & \mathbf{0.8586} \\ -0.0989 & -0.1456 & 0.0423 & 0.2451 & \mathbf{0.7634} & 1 & \mathbf{0.8451} & \mathbf{0.8918} \\ 0.0901 & -0.1196 & -0.0296 & \mathbf{0.6482} & \mathbf{0.8103} & \mathbf{0.8451} & 1 & \mathbf{0.9717} \\ 0.1092 & -0.0694 & 0.0394 & 0.4712 & \mathbf{0.8586} & \mathbf{0.8918} & \mathbf{0.9717} & 1 \end{bmatrix}$$

Figure 6: Correlation matrix obtained by Melcher et al. [4]

As can be observed, a strong positive correlation between the two measured widths of the profiles, b_1 and b_2 , was obtained. An even stronger positive correlation can be seen between the thickness of the upper (t_{21}) and the lower flange (t_{22}). Furthermore, as could be expected, the thicknesses of the web and the flanges correlate quite heavily with the area and the plastic section modulus around the strong axis.

Timothy Kyle Jaquess (1998):

Jaquess (1998) [14] has written a thesis at the University of Texas about a similar subject as the one of the present thesis. Among other things, his thesis characterizes the geometric properties of steel rolled sections. He investigated 17 wide-flange sections (equivalent to H-sections in Europe) produced in the United States, Great Britain and Luxembourg. The cross-sectional dimensions regarding the section height d , flange width b_f , flange thickness t_f and web thickness t_w were measured. Thereby, the following figure illustrates the measured quantities:

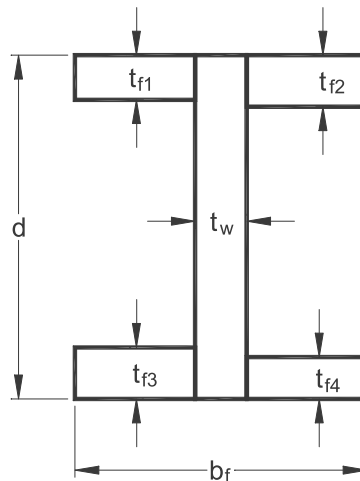


Figure 7: Illustration of the investigated geometrical dimensions by Jaquess [14]

Based on the measurement data of Jaquess, the following normalized mean values and coefficients of variations can be calculated for the sectional dimensions:

Table 3: Normalized mean values and coefficients of variation of sectional dimensions according to Jaquess [14]

	t_{f1}	t_{f2}	t_{f3}	t_{f4}	t_w	d	b_f
mean/nom [-]	0.980	0.978	0.980	0.969	1.008	1.000	1.003
c.o.v. [%]	2.732	2.869	2.898	3.188	3.036	0.414	0.972

Furthermore, some sectional properties based on the measured dimensions were calculated and compared to their nominal values using a simplified approach. The following table summarizes the obtained mean values of the normalized sectional properties and the corresponding coefficients of variation which are calculated based on the results stated by Jaquess. The area is denoted by A , the moment of inertia is indicated by I and the elastic and plastic section moduli are represented with W_{el} and W_{pl} respectively. Thereby, the y -axis represents the strong axis, while the z -axis represents the weak axis of the steel sections.

Table 4: Normalized mean values and coefficients of variation of sectional properties according to Jaquess [14]

	A	I_y	I_z	$W_{el,y}$	$W_{el,z}$	$W_{pl,y}$	$W_{pl,z}$
mean/nom [-]	0.990	0.987	0.986	0.991	0.985	0.988	0.984
c.o.v. [%]	1.82	2.23	3.25	1.92	2.64	1.92	2.54

G. A. Alpsten (1972):

G. A. Alpsten published a report about variations in mechanical and cross-sectional properties of steel profiles in 1972 [15]. Among other things, he intensively investigated the geometric properties of the cross-sections of rolled profiles. He evaluated the statistical data of about 5000 measured cross-sections rolled at European steel mills and obtained the following histograms:

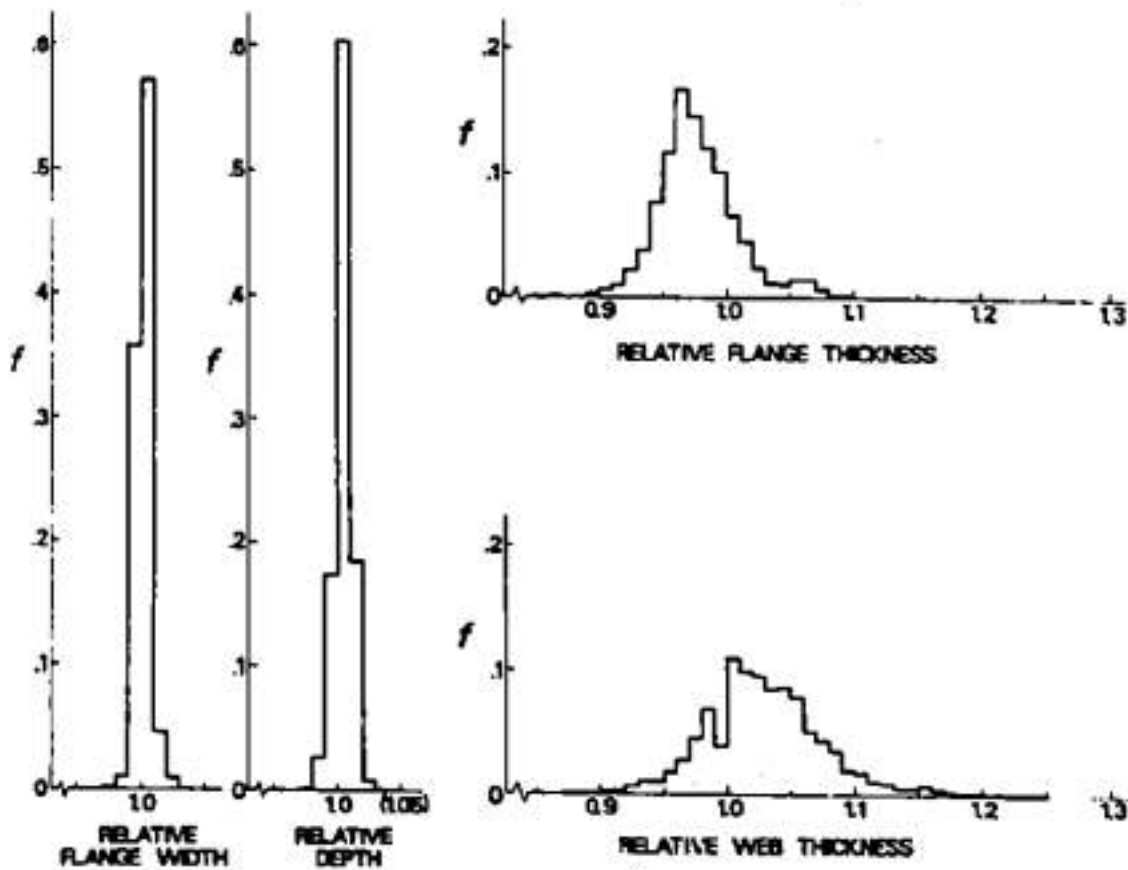


Figure 8: Variations of cross-sectional dimensions of 4816 H-shapes according to G. A. Alpsten [15]

Thereby, the flange width represents the profile width while the depth represents the profile height. It is pointed out that the relative quantities are plotted, meaning that all the measurements were normalized by the standardized nominal value. When looking at the histograms, it is directly observed that the relative variation of the profile width and profile height is much

smaller than the one of the flange and web thicknesses. Unfortunately, there are no numerical values stated for the coefficients of variation or something similar. Furthermore, it is seen that there is a tendency that the majority of the web thicknesses is thicker than the nominal values, while for the flange thicknesses it is the other way around. The measured profile widths and profile heights exhibit a mean value somewhere close around the nominal value.

In addition to the cross-sectional dimensions, G. A. Alpsten also studied some sectional properties based on the same sample as used in Figure 8. However, it must be noted that it is not exactly clear which assumptions or simplifications were made in order to calculate the sectional properties. The following histograms are the result of this evaluation:

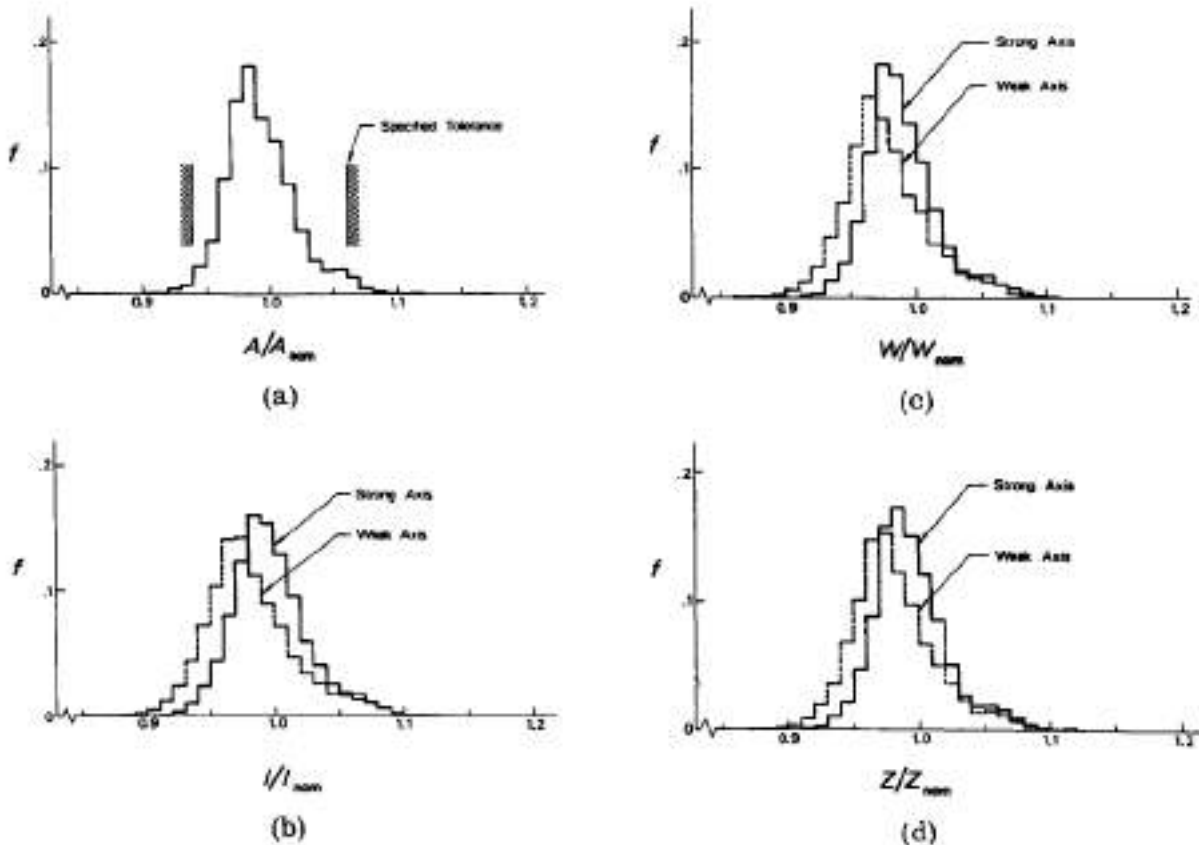


Figure 9: Variations of sectional properties of 4816 H-shapes according to G. A. Alpsten [15]

The four histograms represent the area A , the moments of inertia I , the elastic section moduli W and the plastic section moduli Z respectively. Again, the normalized quantities are plotted. It is identified that all the quantities tend to be smaller than the nominal value on average. This is a direct consequence of the observation that the measured flange thicknesses are thinner than the nominal values (see Figure 8). This shows once more the significance of the flanges of hot-rolled profiles on the structural behaviour. Moreover, the discrepancy to the nominal values tends to be even higher for the sectional properties around the weak axis compared to the strong axis.

As the report of G. A. Alpsten is from the year 1972, it will be interesting to observe how the production process of rolled profiles may have changed regarding the measured dimensions nowadays more than 50 years later.

2. Measuring concept

As this thesis is building on the bachelor thesis of Ackermann & Reinhardt [5], the measuring concept and its findings are adopted accordingly. However, some adjustments were made. For the sake of clarity, the applied measuring concept is explained in detail in the following. A uniform measuring procedure is important to ensure the comparability and consistency between the measured dimensions. Furthermore, it enables the reproducibility of the measurement process.

The measuring process was limited to the commonly used steel profiles IPE, HEA and HEB. The mentioned sections were investigated in the size range 200-600. For the IPE sections, additionally the sizes 160 and 180 were measured in order to enable a comparison to the data of Melcher et al. [4], as introduced in section 1.5.

After clarifying the measuring concept and the used measurement devices, some special investigations will be explained in this chapter. At the end of this chapter, some possible measurement errors will be studied.

2.1. Measured quantities

The following chapters present the measured quantities. Due to reasons of accessibility, these measurements were carried out at the ends of the steel beams. In chapter 2.3, it will be explained how it is checked whether the geometrical dimensions at the ends of the steel beams represent the dimensions along the whole length.

2.1.1. Height and Width

The following figure illustrates how the height and the width of the profiles were measured:

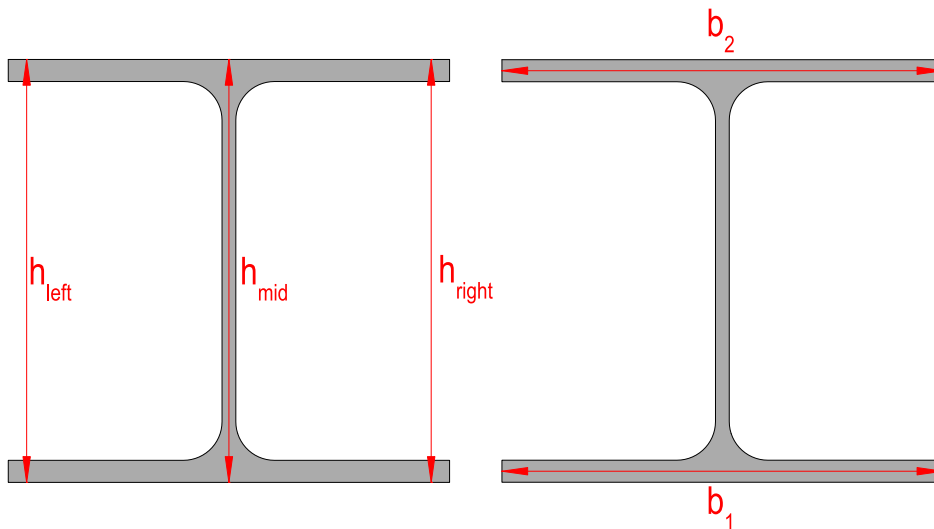


Figure 10: Measuring procedure for height (left) and width (right)

For the height, it is considered that both flanges may have some skewness in the cross-sectional plane. This induces a pronounced effect on the measured height depending on the location of the measurement. Therefore, the height was measured at three different locations, as can be seen in Figure 10.

Furthermore, it was observed that there may be some local surface irregularities for some profiles prohibiting a precise measurement of the height. In these cases, a small steel plate was used (similarly as will be introduced in Figure 13 für the a -value) to guarantee a flat measurement surface. The thickness of this steel plate was finally subtracted to get the profile height.

The profile width was measured at both levels of the flanges. The purpose of measuring the width of each profile at two different locations was to recognize and minimize measuring errors. Furthermore, there may be some deviations between the width of the upper and the lower flange.

2.1.2. Flange and web thicknesses

The thickness of the flange was measured four times for each flange in order to detect some possible variations within a flange. For the same reason, the thickness of the web was measured three times. The following figure shows the measured quantities:

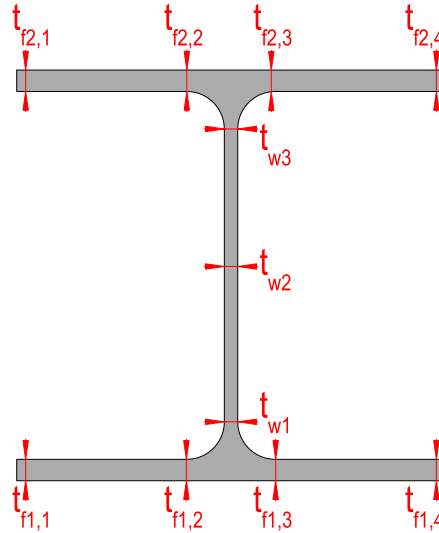


Figure 11: Measuring procedure for the flange & web thicknesses

The flange thicknesses were measured at the outer flange ends ($t_{f1,1}$, $t_{f1,4}$, $t_{f2,1}$ and $t_{f2,4}$) and at the transition to the roundings ($t_{f1,2}$, $t_{f1,3}$, $t_{f2,2}$ and $t_{f2,3}$). The thickness of the web was measured approximately in the middle of the profile height (t_{w2}) and at the transition to the roundings (t_{w1} and t_{w3}).

2.1.3. Radius of the root fillets

It was decided to measure each root fillet radius of the cross-sectional plane, as can be seen in Figure 12. In this way, measuring errors can be reduced and deviations between the individual radii can be discovered. The measurement results of the root fillet radius should be treated with caution because the measured values are extensively prone to variations depending on the positioning of the measurement device. This is based on the fact that the root fillet radii are not always constant as they are not produced as perfect quarter circles.

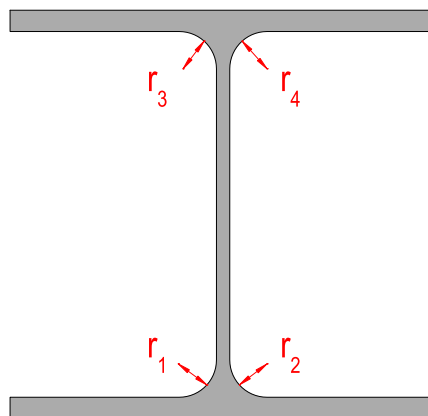


Figure 12: Measuring procedure for the root fillet radii

2.1.4. A-value

In order to measure the a-value, a short steel bar and a small steel plate was used, as illustrated in Figure 13. With the known or measured dimensions t_{plate} , t_{bar} , t_w and x_{mes} , the dimension a_1 can be calculated:

$$a_1 = x_{mes} - t_{bar} - t_{plate} - t_w \tag{1}$$

The same procedure is repeated for the a-value a_2 on the other side. The a-values will be used later to derive a web eccentricity of the measured profiles.

It is noted that for the web thickness t_w , the arithmetic mean of the three measured quantities (see section 2.1.2) is inserted in equation (1).

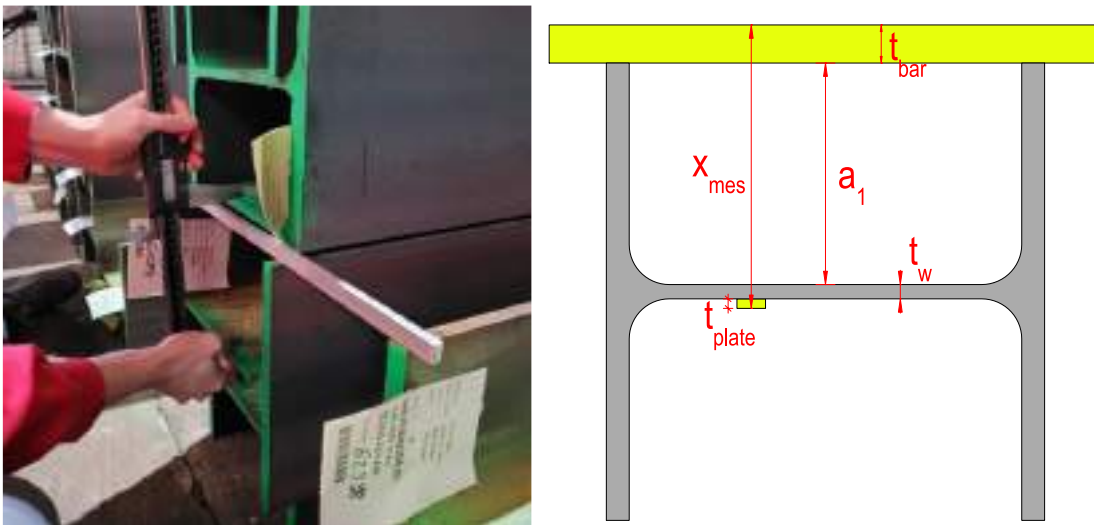


Figure 13: Measuring procedure to obtain the a-value

2.2. Measurement devices

The following measurement devices were used:

2.2.1. Caliper

Name: Mitutoyo Digital ABS AOS Caliper

Maximum range: 600 mm

Application: Profile height and width & a-value

2.2.2. Electronic quick probe

Name: Kroeplin K450

Maximum range: 50 mm

Application: Flange & web thickness

2.2.3. Root fillet radii measurement device

Name: Insize digital radii measurement device

Measurement range: 7-910 mm (internal radius)

Application: Root fillet radius



Figure 14: Caliper, electronic quick probe and radii measurement device

2.3. Longitudinal measurements

In addition to the measurements at the ends of the girders, it was decided to conduct some measurements along the length of the beams as well. The goal of this procedure is to figure out how the individual measured dimensions from chapter 2.1 behave along the length of the beam and if the measured dimensions at the ends of the beams represent the dimensions along the whole beam. It must be noted that not all dimensions mentioned in chapter 2.1 could be measured along the length. It was for example not possible to measure the web thickness due to accessibility reasons. The measured quantities are the flange thickness, the profile height, the profile width and the root fillet radius. In the process of the longitudinal measurements, for each of these quantities only one measurement in the cross-sectional plane was carried out in contrast to the explanations in chapter 2.1. The following figure illustrates the measured quantities:

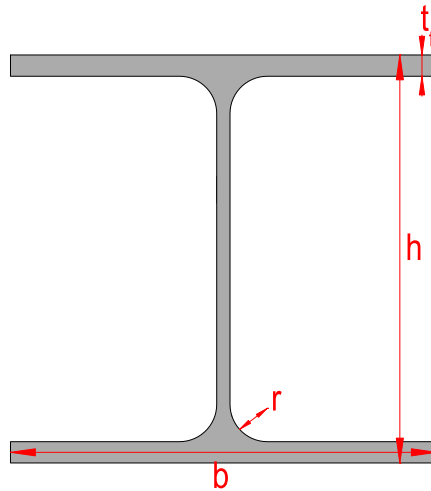


Figure 15: Longitudinal measurement quantities

These measurements are sufficient to investigate the longitudinal scatter. For some girders, not all of the mentioned four quantities could be measured due to the local accessibility.

The length of the investigated steel girders covers a range from 12 m to 26 m. The longitudinal measurements were conducted at regular distances of about two meters. It was tried to cover all profile types (IPE, HEA and HEB) and a wide size range in the measurements. However, it must be noted that not each profile size could be measured due to the local accessibility along the length. On the other hand, some profile types were measured more than once. The evaluation of these measurements will be conducted in section 3.2.

2.4. Repetitive measurements – Uncertainty in measurement

When measuring a physical quantity, the result will always only be an estimate of the true value and there will always be some kind of uncertainty related to this measurement. Therefore, the quality of the measurement procedure should be described somehow quantitatively. In order to achieve that, it was decided to measure the same geometrical quantity 15 times at the same location. This procedure was repeated for several geometrical quantities and three different steel girders. The evaluation is done based on chapter 4.2 of the ISO Guide 93-3:2008 [6]. The guide suggests that the arithmetic mean \bar{q} of n independent observations q_k is the best available estimate of the expected value μ_q of a quantity q :

$$\bar{q} = \frac{1}{n} \cdot \sum_{k=1}^n q_k \quad (2)$$

Furthermore, the experimental variance of the observations, which estimates the variance σ^2 of the probability distribution of q , is given by:

$$s^2(q_k) = \frac{1}{n-1} \cdot \sum_{j=1}^n (q_j - \bar{q})^2 \quad (3)$$

The experimental standard deviation follows consequently:

$$s(q_k) = \sqrt{s^2(q_k)} \quad (4)$$

Based on the assumption that the individual measurements are normally distributed with unknown mean and standard deviation, a confidence interval can be constructed. For its derivation, it is made use of the assumption that the unknown mean and standard deviation of the individual measurements can be estimated by the arithmetic mean and the experimental standard deviation respectively. The assumption of a normal distribution makes sense for geometric dimensions according to the lecture material of Prof. Dr. Bruno Sudret [13].

According to the lecture material of Dr. Lukas Meier [8], the symmetric $(1 - \alpha)$ -confidence interval can be calculated as:

$$I = \bar{q} \pm s(q_k) \cdot t_{n-1, 1-\alpha/2} \quad (5)$$

Where \bar{q} is the arithmetic mean of n measurements according to equation (2), $s(\bar{q})$ is the experimental standard deviation of the mean according to equation (4) and $t_{n-1, 1-\alpha/2}$ is the $((1 - \alpha/2) \times 100)\%$ quantile of the t-distribution (or Student's distribution) with $n - 1$ degrees of freedom. The confidence interval according to equation (5) has the meaning that with a probability of $(1 - \alpha)$, an individual measurement result lies within this interval. Therefore, it somehow describes the reliability and accuracy of the measurement process and how much the individual measurements scatter. The investigated girders will be evaluated in section 3.3.

2.5. Possible measurement errors

There is a large variety of possible measurement errors that could occur and should be kept in mind. In the following, they will be explained in more detail.

Human errors:

If the persons performing the measurements do not pay enough attention, there are several sources of errors. There are a lot of examples like misreading the scale, writing down the wrong value, using the wrong measurement device or using the wrong measuring technique (by applying too much or too less force when measuring a quantity for example). Furthermore, the persons should be familiar with the functions of each measurement device and should apply them only when appropriate. For the fillet radius measurement device, it is for example important to use the correct attachment.

Instrumental errors:

Instrumental errors may occur if the measurement devices themselves show some defects or are calibrated inadequately. For example, the used caliper may be misaligned. This type of error also occurs when the zeroing of the device is done incorrectly by the instrument. However, if the wrong zeroing is caused by the person using it, the error will be categorized to human errors.

The limitations in the resolution of the measuring device are also counted as instrumental errors. For example, using a caliper with an insufficient number of decimal places will induce an error as well.

Environmental errors:

When measuring geometrical dimensions, the surrounding environment may influence the measurements results due to vibrations, humidity or temperature for example. However, since the measurements of this thesis were done inside a dry storage hall, these effects should not have played a pronounced role.

Random errors:

There are always some unpredictable natural variations in the measurement process or in the object being measured. Therefore, random errors cannot be excluded from the measurement process. However, this kind of error can be minimized by carrying out repeated measurements.

Systematic errors:

In contrast to the random errors, there may also be some systematic errors. These occur when there is a consistent shift in the measurement process. They cannot be minimized by conducting repeated measurements. For example, the used caliper may consistently measure a distance too long or too short.

Considering all these potential sources of measurement errors, it is essential to pay the greatest attention when carrying out the measurements. Furthermore, reliable measurement devices and well-defined measurement techniques should be used. One should always be aware of these potential sources of errors.

3. Measurement results & statistical evaluation

In this chapter, the most important measurement results are presented and discussed. Furthermore, the statistical evaluation will be conducted. It is noted that due to the large amount of data, not all measurement results are showed here extensively, rather focusing on the most important ones. A full version of all results is given in Appendix A.2.

For more detailed insights into the results, the statistical evaluation of the data will be done for six different categories, each category containing a specific group of profiles:

Table 5: Selected statistical evaluation categories

	Specification	Number of investigated profiles
Category "Total"	All measured profiles	561
Category "Small"	Small size profiles (160-340)	340
Category "Large"	Large size profiles (360-600)	221
Category "HEA"	HEA profiles	217 (140 small, 77 large)
Category "HEB"	HEB profiles	190 (116 small, 74 large)
Category "IPE"	IPE profiles	154 (84 small, 70 large)

The threshold size between the categories "Small" and "Large" is chosen mainly based on the characteristics of the measurement results, as will be seen later (see also Appendix A.3 & A.4).

At the beginning of this chapter, it will be explained how the measurement data are statistically post-processed. Afterwards, the results of the longitudinal measurements and the repetitive measurements will be stated and discussed. Subsequently, the statistical evaluation of the general measurements will follow, particularly focusing on the flange thicknesses. Finally, an additional investigation regarding the tolerance exceedances will be made.

3.1. Statistical post-processing of the data

To draw some conclusions out of the measured quantities explained in the previous chapters, the data need to be post-processed. In order to do that, the measured dimensions are normalized with respect to the corresponding standardized nominal value from the SZS C5/18 tables [7] leading to a dimensionless quantity:

$$x_{normalized} = \frac{x_{measured}}{x_{nominal}} \quad (6)$$

The advantage of this procedure is that the percentage deviation from the standardized value is obtained directly. Furthermore, the measurements from different profile sizes can be compared directly in this way. For the sake of completeness, the used nominal values from the SZS C5/18 tables are displayed in Appendix A.1.

In the following, some statistical quantities are explained based on the lecture material of Dr. Lukas Meier [8]. In all these equations, the normalized quantities explained above (equation (6)) will be inserted.

3.1.1. Mean value

The arithmetic mean value is a commonly used parameter to describe a central value of a data sample. It is calculated using the following formula, n being the number of measurements and x_i being the normalized variable (see equation (6)) of one of the measured quantities for the i -th profile:

$$\bar{x} = \frac{1}{n} \cdot \sum_{i=1}^n x_i \quad (7)$$

3.1.2. Empirical variance and empirical standard deviation

The unbiased empirical variance and the empirical standard deviation are statistical measures that represent the variability of a data set. Therefore, they are indicators of how spread out the data is from the mean. The unbiased empirical variance can be calculated making use of the mean value defined above:

$$s^2 = \frac{1}{n-1} \cdot \sum_{i=1}^n (x_i - \bar{x})^2 \quad (8)$$

The same definitions made in section 3.1.1 still hold.

The empirical standard deviation is the square root of the empirical variance and follows consequently:

$$s = \sqrt{s^2} = \sqrt{\frac{1}{n-1} \cdot \sum_{i=1}^n (x_i - \bar{x})^2} \quad (9)$$

3.1.3. Empirical covariance and empirical Pearson's correlation coefficient:

The empirical covariance represents the degree to which two variables in a data set vary together. The empirical covariance between two variables x and y can be obtained as follows:

$$s_{xy} = \frac{1}{n-1} \cdot \sum_{i=1}^n (x_i - \bar{x}) \cdot (y_i - \bar{y}) \quad (10)$$

It should be noted that the empirical covariance can be affected by the scale of the variables and consequently depends on the units chosen for the two variables. To address this issue, a standardized quantity is useful to use, leading to the correlation coefficient.

The empirical Pearson's correlation coefficient is an important indicator to detect the linear dependency of two quantities. It can be calculated by using the empirical covariance and standardizing it by dividing it by the product of the standard deviations of the two variables:

$$r_{xy} = \frac{s_{xy}}{s_x \cdot s_y} \quad (11)$$

Since it is a standardized unitless measure, the Pearson's correlation coefficient will always lie between -1 and 1. A large positive value represents a strong positive correlation while a large negative value represents a strong negative correlation. One of the disadvantages of the Pearson's correlation coefficient is the fact that it only characterizes the linear relationship between two parameters. There is no information about a nonlinear dependency between two parameters. Therefore, the scatterplots between two parameters should also be looked at carefully in order to detect a potential nonlinear dependency.

3.1.4. Coefficient of variation:

The coefficient of variation describes the ratio between the empirical standard deviation and the mean value:

$$CV = \frac{s}{\bar{x}} \cdot 100 \% \quad (12)$$

The dimensionless coefficient of variation can be seen as a normalized measure which allows to compare different data sets with different units. It represents the relative variability of a data set with respect to its mean value. A low coefficient of variation implies that the data points are closely spread around the mean and vice versa.

3.2. Longitudinal measurements

The goal of the longitudinal measurements is to figure out how the measured dimensions behave along the length of the steel beams. As explained in chapter 2.3, the measured quantities include the flange thickness, the profile height, the profile width and the root fillet radius. In the subsequent figures, the behaviour of these measured quantities along the length is presented for the investigated beams. It is noted that on the y-axis, the normalized quantities according to equation (6) are plotted. The relative position along the length of the girder is depicted on the x-axis.

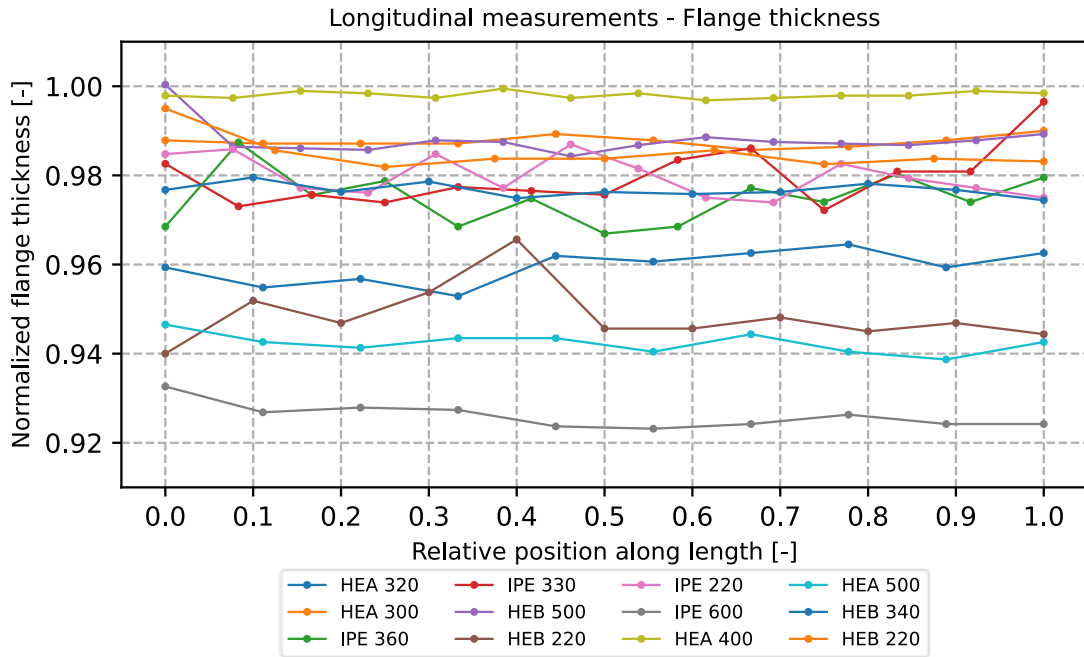


Figure 16: Normalized flange thickness along the length of the beams

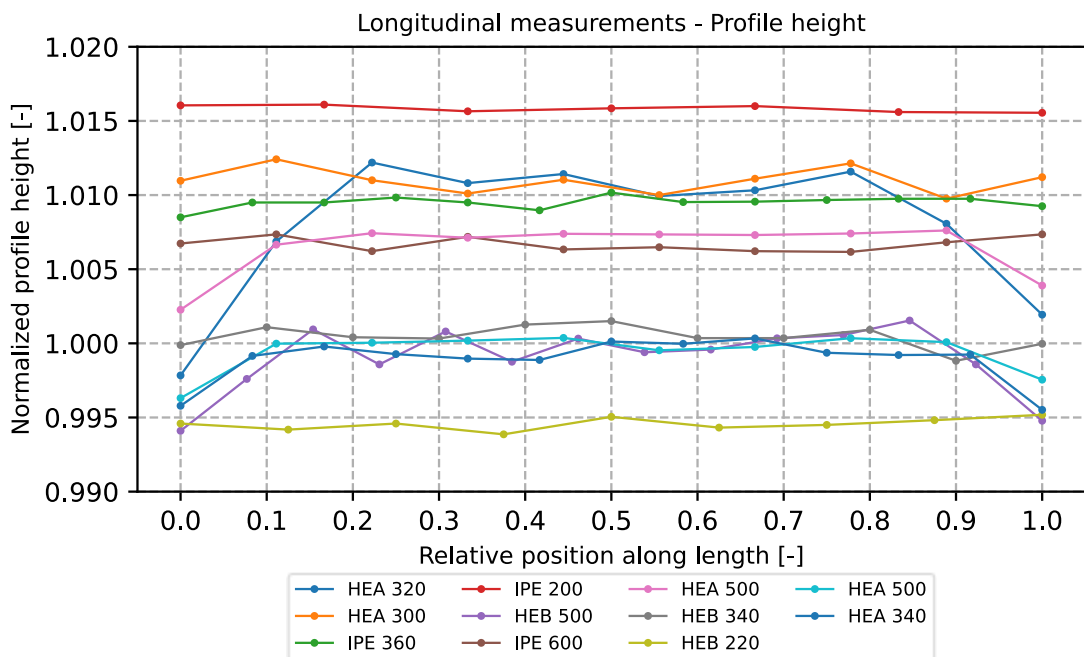


Figure 17: Normalized profile height along the length of the beams

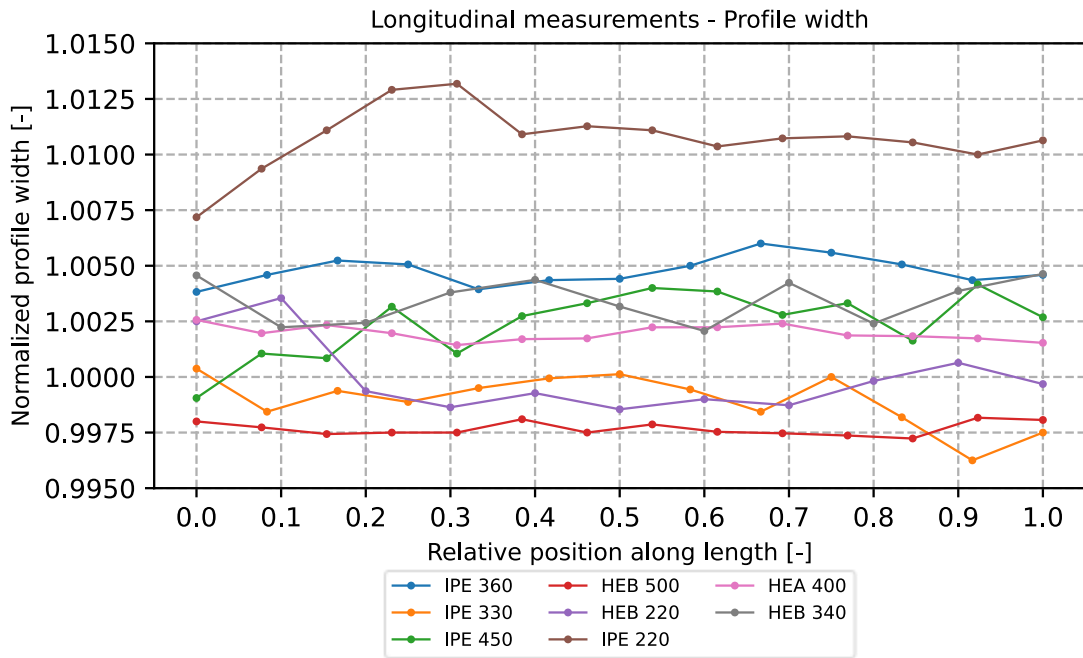


Figure 18: Normalized profile width along the length of the beams

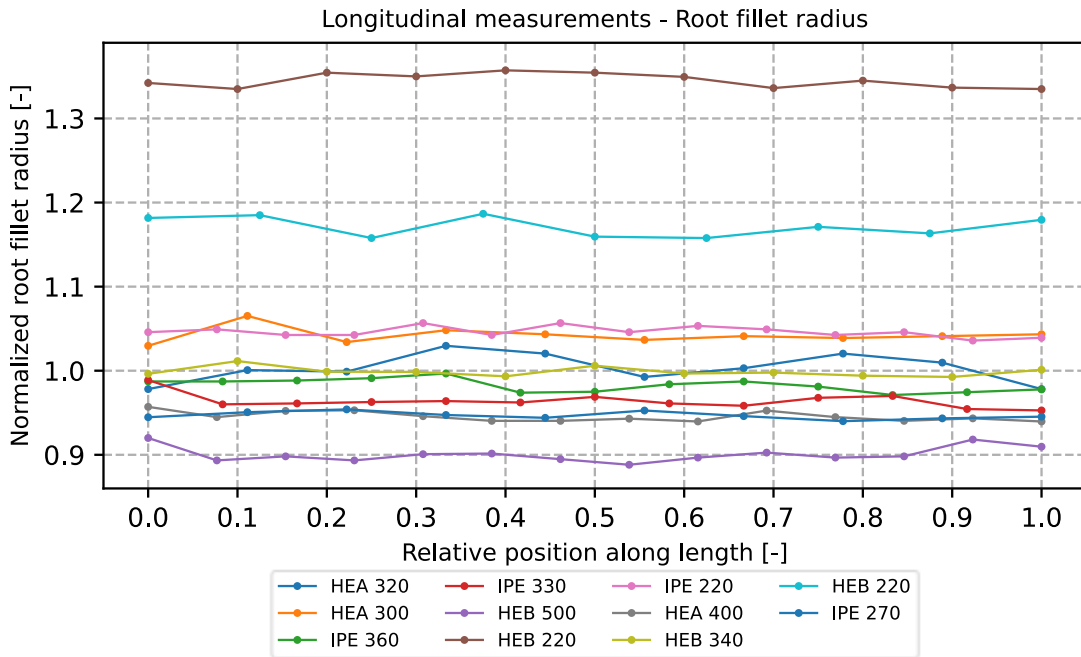


Figure 19: Normalized root fillet radius along the length of the beams

In the presented figures, it is observed that the imperfect geometry remains relatively constant along the length of the beam. For the profile height, it is seen that five of the investigated beams show a smaller height at both ends compared to the values along the rest of the length. However, it must be considered that the height of the profiles was not measured at the level of the web, but at an external location, as displayed in Figure 15. Therefore, as an additional consideration, the profile height was measured at the two end faces of the beam at the level of the web (h_{mid} in Figure 10) for three of the five mentioned beams. In the following table, the results are summarized. The measured values of h_{mid} at the two end faces are denoted by $h_{mid,0}$ and $h_{mid,1}$ respectively, while the measured values of h according to Figure 15 at the two ends of the beams are denoted by h_0 and h_1 . Furthermore, the mean value of the remaining measurements along the length (apart from

the ones at the two ends) is stated as h_{avg} . In other words, h_0 and h_1 represent the end values of Figure 17, while h_{avg} is an indicator for the measured height along the rest of the beams.

Table 6: Results of the additional consideration regarding the longitudinal variation of the profile height

Profile	$h_{mid,0}$ [mm]	$h_{mid,1}$ [mm]	h_0 [mm]	h_1 [mm]	h_{avg} [mm]
HEA 500	493.13	493.30	491.11	491.91	493.57
HEA 340	330.09	329.89	328.61	328.52	329.83
HEA 500	489.85	489.99	488.19	488.80	490.02

It is observed that while the measured heights h_0 and h_1 are considerably smaller than the average of the remaining values, the measured heights $h_{mid,0}$ and $h_{mid,1}$ are still approximately the same as the average of the values along the length. This means that if the heights $h_{mid,0}$ and $h_{mid,1}$ would be plotted in Figure 17 instead of h_0 and h_1 , there would not be the same pattern noticed that the measured heights at the two ends are smaller than along the rest of the length. The corresponding figure is shown in Appendix A.2.2. The reduced height at the two ends of the beams seems to be limited to the heights which are measured away from the web level (according to Figure 15). This may be explained by the cutting process during the production of these beams. Depending on the cutting technique, there may be some major initiation of forces at these end locations which can cause some residual stresses. As a consequence, the height can be reduced at these locations. However, it seems that the height at the web level (h_{mid} in Figure 10) is not affected by this and remains unchanged.

As a conclusion, it can be stated that it does not make sense to further consider the two measured heights h_{left} and h_{right} according to the measuring concept (see Figure 10) as these are measured at the ends of the steel beams. There will be some beams for which the heights h_{left} and h_{right} will not represent the height along the whole length because they may be reduced for example due to the mentioned residual stresses. Therefore, it is decided to only consider the height h_{mid} of Figure 10 for the profile height in the following. As it is measured at the web level, it can still be assumed that it represents the profile height along the whole length of the steel beam.

Besides the profile height, the measured quantities don't show a major variation along the length of the beam. There are still some minor discrepancies which however may also be a result of measurement errors (as discussed in section 2.5). Overall, it seems reasonable to measure all the quantities just at the end of the beam and to assume their constancy along the length. In order to strengthen this statement, the following table shows the coefficients of variation along the length of the investigated beams:

Table 7: Coefficients of variation along the length of the beams (in %)

Profile	t_f	h	b	r
HEA 320	0.387	0.468	-	1.734
HEA 300	0.128	0.085	-	0.924
IPE 360	0.603	0.041	0.063	0.792
IPE 330	0.680	-	0.118	0.938
IPE 450	-	-	0.147	-
IPE 200	-	0.023	-	-
HEB 500	0.381	0.222	0.031	1.024
HEB 220	0.712	-	0.164	0.635
IPE 220	0.460	-	0.141	0.593
IPE 600	0.308	0.047	-	-
HEA 400	0.076	-	0.034	0.618
HEA 500	0.239	0.182	-	-
HEB 340	0.157	0.075	0.100	0.566
HEB 220	0.401	0.042	-	1.031
IPE 270	-	-	-	0.466
HEA 500	-	0.137	-	-
HEA 340	-	0.116	-	-

When comparing these values with the values from the general measurements (section 3.5.1), one can see that the variation along the length is much smaller than the variation of the general measurements themselves. This confirms the conclusion made above.

For the radius of the root fillets, it can be seen in Figure 19 that two of the investigated beams have quite larger radii than the nominal values. As already explained in section 1.2, the value for the fillet radius is not strictly standardized and the values from the SZS C5/18 tables [7] are just recommendations which can be modified depending on the producer's preference. Therefore, it seems that the producer of these beams decided to produce a larger radius than the recommended one. However, this does not affect the variability along the length of the beams, as the chosen radii remain approximately unchanged along the length.

As mentioned in chapter 2.3, it was not possible to measure the web thickness along the length of the profiles. By taking into consideration the result patterns of the other dimensions, as shown in the previous figures, it is assumed in the following that the web thicknesses remain constant along the length as well and that the measured web thicknesses at the ends of the girders can be regarded as representative for the whole length.

In the thesis of Jaquess (1998) [14], which was already mentioned in section 1.5, the variation of the geometrical dimensions in the longitudinal direction of the beam was investigated as well. He also observed that the measured dimensions were nearly constant along the length of the members. It should be noted, however, that he only measured the dimensions at two locations along the length and not on a regular distance along the whole beam. Nevertheless, the key message of relatively constant dimensions along the length is the same as made above.

3.3. Uncertainty in measurement

It was tried to cover each profile type and a large size range when conducting the measurements regarding the quantification of the measurement accuracy, as introduced in section 2.4. Therefore, the following three profiles were investigated: IPE 180, HEA 340 and HEB 600. It was decided to measure the flange thickness, the web thickness, the height, the width, the a-value and the root fillet radius, repeating the measurement for each dimension 15 times. The following tables summarize the arithmetic mean and the coefficient of variation for each dimension:

Table 8: Arithmetic mean values of the measured dimensions

Profile	t_f [mm]	t_w [mm]	h [mm]	b [mm]	a [mm]	r [mm]
IPE 180	8.10	5.51	179.69	92.26	43.52	9.03
HEA 340	16.43	9.42	332.48	300.64	145.71	27.48
HEB 600	29.32	15.18	602.32	299.06	141.14	30.98

Table 9: Coefficients of variation of the measured dimensions (in %)

Profile	t_f [%]	t_w [%]	h [%]	b [%]	a [%]	r [%]
IPE 180	0.444	0.544	0.054	0.042	0.551	0.914
HEA 340	0.070	0.067	0.069	0.022	0.108	1.206
HEB 600	0.164	0.183	0.006	0.029	0.328	1.837

It can be observed that the coefficients of variation are quite small, especially for the larger dimensions as the profile height and width. Furthermore, it is seen that the measurements of the root fillet radii show the largest variation. This confirms that the measurement of the radii is more prone to variations depending on the positioning of the measurement device compared to the other dimensions. However, the coefficients of variation for the radii are still small (max. 1.837 %) when comparing them with the coefficients of variation of the general measurements (see section 3.5.1). It can be generally said that the coefficients of variations stated in Table 9 are much smaller than the ones of the general measurements in section 3.5.1, leading to the conclusion that a satisfying measurement accuracy is ensured.

Based on the explanations in section 2.4, the following 95 % confidence intervals can be calculated for each investigated profile and dimension:

Table 10: Obtained 95 % confidence intervals for the investigated dimensions

	IPE 180	HEA 340	HEB 600
t_f	$l = 8.10 \text{ mm} \pm 0.0771 \text{ mm}$	$l = 16.43 \text{ mm} \pm 0.0246 \text{ mm}$	$l = 29.32 \text{ mm} \pm 0.1034 \text{ mm}$
t_w	$l = 5.51 \text{ mm} \pm 0.0643 \text{ mm}$	$l = 9.42 \text{ mm} \pm 0.0136 \text{ mm}$	$l = 15.18 \text{ mm} \pm 0.0595 \text{ mm}$
h	$l = 179.69 \text{ mm} \pm 0.2080 \text{ mm}$	$l = 332.48 \text{ mm} \pm 0.4948 \text{ mm}$	$l = 602.32 \text{ mm} \pm 0.0777 \text{ mm}$
b	$l = 92.26 \text{ mm} \pm 0.0825 \text{ mm}$	$l = 300.64 \text{ mm} \pm 0.1440 \text{ mm}$	$l = 299.06 \text{ mm} \pm 0.1870 \text{ mm}$
a	$l = 43.52 \text{ mm} \pm 0.5141 \text{ mm}$	$l = 145.71 \text{ mm} \pm 0.3389 \text{ mm}$	$l = 141.14 \text{ mm} \pm 0.9918 \text{ mm}$
r	$l = 9.03 \text{ mm} \pm 0.1769 \text{ mm}$	$l = 27.48 \text{ mm} \pm 0.7110 \text{ mm}$	$l = 30.98 \text{ mm} \pm 1.2205 \text{ mm}$

The same confidence intervals can also be stated in percentage values:

Table 11: Obtained 95 % confidence intervals for the investigated dimensions stated in percentage values

	IPE 180	HEA 340	HEB 600
t_f	± 0.952 %	± 0.150 %	± 0.353 %
t_w	± 1.168 %	± 0.144 %	± 0.392 %
h	± 0.116 %	± 0.149 %	± 0.013 %
b	± 0.089 %	± 0.048 %	± 0.063 %
a	± 1.181 %	± 0.233 %	± 0.703 %
r	± 1.960 %	± 2.587 %	± 3.940 %

When comparing these confidence intervals with the coefficients of variation of the general measurements (see section 3.5.1), it can be confirmed once again that the measuring process seems to be accurate enough. For example, for the flange thicknesses, it will be observed in section 3.5.1 that the coefficient of variation is approximately 3 % which means that the standard deviation is 3 % of the mean value. At the same time, the 95 % confidence interval in percentage values for the flange is ± 0.35-0.95 % (see Table 11). This shows impressively that when relating the accuracy of the measurement process to the scatter of the general measurements, it can be generally said that the individual measurements are reliable and there is not a large scatter when repeating the same measurement. The used measurement process seems to be accurate. However, this statement presumes the absence of systematic errors which cannot be excluded especially for the measured a-values as will be discussed in section 3.5.1.

3.4. Investigation of the measured flange thicknesses

In this section, the measured flange thicknesses are investigated separately before all further measurements are evaluated in chapter 3.5. The flanges are quite important for the structural resistance of hot-rolled profiles, as Melcher et al. [4] already observed the crucial role of the variability of the flanges (see Figure 1). Therefore, it is reasonable to study them in more detail.

3.4.1. Mean values and coefficients of variation

The thicknesses of the flanges were measured at four different locations for each flange, as explained in section 2.1.2. The following two tables show the mean values of the normalized measurements and the coefficients of variation for each category:

Table 12: Mean values of the normalized flange thicknesses

cat.	$\frac{t_{f1,1}}{t_{f,nom}}$	$\frac{t_{f1,2}}{t_{f,nom}}$	$\frac{t_{f1,3}}{t_{f,nom}}$	$\frac{t_{f1,4}}{t_{f,nom}}$	$\frac{t_{f2,1}}{t_{f,nom}}$	$\frac{t_{f2,2}}{t_{f,nom}}$	$\frac{t_{f2,3}}{t_{f,nom}}$	$\frac{t_{f2,4}}{t_{f,nom}}$
Total	0.9608	0.9903	0.9913	0.9685	0.9602	0.9868	0.9948	0.9708
Small	0.9619	0.9920	0.9910	0.9667	0.9607	0.9871	0.9960	0.9703
Large	0.9591	0.9876	0.9918	0.9714	0.9594	0.9864	0.9929	0.9717
HEA	0.9602	0.9946	0.9952	0.9675	0.9625	0.9925	0.9995	0.9714
HEB	0.9607	0.9894	0.9948	0.9728	0.9595	0.9873	0.9979	0.9738
IPE	0.9616	0.9853	0.9816	0.9648	0.9577	0.9781	0.9843	0.9665

Table 13: Coefficients of variation (in %) of the normalized flange thicknesses

cat.	$\frac{t_{f1,1}}{t_{f,nom}}$	$\frac{t_{f1,2}}{t_{f,nom}}$	$\frac{t_{f1,3}}{t_{f,nom}}$	$\frac{t_{f1,4}}{t_{f,nom}}$	$\frac{t_{f2,1}}{t_{f,nom}}$	$\frac{t_{f2,2}}{t_{f,nom}}$	$\frac{t_{f2,3}}{t_{f,nom}}$	$\frac{t_{f2,4}}{t_{f,nom}}$
Total	3.178	3.355	3.288	3.214	3.121	3.291	3.423	3.233
Small	3.401	3.736	3.673	3.568	3.334	3.673	3.763	3.574
Large	2.797	2.642	2.596	2.563	2.766	2.602	2.814	2.632
HEA	3.202	3.546	3.655	3.340	2.952	3.358	3.498	3.443
HEB	2.601	2.521	2.580	2.662	2.598	2.522	2.634	2.542
IPE	3.756	3.881	3.341	3.600	3.859	3.830	3.950	3.644

In Table 12, it can be observed that the mean values of the measured flange thicknesses are smaller than the standardized ones for each category. This may be due to the fact that there is quite a large allowed tolerance for the flange thickness given in EN 10034 [2], see also Figure 3. Therefore, the producers may try to save costs by producing flange thicknesses at the very lower end of the tolerances. However, one should be aware that the production of thinner flanges may induce unfavourable consequences on the structural behaviour, as will be further studied in section 4 and 5.

The classification into the different categories does not have a huge relevance for the mean values, as there is not a considerable variation when comparing the values of the different categories. However, it seems that the flange thicknesses of the IPE sections are produced slightly thinner compared to the other categories.

When studying the mean values in more detail, it can be noticed that the measured outer flange thicknesses ($t_{f1,1}$, $t_{f1,4}$, $t_{f2,1}$ and $t_{f2,4}$) are much smaller than the ones that are closer to the web. This pattern can be observed for each category. It seems that the flanges are produced thicker in the proximity of the web than further away. This induces a pronounced impact on the structural behaviour around the weak axis, as there the outer flange part is responsible for providing the majority of the bending resistance and the bending stiffness. This simply comes from the fact that the areas further away from the neutral axis contribute the most to the structural behaviour in bending. Furthermore, the outer flange part is typically a location where connections to other structural elements are made, inducing additional forces at these parts. A reduced flange thickness may not provide enough resistance to take these forces then.

For the coefficients of variation, it can be generally observed that the smaller cross-sections show larger coefficients of variation compared to the larger profiles. Furthermore, the HEB sections show smaller variations than the other profile types. This may be due to the production process of the rolled profiles. More specifically, the production equipment has a specific accuracy. Due to the limited accuracy, the machine produces cross-sections with slightly different dimensions than the nominal ones. Obviously, this limited accuracy induces a larger percentage deviation from the nominal value for smaller profiles compared to larger profiles. The smaller the quantity, the larger is the percentage deviation of the same absolute deviation. As the HEB sections have thicker flanges, it will induce a smaller percentage deviation there compared to the other profile types. The observation of larger variations for smaller profiles is not limited to the flange thicknesses, but holds true for all measured dimensions, as will be seen in the subsequent chapters.

The following figure serves as an illustration for the observation that the variation decreases the larger the profile gets. In the left part of the figure, the normalized flange thickness $t_{f1,1}$ is plotted against the profile size. The corresponding histogram is shown on the right. Furthermore, the different profile types (HEA, HEB, IPE) are shown with different colours. In this plot, it can also be seen why the threshold size between the categories “Small” and “Large” is chosen at the size 360, because the pattern of the results in terms of variability seems to change in this region. This holds true for almost all measured dimensions.

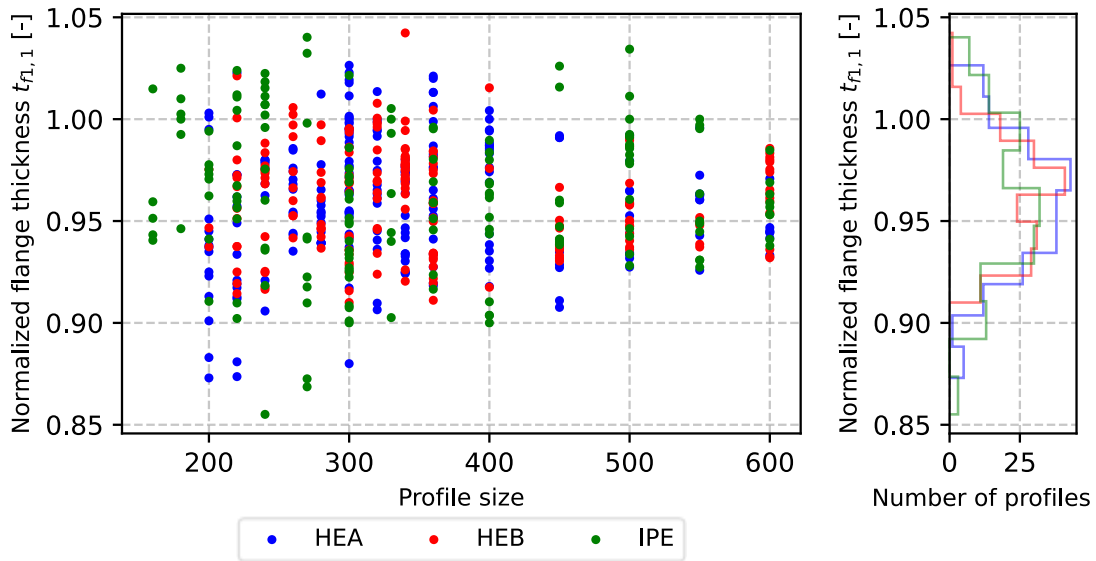


Figure 20: Plot of the normalized flange thickness $t_{f1,1}$ against the profile size (left) with the corresponding histogram (right)

For the other measured flange thicknesses, these plots look very similar, as shown in Appendix A.3.1.

3.4.2. Correlation study

The goal of this subchapter is to study the correlation behaviour of the measured flange dimensions. In order to do this, the correlation matrices are calculated and shown. A correlation matrix contains the calculated Pearson's correlation coefficients between two parameters in a tabular form. Obviously, the matrix is symmetric with ones on the diagonal.

For the category "Total", the following correlation matrix can be derived:

Table 14: Correlation matrix of the measured flange thicknesses for the category "Total"

	$t_{f1,1}$	$t_{f1,2}$	$t_{f1,3}$	$t_{f1,4}$	$t_{f2,1}$	$t_{f2,2}$	$t_{f2,3}$	$t_{f2,4}$
$t_{f1,1}$	1							
$t_{f1,2}$	0.806	1						
$t_{f1,3}$	0.593	0.746	1					
$t_{f1,4}$	0.601	0.608	0.808	1				
$t_{f2,1}$	0.723	0.593	0.635	0.680	1			
$t_{f2,2}$	0.595	0.700	0.805	0.699	0.799	1		
$t_{f2,3}$	0.636	0.818	0.744	0.621	0.574	0.724	1	
$t_{f2,4}$	0.688	0.725	0.691	0.729	0.606	0.649	0.838	1

There is a strong positive linear correlation between all measured flange thicknesses, as all entries of the matrix are above 0.55. This means that, in general, when one flange thickness is produced too thin, there is a strong tendency that all the other flange thicknesses are produced too thin as well and vice versa.

Furthermore, it seems that the correlation between the outer and the corresponding inner part of each half of the flanges is particularly pronounced. The corresponding correlation coefficients are highlighted in green in Table 14. This pattern can be observed even more when plotting the normalized inner flange thickness against the normalized outer flange thickness for all four flange halves, as can be seen in the following figure. Thereby, the different colours represent the four different flange halves (see illustration at the lower left corner of the figure).

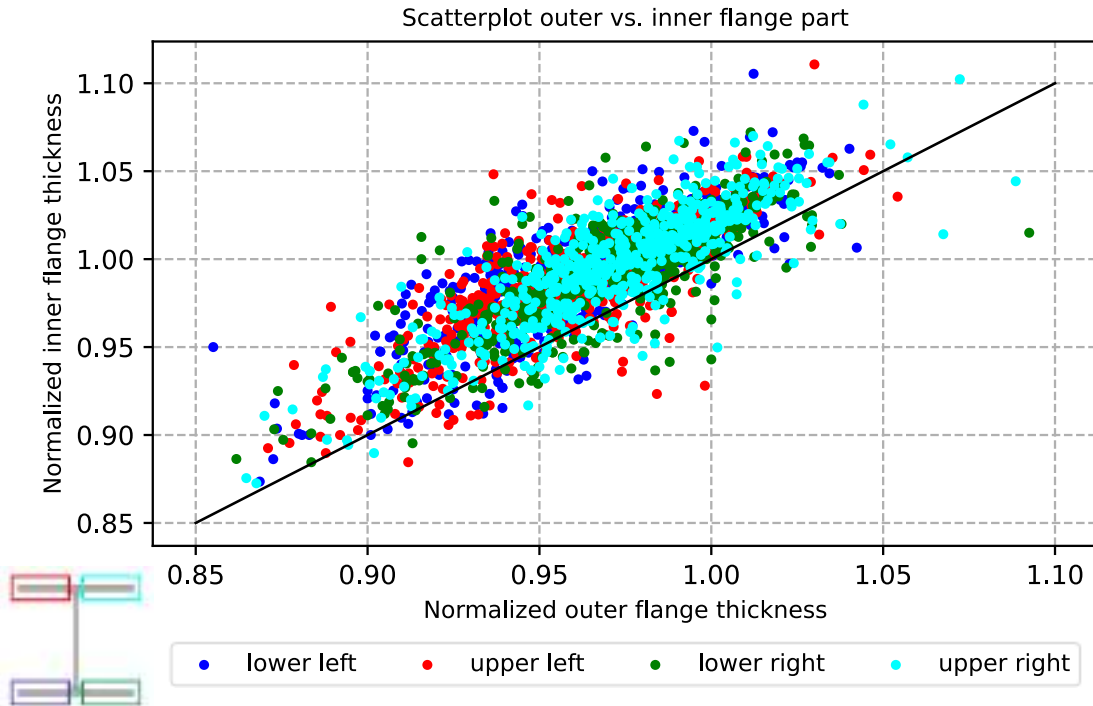


Figure 21: Scatterplot of normalized outer flange thicknesses against normalized inner flange thicknesses

The black line in Figure 21 highlights once again that the vast majority of the investigated flanges have thinner dimensions at the outer parts compared to the inner ones, as most of the points lie above the black line. Since the mentioned line has an inclination of 45 degrees, points lying on the black line would imply equal thicknesses for the outer as well as the inner part of the flanges.

To summarize, there is a quite strong positive correlation between all the measured flange thicknesses observed. A particular strong correlation is obtained between the outer part of the flange and the corresponding inner part of the same flange half. The same correlation pattern can be observed for each category with slightly differing values. The corresponding correlation matrices for each category can be found in Appendix A.3.2.

3.5. General statistical evaluation

In this chapter, the most important measurement results according to the procedure of section 2.1 are displayed and statistically evaluated. A compilation of all the measurements can be found in Appendix A.2, while the subsequently explained measurement results are visualized in Appendix A.4.3.

Before conducting the statistical evaluation of the data, some simplifications are made. As the measured flange thicknesses were already extensively investigated in section 3.4, they are averaged for the lower and the upper flange in order to reduce the number of quantities:

$$t_{f,lower} = \frac{t_{f1,1} + t_{f1,2} + t_{f1,3} + t_{f1,4}}{4} \tag{13}$$

$$t_{f,upper} = \frac{t_{f2,1} + t_{f2,2} + t_{f2,3} + t_{f2,4}}{4} \tag{14}$$

The four measured root fillet radii are investigated in detail in Appendix A.4.1. It is observed that although there are differences depending on the considered category (IPE and HEB sections exhibit significantly larger radii than HEA sections for example), there are no considerable discrepancies between the four measured radii of the same category (considering the large coefficients of variation). They show similar mean values and coefficients of variation. Furthermore, there is quite a

strong positive linear correlation between all the root fillet radii. Therefore, it seems to be reasonable to average the four measured radii for each profile without losing much information:

$$r = \frac{r_1 + r_2 + r_3 + r_4}{4} \quad (15)$$

For the web thicknesses, the same statements as for the root fillet radii hold, see Appendix A.4.2 for a more detailed evaluation. The three measured web thicknesses are all equally strong correlated among each other and don't show considerable differences in the calculated mean and coefficient of variation of the same category. Therefore, they will be averaged to one quantity as well:

$$t_w = \frac{t_{w1} + t_{w2} + t_{w3}}{3} \quad (16)$$

For the profile height, only the quantity measured at the level of the web (h_{mid}) is considered:

$$h = h_{mid} \quad (17)$$

This is done based on the results of section 3.2, where it was concluded that the other two measured heights do not represent the profile height along the whole length.

In contrast, both measured profile widths, b_1 and b_2 , and both measured a-values, a_1 and a_2 , are considered for the statistical evaluation.

3.5.1. Mean values and coefficients of variation

The following table summarizes the mean values of the mentioned quantities for the different categories:

Table 15: Mean values of measurement data for the different categories (normalized quantities)

cat.	$\frac{t_{f,low}}{t_{f,nom}}$	$\frac{t_{f,up}}{t_{f,nom}}$	$\frac{t_w}{t_{w,nom}}$	$\frac{h}{h_{nom}}$	$\frac{b_1}{b_{nom}}$	$\frac{b_2}{b_{nom}}$	$\frac{r}{r_{nom}}$	$\frac{a_1}{a_{nom}}$	$\frac{a_2}{a_{nom}}$
Total	0.9777	0.9782	1.0139	1.0051	1.0014	1.0015	1.0126	1.0040	1.0022
Small	0.9779	0.9785	1.0180	1.0053	1.0019	1.0020	1.0133	1.0060	1.0015
Large	0.9775	0.9776	1.0077	1.0046	1.0006	1.0007	1.0114	1.0009	1.0034
HEA	0.9794	0.9815	1.0205	1.0047	0.9992	0.9992	0.9973	1.0017	0.9990
HEB	0.9794	0.9796	1.0051	1.0056	0.9995	0.9993	1.0191	1.0016	1.0018
IPE	0.9733	0.9717	1.0155	1.0050	1.0066	1.0074	1.0260	1.0101	1.0073

Additionally, the coefficient of variation is stated here for the same quantities and for each category:

Table 16: Coefficients of variation (in %) for the different categories

cat.	$\frac{t_{f,low}}{t_{f,nom}}$	$\frac{t_{f,up}}{t_{f,nom}}$	$\frac{t_w}{t_{w,nom}}$	$\frac{h}{h_{nom}}$	$\frac{b_1}{b_{nom}}$	$\frac{b_2}{b_{nom}}$	$\frac{r}{r_{nom}}$	$\frac{a_1}{a_{nom}}$	$\frac{a_2}{a_{nom}}$
Total	2.863	2.878	3.547	0.507	0.608	0.634	7.913	1.298	1.336
Small	3.163	3.168	3.877	0.564	0.671	0.695	8.702	1.286	1.362
Large	2.333	2.368	2.855	0.402	0.488	0.516	6.525	1.256	1.291
HEA	3.062	2.947	3.543	0.510	0.466	0.475	8.132	1.056	0.985
HEB	2.238	2.203	3.469	0.510	0.387	0.388	9.074	1.294	1.247
IPE	3.213	3.388	3.449	0.498	0.687	0.691	5.407	1.411	1.679

Table 15 and Table 16 provide some useful insight into the measurement results. Generally, it is seen that the smaller cross-sections show larger coefficients of variation for all measured dimensions compared to the larger profiles. As already stated in section 3.4.1, this may be due to the limited accuracy of the production equipment which induces a larger percentage deviation from the nominal value for smaller profiles and smaller dimensions compared to larger profiles and larger dimensions.

Looking into the numbers more specifically, it is seen that the profile width and profile height show a much smaller variation compared to all other parameters. At least partially, this can be explained again by the fact that the height and the width are larger dimensions compared to the others. Therefore, a limited production equipment accuracy induces a smaller percentage deviation. The mean values of the measured heights and widths are quite close to the nominal values, yielding in normalized mean values around 1.00. Together with the small coefficient of variation of these dimensions, it seems that these dimensions are produced quite precisely in accordance with the standardized quantities presented in section 1.2. Moreover, it is observed that the profile widths are produced in average approximately 0.5 % larger for the IPE profiles compared to the other profile types.

Generally, it can be stated that the measured web thicknesses are larger than the nominal values on average, while a large part of the measured flange thicknesses are smaller than the nominal ones, resulting in mean values of the normalized measurements below 1.00 (as already seen in section 3.4). Furthermore, it is observed that there are quite some discrepancies of the normalized mean value of the web thicknesses depending on the considered category. It seems that the web thicknesses of large profiles and HEB sections are produced considerably thinner compared to the other profiles.

As could be expected, the measured root fillet radii exhibit the largest coefficient of variation. This relates to the measuring procedure which is extensively prone to variations as the radii are not perfect quarter circles, as already explained in section 2.1.3. Moreover, the producer may decide himself which radius to produce, as stated in section 1.2. In Appendix A.4.3, it can be observed that there are obviously some measurements of profiles where the root fillet radius chosen by the producer deviates one or even two size classes from the recommended one in the SZS C5/18 tables [7]. Furthermore, it is observed in Table 15 that the root fillet radii seem to be produced considerably thinner for HEA sections compared to the other profile types. In order to show that this observation still holds true even when neglecting the profiles for which the producer obviously decided to produce other radii than the recommended ones, the mean values and the coefficients of variation are calculated once again, neglecting these outliers, see Appendix A.4.4. Whenever the value between the observed mean root fillet radius according to equation (15) deviates more than 2.5 mm from the recommended nominal value of the SZS C5/18 tables [7], it is defined as an outlier. This is based on the observation that the recommended root fillet radii size classes have size steps of 3 mm between each other. The derived mean values still show the pattern of smaller root fillet radii for HEA sections compared to the other categories, see Appendix A.4.4 for more details. The root fillet radii of IPE sections are produced the largest.

When looking at the mean values of the two measured a -values, it seems that there is some kind of systematic error made during the measurement process, as the a -values should be the difference between the profile width and the web thickness. For the measurement results in Table 15, it is seen that the normalized mean value of the profile width is around 1.00, while the normalized mean value of the web thickness is above 1.00. This would mean that the mean values of the a -values should be below 1.00 to guarantee compatibility. However, the observed a -values are slightly larger than 1.00 on average. Therefore, it is suspected that there is some small systematic error which has the consequence that the measured a -values are slightly larger than the real ones. An example for a plausible systematic error may be that there is too less force applied when measuring the a -values, which are obtained with the help of a steel bar (see Figure 13). This would explain why the measured a -values are larger than the expected ones. Nevertheless, as the a -values will only be used to calculate the eccentricity of the web later, the systematic error will cancel out, see section 4.2.1. The two a -values will be subtracted from each other, therefore eliminating the systematic error.

3.5.2. Correlation study

In the following, a correlation study for the quantities specified above is conducted. For each category, the correlation matrix will be shown. All entries above +0.4 will be marked green while all values below -0.4 will be marked red. Using this colour coding, the green entries indicate quite a large positive linear correlation, while the red entries indicate a negative one.

Furthermore, a scatter plot matrix is shown for each category in Appendix A.4.3. The scatter plot matrix is a convenient way to present the results in a compact form. On the diagonal, the histogram of each quantity is shown. On the off-diagonal entries, the scatter plot between two quantities is plotted. A scatter plot is a useful graphical way to detect a possible correlation. In contrast to the Pearson's correlation coefficient, a potential nonlinear correlation between two quantities can be discovered when looking at the scatter plots.

Category "Total":

Table 17: Correlation matrix for category "Total"

	$t_{f,lower}$	$t_{f,upper}$	t_w	h	b_1	b_2	r	a_1	a_2
$t_{f,lower}$	1								
$t_{f,upper}$	0.898	1							
t_w	-0.266	-0.244	1						
h	-0.156	-0.143	0.050	1					
b_1	-0.143	-0.142	-0.006	0.011	1				
b_2	-0.118	-0.146	0.044	-0.004	0.851	1			
r	-0.371	-0.339	-0.163	-0.006	0.217	0.170	1		
a_1	-0.071	-0.071	0.018	0.078	0.504	0.499	0.042	1	
a_2	0.004	-0.008	-0.234	-0.044	0.421	0.405	0.253	-0.138	1

Category "Small":

Table 18: Correlation matrix for category "Small"

	$t_{f,lower}$	$t_{f,upper}$	t_w	h	b_1	b_2	r	a_1	a_2
$t_{f,lower}$	1								
$t_{f,upper}$	0.920	1							
t_w	-0.282	-0.266	1						
h	-0.152	-0.120	-0.035	1					
b_1	-0.139	-0.139	-0.012	-0.001	1				
b_2	-0.132	-0.165	0.057	-0.017	0.850	1			
r	-0.450	-0.436	-0.158	0.040	0.219	0.162	1		
a_1	-0.109	-0.115	0.001	0.042	0.562	0.578	0.020	1	
a_2	0.028	0.018	-0.244	-0.039	0.455	0.437	0.263	-0.266	1

Category “Large”:

Table 19: Correlation matrix for category "Large"

	$t_{f,lower}$	$t_{f,upper}$	t_w	h	b_1	b_2	r	a_1	a_2
$t_{f,lower}$	1								
$t_{f,upper}$	0.836	1							
t_w	-0.234	-0.199	1						
h	-0.169	-0.218	0.265	1					
b_1	-0.162	-0.159	-0.044	0.018	1				
b_2	-0.081	-0.103	-0.048	0.005	0.850	1			
r	-0.152	-0.072	-0.188	-0.143	0.210	0.189	1		
a_1	0.000	0.006	-0.031	0.122	0.367	0.317	0.085	1	
a_2	-0.048	-0.062	-0.195	-0.041	0.387	0.379	0.240	0.102	1

Category “HEA”:

Table 20: Correlation matrix for category "HEA"

	$t_{f,lower}$	$t_{f,upper}$	t_w	h	b_1	b_2	r	a_1	a_2
$t_{f,lower}$	1								
$t_{f,upper}$	0.919	1							
t_w	-0.287	-0.280	1						
h	-0.191	-0.132	0.043	1					
b_1	-0.116	-0.093	-0.162	0.036	1				
b_2	0.009	0.013	-0.142	0.031	0.864	1			
r	-0.525	-0.486	-0.101	0.033	0.346	0.216	1		
a_1	0.101	0.066	-0.144	0.090	0.444	0.465	0.117	1	
a_2	-0.120	-0.066	-0.246	-0.051	0.475	0.452	0.205	-0.403	1

Category “HEB”:

Table 21: Correlation matrix for category "HEB"

	$t_{f,lower}$	$t_{f,upper}$	t_w	h	b_1	b_2	r	a_1	a_2
$t_{f,lower}$	1								
$t_{f,upper}$	0.921	1							
t_w	-0.057	-0.066	1						
h	0.062	0.070	0.035	1					
b_1	-0.254	-0.264	-0.099	-0.046	1				
b_2	-0.159	-0.202	-0.091	-0.097	0.763	1			
r	-0.500	-0.482	-0.192	-0.011	0.175	0.065	1		
a_1	0.049	0.021	0.010	-0.010	0.406	0.387	-0.094	1	
a_2	-0.172	-0.130	-0.300	0.035	0.265	0.227	0.391	0.057	1

Category “IPE”:

Table 22: Correlation matrix for category “IPE”

	$t_{f,lower}$	$t_{f,upper}$	t_w	h	b_1	b_2	r	a_1	a_2
$t_{f,lower}$	1								
$t_{f,upper}$	0.861	1							
t_w	-0.436	-0.375	1						
h	-0.314	-0.346	0.135	1					
b_1	-0.035	0.017	0.172	0.048	1				
b_2	-0.117	-0.104	0.306	0.044	0.747	1			
r	0.050	0.081	-0.174	-0.117	0.059	0.148	1		
a_1	-0.268	-0.161	0.176	0.191	0.457	0.439	0.058	1	
a_2	0.274	0.194	-0.186	-0.131	0.352	0.347	0.072	-0.348	1

When studying the correlation matrices, there are some general patterns that can be observed. It can be immediately seen that there is a large positive correlation between the thicknesses of the two flanges of the measured profiles. This observation holds true for every category, however being even more pronounced for smaller than for larger profiles and more pronounced for HEA and HEB profiles than for IPE profiles. The strong correlation between the flanges is not a surprise, as the same conclusion was already made in section 3.4. A similar observation can be made for the two measured profile widths b_1 and b_2 , although being a bit less pronounced than for the flange thicknesses. They are also quite strongly positively correlated.

As could be expected, the a -values correlate positively with the measured profile widths. This comes from the fact that a larger profile width automatically induces a larger a -value when the web thickness is assumed to remain unchanged. Moreover, there is a small negative correlation between the web thickness and the flange thicknesses for IPE and HEA profiles which is not observed for the HEB profiles.

Furthermore, a moderate negative correlation between the flange thicknesses and the root fillet radius can be observed for HEA and HEB sections and especially for small profiles. For IPE profiles, this behaviour cannot be noticed. However, as already stated in section 3.5.1, there are obviously some measurements of the root fillet radii which were intentionally chosen by the producer to deviate one or two size classes from the recommended one according to the SZS C5/18 tables [7]. Such outliers can influence the correlation behaviour quite heavily. Therefore, the same correlation study is carried out ignoring these outliers, see Appendix A.4.4. The outliers are defined in the same way as described in section 3.5.1. The whole measurement series, meaning all measured dimensions of one specific measured profile, is removed when an outlier is observed for the root fillet radii. This is done because there needs to be the same number of measurements for all dimensions in order to derive a correlation matrix. When conducting this evaluation, it is observed that the negative correlation between the flange thicknesses and the root fillet radii almost fully disappears. This evaluation without considering the outliers of the root fillet radii shows impressively how the radii chosen by the producer can falsify the results of the correlation study when not properly considering it.

3.5.3. Choice of the probability distribution family

In practise, it would be useful to know which probability distribution is fitting to the obtained data, as the design standard prEN 1993-1-1 [9] presumes a lognormal distribution for the geometrical dimensions, as mentioned by Kuhlmann et al. (2020) [1]. There are several ways to choose an appropriate probability density function (PDF). One way is to plot the normalized histograms of the data and some PDFs in the same figure. Based on this visual comparison, one can qualitatively judge which PDF is fitting the best. This is done in the framework of this thesis for the normal and the lognormal probability density function. The following equations are all adopted from the lecture material of Prof. Dr. Bruno Sudret [13].

A normal random variable behaves according to the following PDF:

$$f_X(x) = \frac{1}{\sqrt{2 \cdot \pi} \cdot \sigma} \cdot e^{-0.5 \cdot \left(\frac{x-\mu}{\sigma}\right)^2} \quad (18)$$

The parameters μ and σ can be estimated based on the obtained data and making use of the method of moments:

$$\mu = \frac{1}{n} \cdot \sum_{i=1}^n x_i \quad (19)$$

$$\sigma = \sqrt{\frac{1}{n-1} \cdot \sum_{i=1}^n (x_i - \bar{x})^2} \quad (20)$$

Which is nothing else than the mean value and the empirical standard deviation of the sample.

A lognormal random variable behaves according to the following PDF:

$$f_X(x) = \frac{1}{\sqrt{2 \cdot \pi} \cdot \zeta \cdot x} \cdot e^{-0.5 \cdot \left(\frac{\ln x - \lambda}{\zeta}\right)^2} \quad (21)$$

The parameters λ and ζ can be estimated again by applying the method of moments:

$$\lambda = \ln \frac{\bar{x}}{\sqrt{1 + \left(\frac{s}{\bar{x}}\right)^2}} \quad (22)$$

$$\zeta = \sqrt{\ln \left(1 + \left(\frac{s}{\bar{x}}\right)^2\right)} \quad (23)$$

Where the empirical mean \bar{x} and the empirical standard deviation s are adopted from the equations (7) and (9).

Another way to study graphically which distribution is fitting to the data is by comparing the theoretical quantiles of a selected probability distribution with the empirical quantiles obtained from the data. This can be done by constructing so-called quantile-quantile plots (QQ-plots) [8]. The idea is to plot the theoretical quantiles on the x-axis while plotting the empirical quantiles on the y-axis. If the theoretical distribution function is fitting to the data, the points should approximately lie on a line with an inclination of 45 degree, meaning that the theoretical and the empirical quantiles coincide.

According to the lecture Material of Dr. Lukas Meier [8] the following $(\alpha_k \times 100)\%$ quantiles are considered:

$$\alpha_k = \frac{k - 0.5}{n}, \quad k = 1, \dots, n \quad (24)$$

With n being the number of measurements. Using this choice of the quantiles, the measurement $x_{(k)}$ is directly the corresponding empirical quantile. Thereby, $x_{(k)}$ is the k -th measurement of the measurement series which is sorted in ascending order. The theoretical quantiles on the other side can be calculated with $F^{-1}(\alpha_k)$, where F is the cumulative distribution function of the theoretical distribution. Therefore, the following points are plotted in the QQ-plot:

$$\{F^{-1}(\alpha_k), x_{(k)}\}, \quad k = 1, \dots, n \quad (25)$$

Based on the definitions above, the histograms with the theoretical PDFs and the QQ-plots are constructed for the dimensions introduced in this chapter except for the a -values. It is pointed out that for the histograms the probability density is

always chosen such that the area under the histogram integrates to 1.00. This enables a direct comparison between the theoretical PDF and the obtained data. The figures for the lower flange thickness are shown here for instance:

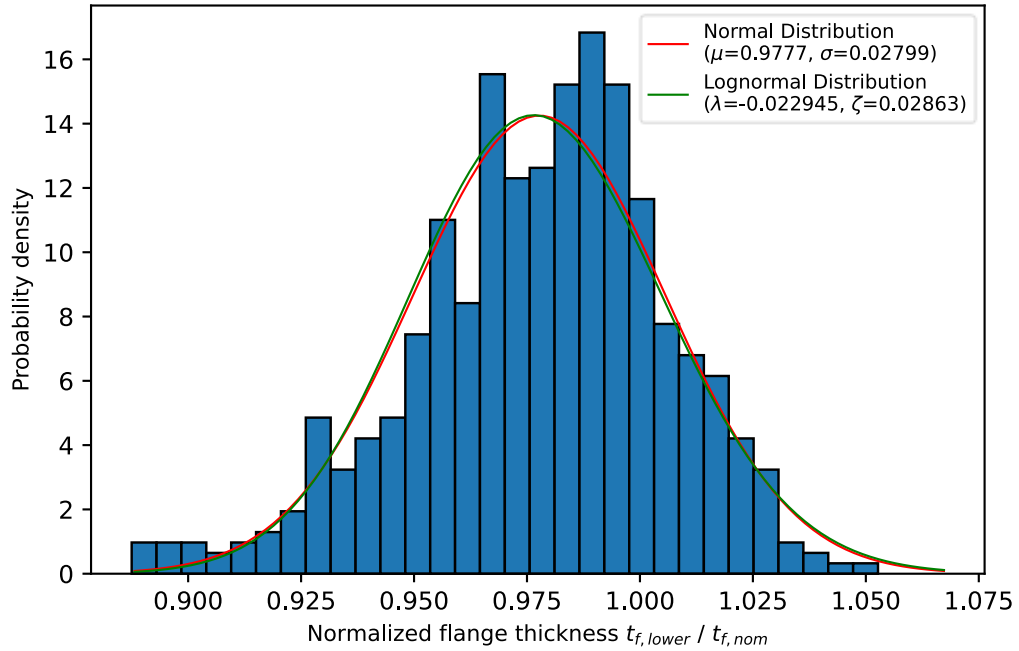


Figure 22: Histogram and probability density functions (normal and lognormal) for lower flange thickness

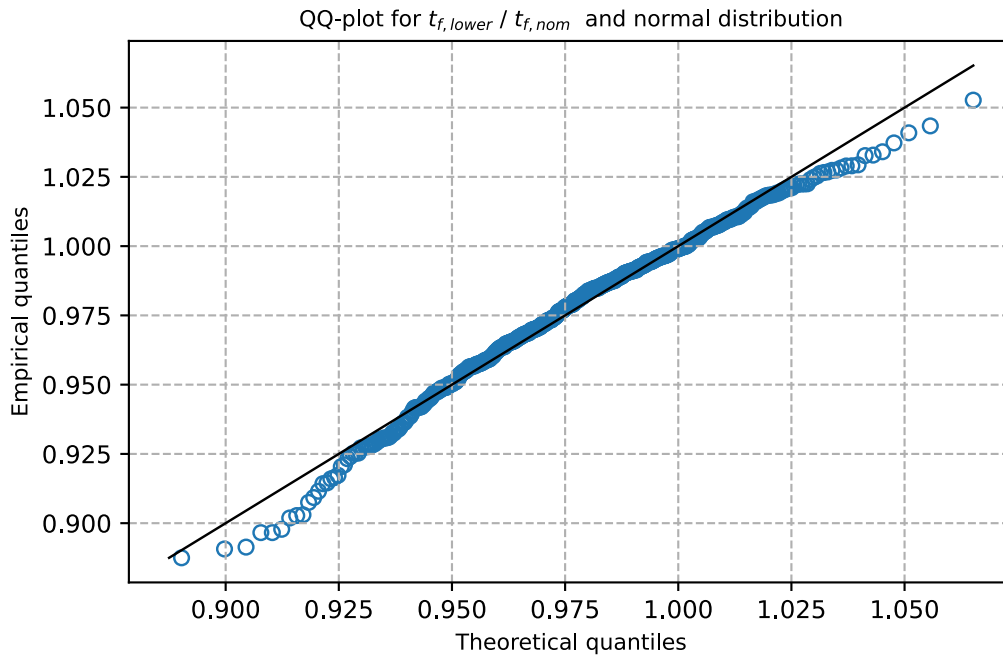


Figure 23: QQ-plot for lower flange thickness and normal distribution function

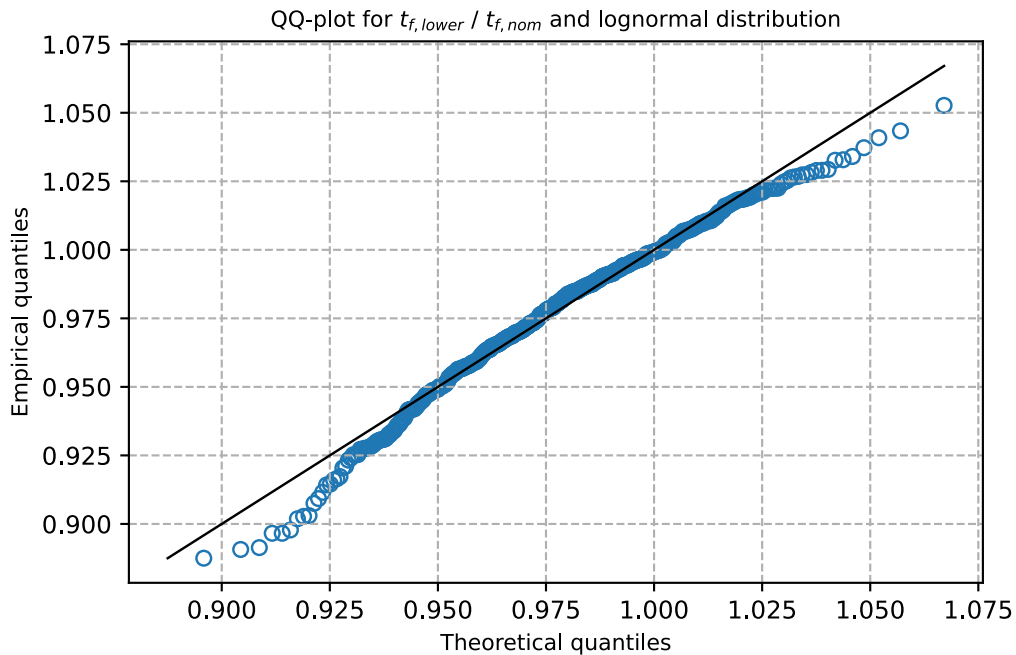


Figure 24: QQ-plot for lower flange thickness and lognormal distribution function

For the other dimensions, these figures can be found in Appendix A.4.5.

It is immediately seen that there are no large differences between the two PDFs. This comes simply from the fact that the obtained data are clearly in the range of positive numbers and far away from zero. Furthermore, the relative variation of the results is too small to induce major differences between the two distributions. In the case of the lower flange thickness, both PDFs reproduce the data quite well with slight discrepancies in the region of the very lower and the very upper quantiles.

For the upper flange thickness, a similar pattern is observed. An even better fit of the data to the theoretical probability distribution functions is derived for the web thickness and the profile height, as can be seen in Appendix A.4.5. The data points lie almost perfectly on the 45-degree line in the QQ-plots. For the measured profile widths and the root fillet radii, however, there are significant discrepancies observed mainly in the region of the very upper quantiles. It seems that the empirical quantiles are much larger than the theoretical ones in this region for both dimensions. This means that there are some measured profile widths and root fillet radii which would not be predicted by the two theoretical PDFs.

3.5.4. Comparison with literature

As mentioned in section 1.5, there are some investigations which have already been carried out about similar topics as the one of the present thesis. In this chapter, the results of these investigations will be compared with the ones obtained within the scope of this thesis.

SAFEBRICKTILE:

The recommended distributions of the geometrical dimensions according to the SAFEBRICKTILE project [3] are summarized in Table 1. The corresponding quantities obtained within this thesis are summarized in Table 15 and Table 16. It is seen that the derived mean values are quite well in agreement with the suggested values of the SAFEBRICKTILE project. For the web, the observed mean values are a little bit higher than the ones recommended in Table 1 (approximately 0.5-2 % larger depending on the category). For the profile height, the obtained mean values are around 0.5 % larger. The derived mean values of the remaining parameters are close to the ones recommended by the SAFEBRICKTILE project.

For the coefficients of variation, there are larger discrepancies between the recommended values and the ones obtained during this thesis. For the profile width and height, the derived coefficients of variation are clearly smaller than the recommended ones. The coefficients of variation of the flange and web thicknesses of the category "Large" are well in agreement

with the suggested values. However, larger coefficients of variations were observed for the smaller profiles compared to the ones suggested by the SAFEBRICTILE project.

Annex E in prEN 1993-1-1:

As mentioned in section 1.4, the Annex E of the new draft standard prEN 1993-1-1 [9] gives some information about the assumed statistical distribution of the geometrical properties underlying the usage of the partial safety factors recommended by the Eurocode 3. The relevant excerpt is repeated here:

Parameter	Mean value X_m	Coefficient of variation	Upper reference value $X_{5\%}$	Lower reference value $X_{0,12\%}$
Depth h	1,0 h_{nom}^a	0,9 %	0,98 h_{nom}^a	0,97 h_{nom}^a
Width b	1,0 b_{nom}^a	0,9 %	0,98 b_{nom}^a	0,97 b_{nom}^a
Rolled and welded I- and H-sections: flange thickness t_f	0,98 $t_{f,nom}^a$	2,5 %	0,95 $t_{f,nom}^a$	0,91 $t_{f,nom}^a$
Rolled and welded I- and H-sections: web thickness t_w	1,0 $t_{w,nom}^a$	2,5 %	0,96 $t_{w,nom}^a$	0,93 $t_{w,nom}^a$

Figure 25: Excerpt of Annex E of prEN 1993-1-1 [9]

As these values are obtained primarily based on the SAFEBRICTILE project, the stated values are almost the same as recommended by the mentioned project. The only difference is concerning the normalized mean value of the flange thickness, being 0.98 in the Annex E of prEN 1993-1-1, while being recommended as 0.975 by the SAFEBRICTILE project. The derived mean values of the present thesis lie somewhere between these two values.

As all other mean values and coefficients of variation stated in Annex E of prEN 1993-1-1 are the same as suggested by the SAFEBRICTILE project, the same statements hold as already made for the comparison between the SAFEBRICTILE project and the data of this thesis. Therefore, it is recommended to think about adjusting the structure of the values given in Annex E of prEN 1993-1-1. Based on the observations of this thesis, it might be reasonable to subdivide the coefficients of variation further into different categories based on the profile size at least for the flange and web thicknesses. A common value for all profile sizes is a severe simplification. Larger profiles almost always have smaller coefficients of variation compared to smaller profiles, simply due to the accuracy of the production equipment which induces a larger percentage variation for smaller dimensions, as already indicated further above. The current values stated in Annex E of prEN 1993-1-1 for the coefficients of variation of the flange and the web thicknesses fit well for the investigated large profiles. However, for the small profiles, the observed coefficients of variation are clearly larger than recommended by the draft code.

Furthermore, it is emphasized once again that it was observed that there is a significant variability of the flange thickness within the cross-sectional plane. The measured outer flange thicknesses are considerably thinner than the inner flange thicknesses, as seen in section 3.4. In Figure 25, however, there is a constant mean value given for the flange thickness. This should be kept in mind as well.

As an additional check, the upper and lower reference fractile values according to Figure 25 ($X_{5\%}$ and $X_{0,12\%}$) can be compared to the ones of the measured profiles. The following table displays the corresponding values:

Table 23: Upper and lower reference values of the investigated profiles

	$\frac{t_{f,low}}{t_{f,nom}}$	$\frac{t_{f,up}}{t_{f,nom}}$	$\frac{t_w}{t_{w,nom}}$	$\frac{h}{h_{nom}}$	$\frac{b_1}{b_{nom}}$	$\frac{b_2}{b_{nom}}$
$X_{5\%}$	0.9278	0.9294	0.9610	0.9970	0.9929	0.9926
$X_{0,12\%}$	0.8875	0.8814	0.8920	0.9877	0.9838	0.9874

It is identified that the reference values of the flange thicknesses are significantly smaller than the ones recommended in Annex E of the standard prEN 1993-1-1. For the web thickness, the upper reference value is quite in agreement with the standard, while the lower reference value is clearly below the value stated in the standard. For the profile height and the profile width, the upper as well as the lower reference values are larger than recommended in the standard. However, it must be emphasized that the reference values of the investigated profiles should be treated with caution. One would need to investigate a lot more profiles than the 561 sections measured during this thesis to get meaningful conclusions regarding these reference values. For a number of 561 profiles, the lower reference value $X_{0.12\%}$ corresponds to the smallest measurement for each dimension. Therefore, it's clear that one single measurement can have a pronounced impact on this reference value.

Melcher et al. (2004):

Neither in the SAFEBRICTILE project, nor in the new Annex E of prEN 1993-1-1, there is an investigation about the correlation between the individual geometrical parameters. However, there was the experimental research project by Melcher et al. [4] investigating the correlation among other things, as mentioned in section 1.5.

As Melcher et al. investigated IPE profiles in the size range 160-240, the calculations made in section 3.5.1 and 3.5.2 are repeated here by only considering the same profile range as Melcher et al. in order to allow for a consistent comparability. There are 45 investigated profiles which fall into this category. The following correlation matrix is derived:

Table 24: Correlation matrix for the measured IPE profiles in the size range 160-240

	$t_{f,lower}$	$t_{f,upper}$	t_w	h	b_1	b_2
$t_{f,lower}$	1					
$t_{f,upper}$	0.844	1				
t_w	-0.494	-0.429	1			
h	-0.157	-0.180	-0.035	1		
b_1	-0.253	-0.287	0.305	0.066	1	
b_2	-0.388	-0.473	0.399	0.016	0.773	1

It should be kept in mind that 45 profiles are only a limited number compared to the 371 profiles which were investigated by Melcher et al. Furthermore, it is pointed out that Melcher et al. didn't investigate the a-values and the root fillet radii of the steel profiles, therefore being omitted in Table 24.

Comparing the correlation matrix obtained by Melcher et al. (see Figure 6) with the derived correlation matrix above, it can be identified that the correlation between the two flange thicknesses is quite similar, being even more remarkable using the data of this thesis (0.844 vs. 0.763). The same holds true for the correlation between the two measured profile widths, also being more pronounced using the data of this thesis (0.773 vs. 0.623). However, not all observed particularities derived above can also be seen in the data of Melcher et al. For example, there is quite a moderate negative correlation observed between the flange thicknesses and the web thickness using the data of this thesis, while Melcher et al. derived a weak positive correlation between these parameters. Another characteristic is the observation that there is quite a moderate positive correlation between the web thickness and the profile widths using the data of this thesis while Melcher et al. obtained a weak negative correlation. However, it should be kept in mind that the correlation matrix in Table 24 is based on only 45 profiles. Therefore, one single measurement can have a large influence on the correlation coefficients.

Overall, the remarkable pattern of strongly correlating flange thicknesses and profile widths observed during this thesis can be confirmed using the data of Melcher et al.

As Melcher et al. didn't only investigate the correlation behaviour, but also the mean values and the standard deviations of the parameters, some further comparisons can be made. The following table summarizes the normalized mean values and the coefficients of variation for the 45 IPE profiles in the size range 160-240 investigated during this thesis:

Table 25: Normalized mean values and coefficients of variation for the measured IPE profiles in the size range 160-240

	$\frac{t_{f,low}}{t_{f,nom}}$	$\frac{t_{f,up}}{t_{f,nom}}$	$\frac{t_w}{t_{w,nom}}$	$\frac{h}{h_{nom}}$	$\frac{b_1}{b_{nom}}$	$\frac{b_2}{b_{nom}}$
mean [-]	0.9811	0.9815	1.0199	1.0047	1.0120	1.0121
c.o.v. [%]	3.309	3.081	4.406	0.666	0.813	0.814

Comparing these values with the ones stated by Melcher et al. (see section 1.5), it is noticed that the derived mean value for the web thickness is approximately 3 % smaller (1.020 vs. 1.055). For the remaining parameters, the observed mean values coincide quite well with the ones specified by Melcher et al. For one flange thickness, Melcher et al. obtained a mean value which is 1-2 % larger (0.981 vs. 0.998).

Finally, the coefficients of variations are compared. There are quite some differences for each parameter. For the profile height and the web thickness, Melcher et al. obtained smaller coefficients of variation, while for the flange thicknesses and the profile widths larger coefficients of variation were noticed. However, once again it is noted that only 45 profiles are investigated here while Melcher et al. studied 371 profiles. A possible measurement error has a stronger impact on the result when measuring less profiles. Furthermore, it is not exactly documented how accurate and with which instruments Melcher et al. carried out their investigations. Therefore, it is difficult to draw some final conclusions.

Timothy Kyle Jaquess (1998):

Additionally, the obtained results can be compared to the thesis of Jaquess [14], as introduced in section 1.5. The mean values and coefficients of variation according to Jaquess are summarized in Table 3. It is identified that the mean values obtained during this thesis coincide quite well with the values of Jaquess. The biggest deviation can be observed for the web thickness where he got a mean value which is approximately 1 % lower than the value derived during this thesis. The obtained coefficients of variation are in accordance with the values of Jaquess as well. No large discrepancies are observed. This holds true even though Jaquess investigated only 17 profiles.

G. A. Alpsten (1972):

As there are no specific numbers given by G. A. Alpsten (1972) [15] for the mean values or coefficients of variations, the results can only be compared qualitatively. In Figure 8, it is seen that G. A. Alpsten obtained a much smaller variation for the profile height and profile width compared to the web and flange thicknesses. The same is observed when looking at the data of this thesis (see Table 13 and Table 16). Moreover, G. A. Alpsten derived mean values for the measured profile widths and profile heights somewhere close around the nominal value. For the web thicknesses, the mean value is larger than the nominal value and for the flange thicknesses it is vice-versa. The same pattern for the mean values is seen in the evaluation of this thesis (see Table 12 and Table 15).

In conclusion, it can be stated that although the report of G. A. Alpsten is from the year 1972, the general pattern of the measured dimensions of rolled steel sections does not seem to have changed considerably. The same patterns are still observed more than 50 years later.

3.5.5. Exceedance of tolerances

As an additional investigation, it is studied how many times the geometrical tolerances introduced in section 1.3 were exceeded by the measurement results. The investigated dimensions are the profile height, the profile width, the web thickness and the flange thickness. For the profile width, the arithmetic mean of b_1 and b_2 is used. For the profile height, only the height measured at the level of the web, h_{mid} , is considered. For the web thickness, the arithmetic mean of the three measured web thicknesses t_{w1} , t_{w2} and t_{w3} is used according to equation (16). Finally, for the flange, it is distinguished between the upper and the lower flange, using the arithmetic mean in each case, see equations (13) and (14). According to the standard EN 10034 [2], it must be differentiated between positive and negative exceedances of the tolerances. The positive exceedances indicate that the measured dimensions are larger than the largest allowed ones while the negative exceedances correspond to measured dimensions which are smaller than the lowest allowed ones. The following table summarizes the results of this investigation, stating the number of positive (+) and negative (-) tolerance exceedances for each dimension:

Table 26: Number of positive (+) and negative (-) tolerance exceedances

	IPE		HEA		HEB		Total	
	+	-	+	-	+	-	+	-
h	3	0	11	2	16	1	30	3
b	0	0	0	1	0	0	0	0
t_w	0	0	0	0	1	0	1	0
t_f	0	0	0	0	0	0	0	0

It is observed that apart from one measured web thickness, only the profile height shows some exceedances of the standardized tolerances. Furthermore, it's conspicuous that these exceedances are almost exclusively positive ones, meaning that the measured dimensions are larger than the standardized one.

4. Investigation of the sectional properties

It was already mentioned in section 1 that the deviation of the geometrical dimensions of steel I-sections to the standardized dimensions will induce some effects on the structural behaviour in terms of cross-sectional resistance. To investigate these effects in a simplified way, the goal of this chapter is to calculate some sectional properties of the real measured cross-sections. Additionally, these sectional properties are calculated for the nominal and for the idealized cross-sections. The latter ones have some idealizations, as will be explained in the following. The primary goal of introducing an idealized cross-section is to create a cross-section which is quite near to the real measured cross-section, while only considering as little different dimensions as possible. Furthermore, the idealized cross-section will allow to draw some additional conclusions about the structural behaviour when comparing it with the real one.

The sectional properties refer to the geometric characteristics of a cross-section. However, the calculated sectional properties provide some useful information about the structural behaviour of the cross-sections as well. For example, the area directly influences the resistance to axial loads while the section moduli indicate the bending resistance. The sectional properties could be used in a further step to calculate some simplified cross-sectional resistances when multiplying the corresponding quantities by the steel yield strength. However, the cross-sectional resistance and the comparison between the idealized and the real cross-section will be investigated in more detail in section 5 by considering some further phenomena such as the local buckling phenomenon for example. The sectional properties determined in the current chapter will be used for some plausibility checks there.

4.1. Nominal cross-section

The nominal cross-section is defined by the standardized nominal dimensions stated in the SZS C5/18 tables [7], as introduced in chapter 1.2. In the current subchapter, it will be explained how the sectional properties of the nominal cross-sections (presented in Appendix A.1) are calculated. A sketch of a cross-section with all the variables used in this section can be found in Appendix A.1. The derived sectional properties of the nominal cross-section serve as reference values for the other types of cross-sections.

4.1.1. Cross-sectional area

The area of the cross-section is calculated by adding up the individual subareas of the I-section:

$$A = 2 \cdot b \cdot t_f + h_2 \cdot t_w + (4 - \pi) \cdot r^2 \quad (26)$$

It is noted that the height h_2 is a helping variable which allows to write the equation in a compact and convenient way. It is the height of the profile subtracting the flange thicknesses and can be calculated as follows:

$$h_2 = h - 2 \cdot t_f \quad (27)$$

This helping variable will be used in the following chapters as well.

4.1.2. Moment of inertia

The moment of inertia of the rolled profiles is obtained by applying the Steiner’s theorem to the individual parts of the cross-section, as can be seen in the subsequent equations. The following tabulated values of the moments of inertia are used [10]:

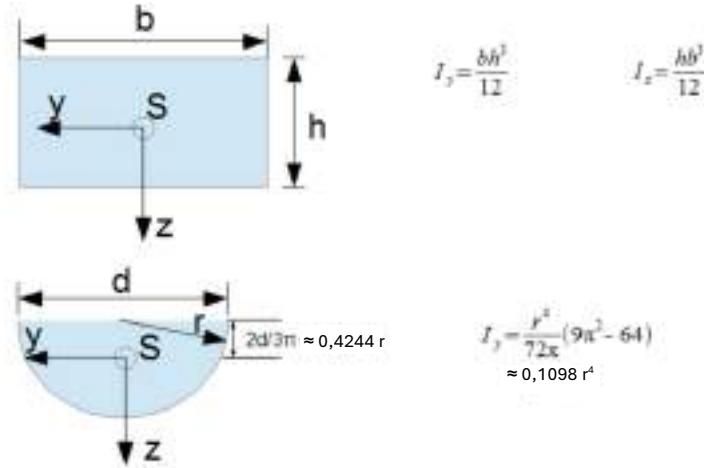


Figure 26: Tabulated moments of inertia [10]

$$I_y = 2 \cdot \frac{b \cdot t_f^3}{12} + 2 \cdot \left(\frac{t_f + h_2}{2}\right)^2 \cdot t_f \cdot b + \frac{t_w \cdot h_2^3}{12} + 2 \cdot \left[\frac{2 \cdot r^4}{12} + \left(\frac{h_2 - r}{2}\right)^2 \cdot 2 \cdot r^2 - 0.1098 \cdot r^4 - \left[\frac{h_2}{2} - (1 - 0.4244) \cdot r\right]^2 \cdot \frac{\pi \cdot r^2}{2}\right] \tag{28}$$

$$I_z = 2 \cdot \frac{b^3 \cdot t_f}{12} + \frac{t_w^3 \cdot h_2}{12} + 2 \cdot \left[\frac{2 \cdot r^4}{12} + \left(\frac{t_w + r}{2}\right)^2 \cdot 2 \cdot r^2 - 0.1098 \cdot r^4 - \left[\frac{t_w}{2} + (1 - 0.4244) \cdot r\right]^2 \cdot \frac{\pi \cdot r^2}{2}\right] \tag{29}$$

Thereby, the y-axis represents the strong axis of the rolled profiles while the z-axis represents the weak axis. This definition will also be used in the following.

4.1.3. Section modulus

The section modulus is an important indicator of the theoretical cross-sectional bending resistance.

The elastic section modulus can be calculated based on the obtained moments of inertia:

$$W_{el,y} = \frac{I_y}{h/2} \tag{30}$$

$$W_{el,z} = \frac{I_z}{b/2} \tag{31}$$

The plastic section modulus is derived as follows:

$$W_{pl,y} = \sum_i A_i \cdot z_i = 2 \cdot t_f \cdot b \cdot \left(\frac{h_2 + t_f}{2}\right) + t_w \cdot \frac{h_2^2}{4} + 2 \cdot r^2 \cdot (h_2 - r) - \pi \cdot r^2 \cdot \left[\frac{h_2}{2} - (1 - 0.4244) \cdot r\right] \tag{32}$$

$$W_{pl,z} = \sum_i A_i \cdot y_i = 2 \cdot \frac{b^2}{4} \cdot t_f + \frac{t_w^2}{4} \cdot h_2 + 2 \cdot r^2 \cdot (t_w + r) - \pi \cdot r^2 \cdot \left[\frac{t_w}{2} + (1 - 0.4244) \cdot r\right] \tag{33}$$

4.2. Real cross-section

For the real cross-section, all the measured dimensions of chapter 2.1 are considered. For the height, however, only the height h_{mid} is taken into account based on the conclusions of section 3.2.

4.2.1. Web eccentricity

It is noted that for the calculation with the real measured cross-sectional dimensions, a web eccentricity based on the measurements of a_1 and a_2 is considered:

$$e_{web} = \frac{a_1 - a_2}{2} \tag{34}$$

In chapter 2.1.4, it was explained how the a-values were measured. The web eccentricity is visualized in Figure 27.

4.2.2. Definition of the coordinates

The following sketch shows the definition of the coordinates of the cross-section. The coordinates of the points 1-22 are calculated automatically with the help of a written Python code when inserting all the dimensions of the cross-section.

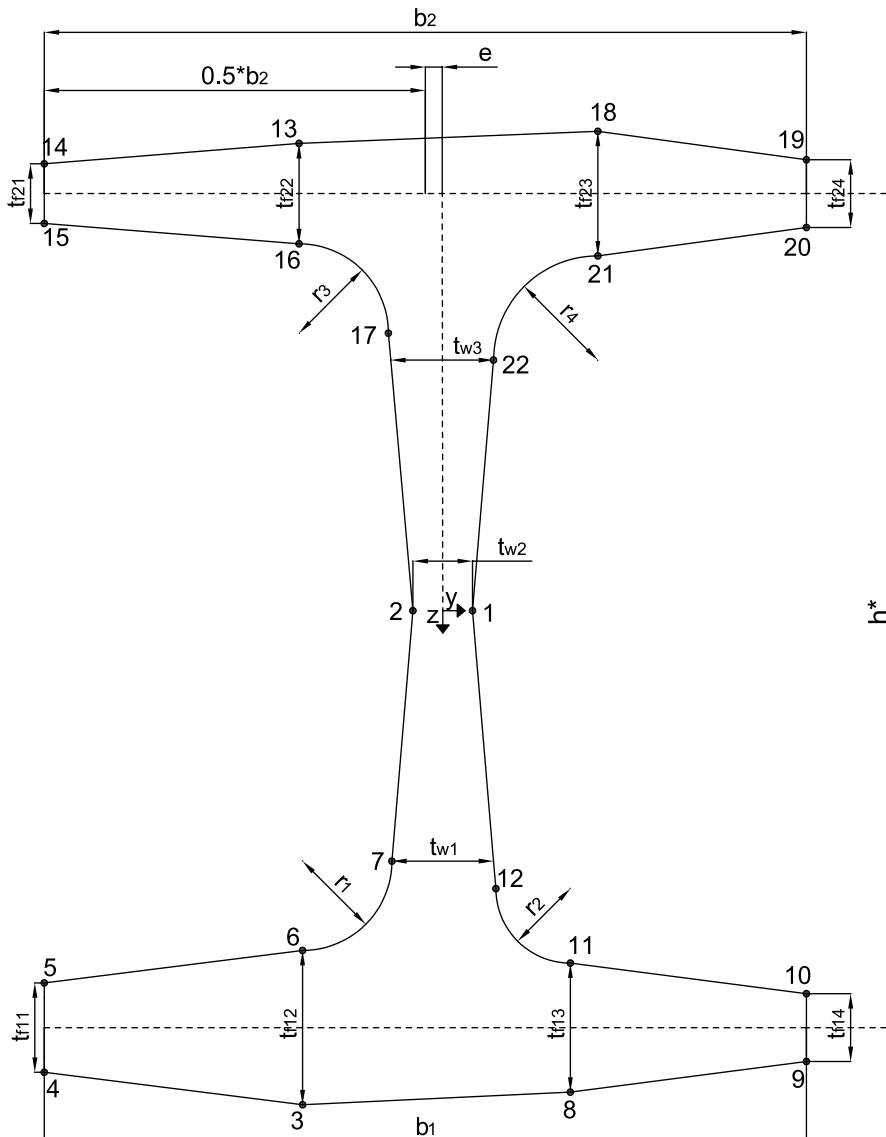


Figure 27: Sketch of the modelled cross-section

It is emphasized that it is assumed that the dimensions $t_{f1,2}$, $t_{f1,3}$, $t_{f2,2}$, $t_{f2,3}$, t_{w1} and t_{w3} are located directly at the respective boundary to the roundings. In Figure 27, the web thicknesses t_{w1} and t_{w3} are assumed to be at the points 7 and 22 respectively. However, this is just an illustrative example. The written Python code will automatically check whether point 7 or 12 and whether point 17 or 22 are lying closer towards the middle of the web (meaning towards points 1 and 2). The web thicknesses t_{w1} and t_{w3} are then automatically defined at the points that are lying closer towards the middle of the web. For the other points, an extrapolation of the inclination of the web is assumed, as exemplary illustrated in Figure 27 for the points 12 and 17.

The dimensions $t_{f1,1}$, $t_{f1,4}$, $t_{f2,1}$ and $t_{f2,4}$ are located at the outer boundaries of the flanges, while the thickness t_{w2} is assumed to be in the middle of the height.

A further significant assumption is that the thicknesses of the flanges are always referred to the middle lines of the flanges which are assumed to be horizontal, see Figure 27. In a simplified way, the height between the two middle lines of the flanges is calculated with the following equation:

$$h^* = h - 0.25 \cdot ((t_{f1,2} + t_{f1,3}) + (t_{f2,2} + t_{f2,3})) \quad (35)$$

Except for the roundings, always a linear transition from one defined coordinate point to the other is assumed, as illustrated in Figure 27.

4.2.3. Shift of the centroid

Due to the varying dimensions of the profile width, the flanges, the web and the root fillet radii and due to the introduction of a web eccentricity, the centroid of the real cross-section will not lie in the middle between the points 1 and 2 (see Figure 27) anymore as it would be the case for a nominal cross-section. This has to be considered when calculating the sectional properties in the following chapter.

The coordinates of the cross-sectional centroid, C_y and C_z , are calculated by approximating the cross-section with a closed polygon and applying the following equations according to Paul Bourke [27]:

$$C_y = \frac{1}{6 \cdot A} \cdot \sum_{i=0}^{n-1} (y_i + y_{i+1}) \cdot (y_i \cdot z_{i+1} - y_{i+1} \cdot z_i) \quad (36)$$

$$C_z = \frac{1}{6 \cdot A} \cdot \sum_{i=0}^{n-1} (z_i + z_{i+1}) \cdot (y_i \cdot z_{i+1} - y_{i+1} \cdot z_i) \quad (37)$$

where A is the polygon's area:

$$A = \frac{1}{2} \cdot \sum_{i=0}^{n-1} (y_i \cdot z_{i+1} - y_{i+1} \cdot z_i) \quad (38)$$

It is pointed out that for the roundings of the profiles, five intermediate points are defined respectively in order to get a polygon close to the real geometry. However, it must be kept in mind that the used geometry remains an approximation of the real geometry.

The coordinate system introduced in Figure 27 is used. The resulting centroidal coordinates for all 561 cross-sections can be found in Appendix B.1.1.

4.2.4. Sectional properties

As there is no double symmetry given, the sectional properties of the real cross-sections are not calculated by hand anymore. Instead, it is made use of the structural engineering plug-in Karamba3D [28] for Grasshopper which itself is a plug-in for the modelling tool Rhinoceros [29]. The same polygonal approximation introduced in section 4.2.3 (five intermediate points for the roundings) is used. Therefore, it must be emphasized that the calculated sectional properties are only approximations of the real sectional properties.

When inserting the corresponding coordinates of the polygon, Karamba3D automatically calculates the cross-sectional properties, such as the area, the moments of inertia or the elastic and plastic section moduli. The moments of inertia and the section moduli are computed at the cross-sectional centroids and without rotating the coordinate system introduced in Figure 27. Since there is no double symmetry given, the elastic section moduli have different values in the positive direction compared to the negative one, which has to be taken into account. Furthermore, the y - and z -axis introduced in Figure 27 are not the principal axes which leads to the occurrence of a deviation moment I_{yz} . Strictly speaking, a small rotation of the coordinate system would be necessary in order to get the principal axes. However, the values of I_{yz} are negligibly small compared to I_y and I_z , leading to the conclusion that the principal moments of inertia will not deviate much from I_y and I_z . Furthermore, a direct comparability to the nominal and idealized cross-sections is ensured when neglecting the rotation of the coordinate system.

The plausibility of the sectional properties calculated by Karamba3D was checked by comparing the values with the values of the idealized (section 4.3) and the nominal cross-sections (section 4.1).

4.3. Idealized cross-section

In this section, an idealized cross-section will be introduced. The goal is to depict the real cross-section as accurate as possible while considering as little dimensions as possible. However, there will be some severe simplifications compared to the real cross-section which will allow to calculate the sectional properties still by hand.

As a reminder, the following figure summarizes the measured dimensions of the real cross-sections:

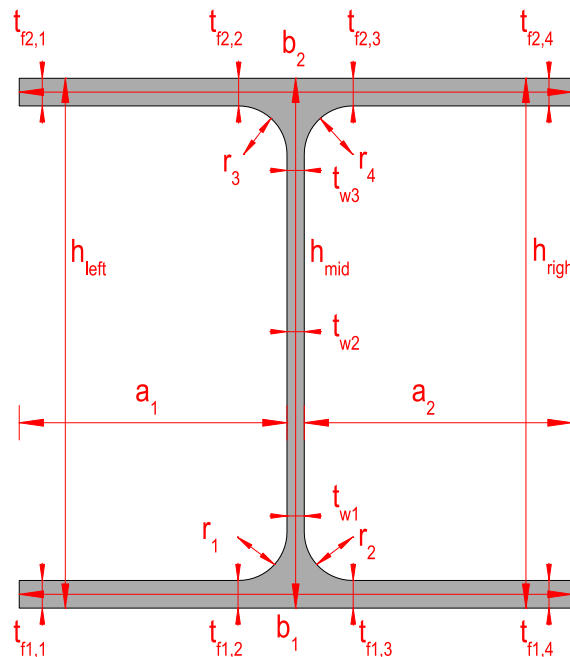


Figure 28: Measured dimensions of the cross-section

In the following subsections, it is explained how these measurements are used in order to define an idealized cross-section. The idealized dimensions introduced in the following sections (h , b , r , t_w and t_f) can then be inserted in the equations of section 4.1 to obtain the sectional properties of the idealized cross-section.

4.3.1. Height and width

Both the height and the width of the profiles are assumed to be constant for the idealized cross-section. In a simplified way, only the height measured at the level of the web is considered based on the conclusions of section 3.2:

$$h = h_{mid} \quad (39)$$

For the profile width, the arithmetic mean of the two measured quantities, b_1 and b_2 is considered:

$$b = \frac{b_1 + b_2}{2} \quad (40)$$

4.3.2. Root fillet radius

For the root fillet radius, the same value is considered for all four radii of a cross-section. This value is approximated as the arithmetic mean of the four measurements r_1 , r_2 , r_3 and r_4 (see Figure 28):

$$r = \frac{r_1 + r_2 + r_3 + r_4}{4} \quad (41)$$

4.3.3. Flange and web thickness

The goal of defining an idealized cross-section is to use as little different dimensions as possible. Therefore, the flange and web thicknesses are assumed to be constant as well. However, these parameters should somehow depict the real measurements. Both thicknesses are defined based on the regulations in the tolerance standard EN 10034:1993 [2] where it is specified that the flange thickness should be measured at the quarter points of the flanges and the web thickness should be measured at the middle of the profile height, as also depicted in Figure 2. These values can be estimated based on the measured dimensions illustrated in Figure 28 and the variables introduced in the previous subchapters:

$$t_w = t_{w2} \quad (42)$$

$$t_{f,upper,left} = t_{f2,1} + (t_{f2,2} - t_{f2,1}) \cdot \left(\frac{b_2/4}{b_2/2 - t_w/2 - r} \right) \quad (43)$$

$$t_{f,upper,right} = t_{f2,4} + (t_{f2,3} - t_{f2,4}) \cdot \left(\frac{b_2/4}{b_2/2 - t_w/2 - r} \right) \quad (44)$$

$$t_{f,lower,left} = t_{f1,1} + (t_{f1,2} - t_{f1,1}) \cdot \left(\frac{b_1/4}{b_1/2 - t_w/2 - r} \right) \quad (45)$$

$$t_{f,lower,right} = t_{f1,4} + (t_{f1,3} - t_{f1,4}) \cdot \left(\frac{b_1/4}{b_1/2 - t_w/2 - r} \right) \quad (46)$$

It should be noted that the resulting values of the flanges are just estimations of the real flange thicknesses at the quarter points. The equations are only strictly valid if there is a linear transition between the inner and the outer measured flange thickness, as assumed in Figure 27. In reality, there may be a non-linearity for these transitions.

It is pointed out that for both flanges, the same constant thickness t_f is used in the following for calculating the idealized sectional properties. This thickness is calculated as the arithmetic mean of the quantities obtained in the equations (43)-(46):

$$t_f = \frac{t_{f,upper,left} + t_{f,upper,right} + t_{f,lower,left} + t_{f,lower,right}}{4} \quad (47)$$

Among other things, the goal of introducing an idealized cross-section is to determine how the sectional properties and the cross-sectional resistances are influenced when one neglects the variability of the flange thicknesses in the cross-sectional plane.

4.3.4. Sectional properties

The idealized dimensions introduced in the preceding sections (h , b , r , t_w and t_f) can be inserted in the equations of section 4.1 in order to obtain the sectional properties of the idealized cross-section. It is emphasized that some possible web eccentricity is not considered for the idealized cross-section, therefore still assuming double symmetry. Furthermore, it should be noted that the assumption of a constant flange thickness is a severe simplification, mainly for the behaviour around the weak axis. In section 3.4, it was observed that for the real measured cross-sections the outer parts of the flanges are much smaller than the inner parts, which has a non-negligible impact on the structural behaviour around the weak axis. This will be observed in the following section when comparing the sectional properties of the real cross-sections with the ones of the idealized cross-sections.

4.4. Evaluation of the sectional properties

In this chapter, the sectional properties explained above are calculated inserting the dimensions of the 561 measured profiles and subsequently evaluated for both the real and the idealized measured cross-sections. It is emphasized that the normalized quantities according to equation (6) are used. Thereby, the nominal sectional properties are calculated according to section 4.1 (see Appendix A.1).

A full table with all the calculated quantities for each profile is displayed in Appendix B.1 (real cross-sections) and Appendix B.2 (idealized cross-sections). A visualization of the results (histograms and scatter plots) can also be found in the respective Appendix. Additionally, some QQ-plots for the theoretical normal and lognormal probability distributions are shown for the sectional properties of the real cross-sections, using the same procedure introduced in section 3.5.3.

4.4.1. Real vs. nominal cross-sections

The mean values and the coefficients of variation of the normalized sectional properties are presented in the following tables for the real cross-sections:

Table 27: Mean values of the sectional properties for the different categories (real vs. nominal cross-sections)

cat.	$\frac{A_{real}}{A_{nom}}$	$\frac{I_{y,real}}{I_{y,nom}}$	$\frac{I_{z,real}}{I_{z,nom}}$	$\frac{W_{el,y,real,pos}}{W_{el,y,nom}}$	$\frac{W_{el,y,real,neg}}{W_{el,y,nom}}$	$\frac{W_{el,z,real,pos}}{W_{el,z,nom}}$	$\frac{W_{el,z,real,neg}}{W_{el,z,nom}}$	$\frac{W_{pl,y,real}}{W_{pl,y,nom}}$	$\frac{W_{pl,z,real}}{W_{pl,z,nom}}$
Total	0.9957	1.0012	0.9779	0.9939	0.9948	0.9744	0.9714	0.9975	0.9813
Small	0.9972	1.0029	0.9796	0.9943	0.9954	0.9751	0.9715	0.9990	0.9827
Large	0.9933	0.9986	0.9753	0.9933	0.9939	0.9734	0.9713	0.9952	0.9793
HEA	0.9950	0.9991	0.9730	0.9909	0.9929	0.9716	0.9687	0.9960	0.9782
HEB	0.9919	1.0000	0.9733	0.9927	0.9926	0.9727	0.9688	0.9952	0.9782
IPE	1.0015	1.0056	0.9907	0.9996	1.0001	0.9805	0.9784	1.0024	0.9895

Table 28: Coefficients of variation (in %) of the sectional properties for the different categories (real vs. nominal cross-sections)

cat.	$\frac{A_{real}}{A_{nom}}$	$\frac{I_{y,real}}{I_{y,nom}}$	$\frac{I_{z,real}}{I_{z,nom}}$	$\frac{W_{el,y,real,pos}}{W_{el,y,nom}}$	$\frac{W_{el,y,real,neg}}{W_{el,y,nom}}$	$\frac{W_{el,z,real,pos}}{W_{el,z,nom}}$	$\frac{W_{el,z,real,neg}}{W_{el,z,nom}}$	$\frac{W_{pl,y,real}}{W_{pl,y,nom}}$	$\frac{W_{pl,z,real}}{W_{pl,z,nom}}$
Total	1.665	1.997	3.101	1.914	1.945	2.872	2.943	1.812	2.720
Small	1.780	2.165	3.384	2.097	2.114	3.163	3.243	1.938	2.971
Large	1.441	1.677	2.587	1.593	1.650	2.357	2.418	1.574	2.268
HEA	1.687	2.043	3.126	2.004	2.022	3.091	3.012	1.857	2.842
HEB	1.401	1.811	2.200	1.567	1.573	2.176	2.116	1.543	1.972
IPE	1.777	2.094	3.596	2.053	2.145	3.207	3.546	1.963	3.136

The mean of the calculated cross-sectional areas is little below 1.00 for each category except the IPE profiles, mainly due to the fact that the flanges are produced thinner than the nominal values, as seen in section 3.4. The negative impact of the reduced flange thicknesses seems to be bigger than the positive influence of the larger web thicknesses. For the IPE profiles the flanges make a smaller portion of the whole cross section area compared to the other profile types and therefore it's reasonable that the undersized flanges don't have the same impact onto the area, leading to a higher normalized mean value for the area for the IPE profiles.

The observation that the mean values of the normalized areas do not deviate much from 1.00 may explain why the web thicknesses are produced thicker than the nominal values, as observed in section 3.5. It seems that the web thicknesses are produced thicker in order to compensate for the lost area due to the thinner flanges. When compensating for this part of the area, the producer can avoid that the mass of the sold girders is noticeably smaller than the mass of the nominal girders. Even though the tolerance standard EN 10034 [2] permits a mass tolerance of $\pm 4\%$, it seems that the producers do not want to sell girders with a distinctive small mass. It's likely that the customer will check the mass of the bought steel girders. When there is no large discrepancy to the mass of the nominal girders, the producer can avoid unpleasant questions and claims.

For the calculated moments of inertia and section moduli around the weak axis, the mean values are significantly below 1.00 for all categories, yielding a similar pattern as was observed for the flange thicknesses in section 3.4. Conversely, the moments of inertia and section moduli around the strong axis exhibit mean values quite close around 1.00. Moreover, it can be observed that the mean values for the moments of inertia and the section moduli around both axes are higher for IPE profiles than for HEA and HEB profiles. This again relates to the fact that the flanges are produced thinner than the nominal value on average, but make a smaller portion of the cross-section of IPE profiles compared to the other profile types. The reduced values of the moments of inertia and section moduli around the weak axis compared to the strong axis comes from the fact that the flanges have a larger percentage contribution to these quantities around the weak axis than around the strong axis. For the strong axis, the internal lever arm of the flanges is more important, more specifically the profile height plays the predominant role there.

Studying the coefficients of variation, the typical pattern is again seen that the smaller cross sections have a larger percentage variation due to the limited production equipment accuracy which induces a larger percentage deviation for smaller sections, as already stated several times. Furthermore, the HEB sections show significantly smaller variations than the other profile types. As the HEB sections have thicker flanges, the limited production accuracy will induce a smaller percentage deviation there compared to the other profile types.

The moments of inertia and the section moduli around the weak axis have a larger variation compared to the strong axis because these quantities are highly impacted by the flange thicknesses which themselves have considerable variations, as observed in section 3.4. In contrast, the coefficients of variation are smaller for these quantities around the strong axis as a consequence of the larger influence of the profile height for these quantities. The profile height itself shows a severely reduced variation compared to the flange thicknesses, as seen in section 3.5. The cross-sectional area also shows quite low variations as this quantity is highly influenced by the profile height and profile width which themselves have small variations, as has been observed.

4.4.2. Real vs. ideal cross-sections

For the idealized cross-section, the comparison to the real cross-section is of larger interest than the comparison to the nominal cross-section. Therefore, the results of the idealized cross-sections are used to calculate the relation between the real and the idealized sectional properties:

$$x_{real \text{ vs. ideal}} = \frac{x_{real}}{x_{ideal}} \quad (48)$$

The following table presents the mean values and the coefficients of variation of this relation for all sectional properties for the category "Total". More detailed tables containing a subdivision into the different categories can be found in Appendix B.2.3.

Table 29: Mean values and coefficients of variation for real vs. idealized sectional properties (category “Total”)

	$\frac{A_{real}}{A_{ideal}}$	$\frac{I_{y,real}}{I_{y,ideal}}$	$\frac{I_{z,real}}{I_{z,ideal}}$	$\frac{W_{el,y,real,pos}}{W_{el,y,ideal}}$	$\frac{W_{el,y,real,neg}}{W_{el,y,ideal}}$	$\frac{W_{el,z,real,pos}}{W_{el,z,ideal}}$	$\frac{W_{el,z,real,neg}}{W_{el,z,ideal}}$	$\frac{W_{pl,y,real}}{W_{pl,y,ideal}}$	$\frac{W_{pl,z,real}}{W_{pl,z,ideal}}$
mean [-]	1.0011	0.9999	0.9916	0.9976	0.9985	0.9896	0.9865	1.0007	0.9954
c.o.v [%]	0.265	0.237	0.504	0.602	0.553	0.685	0.808	0.259	0.349

Some discrepancies between the real and the idealized sectional properties can be observed mainly for the structural behaviour around the weak axis. The mean values of the section moduli and the moment of inertia around the weak axis are considerably smaller for the real measured cross-sections compared to the idealized ones. This comes simply from the fact that for the idealized cross-section a major assumption was the definition of a constant flange thickness, which was calculated according to section 4.3.3. The real cross-section, however, shows variations in the flange thicknesses, mainly between the inner and the outer flange parts, as already observed in chapter 3.4. It was observed that the outer flange thicknesses are substantially thinner than the inner ones. This leads to a remarkable effect on the structural behaviour of the real cross-sections, as around the weak axis the outer parts of the flanges have the largest lever arm and therefore contribute the most to the structural resistance around this axis. This effect is more pronounced for the elastic section moduli compared to the plastic section moduli.

For the area and the sectional properties around the strong axis, no significant differences can be seen between the real and the idealized cross-sections. This is based on the fact that the thinner outer flange thicknesses do not have this strong impact as for the behaviour around the weak axis. For the behaviour around the strong axis, the profile height is much more decisive. For the latter, the same value was selected for the idealized cross-section as for the real one. As for the flange thickness some kind of an average value was chosen (quarter points, see section 4.3), it also makes sense that there are no large deviations between the real and the idealized cross-sectional area.

The conclusions made in the current section are some of the reasons why an idealized cross-section was introduced in section 4.2. The intention is to illustrate that the idealized cross-section with a constant flange thickness does not precisely depict the structural behaviour of the real measured cross-section that exhibits a significant variability of the flange thicknesses in the cross-sectional plane. This will be further investigated in section 5.

4.4.3. Comparison with literature

Melcher et al. (2004):

Melcher et al. [4] investigated the cross-sectional area and the plastic section modulus around the strong axis, as seen in Figure 5 and Table 2. These quantities are investigated here for the same profile range (IPE 160-240) separately using the data of this thesis for the real measured cross-sections:

Table 30: Mean value and coefficient of variation of sectional properties for IPE 160-240 (real vs. nominal cross-sections)

	$\frac{A_{real}}{A_{nom}}$	$\frac{W_{pl,y,real}}{W_{pl,y,nom}}$
mean [-]	1.0131	1.0152
c.o.v [%]	1.621	1.618

As already mentioned in section 3.5.4, 45 investigated profiles fall into this category.

When comparing the values above with the ones obtained by Melcher et al., it is seen that Melcher et al. derived mean values for both quantities which are approximately 0.5-1.0 % larger. On the one hand, this can be explained by the fact that Melcher

et al. measured quite larger values for the web thicknesses, as mentioned in section 3.5.4. On the other hand, Melcher et al. measured slightly larger flange thicknesses and assumed a constant flange thickness.

For the coefficients of variation, larger discrepancies are observed. For both quantities, Melcher et al. derived coefficients of variation which are approximately 1.5 % larger compared to the values of this thesis. This is a direct consequence of the larger variations of the flange thicknesses and the profile widths which were investigated by Melcher et al., as already seen in section 3.5.4.

Additionally, it must be said that it is not exactly known at which locations of the web and the flanges the respective thicknesses were measured by Melcher et al. Depending on the used approaches, this may also induce some deviations to the values of this thesis.

Timothy Kyle Jaquess (1998):

Jaquess [14] investigated quite extensively the sectional properties of 17 steel profiles using a simplified approach. He investigated the cross-sectional area, the moments of inertia around both axes and the elastic and plastic section moduli around both axes. The mean values and coefficients of variation are summarized in Table 4. The values coincide quite well with the normalized results of the idealized cross-sections of this thesis which are summarized in the following table:

Table 31: Mean values and coefficients of variation ideal vs. nominal cross-sections (category "Total")

	$\frac{A_{ideal}}{A_{nom}}$	$\frac{I_{y,ideal}}{I_{y,nom}}$	$\frac{I_{z,ideal}}{I_{z,nom}}$	$\frac{W_{el,y,ideal}}{W_{el,y,nom}}$	$\frac{W_{el,z,ideal}}{W_{el,z,nom}}$	$\frac{W_{pl,y,ideal}}{W_{pl,y,nom}}$	$\frac{W_{pl,z,ideal}}{W_{pl,z,nom}}$
mean [-]	0.9946	1.0013	0.9862	0.9962	0.9847	0.9968	0.9859
c.o.v [%]	1.707	2.008	3.110	1.851	2.888	1.830	2.748

Therefore, the values of Jaquess show similar deviations to the real sectional properties of this thesis as discussed in section 4.4.2. The largest discrepancy between the results of Jaquess and the results of the idealized cross-sections of this thesis is identified for the sectional properties around the strong axis, as Jaquess obtained slightly smaller values. This is based on the observation that Jaquess measured profile heights which are approximately 0.5 % smaller than the ones of this thesis. As the profile height is a decisive parameter for the sectional properties around the strong axis, this automatically induces the observed discrepancies.

As Jaquess measured the flange thicknesses somewhere in the region of the flange quarter points and assumed a constant flange thickness, the similarity of the results to the idealized cross-section of this thesis seems to be reasonable.

G. A. Alpsten (1972):

A review of some sectional properties based on almost 5000 measurements is mentioned in the report of G. A. Alpsten [15], as seen in chapter 1.5. It is pointed out that the same patterns observed by G. A. Alpsten (see Figure 9) can still be observed looking at the data of this thesis. All sectional properties investigated by G. A. Alpsten still tend to have mean values below 1.00 using the data of this thesis. Moreover, the quantities around the strong axis have larger normalized mean values compared to the quantities around the weak axis, as already observed by G. A. Alpsten. It is noted that more specific comparisons cannot be conducted, as G. A. Alpsten didn't state any numerical values for the mean values or the coefficients of variation.

As already noted in section 3.5.4, it is impressive that the rough conclusions made out of the data of more than 50 years back still hold nowadays, although there have certainly been some major changes in the production process of rolled steel profiles in the meantime.

5. Numerical investigation of the cross-sectional resistance

The results of the investigation of the sectional properties in section 4 could be used as a basis for calculating some simplified cross-sectional resistances according to prEN 1993-1-1 [9]. However, in order to get some more meaningful conclusions, the goal of the current chapter is to further investigate the cross-sectional resistance of the non-idealized cross-section geometry using some advanced numerical approaches. This will be done by using the general-purpose programming language Python [23] and the finite element method program Simulia Abaqus [24].

5.1. Methodology

In order to be able to investigate several hundreds of cross-sections with the aid of the finite element method (FEM), a parametrized Python script automatically generating the input files for the FE-models was written. The finite element method is a powerful computer-based method used to solve structural problems by dividing the structure into small, finite elements and applying mathematical models to simulate the behaviour of the structure [16]. Simply put, FEM is a method for breaking down a complex problem into smaller elements that are interconnected and assembled to form an approximation of the original structure. The structural behaviour of each finite element is mathematically described by the behaviour of the nodes of the elements and the behaviour between the nodes (using shape functions). When introducing relationships between strains and deformations, as well as between strains and stresses, some equilibrium equations can be derived for each element using energy principles [18]. Afterwards, the individual finite elements are assembled back together to derive global equations and to apply some specific boundary conditions. Finally, the set of equations can be solved numerically to get the quantities of interest (e.g. displacements or stresses). However, one must bear in mind that the models are always simplified idealizations and don't reproduce the behaviour of the real structure completely accurate.

For this thesis, the finite element method is used to simulate the several hundreds of measured cross-sections to obtain their cross-sectional resistances. The advantage of using the FEM for this task is that one can go much more into detail compared to simplified hand calculations, as done in chapter 4. One can apply much more advanced assumptions and approaches behind the calculations. In the following chapter, it will be explained which approaches are followed and how the finite element model in Abaqus is derived. Due to the large number of models, the FE-calculations are conducted with the aid of the high-performance Euler cluster at ETH Zurich [19].

Each measured section of chapter 3 will be investigated in three ways: Once with the real cross-sectional dimensions measured (considering a web eccentricity as explained in chapter 4.2), once with the nominal cross-sectional dimensions and once with the idealized cross-sectional dimensions introduced in chapter 4.3 (constant flange thicknesses etc.). Analogously to the equation (6), the derived cross-sectional resistances are finally normalized with respect to the corresponding cross-sectional resistance obtained for the nominal cross-section. The comparison of these dimensionless quantities will then lead to meaningful conclusions. Furthermore, three different loading situations are considered for each profile: Pure compression, bending around the strong axis and bending around the weak axis. For the investigation with the real measured cross-sectional dimensions, a positive as well as a negative bending moment needs to be considered, as there is no double symmetry given.

5.2. Abaqus model

This chapter describes the assumptions and approaches behind the Abaqus models and how these are built up. In chapter 5.3, it will be explained how it is reached that the Abaqus model is automatically generated for all cross-sections. In the current section, the focus is set on an individual model for one cross-section.

5.2.1. Types of analyses

There are two types of analyses that are carried out for each profile: A linear buckling analysis (LBA) and a geometrically and materially non-linear analysis with imperfections (GMNIA). The LBA represents the bifurcation problem with linear elastic material properties and perfect geometry along the length. The bifurcation of the geometry means that an initially perfect geometry can suddenly have all possible deformation stages at a certain load level. In other words, the system becomes a zero-stiffness system at this load. The primary goal of the LBA is to retrieve the buckling eigenmodes and to scale them to

get the imperfection shape of the GMNIA model. It is emphasized that only local buckling eigenmodes are looked for, avoiding global buckling modes since the focus is set on the cross-sectional resistance of the profiles and not on the global member resistance. The GMNIA is finally used to predict the cross-sectional resistance of the profiles considering local buckling phenomena. It is noted that the classification of the cross-sections according to the classical design checks of prEN 1993-1-1 [9] is not required anymore when carrying out a GMNIA, as the local buckling phenomena are covered by the analysis itself.

As the solution path of the load-displacement of the GMNIA is strongly non-linear, the solution requires iterations for the convergence of the equilibrium (e.g. Newton-Raphson), following the non-linear load-displacement path through linearizations [18]. Usually, also a load-step subdivision is required. This is done in Abaqus by controlling the time step increments. The following values are chosen:

Total time of step: 1

Initial time increment: 0.05

Maximum time increment: 0.1

Minimum time increment: 10^{-9}

Maximum number of increments: 1000

The failure is reached as soon as Abaqus cannot find any convergence of the equilibrium anymore and aborts the analysis. This means that a larger load than the failure load needs to be applied such that the failure can be reached once during the iterations for the load-displacement curve. This is done by estimating the plastic failure load with the help of the idealized sectional properties of section 4.3 and applying this estimated load with an overload factor of two. This means for example that when the sectional properties of section 4.3 suggest a normal force capacity of 5 MN, then a normal force of 10 MN will be applied in the Abaqus model. Using this approach, it is ensured that the applied load is larger than the cross-sectional resistance and the failure will be reached once during the iterations.

For the LBA, six eigenvalues and eigenmodes are determined. However, only the first non-negative eigenvalue and the corresponding eigenmode is finally used, as will be explained in section 5.2.7.

5.2.2. Model and element types

In order to avoid global instabilities (see section 5.2.1), very short girders are modelled. However, it is not possible to just model the cross-section with zero length since the local buckling eigenmodes of the LBA need to be derived and implemented in the GMNIA, which would not be possible otherwise. The length of each profile is determined using the following equations:

$$L = 2 \cdot \max(h_{web}, b_1, b_2) \quad (49)$$

$$h_{web} = h - 0.5 \cdot (t_{f1,2} + t_{f1,3}) - 0.5 \cdot (t_{f2,2} + t_{f2,3}) - 0.5 \cdot (r_1 + r_2) - 0.5 \cdot (r_3 + r_4) \quad (50)$$

Where the variables symbolize the quantities stated in Figure 28, h being the height of the profile at the level of the web, $h = h_{middle}$. It is seen that the web height h_{web} is approximated by using the arithmetic mean of some measured flange thicknesses and root fillet radii.

The equation (49) is chosen based on the “garland curves” [18], which show that the minimum of the buckling stress is not heavily influenced by the number of buckling waves in longitudinal direction after a certain length of the plates. However, it must be considered that the chosen boundary conditions (see section 5.2.5) deviate from the classical case of a plate with hinged boundary conditions on four sides due to the clamping effect. This is the reason why a factor of 2 is chosen in equation (49) instead of a factor of 1. It is omitted to use an even larger length, as on the one hand there would be some influences from global instability phenomena after a certain length which are not desired when investigating the cross-sectional resistance and on the other hand the required computational time would significantly increase which is a key point when conducting the calculations for over 500 profiles and several loading situations. Furthermore, as the results are anyways

always normalized with the results of the nominal cross-section (as explained in chapter 5.1), the chosen length does not play a pronounced role as long as a reasonable value is selected. It has been observed that the number of longitudinal local buckling waves lies between one and three for the length of the profiles according to equation (49), depending on the investigated profile.

The elements of the steel profiles are modelled as 3D solids. A modelling with shell elements would also be possible, however the behaviour of the transition zone between the web and the flange of hot-rolled profiles can be modelled much more precisely when using 3D solid elements. The drawback of using solids is the higher computational effort. The used element type is C3D20R, meaning that the element is a 3D continuum with 20 nodes (illustrated in Figure 29) and that a reduced integration is applied. The reduced integration implies that there are fewer Gauss points than nodes when applying the Gauss integration to the element, the Gauss integration being the treatment of integrals by approximate sums in the determination of the stiffness matrices of each element [18]. Furthermore, using 20 nodes means that for the shape function of each element, a parabolic function is formulated.

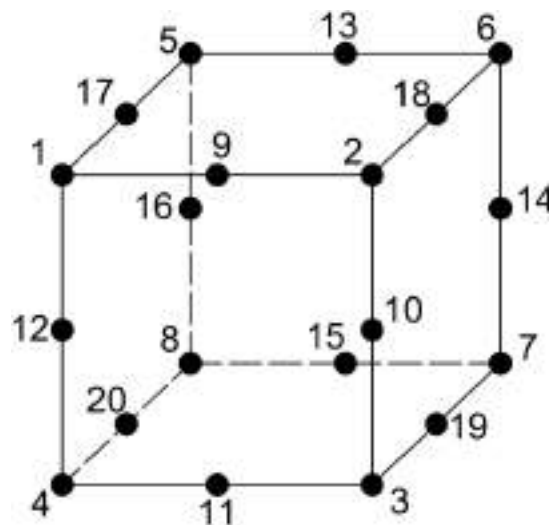


Figure 29: Illustration of the used C3D20R elements

5.2.3. Material properties

As the LBA represents the linear bifurcation problem, only the elastic material properties (Young's modulus E and Poisson's ratio ν) need to be modelled:

Table 32: Elastic properties modelled for the LBA

E [GPa]	210
ν [-]	0.3

The material model used for the GMNIA is a bilinear model (linear elastic – perfectly plastic) with a nominal plateau slope of $E/10'000$ for the numerical stability, as recommended by prEN 1993-1-14 [17]:

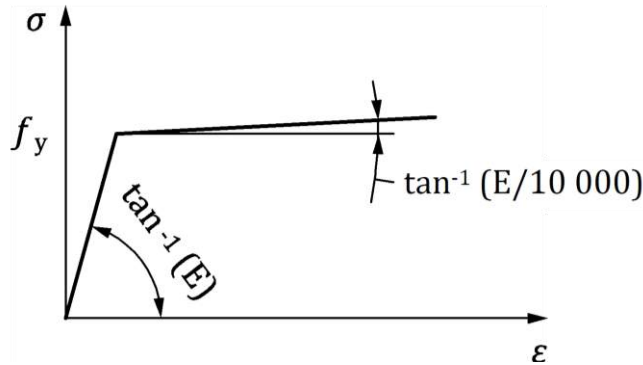


Figure 30: Bilinear material model used for the GMNIA [17]

It is omitted to use a more refined material model, as the standard prEN1993-1-1 [9] also makes use of the linear elastic - perfectly plastic model when calculating the cross-sectional resistances. Therefore, a better comparability between the standard and the carried-out calculations is ensured.

The same elastic properties as used for the LBA are implemented for the GMNIA. In addition, the yield stress is assumed to be at $f_y = 355 \text{ MPa}$. It is pointed out that the nominal stresses and nominal strains of the material model need to be converted into true stresses and true strains for a consistent use in Abaqus:

$$\sigma_{true} = \sigma_{nom} \cdot (1 + \epsilon_{nom}) \tag{51}$$

$$\epsilon_{true} = \ln(1 + \epsilon_{nom}) \tag{52}$$

5.2.4. Mesh

The mesh of the nodes is chosen in Abaqus such that there are always 12 elements in longitudinal direction, as can be seen in the following figure. This number of elements is sufficient, as the shape functions of the individual elements are parabolic ones, as explained in section 5.2.2. Furthermore, the computational time would increase substantially when choosing a larger number of elements in the longitudinal direction.



Figure 31: Illustration of the chosen mesh pattern in Abaqus

In the thickness direction, two elements are chosen for the web, while three elements are chosen for the flanges. For the respective other direction in the cross-sectional plane, the number of elements is selected such that the aspect ratio of the individual elements does not exceed a value of 2.5. For the transition zones between the flanges and the web, a total number of 28 elements per rounding is modelled in such a way that the mesh is as regular as possible in these regions, as can be seen in Figure 32 for a nominal cross-section:

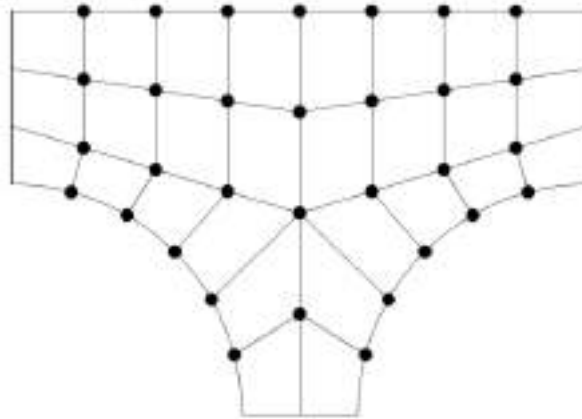


Figure 32: Illustration of the selected mesh pattern in the roundings

For the cross-sections with the real measured dimensions, some little adjustments are made, keeping the number of elements per rounding to 28. The following figure shows exemplary the generated mesh for a cross-section with exaggerated dimensions and a large web eccentricity:

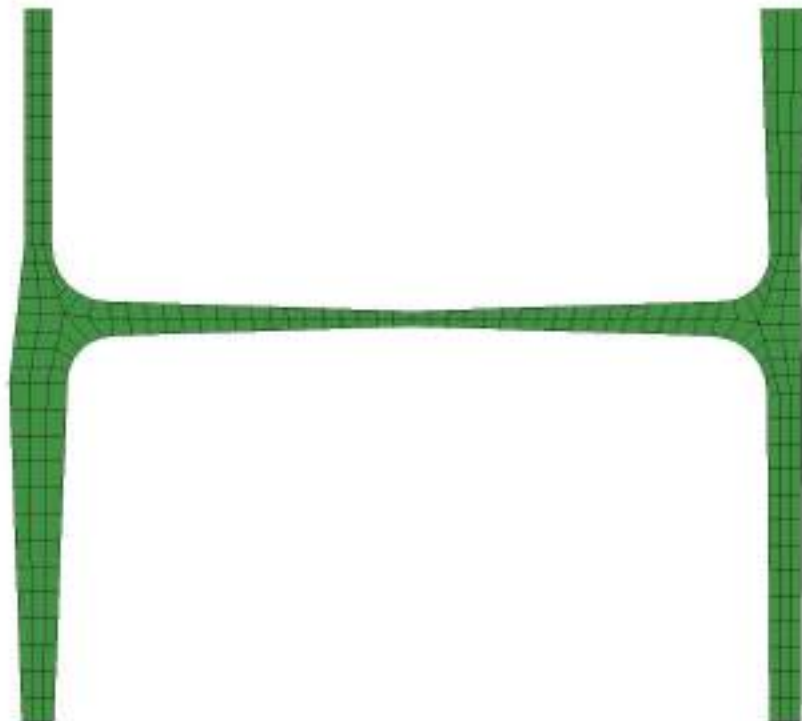


Figure 33: Illustration of the mesh with exaggerated dimensions

It is observed that one can define heavily varying dimensions, as for example quite different flange thicknesses within the same flange. The corresponding mesh is generated automatically by the written Python code. In section 5.3, the procedure of this algorithm will be explained in more detail.

5.2.5. Boundary conditions and loads

At the cross-sectional centroids at the ends of the profile (RP-1 and RP-2 in Figure 35), the displacement in the global y- and z-direction, as well as the rotation around the global x-direction is restrained to zero:



Figure 34: Boundary conditions applied at the ends of the profile

It is noted that the global coordinate system is shown in Figure 35.

Furthermore, at the ends of the profile, two multi-point constraints (MPC's) are introduced that couple all cross-sectional nodes to the cross-sectional centroid, as can be seen in the following figure:

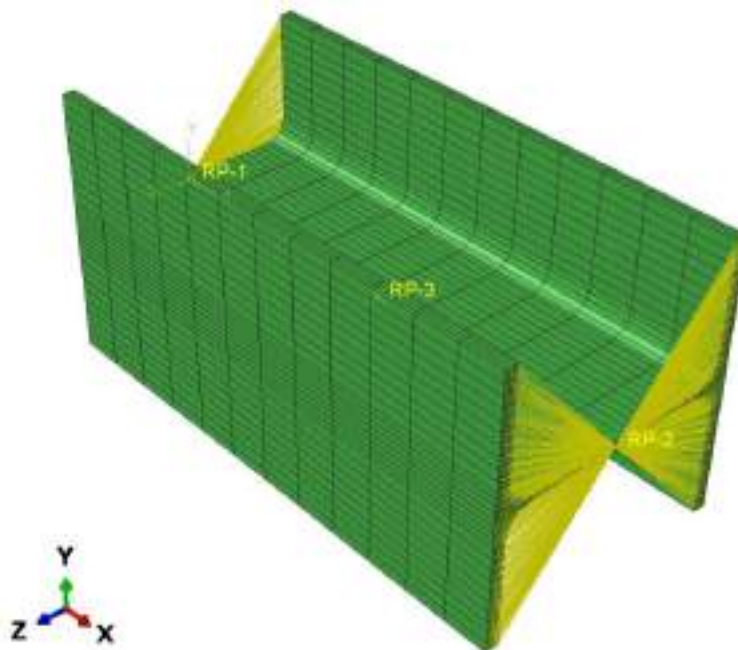


Figure 35: Illustration of the multi-point constraints at the ends of the profile

The MPC type BEAM is chosen in Abaqus, which means that a rigid beam between all nodes and the cross-sectional centroid is modelled that constrains the displacement and the rotation of all nodes to the displacement and the rotation at the centroid, corresponding to the presence of a rigid beam between these nodes [20]. This leads to a clamping effect.

It is noted that for a real measured cross-section, the centroid may lie outside the web depending on the web eccentricity and the measured geometrical dimensions of the cross-section. In these cases, the boundary conditions need to be adjusted. This will be checked in the Python code when generating the input files, as will be shown in section 5.3. For the 561 measured cross-sections, the centroid always lies within the web area.

In order to ensure the global stability, the deformation of the central web node in the middle of the longitudinal direction (RP-3 in Figure 35) is restrained to zero in global x-direction. Furthermore, in the case of bending around the strong axis, the

displacement in global y-direction of one node per rounding is restrained to zero along the whole length as an additional boundary condition, as illustrated in the following figure:

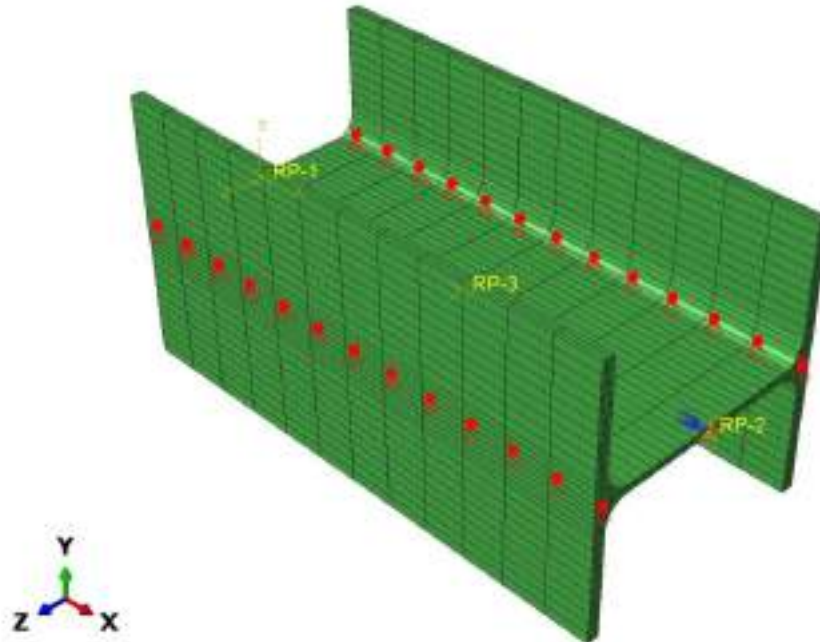


Figure 36: Additional boundary conditions in the roundings (marked in red) in the case of bending around the strong axis

The intention of this boundary condition is to prevent the global lateral yielding of the girder around the weak axis, as shown in the following figure in an exaggerated way:

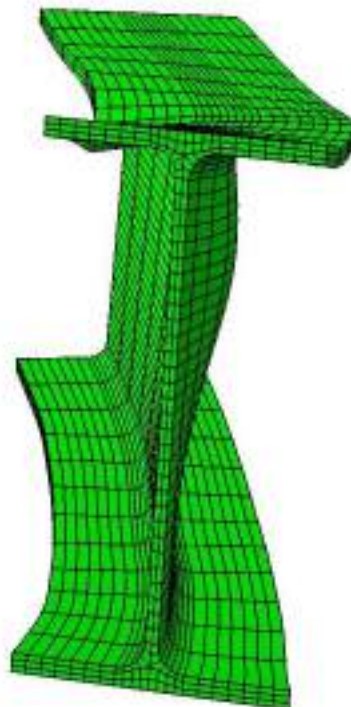


Figure 37: Exaggerated visualization of the global yielding around the weak axis when not considering the additional boundary conditions

This prevention is needed as only the cross-sectional resistances are investigated, neglecting some possible global instability phenomena. For the other loading situations (pure compression and bending around the weak axis), this global phenomenon is not observed. Therefore, these additional boundary conditions are omitted in these cases.

The loads are introduced as point loads at the two cross-sectional centroids at the ends of the profile (RP-1 and RP-2 in Figure 35). For each load case, the corresponding load is applied at both points, but with opposite algebraic sign. For example, for the load case “pure compression”, a positive force in x-direction is applied at RP-1, while a negative force in x-direction is applied at RP-2. The same holds true analogously for bending around both axes. As explained in section 5.2.1, the magnitude of the load is determined by using the idealized sectional properties of section 4.3 and applying an overload factor of two.

Using the centroids as the load introduction points ensures that the load case “pure compression” can be reached without bending effects when introducing a compressive normal force. However, in reality, one needs to consider properly where the normal force is acting. It may occur that the load is introduced in the central web node (between point 1 and 2 in Figure 27) due to a certain connection to another component. In this case, certain bending effects will automatically be induced for the real measured cross-sections due to the shift of the centroid, as explained in section 4.2.3. This aspect is not further investigated in the framework of this thesis, it will just be focused on the pure compression load case without bending due to a potential load eccentricity. For the bending load case, the load introduction point does not play a role. For consistency, the centroid is selected as the load introduction point for all load cases.

5.2.6. Units

As Abaqus has no built-in systems of units, the units chosen by the user have to be self-consistent. It is decided to insert all dimensions in mm and all forces in N. This leads to stresses in the unit MPa:

Table 33: Selected units in Abaqus (red) [25]

Quantity	SI	SI (mm)	US Unit (ft)	US Unit (inch)
Length	m	mm	ft	in
Force	N	N	lbf	lbf
Mass	kg	tonne (10 ³ kg)	slug	lbf s ² /in
Time	s	s	s	s
Stress	Pa (N/m ²)	MPa (N/mm ²)	lbf/ft ²	psi (lbf/in ²)
Energy	J	mJ (10 ⁻³ J)	ft lbf	in lbf
Density	kg/m ³	tonne/mm ³	slug/ft ³	lbf s ² /in ⁴

5.2.7. Geometrical Imperfections

A key aspect of the GMNIA is that geometrical imperfections need to be implemented. The introduction of a geometrical imperfection is not done in the analytical solutions of the classical design, as these effects are already built-in in the calibrated formulas of the standards. However, when investigating the cross-sectional resistance with the FEM properly, these imperfections need to be modelled explicitly.

As mentioned in section 5.2.1, the LBA is carried out in order to obtain an appropriate geometrical imperfection shape for the GMNIA. It is assumed that the buckling eigenmode belonging to the first non-negative eigenvalue is the most unfavourable imperfection shape. The buckling eigenmodes are obtained under pure compression. It is emphasized that the buckling eigenmodes belonging to pure compression are implemented for all loading situations in the GMNIA. In the case of a bending LBA, the buckling eigenmodes would show no buckling waves in the tensile zones which is not representative of real distributions of geometrical imperfections. Therefore, it's more realistic to introduce the buckling eigenmodes obtained under pure compression as the imperfection shapes for bending loading as well.

The buckling eigenmodes obtained in the LBA are normalized to a maximum deformation magnitude of 1.00 in the unit which is chosen in Abaqus (mm for this thesis). Therefore, these eigenmodes need to be scaled properly in order to comply with the code provisions of prEN 1993-1-14 [17]. For the imperfection magnitude $f_{magnitude}$, it is decided to select the following value according to chapter 5.4 of prEN 1993-1-14:

$$f_{magnitude} = \frac{a_i}{200} \quad (53)$$

Where the characteristic buckling length a_i is calculated for the web as follows using the definitions of Figure 28 and $h = h_{middle}$:

$$a_w = h - 0.5 \cdot (t_{f1,2} + t_{f1,3} + t_{f2,2} + t_{f2,3}) - 0.5 \cdot (r_1 + r_2 + r_3 + r_4) \quad (54)$$

Analogously, the characteristic buckling length can be calculated for the flanges:

$$a_f = 0.5 \cdot (b_1 + b_2) - 0.5 \cdot (t_{w1} + t_{w3}) - 0.5 \cdot (r_1 + r_2 + r_3 + r_4) \quad (55)$$

It is emphasized that according to the standard prEN 1993-1-14, the imperfection magnitude introduced in equation (53) is strictly valid only when modelling equivalent geometric imperfections including residual stresses. For this thesis however, the residual stresses are modelled explicitly, as will be shown in section 5.2.8. Nevertheless, when looking at individual plates and the local buckling of these plates, it does not make sense to introduce other imperfection magnitudes when considering residual stresses explicitly compared to the case where the residual stress state should be included in the imperfection shape. This is due to the fact that the code cannot know in advance where this individual plate will be located in the cross-section. As the code provisions have to hold for all types of individual plates, the residual stresses cannot be included in these equivalent geometric imperfections for individual plates. This is in contrast to the equivalent geometric imperfections of whole profiles when looking at the global buckling where it makes sense to distinguish between equivalent geometric imperfections and purely geometric imperfections when the residual stresses are modelled explicitly, as indeed, the global buckling will be influenced by the distribution of the residual stress state. Furthermore, Gérard et al. [26] also recommend to select the geometrical imperfection magnitude according to equation (53) when looking at the local plate buckling of hot-rolled I-sections even when the residual stresses are modelled explicitly, as this should lead to reasonable resistance predictions.

In the equations (53) - (55), it can be observed that the flanges have other imperfection magnitudes compared to the web. However, in the Abaqus GMNIA model, only one overall scaling factor for the whole cross-section is applied to the LBA eigenmode which has its maximum deformation magnitude (=1.00) either in the web or in the flanges. This overall scaling factor is determined by looking at the maximum deformation magnitude of the web and flanges of the obtained LBA eigenmode respectively. Afterwards, the required scaling factor to reach the imperfection magnitude according to equations (53) - (55) for the individual cross-sectional parts is calculated. Finally, the minimal scaling factor is chosen, such that the imperfection magnitude of equations (53) - (55) is fulfilled at the critical cross-sectional part (web or flange).

5.2.8. Residual stresses

Hot-rolled steel profiles always have some residual stresses locked in the members. These are also some types of imperfections in the structure that need to be considered explicitly when using the FEM in contrast to the classical design. In the course of this thesis, the residual stresses are modelled according to the model of the standard prEN 1993-1-14 [17]:

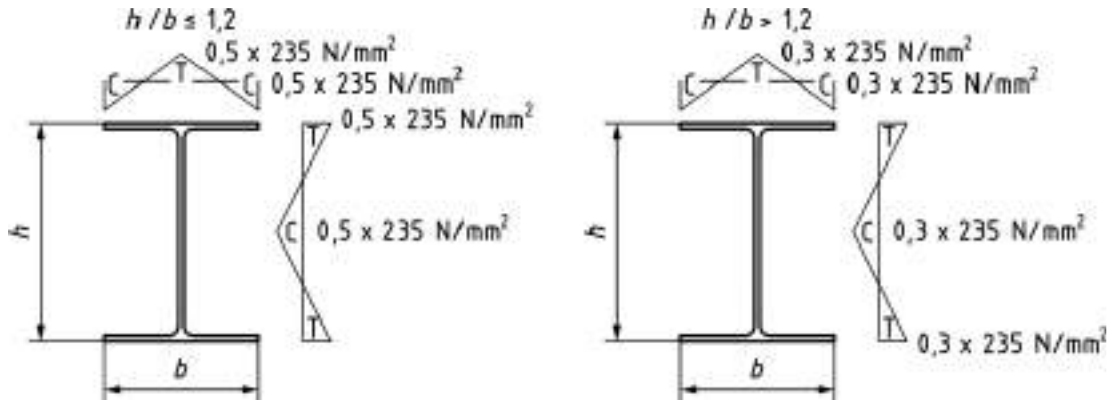


Figure 38: Residual stresses for hot-rolled I-sections according to prEN 1993-1-14 [17]

It is noted that the residual stresses from Figure 38 are implemented in an approximate way in Abaqus, as can be seen in Figure 39. The linear residual stress model from Figure 38 is approximated by a stepwise determination and implementation of the residual stress at the middle of each mesh element. There is a constant residual stress modelled for each mesh element. Furthermore, as a simplification, a constant tensile residual stress is modelled in the roundings. The integral of this tensile stress over the roundings corresponds to the integral of the residual stresses over the rest of the cross-section with a changed sign. Using this approach, it is ensured that the equilibrium is fulfilled and that there is no resulting force developed by the residual stress state. The residual stresses are modelled as predefined stress fields in Abaqus.

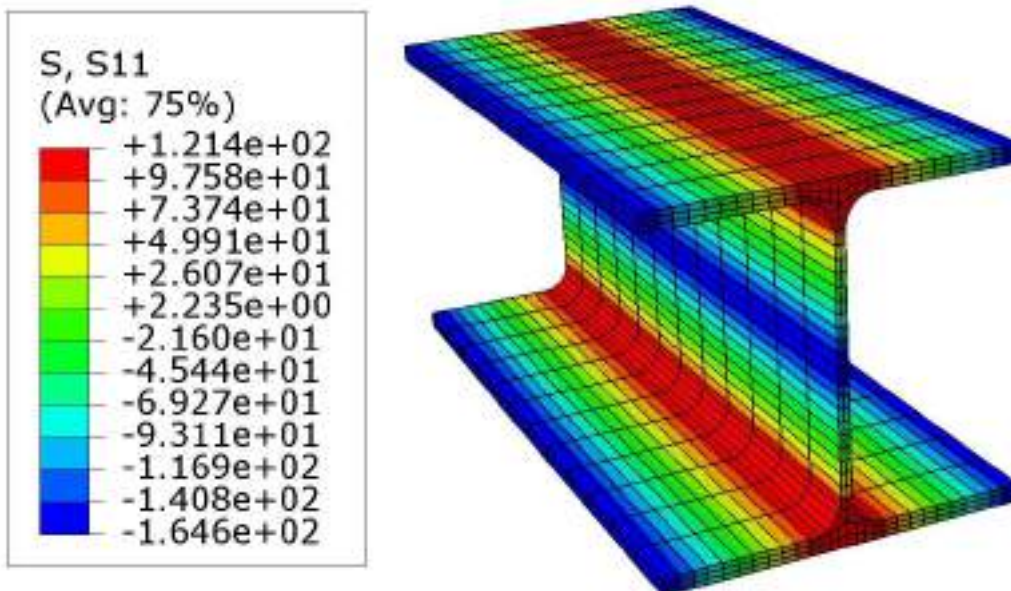


Figure 39: Residual stresses modelled in Abaqus

5.2.9. Model verification

For all types of finite element modelling, a proper model verification is essential. According to the standard prEN 1993-1-14 [17], the verification should check the correctness and the accuracy of the numerical model compared to the mathematical model. In the following, the results of the LBA as well as the GMNIA are verified using some reference calculations.

LBA:

The results of the LBA are the eigenvalues and the corresponding eigenmodes. In order to be able to verify them, some comparative calculations are carried out with the help of the structural analysis software EBPlate [21]. Three different nominal profiles are investigated. The following table summarizes the results obtained by the LBA in Abaqus:

Table 34: LBA results of the Abaqus model

Profile	N [kN]	α_{cr} [-]	σ_{cr} [MPa]
IPE 160	1426	2.2893	1624
HEA 360	10136	2.1119	1497
HEB 500	16943	2.1877	1551

It is noted that the positive sign is used for compression here. Furthermore, α_{cr} represents the first positive eigenvalue. With the help of this eigenvalue α_{cr} and the applied normal force N , the critical elastic buckling stress σ_{cr} can be calculated as follows:

$$\sigma_{cr} = \frac{N \cdot \alpha_{cr}}{A} \quad (56)$$

The values summarized in Table 34 can be verified using EBPlate. As the local buckling of the web was decisive for the three investigated profiles, these webs are modelled in EBPlate accordingly. The same height (without roundings and flange thicknesses), length and thickness of the webs are modelled as in the Abaqus model. The following figure shows exemplary the model of the web of the IPE 160 profile:

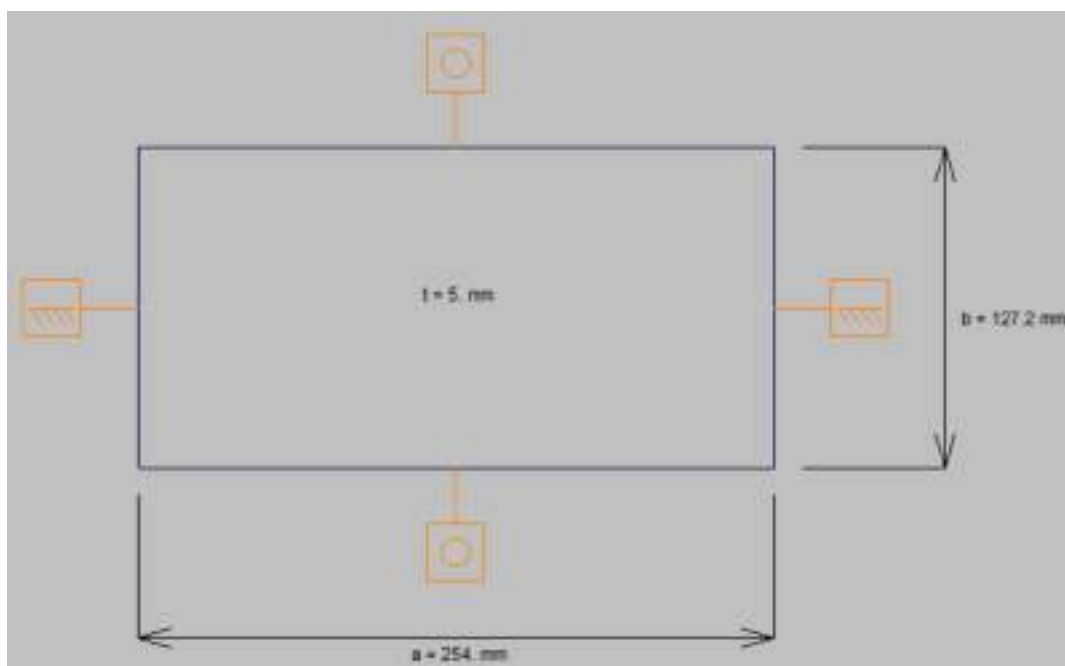


Figure 40: EBPlate model of the IPE 160 web

It is seen that at the upper and lower edge, a pinned support is modelled, while a clamped support is introduced at the two ends in longitudinal direction of the web. These boundary conditions simulate the boundary conditions explained in section

5.2.5 approximately. By using this model for all three profiles, the following critical buckling stresses $\sigma_{cr,EBPlate}$ are obtained in EBPlate:

Table 35: Obtained critical buckling stresses using EBPlate

Profile	$\sigma_{cr,EBPlate}$ [MPa]
IPE 160	1442
HEA 360	1287
HEB 500	1288

It is observed that these values are relatively close to the values obtained with Abaqus (see Table 34), being slightly lower. The deviation to the values of the Abaqus model can be explained by the fact that the EBPlate model with pinned lower and upper edges just considers the stiffness of the web without the slight clamping effect of the flanges. Therefore, it is reasonable that the values obtained with Abaqus are slightly larger, as there, the additional stiffness given by the flanges is automatically considered in the whole model. The largest percentage deviation between the Abaqus model and the EBPlate model can be observed for the HEB 500 profile, as there the thickness of the flanges and accordingly the additional stiffness given by the flanges is larger compared to the other profiles.

The program EBPlate is also able to generate the corresponding eigenmode. The following figure shows a comparison of the buckling shape obtained with Abaqus (left) and the one obtained with EBPlate (right) for the profile IPE 160. It can be observed that the two eigenmodes look similar. One can also see the influence of the slight clamping effect of the flanges in the Abaqus model compared to the hinged boundaries of the EBPlate model.

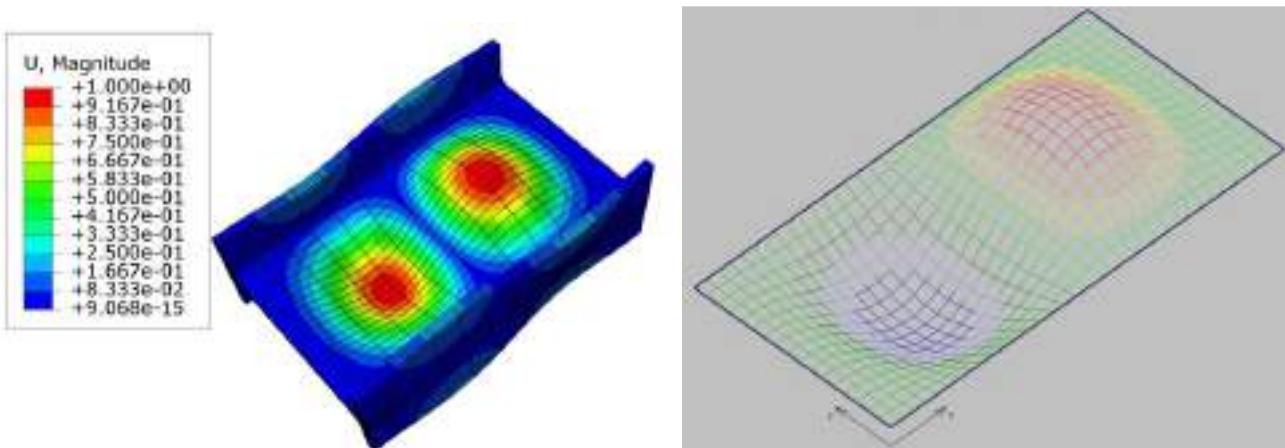


Figure 41: Comparison of the buckling eigenmode for the Profile IPE 160 obtained with Abaqus (left) and EBPlate (right)

A comparison of the elastic buckling load obtained with Abaqus to the one calculated according to the standard prEN 1993-1-5 [22] would also be possible. However, this standard does not state a k_{σ} -value which is suitable for the prevailing boundary conditions. Using the value for a four-sided hinged plate results in a heavily underestimated critical buckling stress, as can be expected. Therefore, it is omitted to show this comparison here. The comparison of the Abaqus model with the EBPlate model illustrates that the Abaqus LBA model seems to work properly.

GMNIA:

For the verification of the GMNIA results, it is decided to model five fictive sections for each load case (pure compression, bending around the strong axis and bending around the weak axis) with different width-to-thickness ratios for each cross-sectional part. Thereby, the first profile (CS 1) is always a cross-section which is clearly a class 1 cross-section according to the classification of prEN 1993-1-1 [9]. The second profile (CS 1/2) is always a cross-section which is at the boundary between a class 1 and class 2 cross-section but still belonging to the class 1. The third profile (CS 2/3) is a cross-section at the boundary between class 2 and class 3, belonging still to the class 2 and the fourth profile (CS 3/4) is a cross-section at the boundary between class 3 and class 4, belonging still to the class 3. Furthermore, the fifth profile (CS 4) is a cross-section which is clearly a class 4 cross-section. Evaluating these profiles and comparing the cross-sectional resistances obtained by the GMNIA with the theoretical plastic failure loads according to prEN 1993-1-1 [9], one can draw some conclusions out of the results.

The following table summarizes the chosen dimensions for the cross-sections:

Table 36: Fictive cross-sections used for the GMNIA verification

	h [mm]	b [mm]	t_w [mm]	t_f [mm]	r [mm]
<u>Compression:</u>					
CS 1	224	196	8	13	24
CS 1/2	255	244	8	13	24
CS 2/3	294	266	8	13	24
CS 3/4	320	350	8	13	24
CS 4	374	456	8	13	24
<u>Bending around strong axis:</u>					
CS 1	424	196	8	13	24
CS 1/2	540	244	8	13	24
CS 2/3	611	266	8	13	24
CS 3/4	858	350	8	13	24
CS 4	1074	456	8	13	24
<u>Bending around weak axis:</u>					
CS 1	224	196	8	13	24
CS 1/2	255	244	8	13	24
CS 2/3	294	266	8	13	24
CS 3/4	320	388	8	13	24
CS 4	374	496	8	13	24

The detailed classification of these cross-sections can be found in Appendix C.1.

The following figure shows exemplarily the failure pattern for the CS 1/2 in the loading case "pure compression" (strongly inflated):

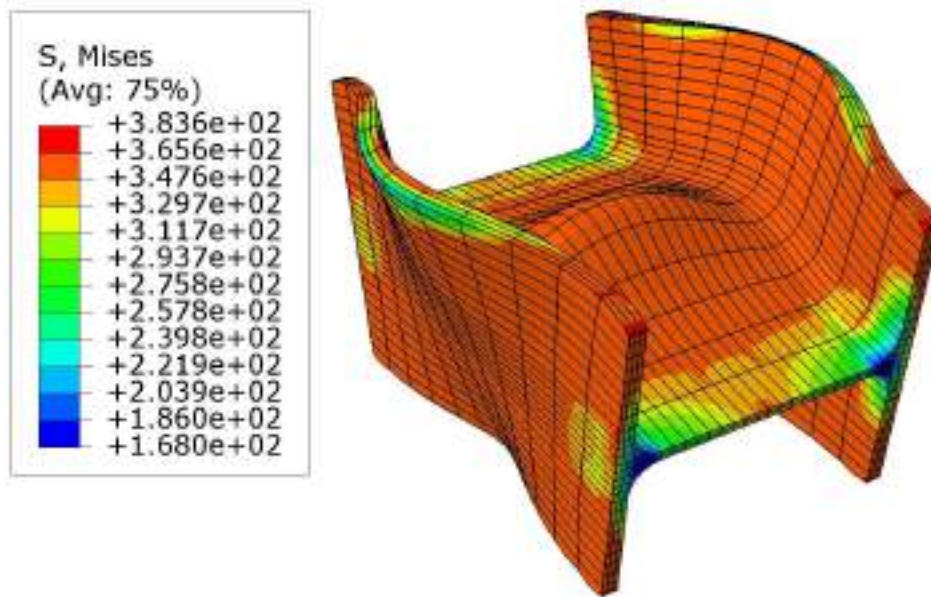


Figure 42: Failure pattern observed for CS 1/2 in the loading case "pure compression" (strongly inflated)

For all profiles and all loading cases, the failure pattern is always a cross-sectional failure in the middle in longitudinal direction, far away from the boundaries. The latter is important, as in this way, it is ensured that the boundary conditions do not have a significant influence on the failure load.

The following table summarizes the obtained failure loads and shows the normalization with the theoretical plastic failure loads according to prEN 1993-1-1 [9]:

Table 37: Obtained failure loads and normalization with theoretical plastic failure loads

	N_{ult} [kN]	N_{ult} / (A*f_y)	M_{y,ult} [kNm]	M_{y,ult} / (W_{pl,y}*f_y)	M_{z,ult} [kNm]	M_{z,ult} / (W_{pl,z}*f_y)
<u>Pure compression:</u>						
CS 1	2571.24	1.0095				
CS 1/2	3095.06	1.0055				
CS 2/3	3398.21	1.0019				
CS 3/4	4223.08	0.9958				
CS 4	4917.49	0.9153				
<u>Bending around strong axis:</u>						
CS 1			523.646	1.0105		
CS 1/2			824.176	0.9988		
CS 2/3			1017.966	0.9907		
CS 3/4			1822.696	0.9452		
CS 4			2542.795	0.8193		
<u>Bending around weak axis:</u>						
CS 1					96.507	1.0557
CS 1/2					142.574	1.0160
CS 2/3					168.825	1.0144
CS 3/4					344.889	0.9834
CS 4					535.775	0.9378

Thereby, the cross-sectional area A and the plastic section moduli around both axes, $W_{pl,y}$ and $W_{pl,z}$ are calculated according to the equations of section 4.1, see Appendix C.1 for a full compilation of the inserted sectional properties.

Looking at the results of Table 37, it can be observed that for all loading cases, the CS 1 reaches a failure load which is above the theoretical plastic failure load. This makes sense as these cross-sections have per definition a large plastic deformation capacity and apart from that can slightly utilize the flat hardening branch which was modelled in the material model (see section 5.2.3) and which is not depicted in the theoretical plastic failure loads according to prEN 1991-1-1 [9]. The utilization of the hardening branch is primarily observed for bending around the weak axis, as the plastic rotation capacity is the largest for this load situation.

Furthermore, it is seen in Table 37 for all loading cases that the normalized cross-sectional capacity decreases continuously the higher the load class gets. This is reasonable, as the plastic deformation capacity is reduced for cross-sections with a higher class compared to the lower class sections. The class 4 cross-sections have the smallest plastic deformation capacity and tend to buckle much before the theoretical plastic failure load can be reached.

In order to get some qualitative conclusions regarding the plastic deformation capacity, the calculations are carried out deformation-based as well. This is done by removing the force-based loading and gradually applying a displacement for the loading situation of pure compression and a rotation for the bending situations. The following figures present the results in the form of normalized load-deformation curves:

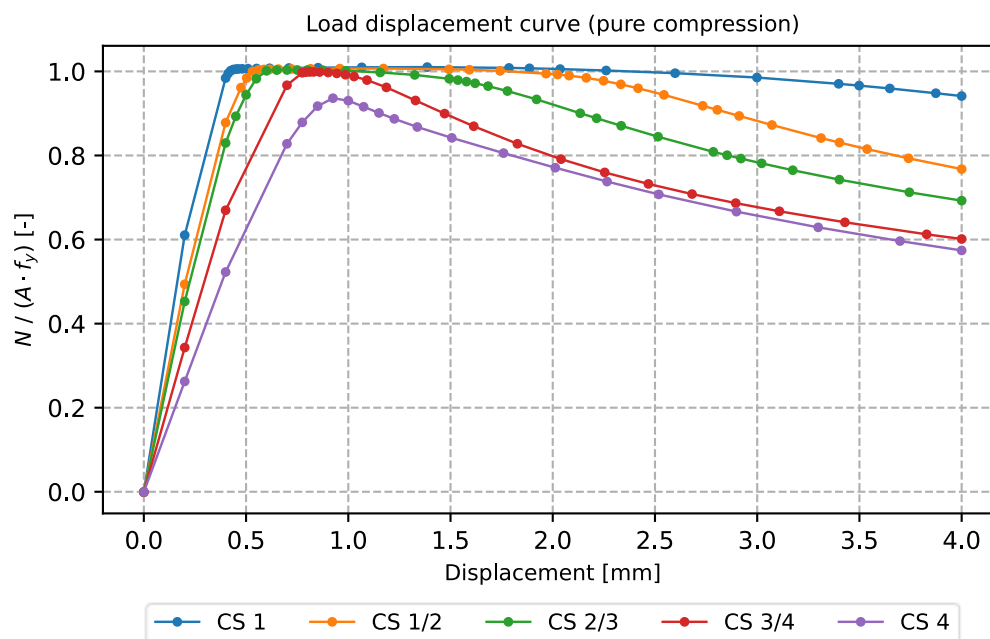


Figure 43: Load displacement curve (pure compression)

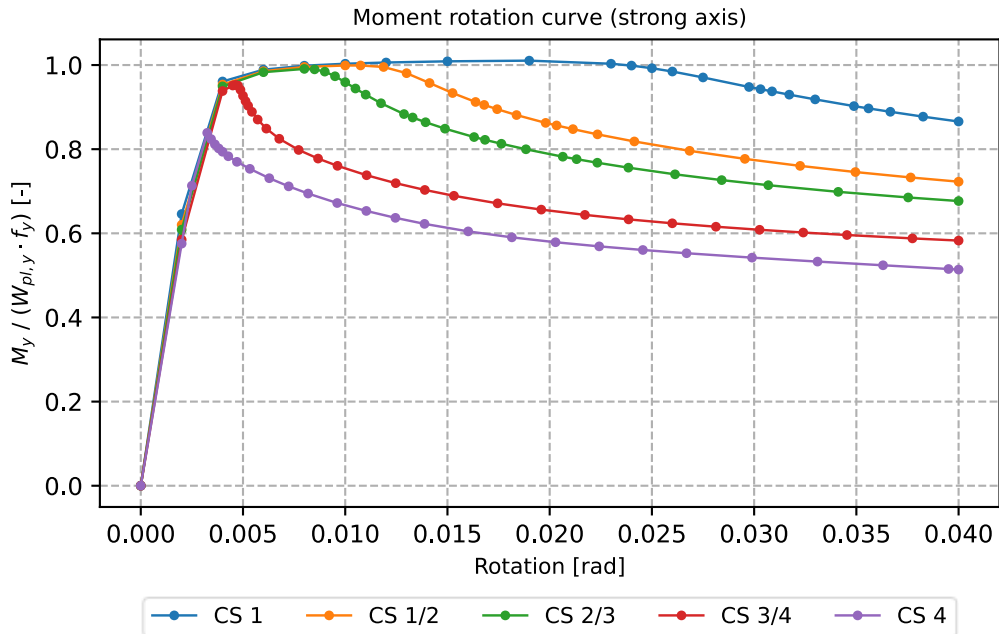


Figure 44: Moment rotation curve (strong axis)

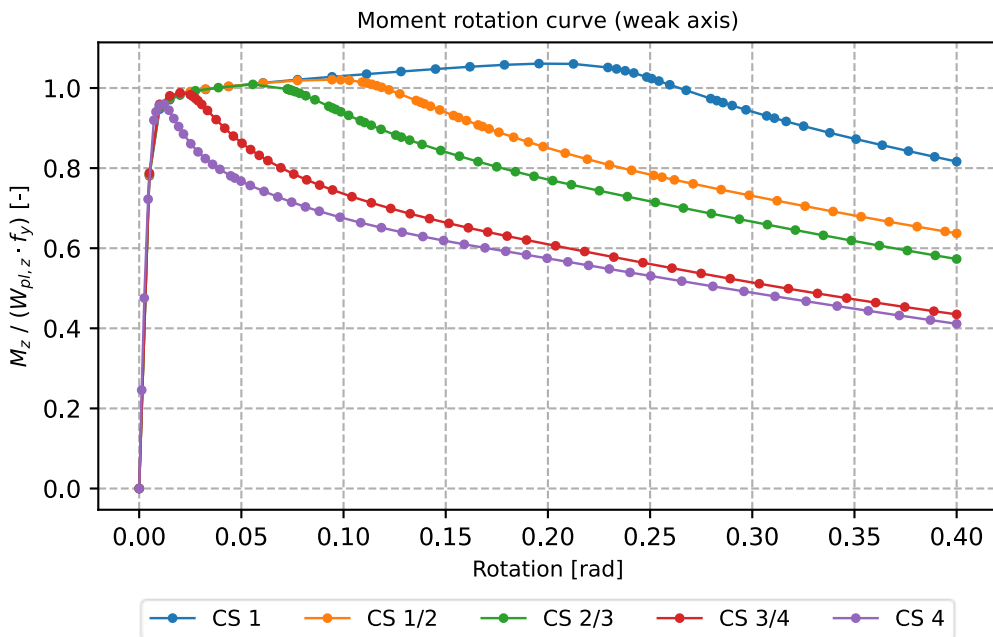


Figure 45: Moment rotation curve (weak axis)

These curves are in accordance with the standard prEN 1991-1-1 [9]. It is observed that the plastic deformation capacity as well as the maximum load gradually decreases as the cross-sectional classes get higher. Obviously, the CS 1 (clearly class 1 cross-section) has the largest plastic deformation capacity as it can maintain a large load for a significant deformation span for all three loading cases. Furthermore, it is observed that there is always an almost linear load-deformation path at the beginning until a specific point where the deformation (displacement or rotation) begins to grow disproportionately at a constant or decreasing load level, as is expected for a sudden local buckling failure or when the whole cross-section is plasticized.

The conducted comparison of the results of five fictive cross-sections for each load case demonstrates that the Abaqus model seems to produce reasonable results for the GMNIA. It is observed that the introduction of a hardening branch in the material model may induce resistances which are above the theoretical ones for class 1 sections. Anyway, the rigorous accuracy of the predicted resistances regarding the compliance with prEN 1993-1-1 [9] has not the highest significance for this thesis, as the results are always normalized with the results of the nominal cross-section in any case.

It is pointed out that in chapter 5.4.1, an additional verification of the Abaqus model will follow.

5.3. Python script

Due to the large number of cross-sections to be investigated, a parameterized Python script was written which automatically generates the Abaqus input files for all cross-sections. Afterwards, each input file creates an Abaqus model with the properties explained in section 5.2. The current section focuses on how it is reached that the Abaqus input files are automatically generated.

5.3.1. General Workflow

The general workflow of the parametrized Python script is divided into five different modules that were written separately. There is a main module and an evaluation module which make use of three further modules, the data module, the input module and the model module. Thereby, the model module contains functions that compute all the required data that are related to the Abaqus model building, as for example the coordinates of the mesh elements among many other things. The input module contains functions that write the Abaqus input files with the corresponding model information from the model module. Finally, the data module includes functions that are able to read and evaluate the results from the LBA and GMNIA calculations. It is for example used to read the eigenmodes from the LBA which are then utilized to model the geometrical imperfections for the GMNIA.

The main module is the leading module when creating the LBA or GMNIA models and the corresponding input files for several cross-sections. Thereby, it refers to the functions of the other modules. The evaluation module on the other hand is the module that is finally used to evaluate the results of the GMNIA. It refers to the functions of the data module.

The following figure illustrates the procedure for creating the input files:

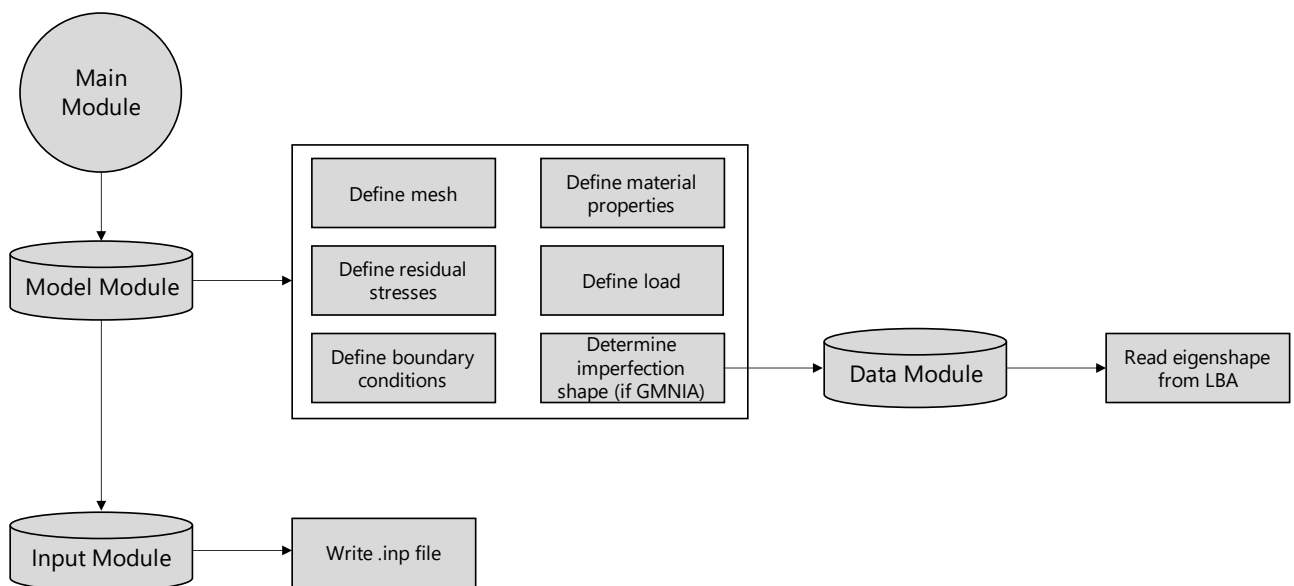


Figure 46: Illustration of the procedure for creating the Abaqus input files

For a deeper understanding of the workflow, the five individual modules are explained in more detail in the following sections. Furthermore, the main assumptions lying behind the programmed functions are stated.

5.3.2. Main module

The main module is split into four principal parts. In the first part, the geometrical dimensions of the cross-sections to be modelled are read in with the aid of a .csv file. The Figure 28 shows which dimensions can be inserted into the .csv file. However, in contrast to Figure 28, only one profile height h is demanded in the .csv file. This was decided based on the results of chapter 3.2 where it was figured out that only the height measured at the level of the web properly represents the height along the whole length of the measured profiles. As a further change to Figure 28, a web eccentricity according to equation (34) can be inserted into the .csv file.

In the second part, one can define the material parameters to be used, as for example the Young's modulus E . Furthermore, the user can decide which analysis to be made (LBA or GMNIA) and which loading case should be investigated (pure compression, bending around the strong axis or bending around the weak axis).

The third part is the model building part. Here, the main module refers to the functions written in the model module to compute all the data that are required to form an Abaqus model. This part also includes a section where the geometrical imperfections are implemented if the type of analysis is a GMNIA.

Finally, the fourth part writes the Abaqus input files with the aid of the functions of the input module.

5.3.3. Model module

In the first part of the model module, some basic information such as the desired aspect ratio of the mesh elements or the identification numbers of the nodes and elements are defined. Afterwards, several functions follow that are needed to compute all the required model data. In the following, the individual functions and the underlying assumptions are explained.

Function defineMeshProperties:

Roughly speaking, this function defines the number of elements for the finite element mesh and calculates the corresponding element dimensions. Thereby, the cross-section is split into eight parts:

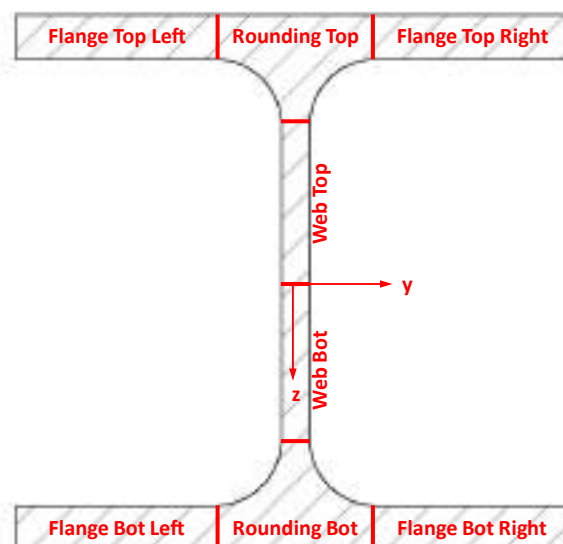


Figure 47: Segmentation of the cross-section into eight parts

Furthermore, the Figure 27 shows the numbering of the points (points 1-22) that is used in the Python code. All assumptions made in section 4.2 are applied accordingly. Based on all these assumptions, the function calculates the number of elements and the dimensions of these elements taking into account the general mesh properties explained in section 5.2.4.

Moreover, the function `defineMeshProperties` also calculates the cross-sectional centroids of all the cross-sections, as explained in section 4.2.3. These centroids are later used to apply the boundary conditions and to introduce the loads. With the aid of an additional if-loop, it is checked whether the centroid lies within the web area or not. If the centroid of an inserted cross-section lies outside the web area, a warning message including the prompt to adjust the boundary conditions and the load introduction will be displayed in the Python console.

Function `analyseNumberOfNodes`:

As the name of the function indicates, the number of nodes for the mesh is calculated here making use of the mesh properties calculated in the previous function. In the two-dimensional plane, it is differentiated between corner and edge nodes, while in the three-dimensional case, it is distinguished between main and side nodes, as the following figure illustrates:

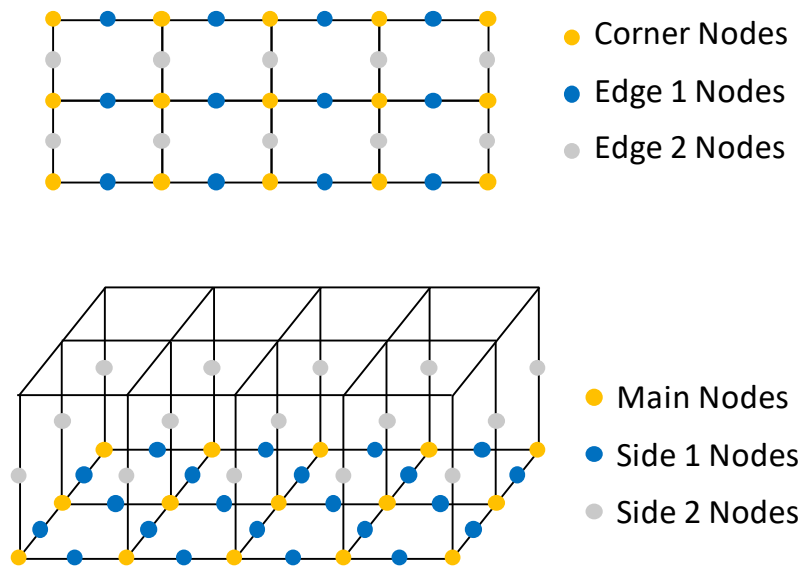


Figure 48: Differentiation between corner and edge nodes (2D case) and main and side nodes (3D case)

Function `analyseNumberOfElements`:

Similar to the preceding function, the number of mesh elements is determined here.

Function `getNode2D`:

This function is a fundamental one, as it defines the node grid with all the coordinates of the nodes in the two-dimensional cross-section plane taking into account all the assumptions made above and the mesh properties defined in section 5.2.4. It treats all the individual cross-sectional parts (see Figure 47) separately. It is noted that the points at the boundaries of the roundings to the web and flanges are considered in the respective web or flange parts. Furthermore, the nodes at the boundary between the top and the bottom web part are considered in the top web part. In Figure 33, it is shown how the generated cross-sectional mesh of nodes looks like for an exaggerated case.

Function `getNode3D`:

Analogously to the two-dimensional case, this function defines the three-dimensional node grid by extending the two-dimensional node grid into the longitudinal direction.

Function `getElements`:

This function defines the individual finite element mesh elements in terms of the corresponding node numbers. Based on the defined three-dimensional node grid of the preceding function, the 20 nodes introduced in Figure 29 are saved for each element. This is again done for each cross-sectional part of Figure 47 separately.

Function `getNodeSets`:

In this function, some node sets are defined. Node sets are a helpful tool in Abaqus to generate some groups of nodes. For example, all nodes at the longitudinal ends of the profile can be saved into one node set to create a multi-point constraint later, as explained in section 5.2.5.

Function getElementSets:

Analogously to the preceding function, this function creates some element sets. Some of these element sets are used later when the residual stresses are defined.

Function getSurfaces:

This function defines surfaces at the longitudinal boundaries of the model, making use of some defined element sets.

Function getResidualStresses:

As the name already indicates, this function calculates the residual stresses introduced in section 5.2.8. All cross-sectional parts of Figure 47 are treated separately. As demonstrated in Figure 39, the written code calculates the residual stress at the middle of each element according to the residual stress model of the standard prEN 1993-1-14 [17]. For each element, the residual stress is kept constant then. Furthermore, the code always summarizes some elements into groups with the help of some element sets. For the flange for example, the adjacent elements in thickness direction are always summarized into the same group and therefore get the same residual stress. The same is done analogously for the web. After calculating the residual stresses in the flanges and the web, the written code integrates all the residual stresses over these cross-sectional parts. Then a constant residual stress is defined for the roundings. The magnitude of this residual stress is chosen such that the integral of this constant stress over the roundings corresponds to the integral of the residual stresses over the rest of the cross-section with a changed sign. Using this procedure, it is ensured that there is no resulting force generated from the residual stress state.

Function getAssembly:

This function defines the assembly for the Abaqus model. This means that on the one hand, the reference points for the boundary conditions and on the other hand the multi-point constraints themselves are defined here, as introduced in section 5.2.5.

Function getMaterials:

In this function, the bilinear material model explained in section 5.2.3 is defined by calculating the stress-strain curve in terms of true strains and true stresses.

Function getBoundaryCond:

The boundary conditions explained in section 5.2.5 are generated here.

Function getSteps:

This function defines the calculation steps for the Abaqus model based on whether a LBA or a GMNIA is conducted. This includes the calculation of the load that is modelled, making use of the idealized sectional properties explained in section 4 and applying an overload factor of two, as pointed out in section 5.2.5.

Function addImperfections:

This is a function that is only used when a GMNIA is conducted. The eigenmode of the LBA is taken here and introduced as a geometrical imperfection by applying the scaling factors that were described in section 5.2.7. This is done simply by adjusting the 3D-coordinates of the nodes.

As a control measure, it is programmed that the code will generate an error message as soon as the eigenmode of the LBA has a maximum deformation (flange or web) of less than 0.99 at the longitudinal middle or third point. This makes sure that the eigenmode is a reasonable one, as for one or three longitudinal buckling waves, the maximum deformation (=1.00 in the LBA) should be in the middle due to symmetry, while for two buckling waves, the maximum deformation is expected at the third points for the boundary conditions introduced in section 5.2.5.

5.3.4. Input module

Similar to the model module, the input module contains several functions that are retrieved in the main module. However, the functions in the input module are not aimed at deriving some modelling information as the model module, but focus on the correct writing of the Abaqus input files that are needed to carry out an Abaqus simulation later. At the very top of this module, the user can insert some basic information, as for example the author's name. Afterwards, some functions follow. In the following, the individual functions of the input module are briefly explained.

Function createNewInputFile:

This is a basic function that creates an empty new input file which is subsequently used in the following functions to be extended.

Function writeHeading:

As the name indicates, this function writes the heading lines of the input file with some basic information as for example the author, the analysis type, the loading type or the inserted cross-sectional dimensions. These heading lines have an informative character such that the user can immediately see the type of model that should be generated using this input file.

Function writeParts:

The function writeParts writes the commands in the input file that will create the proper part in Abaqus. A part is in Abaqus a distinct entity of a building component one wants to model. In the case of this thesis, the part is just the modelled profile. Therefore, this function writes the mesh and element properties including the node and element sets that were generated in the model module beforehand. In the case of the GMNIA, the node grid considering the imperfection shape is already adjusted by the function addImperfections of the model module and can be written here in the same way as for the LBA.

Function writeAssembly:

Defining a part is not sufficient in Abaqus. One needs to define an assembly where theoretically several parts could be taken together as instances and positioned at the desired places. In the case of this thesis, the defined part of the cross-section is taken as an instance without considering additional parts. The function writeAssembly makes sure that the assembly is defined properly. Furthermore, it generates the reference points and the multi-point constraints which were defined in the model module beforehand.

Function writeBoundaryCond:

This function writes the appropriate boundary conditions in the input file.

Function writeMaterials:

The function writeMaterials writes some lines in the input file that contain the relevant information of the material model that is selected.

Function writeResidualStresses:

As the function name suggests, the residual stresses obtained in the model module are written here into the input file.

Function writeSteps:

This function writes the analysis steps that need to be carried out later when reading the input file in Abaqus. It differentiates between the LBA and the GMNIA and writes the applied load depending on the loading situation. In the case of the GMNIA, this function writes the incrementation properties mentioned in section 5.2.1. For the LBA, the desired number of eigenvalues and eigenmodes is written. Furthermore, some key words are written that allow to export the LBA eigenmode in a .dat file to import it as an imperfection shape later for the GMNIA.

5.3.5. Data module

The data module contains some functions that are responsible for the data evaluation of the LBA and GMNIA results. These functions are retrieved in the main module and the evaluation module.

Function readEigenshapes:

This function reads the eigenmodes from the written .dat file (see section 5.3.4). Furthermore, it saves the corresponding eigenvalues.

Function readFracOfStepCompl:

There is a .msg file generated as soon as the Abaqus analysis is completed. The task of the function readFracOfStepCompl is to read this file and to extract the information at which iteration step the GMNIA was aborted. This is done by summing up all the completed time increments. Using this information, one can calculate the failure load later. Therefore, this function is only needed when evaluating a GMNIA.

Function readRefLoad:

In order to obtain the failure load with the help of the information of the previous function, one needs to know the reference load that was applied in the considered GMNIA. This is done by the function readRefLoad which reads the GMNIA input file and exports the required information.

Function readNumberOfIncr:

Similar to the readFracOfStepCompl function, this function reads the generated .msg file as well. However, the task of this function is to extract the number of increments needed during the GMNIA analysis and to compare this number to the maximum number of increments specified in chapter 5.2.1. The purpose of this function is to discover the cases where the selected maximum number of increments may be too small for the analysis. It may occur that the analysis is aborted due to this reason. Therefore, the written function does this short check and displays an error message if this was the case.

5.3.6. Evaluation module

The evaluation module is the module that is needed when one wants to evaluate the results of the GMNIA. This module refers to the functions of the data module and reads the failure loads of the considered models. Analogously to the main module, one can simply insert the name of the same .csv file at the very top. Furthermore, one needs to define the type of loading (pure compression, bending around the strong axis or bending around the weak axis) that was applied. Finally, the evaluation module automatically creates a new .csv file with all the failure loads of the considered profiles.

The following figure illustrates the process of evaluating the Abaqus results:

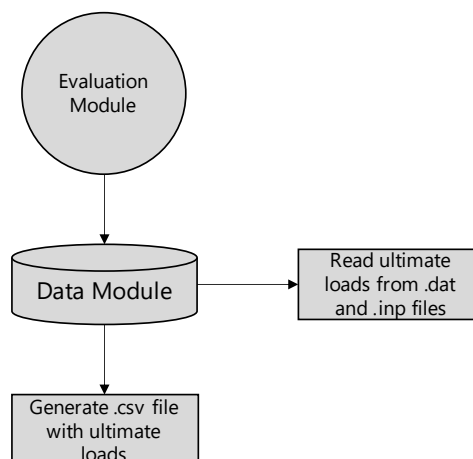


Figure 49: Illustration of the evaluation procedure

5.4. Evaluation of the Abaqus results

As explained in chapter 5.1, there are three investigations carried out for each profile and each load case: Once with the real measured cross-sectional dimensions, once with the nominal cross-sectional dimensions and once with the idealized cross-sectional dimensions introduced in chapter 4.3. Each derived cross-sectional resistance is normalized with respect to the result of the calculation with the nominal dimensions, leading to dimensionless quantities analogously to equation (6). Additionally, the results of the idealized cross-sections are compared to the ones of the real cross-sections in section 5.4.3.

It is pointed out that normally, one would apply some model uncertainty related partial factor γ_{FE} according to the standard prEN 1993-1-14 [17] when calculating a design resistance out of the results of a certain finite element calculation. However, this step is not necessary in the present case, as the results are normalized anyway, as described above.

5.4.1. Nominal cross-sections

The results of the nominal cross-sections are summarized in Appendix C.2. They build the basis for the normalization of the other cross-sections in the following chapters.

Additionally, the classification of the nominal cross-sections is done according to prEN 1993-1-1 [9] in the same way, as already done in Appendix C.1. When comparing the obtained cross-sectional resistances with the theoretical plastic failure loads according to prEN 1993-1-1 and considering the classification of the cross-sections, one can observe that the obtained resistances show a reasonable pattern. The higher the cross-sectional class, the lower is the obtained cross-sectional resistance compared to the theoretical plastic failure load and vice versa. This can be justified by the lower plastic deformation capacity of the cross-sections with a higher class. These observations can be seen as an additional model verification, as already similarly done in section 5.2.9. It is referred to Appendix C.2 for more details.

5.4.2. Real vs. nominal cross-sections

The obtained cross-sectional resistances of the real cross-sections can be found in Appendix C.3.1. Additionally, the normalization with respect to the obtained nominal resistance is given. Furthermore, the corresponding normalized sectional properties are displayed. This allows to check the plausibility of the results, as the normalized resistances should be close to the values of the corresponding normalized sectional properties (normal force close to area and bending moment close to the corresponding plastic section modulus). As most of the investigated cross-sections are class 1 or class 2 cross-sections according to the classification of prEN 1993-1-1 [9] (see classification of the nominal cross-sections in Appendix C.2), it is omitted to display the normalized values of the elastic section moduli as well. It is noted once again that for the real cross-sections the bending resistances vary depending on the sign of the applied load, as there is no double symmetry given. Therefore, the positive as well as the negative bending situation was investigated.

Moreover, the obtained normalized resistances of the real measured cross-sections are visualized in terms of scatter plots and histograms in Appendix C.3.2. Some QQ-plots for the theoretical normal and lognormal probability distributions using the procedure introduced in section 3.5.3 are shown in Appendix C.3.3.

In Table 38 and Table 39, the mean values and the coefficients of variation are presented for the derived normalized quantities for each category introduced in section 3. It is pointed out that in addition to the normalized cross-sectional resistances (N , M_y , M_z), the corresponding normalized sectional properties obtained in section 4.4 (A , $W_{pl,y}$, $W_{pl,z}$) are shown as well. The intention of this is to illustrate the influence and the deviations to the normalized cross-sectional resistances if one would calculate the resistances solely based on the sectional properties by multiplying them with the yield strength without considering the more advanced approaches introduced in section 5.

It is observed that the mean values of the normalized cross-sectional resistances are always smaller than the mean values of the corresponding sectional properties, the discrepancy varying between 0.15 % and 0.6 %. This pattern makes sense as in the current chapter, a more advanced investigation of the cross-sectional resistances was conducted considering for example the local buckling phenomenon. The largest discrepancies (up to 0.6 % depending on the considered category) between the normalized cross-sectional resistances and the corresponding normalized sectional properties are observed for bending around the weak axis. This is reasonable as the outer parts of the flanges are thinner than the inner parts (see section 3.4)

which promotes the local buckling phenomenon especially for bending around the weak axis, as for this loading situation the outer flange parts are loaded the most.

This observation of large discrepancies between the cross-sectional resistances and the sectional properties shows impressively that the sectional properties are just theoretical quantities. There are some factors such as the local buckling phenomenon that are not considered in the sectional properties. Therefore, the sectional properties should be treated with caution when one wants to calculate the cross-sectional resistance as accurate as possible. A more refined analysis is indispensable.

Table 38: Mean values of the cross-sectional resistances and sectional properties (real vs. nominal cross-sections)

cat.	$\frac{N_{real}}{N_{nom}}$	$\frac{M_{y,real,pos}}{M_{y,nom}}$	$\frac{M_{y,real,neg}}{M_{y,nom}}$	$\frac{M_{z,real,pos}}{M_{z,nom}}$	$\frac{M_{z,real,neg}}{M_{z,nom}}$	$\frac{A_{real}}{A_{nom}}$	$\frac{W_{pl,y,real}}{W_{pl,y,nom}}$	$\frac{W_{pl,z,real}}{W_{pl,z,nom}}$
Total	0.9935	0.9954	0.9955	0.9782	0.9765	0.9957	0.9975	0.9813
Small	0.9947	0.9969	0.9970	0.9802	0.9776	0.9972	0.9990	0.9827
Large	0.9915	0.9930	0.9930	0.9751	0.9747	0.9933	0.9952	0.9793
HEA	0.9931	0.9938	0.9939	0.9763	0.9746	0.9950	0.9960	0.9782
HEB	0.9891	0.9933	0.9935	0.9752	0.9721	0.9919	0.9952	0.9782
IPE	0.9993	1.0001	1.0001	0.9845	0.9845	1.0015	1.0024	0.9895

Table 39: Coefficients of variation (in %) for the cross-sectional resistances and sectional properties (real vs. nominal cross-sections)

cat.	$\frac{N_{real}}{N_{nom}}$	$\frac{M_{y,real,pos}}{M_{y,nom}}$	$\frac{M_{y,real,neg}}{M_{y,nom}}$	$\frac{M_{z,real,pos}}{M_{z,nom}}$	$\frac{M_{z,real,neg}}{M_{z,nom}}$	$\frac{A_{real}}{A_{nom}}$	$\frac{W_{pl,y,real}}{W_{pl,y,nom}}$	$\frac{W_{pl,z,real}}{W_{pl,z,nom}}$
Total	1.750	1.876	1.871	2.976	2.989	1.665	1.812	2.720
Small	1.864	2.002	2.004	3.213	3.232	1.780	1.938	2.971
Large	1.541	1.639	1.617	2.540	2.563	1.441	1.574	2.268
HEA	1.717	1.905	1.914	3.112	3.011	1.687	1.857	2.842
HEB	1.445	1.583	1.581	2.230	2.245	1.401	1.543	1.972
IPE	1.967	2.081	2.060	3.456	3.548	1.777	1.963	3.136

When looking at the coefficients of variation in Table 39, it is seen that they are a bit larger for the normalized cross-sectional resistances compared to the corresponding normalized sectional properties for each category. Therefore, the approaches introduced in section 5 seem to increase the variability of the results compared to the pure sectional properties.

When solely looking at the mean values of the obtained normalized cross-sectional resistances without considering the comparison with the sectional properties, one can derive additional conclusions. It is observed that the pure compression resistance of the real cross-sections is not far away from the pure compression resistance of the nominal cross-sections for some categories. The deviation to the nominal resistance is between 0.5 and 1.1 %, as can be seen in Table 38. The main reason for this is the production of thinner flange thicknesses compared to the nominal cross-section, as observed in section 3.4. This leads to a smaller area and an earlier occurrence of the local buckling phenomena due to the increased slenderness of the flanges. However, this effect seems to get attenuated by the fact that the webs are produced thicker than the nominal dimensions, leading to a larger web area which contributes to the pure compression resistance. The largest deviation of the pure compression resistance between the real and the nominal cross-section is observed for the HEB sections as there the comparatively thick and long flanges contribute the most to the cross-sectional area and consequently to the pure compression resistance. Conversely, the smallest deviation is obtained for the IPE sections as for these profiles the flanges are much shorter and the web has a larger contribution to the area there.

For bending around the strong axis, the discrepancy between the real and the nominal cross-sections is slightly less pronounced. However, for bending around the weak axis the differences between the real and the nominal cross-sectional resistances are highly pronounced (up to 2.8 % depending on the category). This can be explained by the increased significance of the flanges for the bending resistance around the weak axis. For the strong axis, the internal lever arm between the two flanges is way more important. For the weak axis, however, the bending resistance is developed primarily based on the flange dimensions. As the flanges are produced thinner for the real cross-sections compared to the nominal ones, the bending resistance consequently gets smaller. Furthermore, the fact that the outer parts of the flanges are produced significantly thinner than the inner parts (see section 3.4) even strengthens this effect, as the outer flange parts have the largest lever arm and therefore contribute the most to the bending resistance. Moreover, the thinner outer flange parts lead to earlier local instabilities due to the increased slenderness compared to the nominal cross-section. In Table 38, it is observed that the IPE sections show considerably larger normalized mean values for the bending resistances around the weak axis compared to the other categories. This can be explained by the smaller widths of the flanges compared to other profile types. Therefore, the thinner flanges do not have the same impact as for the other profile types.

As already indicated further above, there is a difference between the positive and the negative bending resistances, being more pronounced for the weak axis. This phenomenon is mainly based on three factors. Firstly, there may be different flange thicknesses on each half of the profile which leads to different slendernesses and consequently to different bending resistances depending on the sign of the bending moment. Secondly, there is a web eccentricity, as introduced in section 4.2.1. This web eccentricity modifies the flange slendernesses even further depending on the direction of the eccentricity. The difference between the positive and the negative bending resistance around the weak axis is significantly impacted by this. To show this effect, six fictive cross-sections are investigated separately in Appendix C.4.3. It is seen that even a small eccentricity can influence the discrepancy between the positive and the negative bending resistance. A positive web eccentricity induces a larger positive bending resistance compared to the negative one and vice versa when assuming constant flange thicknesses. This is based on the observation that for a positive web eccentricity the shorter flange half is under compressive stresses for a positive bending moment per definition of the chosen coordinate system. By considering the smaller slenderness of the shorter flange half, it's reasonable that the bending resistance is larger compared to the case when the more slender flange half is under compressive stresses.

The third factor is related to the second factor and is also investigated in Appendix C.4.3 for bending around the weak axis. It relates to the pattern of the residual stresses assumed in section 5.2.8. As a consequence of the absence of the double symmetry for the real cross-sections, the assumed residual stress state model automatically induces some bending action. The comparison of the results with and without introducing residual stresses demonstrates the influence of the assumed residual stresses impressively (see Appendix C.4.3). It is observed that the residual stress state increases the discrepancy between the positive and the negative bending resistance for all six investigated profiles compared to the case when neglecting the residual stress state. Depending on the investigated profile, the contribution to this discrepancy can be larger or smaller. It is pointed out that the applied residual stresses are just a modelling assumption used for this thesis. One could also utilize a different residual stress state model.

5.4.3. Real vs. idealized cross-sections

The cross-sectional resistances of the idealized cross-sections are displayed and visualized in Appendix C.4. Similar to the real cross-sections, the normalization with respect to the resistances of the nominal cross-sections as well as the corresponding normalized sectional properties are represented in order to check the plausibility of the results.

In the preceding subchapter, the results of the real cross-sections were studied by comparing them with the results of the nominal cross-sections. As an additional consideration, the idealized and the real cross-sections are compared among each other in the current chapter. Based on this, some valuable conclusions can finally be made.

The following table summarizes the mean values of the ratio between the real and the idealized cross-sectional resistances for the category "Total":

Table 40: Mean values of the cross-sectional resistances for category "Total" (real vs. idealized cross-sections)

	$\frac{N_{real}}{N_{ideal}}$	$\frac{M_{y,real,pos}}{M_{y,ideal}}$	$\frac{M_{y,real,neg}}{M_{y,ideal}}$	$\frac{M_{z,real,pos}}{M_{z,ideal}}$	$\frac{M_{z,real,neg}}{M_{z,ideal}}$
mean [-]	0.9993	0.9989	0.9990	0.9944	0.9927

More detailed tables containing the coefficients of variation and a subdivision into the individual categories can be found in Appendix C.4.3.

This comparison shows how one would over- or underestimate in average the cross-sectional resistances when assuming an idealized cross-section and without considering further aspects such as a potential web eccentricity. For pure compression and bending around the strong axis, the two approaches produce similar results. For bending around the weak axis, however, there are significant differences between the real and the idealized cross-sectional resistances (up to 1 % depending on the category). These discrepancies are mainly based on the fact that for the idealized cross-section a constant flange thickness was chosen. The real measured cross-sections, however, exhibit thinner thicknesses at the outer flange parts which reduces the resistance for bending around the weak axis primarily. Additionally, no web eccentricity was considered for the idealized cross-sections.

To conclude, one should be aware that when just measuring one flange thickness at the quarter points as described in the standard EN 10034 [2] and assuming a constant flange thickness, there may be a considerable overestimation of the cross-sectional bending resistance around the weak axis. Depending on the profile type, this overestimation can even get the magnitude of 1 % in average. It could be thought about considering this by choosing an appropriate safety factor when calibrating the resistance models in the standards, as the current Annex E of prEN 1993-1-1 [9] suggests a constant value for the flange thicknesses and does not consider a potential variability of the flange thicknesses in the cross-sectional plane, as seen in chapter 1.4.

It is pointed out that different assumptions behind the selected dimensions of the idealized cross-section will change the results significantly. Moreover, different results would be obtained when introducing other approaches for the real measured cross-section such as a non-linear transition between the inner and the outer flange thicknesses. The results of this thesis are only valid for the assumptions mentioned in chapter 4.2 and 4.3.

6. Summary & Conclusion

The present thesis addressed the topic of the consequences caused by deviations in the cross-sectional geometry of hot-rolled I-sections. As a first step, the cross-sectional dimensions of 561 cross-sections were measured and statistically evaluated. Due to accessibility reasons, the geometrical dimensions were measured at the ends of the beams. In a side investigation, however, it was proven that the imperfect geometry remains approximately constant along the whole length anyway. For the measured profile height, it was shown that only the height measured at the level of the web (h_{mid} in Figure 10) is representative for the height along the whole length. Furthermore, the accuracy of the measuring concept was proven by conducting repetitive measurements of the same geometrical quantity. However, this statement presumes the absence of systematic errors which cannot be excluded per se.

The statistical evaluation of the measured cross-sectional dimensions was done extensively for six different categories, as mentioned in section 3. For the flange thicknesses, it was observed that they are significantly thinner than the standardized nominal flange thicknesses. Additionally, the outer parts of the flanges are thinner than the inner parts which has a pronounced impact on the structural behaviour around the weak axis as the outer flange parts are responsible for the major part of the resistance in this case. Moreover, the outer flange parts are typically locations where connections to other structures are made, inducing additional forces at these parts. A reduced flange thickness may not provide enough resistance to take these forces. This aspect was not further investigated but should be kept in mind as well.

For the profile height and width, it was figured out that they are produced quite precisely in compliance with the standardized nominal dimensions. For the root fillet radii, large variations could be observed. However, the root fillet radii stated in the SZS C5/18 tables [7] are just recommendations and there are no values strictly standardized. Therefore, each producer can decide himself which radii to produce which is a potential source for the large variation observed. A further cause of this variation is the fact that the measuring process of the root fillet radii was quite prone to variations depending on the position of the measuring device as the radii are not perfect quarter circles.

The conducted correlation study showed that there is a large positive linear correlation between all measured flange thicknesses. A pronounced large correlation is observed between the inner and the corresponding outer flange thickness of the same flange half. Furthermore, a large positive linear correlation between the two measured profile widths could be identified.

To sum up, the recommended mean values of Annex E of the new draft standard prEN 1993-1-1 [9] could be confirmed based on the conducted measurement campaign. The only pronounced deviation could be observed for the web thickness, where the standard prEN 1993-1-1 suggests a mean value of $1.00 \cdot t_{w,nom}$, whereas the data of this thesis yields in a mean value which is 0.5-2 % larger depending on the considered category. For the derived coefficients of variation, some larger discrepancies could be observed compared to the values stated in Annex E of prEN 1993-1-1. It was identified that the stated values coincide quite well with the results of the large profiles. For the smaller cross-sections, however, significantly larger coefficients of variations were derived. Therefore, it is suggested to think about adjusting the structure of the values given in prEN 1993-1-1. A common value for all profile sizes is a severe simplification as for smaller cross-sections larger variations were observed for all measured dimensions.

In a second step, the influence of the imperfect geometry on the cross-sectional resistance was studied, focusing on three load cases: Pure compression, bending around the weak axis and bending around the strong axis. Firstly, this was done by calculating some sectional properties of the investigated cross-sections. As the estimation of the cross-sectional resistance purely based on the sectional properties is not a very accurate prediction, the resistances were examined further making use of the numerical finite element program Abaqus. In order to investigate the 561 cross-sections, a parametrized Python script was programmed.

It was observed that there are large discrepancies between the cross-sectional resistances of the nominal cross-sections compared to the ones of the real measured cross-sections. The main discrepancy could be observed for bending around the weak axis as the reduced flange thicknesses have a pronounced contribution to the resistance for this load case, as already mentioned above. Besides that, it was figured out that the occurring web eccentricity has a certain influence on the bending resistance around the weak axis as well, as the positive and negative bending resistance deviate from each other depending on the magnitude of the web eccentricity. Moreover, the comparison of the numerically derived cross-sectional resistances

with the pure sectional properties showed impressively that there is a certain overestimation of the resistance of the real cross-sections if it is estimated solely based on the sectional properties.

The introduction of an idealized cross-section with constant flange and web thicknesses helped to draw additional conclusions. It was identified that the cross-sectional resistance for bending around the weak axis is overestimated when assuming a constant flange thickness and therefore neglecting the variability of the flange thickness in the cross-sectional plane. In consequence, if one measures the flange thickness at the quarter points of the flanges (as stated in EN 10034 [2]) and assumes a constant flange thickness, the cross-sectional resistance may be overestimated. However, it is pointed out once again that these conclusions are only valid for the assumptions behind the idealized and the real cross-section introduced in the chapters 4.2 and 4.3. If one assumes non-linear transitions between the measurement points of the real cross-section for example, the results could change considerably. In order to investigate this aspect further, one would need to apply for example advanced, more accurate 3D scanning techniques to scan the whole cross-section geometry of the steel profiles.

The results of this thesis have interesting implications for the design practice. For example, the derived statistical information of the sectional dimensions and properties could be incorporated in a further step to detect the influences on the probability of failure, the reliability indices or the safety factors of the standards. This would then enable to optimize the design process and to achieve more reliable structures.

It is pointed out that the present thesis concentrated on the geometrical properties and neglected the influence of the statistical variation of some mechanical properties such as the yield strength. This could be done in a further step as well by considering different steel grades. A subsequent sensitivity analysis would show the relative significance of the variability of the cross-sectional geometry compared to the mechanical properties.

Furthermore, the study regarding the consequences on the structural behaviour was limited to the cross-sectional resistances. In a further step, it would be interesting to see some possible implications of the non-idealized cross-sectional geometry on member resistances by considering global instability phenomena. Moreover, combined loading situations such as a normal force acting together with a bending moment were not investigated during this thesis and would be interesting to study as well.

Finally, the focus of this thesis was lying on hot-rolled profiles. One could do similar investigations for cold-formed and welded profiles as well. It would be interesting to see how the production process can affect the variability of the cross-sectional dimensions and the cross-sectional resistance.

7. Bibliography

- [1] Prof. Dr.-Ing. Ulrike Kuhlmann, Prof. Dr. sc. techn. habil. Markus Knobloch, Univ.-Prof. em. Dr.-Ing. Joachim Lindner, Prof. Dr. techn. Andreas Taras, Fabian Jörg M. Sc., Anna-Lena Bours M. Sc.: Neue Entwicklungen in prEN 1993-1-1:2020. Stahlbau Kalender 2020, chapter 8, pp. 511-609, Stuttgart, 2020.
- [2] Europäisches Komitee für Normung: EN 10034; I- und H-Profil aus Baustahl: Grenzabmasse und Formtoleranzen. Brüssel, 1993.
- [3] Nicoleta Popa, Luís Simões da Silva, Trayana Tankova, Liliana Marques, Carlos Rebelo: SAFEBRICITILE: Standardization of Safety Assessment Procedures across Brittle to Ductile Failure Modes, RFSR-CT-2013-00023, final Report, 2016.
- [4] Melcher Jindrich, Kala Zdenek, Holicky Milan, Fajkus Miroslav, Rozlivka, Lubomir: Design characteristics of structural steels based on statistical analysis of metallurgical products. Elsevier Journal of Constructional Steel Research 60, pp. 795–808, 2004.
- [5] Ackermann Jonas, Reinhardt Melina: Datenerhebung und statistische Auswertung der Querschnittsabmessungen von Walzprofilen. Bachelor thesis, Zürich, 2022.
- [6] International Organization for Standardization: ISO Guide 98-3; Part 3: Uncertainty of measurement – Guide to the expression of uncertainty in measurement (GUM:1995). Geneva, 2008.
- [7] Stahlbau Zentrum Schweiz: Konstruktionstabellen, C5/18 steelwork, Zürich, 2018.
- [8] Dr. Lukas Meier: Statistik und Wahrscheinlichkeitsrechnung. Script of the lecture at ETH Zürich FS18, Zürich, 2018.
- [9] Europäisches Komitee für Normung: prEN 1993-1-1; Bemessung und Konstruktion von Stahlbauten –Teil 1-1: Allgemeine Bemessungsregeln und Regeln für den Hochbau; Deutsche und Englische Fassung; prEN 1993-1-1:2020
- [10] Ingenieurkurse.de: Technische Mechanik 2 Elastostatik – Übersicht Flächenträgheitsmomente für ausgewählte Querschnitte. <https://www.ingenieurkurse.de/technische-mechanik-elastostatik/balkenbiegung/flaechentraegheitsmomente/flaechentraegheitsmomente-in-abhaengigkeit-vom-koordinatensystem.html>, date of access: 24.03.2023.
- [11] Europäisches Komitee für Normung: EN 10365; Warmgewalzter U-Profilstahl, I- und H-Träger - Maße und Masse. Brüssel, 2017.
- [12] Schweizerischer Ingenieur- und Architektenverein: SIA 263/1; Stahlbau – Ergänzende Festlegungen, Zürich, 2020.
- [13] Prof. Dr. Bruno Sudret: Uncertainty Quantification in Engineering. Lecture material at ETH Zürich FS22, Zürich, 2022.
- [14] Jaquess, Timothy K.: Characterization of the Material Properties of Rolled Sections. Master thesis, University of Texas at Austin, December 1998.
- [15] Alpsten, G. A.: Variations in mechanical and cross-sectional properties of steel. Stålbyggnadsinstitutet, Publication No. 42. Proceedings of the international conference on the planning and design of tall buildings. Stockholm, 1972.
- [16] Prof. Dr. Eleni Chatzi, Dr. Patrick Steffen, Dr. Kostas Agathos: Method of Finite Elements I. Lecture material at ETH Zürich FS21, Zürich, 2021.
- [17] European Committee for Standardization: prEN 1993-1-14; Design of steel structures - Part 1-14: Design assisted by finite element analysis; prEN 1993-1-14:2020
- [18] Prof. Dr. A. Taras: Advanced Analysis and Design of Steel and Composite Structures. Lecture material at ETH Zürich FS22, Zürich, 2022.
- [19] ETH Zurich: ScientificComputing: Euler, <https://scicomp.ethz.ch/wiki/Euler>, date of access: 01.05.2023

- [20] Dassault Systemes: SIMULIA User Assistance 2021 Abaqus, https://help.3ds.com/2021/English/DSSIMULIA_Established/SIMACAECSTRefMap/simacst-c-mpc.htm?contextscope=all, date of access: 01.05.2023
- [21] Centre technique industriel de la construction métallique CTICM: EBPlate, version 2.01, <https://www.cticm.com/logiciel/ebplate/>, date of access: 01.05.2023.
- [22] Europäisches Komitee für Normung: prEN 1993-1-5; Bemessung und Konstruktion von Stahlbauten –Teil 1-5: Plattenförmige Bauteile; Deutsche und Englische Fassung; prEN 1993-1-5:2022
- [23] Python Software Foundation: Python Language Reference, version 3.8.10. Available at <http://www.python.org>, date of access: 02.05.2023
- [24] Dassault Systemes: Abaqus, Website: <http://www.simulia.com>, date of access: 02.05.2023
- [25] MIT - Massachusetts Institute of Technology: Abaqus documentation, <https://abaqus-docs.mit.edu/2017/English/SIMACAEGSARefMap/simagsa-c-absunits.htm>, date of access: 03.05.2023
- [26] Lucile Gérard, Liya Li, Markus Kettler, Nicolas Boissonnade: Recommendations on the geometrical imperfections definition for the resistance of I-sections. Elsevier Journal of Constructional Steel Research 162, 2019.
- [27] Bourke, Paul: Calculating the area and centroid of a polygon, <http://paulbourke.net/geometry/polygonmesh/>, date of access: 23.05.2023.
- [28] Preisinger, Clemens: Linking Structure and Parametric Geometry. Architectural Design, 83: 110-113, March 2013.
- [29] Robert McNeel & Associates: Rhinoceros 3D, Website: <https://www.rhino3d.com/>, date of access: 23.05.2023

8. List of figures and tables

Figure 1: Sensitivity analysis between input quantities and load-carrying capacity according to Melcher et al. [4]	4
Figure 2: Prescribed dimensions of hot-rolled I- and H-sections according to EN 10365 [11]	5
Figure 3: Excerpt of the standard EN 10034 [2]	6
Figure 4: Excerpt of the Annex E of the standard prEN 1993-1-1 [9]	7
Figure 5: Excerpt of the results of Melcher et al. [4]	8
Figure 6: Correlation matrix obtained by Melcher et al. [4]	9
Figure 7: Illustration of the investigated geometrical dimensions by Jaquess [14]	9
Figure 8: Variations of cross-sectional dimensions of 4816 H-shapes according to G. A. Alpsten [15]	10
Figure 9: Variations of sectional properties of 4816 H-shapes according to G. A. Alpsten [15]	11
Figure 10: Measuring procedure for height (left) and width (right)	12
Figure 11: Measuring procedure for the flange & web thicknesses	13
Figure 12: Measuring procedure for the root fillet radii	13
Figure 13: Measuring procedure to obtain the a-value	14
Figure 14: Caliper, electronic quick probe and radii measurement device	14
Figure 15: Longitudinal measurement quantities	15
Figure 16: Normalized flange thickness along the length of the beams	20
Figure 17: Normalized profile height along the length of the beams	20
Figure 18: Normalized profile width along the length of the beams	21
Figure 19: Normalized root fillet radius along the length of the beams	21
Figure 20: Plot of the normalized flange thickness $t_{f1,1}$ against the profile size (left) with the corresponding histogram (right)	27
Figure 21: Scatterplot of normalized outer flange thicknesses against normalized inner flange thicknesses	28
Figure 22: Histogram and probability density functions (normal and lognormal) for lower flange thickness	35
Figure 23: QQ-plot for lower flange thickness and normal distribution function	35
Figure 24: QQ-plot for lower flange thickness and lognormal distribution function	36
Figure 25: Excerpt of Annex E of prEN 1993-1-1 [9]	37
Figure 26: Tabulated moments of inertia [10]	42
Figure 27: Sketch of the modelled cross-section	43
Figure 28: Measured dimensions of the cross-section	45
Figure 29: Illustration of the used C3D20R elements	53
Figure 30: Bilinear material model used for the GMNIA [17]	54
Figure 31: Illustration of the chosen mesh pattern in Abaqus	54
Figure 32: Illustration of the selected mesh pattern in the roundings	55
Figure 33: Illustration of the mesh with exaggerated dimensions	55
Figure 34: Boundary conditions applied at the ends of the profile	56
Figure 35: Illustration of the multi-point constraints at the ends of the profile	56
Figure 36: Additional boundary conditions in the roundings (marked in red) in the case of bending around the strong axis	57
Figure 37: Exaggerated visualization of the global yielding around the weak axis when not considering the additional boundary conditions	57
Figure 38: Residual stresses for hot-rolled I-sections according to prEN 1993-1-14 [17]	60
Figure 39: Residual stresses modelled in Abaqus	60
Figure 40: EBPlate model of the IPE 160 web	61
Figure 41: Comparison of the buckling eigenmode for the Profile IPE 160 obtained with Abaqus (left) and EBPlate (right)	62
Figure 42: Failure pattern observed for CS 1/2 in the loading case "pure compression" (strongly inflated)	64
Figure 43: Load displacement curve (pure compression)	65
Figure 44: Moment rotation curve (strong axis)	66
Figure 45: Moment rotation curve (weak axis)	66
Figure 46: Illustration of the procedure for creating the Abaqus input files	67
Figure 47: Segmentation of the cross-section into eight parts	68
Figure 48: Differentiation between corner and edge nodes (2D case) and main and side nodes (3D case)	69
Figure 49: Illustration of the evaluation procedure	72

Table 1: Recommended distributions of geometrical properties according to SAFEBRICTILE [3]	8
Table 2: Calculated coefficients of variation according to the results of Melcher et al. [4].....	8
Table 3: Normalized mean values and coefficients of variation of sectional dimensions according to Jaquess [14].....	9
Table 4: Normalized mean values and coefficients of variation of sectional properties according to Jaquess [14]	10
Table 5: Selected statistical evaluation categories.....	18
Table 6: Results of the additional consideration regarding the longitudinal variation of the profile height	22
Table 7: Coefficients of variation along the length of the beams (in %).....	23
Table 8: Arithmetic mean values of the measured dimensions	24
Table 9: Coefficients of variation of the measured dimensions (in %).....	24
Table 10: Obtained 95 % confidence intervals for the investigated dimensions.....	24
Table 11: Obtained 95 % confidence intervals for the investigated dimensions stated in percentage values.....	25
Table 12: Mean values of the normalized flange thicknesses.....	25
Table 13: Coefficients of variation (in %) of the normalized flange thicknesses.....	26
Table 14: Correlation matrix of the measured flange thicknesses for the category "Total"	27
Table 15: Mean values of measurement data for the different categories (normalized quantities)	29
Table 16: Coefficients of variation (in %) for the different categories.....	29
Table 17: Correlation matrix for category "Total"	31
Table 18: Correlation matrix for category "Small"	31
Table 19: Correlation matrix for category "Large"	32
Table 20: Correlation matrix for category "HEA"	32
Table 21: Correlation matrix for category "HEB"	32
Table 22: Correlation matrix for category "IPE"	33
Table 23: Upper and lower reference values of the investigated profiles	37
Table 24: Correlation matrix for the measured IPE profiles in the size range 160-240.....	38
Table 25: Normalized mean values and coefficients of variation for the measured IPE profiles in the size range 160-240....	39
Table 26: Number of positive (+) and negative (-) tolerance exceedances.....	40
Table 27: Mean values of the sectional properties for the different categories (real vs. nominal cross-sections).....	47
Table 28: Coefficients of variation (in %) of the sectional properties for the different categories (real vs. nominal cross-sections).....	47
Table 29: Mean values and coefficients of variation for real vs. idealized sectional properties (category "Total").....	49
Table 30: Mean value and coefficient of variation of sectional properties for IPE 160-240 (real vs. nominal cross-sections).49	49
Table 31: Mean values and coefficients of variation ideal vs. nominal cross-sections (category "Total")	50
Table 32: Elastic properties modelled for the LBA.....	53
Table 33: Selected units in Abaqus (red) [25]	58
Table 34: LBA results of the Abaqus model.....	61
Table 35: Obtained critical buckling stresses using EBPlate	62
Table 36: Fictive cross-sections used for the GMNIA verification.....	63
Table 37: Obtained failure loads and normalization with theoretical plastic failure loads.....	64
Table 38: Mean values of the cross-sectional resistances and sectional properties (real vs. nominal cross-sections).....	74
Table 39: Coefficients of variation (in %) for the cross-sectional resistances and sectional properties (real vs. nominal cross-sections).....	74
Table 40: Mean values of the cross-sectional resistances for category "Total" (real vs. idealized cross-sections).....	76

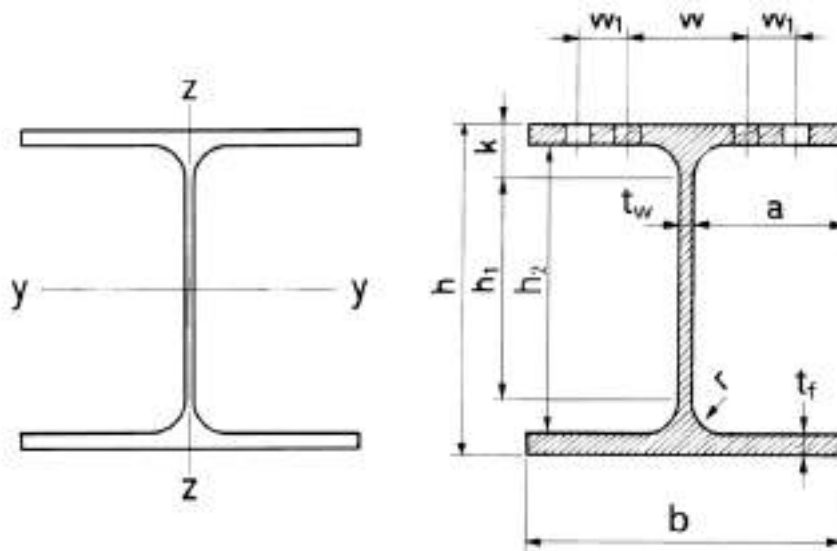
Appendix A – Cross-sectional dimensions

A.1 Nominal values of the sectional dimensions and properties

In this Appendix, the used nominal geometrical dimensions and sectional properties according to the SZS C5/18 tables [7] are displayed as a reference. It is emphasized that all values apart from the pure cross-sectional dimensions were recalculated in order to eliminate the rounding errors. The equations given in chapter 4.1 were used. For the further investigations, the unrounded values are used.

	h [mm]	b [mm]	t _w [mm]	t _r [mm]	r [mm]	h ₁ [mm]	a [mm]	h ₂ [mm]	A [mm ²]	I _y [mm ⁴]	W _{el,y} [mm ³]	W _{el,z} [mm ³]	I _z [mm ⁴]	W _{el,z} [mm ³]	W _{pl,z} [mm ³]	
IPE 160	160	82	82	5	7.4	9	127.2	38.50	145.2	2009.1	108662	123860	683144	16662	26100	
IPE 180	180	91	91	5.3	8	9	146	42.85	164	2394.7	146329	166415	1008503	22165	34600	
IPE 200	200	100	100	5.6	8.5	12	159	2848.4	183	2848.4	194317	220639	1423680	28474	44612	
IPE 220	220	110	110	5.9	9.2	12	177.6	52.05	201.6	3337.1	251985	285406	2048858	37252	58110	
IPE 240	240	120	120	6.2	9.8	15	190.4	56.90	220.4	3911.6	324032	366645	2836334	47272	73924	
IPE 270	270	135	135	6.6	10.2	15	219.6	64.20	249.6	4594.5	428873	483997	4198680	62203	96950	
IPE 300	300	150	150	7.1	10.7	15	248.6	71.45	278.6	5381.2	557074	628356	6037776	80504	125219	
IPE 330	330	160	160	7.5	11.5	18	271	76.25	307	6260.6	713146	803331	7881406	98518	153678	
IPE 360	360	170	170	8	12.7	18	298.6	81.00	334.6	7272.9	903647	10434504	122759	191099	229000	
IPE 400	400	180	180	8.6	13.5	21	331	85.70	373	8446.4	1156419	1307148	13178211	146225	229000	
IPE 450	450	190	190	9.4	14.6	21	378.8	90.30	420.8	9882.1	1499687	1701794	16758582	176406	276380	
IPE 500	500	200	200	10.2	16	21	426	94.90	468	11552.2	1927942	2194118	21416848	214168	335879	
IPE 550	550	210	210	11.1	17.2	24	467.6	99.45	515.6	13441.6	2440602	2787006	26675786	254055	400536	
IPE 600	600	220	220	12	19	24	514	104.00	562	15598.4	3069449	33873374	307940	485649	485649	
HEA 200	190	200	200	6.5	10	18	134	96.75	170	5383.1	386648	429485	13355079	133551	203818	
HEA 220	210	220	220	7	11	18	152	106.50	188	6434.1	54097044	512110	568458	1954590	177687	270594
HEA 240	230	240	240	7.5	12	21	164	116.25	206	7683.6	675060	744624	27688053	230734	351692	
HEA 260	250	260	260	7.5	12.5	24	177	126.25	225	8681.9	104549639	836397	919772	36675584	282120	430168
HEA 280	270	280	280	8	13	24	196	136.00	244	9726.4	136733079	1012838	1112224	47626367	340188	518132
HEA 300	290	300	300	8.5	14	27	208	145.75	262	11252.8	182635121	1259553	1383272	63095513	420637	641165
HEA 320	310	300	300	9	15.5	27	225	145.50	279	12436.8	229286071	1479265	1628090	69852309	465682	709739
HEA 340	330	300	300	9.5	16.5	27	243	145.25	297	13347.3	276931234	1678371	1850476	74359914	495733	755947
HEA 360	350	300	300	10	17.5	27	261	145.00	315	14275.8	330898082	1890846	2088474	78868356	525789	802277
HEA 400	390	300	300	11	19	27	298	144.50	352	15897.8	450694176	2311252	2561800	85638207	570921	872863
HEA 450	440	300	300	11.5	21	27	344	144.25	398	17802.8	637216587	2896439	3215868	94653253	631022	965530
HEA 500	490	300	300	12	23	27	390	144.00	444	19753.8	869748095	3549992	3948858	103670472	691136	1058512
HEA 550	540	300	300	12.5	24	27	438	143.75	492	21175.8	1119322546	4145639	4621818	108190417	721269	1106903
HEA 600	590	300	300	13	25	27	486	143.50	540	22645.8	1412081478	4786717	5350387	112713085	751421	1155656
HEB 200	200	200	200	9	15	18	134	95.50	170	7808.1	5696188	642548	20033672	200337	305812	
HEB 220	220	220	220	9.5	16	18	152	105.25	188	9104.1	80909684	735543	827048	28432645	258479	393881
HEB 240	240	240	240	10	17	21	164	115.00	206	10598.6	112593100	938276	1053146	39226557	326888	498418
HEB 260	260	260	260	10	17.5	24	177	125.00	225	11844.4	149194352	1147649	1282912	51345123	394962	602247
HEB 280	280	280	280	10.5	18	24	196	134.75	244	13136.4	192702826	1376449	1534434	65945170	471037	717571
HEB 300	300	300	300	11	19	27	208	144.50	262	14907.8	251656940	167713	1868675	85628224	570855	870141
HEB 320	320	300	300	11.5	20.5	27	225	144.25	279	16134.3	308235579	1926472	2149241	92388171	615921	939096
HEB 340	340	300	300	12	21.5	27	243	144.00	297	17089.8	366564166	2156260	2408107	96899304	645995	985720
HEB 360	360	300	300	12.5	22.5	27	261	143.75	315	18063.3	431934723	2399637	2682990	101411608	676077	1032489
HEB 400	400	300	300	13.5	24	27	298	143.25	352	19777.8	576805470	2884027	3231740	108190350	721269	1104035
HEB 450	450	300	300	14	26	27	344	143.00	398	21797.8	798875918	3550560	3982371	117213227	781422	1197656
HEB 500	500	300	300	14.5	28	27	390	142.75	444	23863.8	1071758175	4287033	4814568	126239132	841594	1291648
HEB 550	550	300	300	15	29	27	438	142.50	492	25405.8	1366909106	4970579	5590608	130768902	871793	1341142
HEB 600	600	300	300	15.5	30	27	486	142.25	540	26995.8	1710411478	5701372	6425137	135302374	902016	1391057

The following figures taken from the SZS C5/18 tables [7] serves as an illustration of the individual quantities:



A.2 Measurement results

A.2.1 General measurements

#	Description			Measurements																					
	Steel trader	Producer	Type	t _{r1,1}	t _{r1,2}	t _{r1,3}	t _{r1,4}	t _{r2,1}	t _{r2,2}	t _{r2,3}	t _{r2,4}	t _{w1}	t _{w2}	t _{w3}	h _{eff}	h _{mid}	h _{right}	b ₁	b ₂	a ₁	a ₂	r ₁	r ₂	r ₃	r ₄
				[mm]	[mm]	[mm]	[mm]	[mm]	[mm]	[mm]	[mm]	[mm]	[mm]	[mm]	[mm]	[mm]	[mm]	[mm]	[mm]	[mm]	[mm]	[mm]	[mm]	[mm]	[mm]
1	Spaeter	-	HEA 220	10.03	9.97	9.73	9.72	10.03	9.73	9.87	9.77	7.29	7.29	7.35	212.81	210.89	211.02	221.10	220.19	114.25	115.27	25.13	22.67	24.56	22.78
2	Spaeter	Thüringen	HEB 240	16.55	17.16	17.17	16.72	16.70	17.13	17.69	16.91	9.69	9.83	9.75	240.45	240.89	240.60	239.23	239.87	124.82	124.83	20.52	22.71	21.92	20.61
3	Spaeter	-	HEA 240	11.05	11.21	10.98	10.97	11.04	10.95	11.17	10.84	7.95	8.10	8.05	229.34	229.62	230.02	239.89	239.41	124.23	124.00	24.25	23.73	23.37	23.49
4	Spaeter	Arcelor Mittal	HEA 200	9.45	10.31	10.05	9.21	9.55	9.90	10.04	9.29	6.76	6.76	6.89	191.26	191.27	191.81	200.95	200.69	104.58	103.93	17.84	17.51	18.40	16.73
5	Spaeter	Thüringen	IPE 220	9.30	9.58	9.05	8.77	8.75	8.96	9.17	8.87	5.94	5.86	5.96	221.80	222.81	222.85	112.47	111.34	59.93	59.09	13.88	13.62	14.00	13.65
6	Spaeter	-	IPE 200	7.74	8.10	8.30	8.06	7.75	8.13	8.22	8.12	5.87	5.83	5.84	202.88	203.17	203.04	102.09	101.46	53.77	54.43	12.54	12.42	12.41	12.60
7	Spaeter	-	HEA 260	11.79	12.84	12.37	11.80	11.92	12.35	12.81	12.07	7.97	8.06	8.07	250.35	250.50	251.65	260.22	260.78	136.80	137.70	18.76	21.89	20.08	19.97
8	Spaeter	Peiner	HEA 220	9.61	9.94	9.87	9.63	9.77	10.02	10.02	9.57	7.37	7.28	7.18	209.90	210.00	209.37	220.94	220.19	114.89	114.27	22.13	23.33	23.57	23.33
9	Spaeter	Peiner	HEA 200	9.25	9.26	9.16	9.34	9.11	9.31	9.30	9.25	6.58	6.64	6.44	190.36	189.25	189.73	200.06	199.10	103.87	103.83	23.45	19.82	20.38	21.27
10	Spaeter	-	IPE 240	9.98	9.86	9.76	9.81	9.56	9.81	9.67	9.58	6.30	6.07	6.24	238.49	240.22	241.45	120.22	120.18	64.76	62.57	15.40	15.70	14.61	14.75
11	Spaeter	Arcelor Mittal	HEA 200	9.37	9.85	9.71	9.08	8.95	9.53	9.58	9.31	6.91	6.89	7.04	190.68	190.60	191.04	199.64	199.87	102.89	104.78	17.62	17.50	17.39	16.69
12	Spaeter	-	HEB 220	15.22	15.15	15.14	14.93	14.77	15.36	15.51	15.04	9.37	9.30	9.31	221.35	222.11	222.30	218.00	219.25	110.17	118.18	24.25	24.25	23.78	22.70
13	Spaeter	Peiner	HEB 220	14.71	14.98	14.87	14.58	14.93	14.90	14.86	14.41	9.16	9.36	9.34	223.44	221.30	219.17	221.24	220.18	114.48	116.05	23.65	24.34	24.56	23.86
14	Spaeter	-	HEB 280	17.53	18.10	18.27	17.39	17.06	18.12	17.85	17.36	10.55	11.11	10.85	280.08	278.82	277.80	278.52	277.51	146.26	143.68	21.05	27.74	24.30	24.21
15	Spaeter	Arcelor Mittal	HEB 450	24.64	25.45	25.62	25.03	24.64	25.22	25.68	25.10	13.19	13.14	13.28	449.95	450.77	451.32	300.80	301.55	158.26	156.36	26.72	24.72	28.18	27.90
16	Spaeter	Peiner	HEA 450	19.50	20.78	20.94	20.21	19.76	20.91	20.74	19.93	12.23	12.01	12.02	437.58	438.85	437.77	298.24	298.16	155.95	154.71	26.55	28.45	26.08	28.16
17	Spaeter	Peiner	HEB 300	17.66	18.99	19.00	18.69	17.86	19.28	19.23	18.32	11.56	11.33	11.23	303.22	302.71	302.03	300.20	300.33	156.10	154.70	27.01	25.34	27.78	26.58
18	Spaeter	Arcelor Mittal	HEA 300	13.50	14.16	13.56	13.09	13.55	13.90	13.84	13.19	8.13	7.93	7.94	292.93	291.96	291.18	299.66	299.18	152.83	154.71	26.10	24.62	26.51	25.67
19	Spaeter	Arcelor Mittal	HEA 300	13.37	14.06	13.51	13.27	13.19	13.66	13.55	13.19	8.46	7.92	8.29	292.68	292.15	292.88	299.81	298.98	152.69	155.13	27.31	25.11	25.90	23.69
20	Spaeter	Peiner	IPE 550	16.34	17.04	17.37	17.16	16.69	17.40	16.94	16.76	11.78	11.60	11.65	553.02	553.07	553.52	313.41	313.46	111.10	111.11	24.47	24.98	25.47	24.79
21	Spaeter	Arcelor Mittal	HEA 320	14.93	15.66	15.69	15.00	14.83	15.40	15.57	15.10	9.47	9.48	9.67	311.95	311.05	308.99	298.42	299.07	157.06	152.77	27.12	24.62	25.03	24.08
22	Spaeter	Peiner	IPE 300	10.31	10.57	10.19	10.34	10.28	10.11	10.49	10.32	7.01	6.90	7.03	302.35	301.65	301.01	151.23	149.30	78.47	78.68	15.04	15.42	15.44	15.23
23	Spaeter	Peiner	HEB 300	17.91	18.85	19.53	18.69	18.22	19.25	19.28	18.20	10.52	10.75	10.65	301.44	301.40	301.82	299.03	299.99	154.59	155.37	26.36	27.31	26.74	27.12
24	Spaeter	Peiner	HEB 500	27.12	28.32	28.54	27.61	26.73	28.14	28.50	27.85	14.48	14.32	14.55	500.01	499.47	498.82	300.80	300.76	157.97	158.09	25.32	25.41	26.36	27.20
25	Spaeter	-	HEB 500	26.84	27.07	28.47	27.69	26.91	28.03	28.37	27.57	14.35	14.34	14.54	499.50	500.04	499.81	300.78	300.80	158.59	157.21	25.32	25.64	27.20	25.67
26	Spaeter	-	IPE 500	15.37	16.05	15.88	15.70	15.02	15.52	15.57	15.37	10.49	10.39	10.58	503.08	503.17	503.88	300.67	299.90	105.51	105.51	21.33	20.58	20.08	21.11
27	Spaeter	Arcelor Mittal	IPE 300	9.91	10.28	10.09	10.70	10.51	10.92	10.36	9.90	7.45	7.19	7.09	302.24	302.09	301.24	151.89	152.27	79.66	79.73	13.49	13.08	13.08	13.55
28	Spaeter	Peiner	IPE 300	10.18	10.20	10.04	10.16	10.01	9.81	10.16	10.12	6.66	6.70	6.81	300.87	301.08	300.05	150.55	149.75	78.99	78.11	14.85	15.57	15.39	16.09
29	Spaeter	-	IPE 300	10.15	10.28	10.25	10.36	10.20	10.22	10.28	10.13	6.73	6.71	6.91	301.74	301.25	299.88	151.36	149.80	79.99	79.29	14.76	15.70	15.21	14.89
30	Spaeter	-	HEA 280	12.71	13.37	13.75	12.60	12.72	13.17	13.27	12.66	7.97	7.77	7.90	274.06	271.55	273.95	282.37	282.35	146.37	144.31	27.08	28.37	21.39	23.73
31	Spaeter	Peiner	IPE 300	10.37	10.66	10.45	10.71	10.48	11.00	10.30	10.23	7.05	7.17	6.84	300.22	301.23	301.35	150.75	150.00	78.21	79.30	15.36	14.55	13.64	15.16
32	Spaeter	Thüringen	HEA 280	12.40	12.90	12.83	12.47	12.64	13.05	13.14	12.41	7.93	7.90	7.97	270.57	271.79	273.28	281.28	280.66	145.64	143.94	23.21	23.57	24.75	23.78
33	Spaeter	Peiner	HEB 300	18.45	19.45	19.45	19.17	18.52	19.42	19.83	19.24	11.41	11.24	11.25	303.11	302.17	302.72	298.75	298.18	154.67	156.23	27.12	26.86	27.80	26.54
34	Spaeter	Arcelor Mittal	HEB 300	18.40	18.80	19.45	18.67	18.57	19.07	18.94	18.48	10.92	11.05	11.15	299.54	299.86	300.87	300.31	301.15	157.74	154.95	27.67	24.76	26.20	24.17
35	Spaeter	Arcelor Mittal	IPE 300	9.72	10.12	10.63	10.20	10.03	10.49	10.03	9.50	7.82	7.53	7.49	303.34	303.39	303.39	149.75	149.67	78.38	79.21	13.27	13.47	13.34	13.15
36	Spaeter	-	IPE 550	16.25	16.79	16.60	16.33	15.94	16.63	16.75	16.76	11.38	11.26	11.40	551.72	552.29	553.56	310.27	310.24	111.78	110.10	24.47	24.43	25.52	24.30
37	Spaeter	Arcelor Mittal	HEB 300	17.64	17.84	18.13	18.24	17.67	17.31	17.71	18.08	10.81	10.82	10.95	298.48	299.31	299.61	301.86	301.86	157.74	155.68	26.43	25.95	25.69	25.57
38	Spaeter	ACS Transit	HEA 320	15.18	15.79	14.98	14.70	15.04	15.45	15.69	15.16	9.64	9.57	9.65	312.49	312.04	314.36	297.84	297.32	153.38	154.36	26.36	25.03	26.24	25.32
39	Spaeter	Peiner	IPE 400	12.15	12.43	12.58	12.33	12.72	12.64	12.73	12.47	8.69	8.78	8.90	403.28	402.49	401.57	182.14	181.49	94.05	96.32	20.38	20.78	20.55	21.21
40	Spaeter	Peiner	HEB 340	20.87	21.53	21.61	21.11	20.85	21.83	22.02	21.47	11.34	11.24	11.14	339.84	340.19	340.63	299.16	299.32	153.14	158.14	26.88	25.88	27.62	27.69
41	Spaeter	Arcelor Mittal	HEA 320	15.11	15.76	15.30	14.69	15.08	16.03	15.53	14.88	9.94	9.56	9.63	311.95	311.08	310.17	297.90	298.84	151.65	155.88	26.88	24.05	24.88	26.03
42	Spaeter	Arcelor Mittal	HEA 600	24.27	24.58	24.58	24.09	24.52	24.17	25.03	24.40	13.47	13.32	13.55	590.43	593.52	595.62	301.51	302.11	158.41	156.61	31.62	30.77	30.44	32.89
43	Spaeter	Arcelor Mittal	HEA 300	18.91	19.38	18.67	18.32	18.64	18.87	19.00	18.50	10.60	10.66	10.73	304.82	303.68	305.14	300.04	300.81	156.06	156.64	27.33	24.73	24.34	27.69
44	Spaeter	Arcelor Mittal	HEB 340	20.55	21.49	21.00	20.45	20.41	20.81	21.20	20.41	12.19	12.09	12.21	345.05	341.18	342.65	299.78	299.33	157.23	155.05	25.86	24.83	24.99	25.86
4																									

#	Description			Measurements																					
	Steel trader	Producer	Type	t _{f1,1}	t _{f1,2}	t _{f1,3}	t _{f1,4}	t _{f2,1}	t _{f2,2}	t _{f2,3}	t _{f2,4}	t _{w1}	t _{w2}	t _{w3}	h _{eff}	h _{mid}	h _{light}	b ₁	b ₂	a ₁	a ₂	f ₁	f ₂	f ₃	f ₄
				[mm]	[mm]	[mm]	[mm]	[mm]	[mm]	[mm]	[mm]	[mm]	[mm]	[mm]	[mm]	[mm]	[mm]	[mm]	[mm]	[mm]	[mm]	[mm]	[mm]	[mm]	[mm]
81	Debrunner	Arcelor Mittal	HEB 340	20.91	21.58	21.88	21.58	21.29	22.15	22.03	21.56	12.93	13.04	12.88	343.40	343.19	345.01	297.97	297.89	155.50	154.57	24.13	25.86	26.36	23.94
82	Debrunner	-	HEB 340	21.48	21.88	21.91	21.16	21.52	22.02	21.61	20.81	12.37	12.51	12.61	345.18	343.58	343.31	298.92	298.32	155.45	156.11	24.08	26.22	23.62	26.46
83	Debrunner	Thüringen	HEB 340	19.79	20.54	20.90	20.36	19.54	20.44	20.73	20.89	12.84	12.71	12.58	344.00	342.45	341.18	298.08	298.38	157.12	154.69	27.03	27.27	26.88	27.33
84	Debrunner	Arcelor Mittal	HEB 360	20.69	22.10	22.24	21.65	20.01	21.89	22.34	21.54	13.05	13.12	13.17	365.05	363.76	363.72	299.55	300.04	156.94	156.41	26.84	27.03	26.68	26.74
85	Debrunner	Celsa Compagnia	HEB 360	21.41	21.44	21.52	21.83	21.50	21.52	21.37	22.54	12.58	12.93	12.66	363.72	362.37	359.76	302.77	301.14	158.81	155.89	23.34	25.48	28.62	26.08
86	Debrunner	Peiner	HEB 360	22.01	22.77	22.94	22.28	22.35	22.36	22.34	21.83	12.52	12.47	12.50	364.42	364.84	363.86	298.19	299.17	154.46	156.91	24.78	26.32	25.99	23.92
87	Debrunner	Peiner	HEB 360	21.00	21.80	21.90	21.30	20.79	21.73	21.35	21.21	12.70	12.78	12.54	361.48	361.24	362.72	299.62	300.12	158.45	154.75	26.62	27.27	26.80	28.23
88	Debrunner	Peiner	HEB 360	20.97	21.72	21.02	21.34	20.88	21.89	22.02	21.18	12.73	12.76	12.64	361.31	361.01	362.87	299.50	299.88	157.16	155.48	26.42	29.75	26.26	28.45
89	Debrunner	-	HEB 500	26.53	28.08	28.28	27.78	26.89	27.86	27.04	27.62	14.84	14.66	14.77	500.98	500.91	500.35	299.64	299.29	157.22	157.32	25.71	25.77	26.07	29.72
90	Debrunner	Peiner	HEB 360	21.57	22.48	22.47	22.08	21.73	22.40	22.86	22.31	12.14	12.21	11.99	363.32	360.79	361.11	298.55	297.91	154.36	156.15	26.58	28.45	25.03	29.61
91	Debrunner	Arcelor Mittal	HEB 550	27.60	27.91	28.70	28.33	27.65	28.27	28.54	28.35	14.33	14.08	14.39	551.54	552.40	552.45	299.83	299.26	156.47	157.06	24.64	26.62	26.58	25.82
92	Debrunner	Arcelor Mittal	HEB 600	29.22	29.72	30.32	30.04	29.92	30.87	29.74	28.86	15.29	15.13	15.30	600.79	601.28	600.78	299.89	300.19	160.30	156.53	29.53	29.75	29.86	29.50
93	Debrunner	Peiner	HEA 200	8.73	9.18	9.31	9.15	9.12	9.32	9.33	8.87	6.60	6.96	6.71	191.87	191.61	193.09	201.70	200.05	105.03	102.99	17.77	20.21	21.75	19.82
94	Debrunner	Arcelor Mittal	HEA 300	13.18	13.34	14.00	13.98	13.36	13.62	14.33	13.92	9.12	8.92	8.90	293.06	291.47	293.70	302.86	302.72	156.34	156.27	22.56	28.50	26.97	27.55
95	Debrunner	Thüringen	HEA 220	10.70	10.81	10.70	10.40	10.42	10.76	10.94	10.51	7.08	7.00	7.00	212.47	211.96	212.74	220.32	220.88	114.73	113.51	20.02	20.36	20.38	20.44
96	Debrunner	Arcelor Mittal	IPE 220	8.37	8.65	8.71	8.46	8.88	9.12	9.05	8.79	6.14	6.01	6.20	218.75	218.76	219.16	211.02	212.76	110.52	109.76	15.86	17.19	13.45	13.00
97	Debrunner	Arcelor Mittal	IPE 160	7.10	7.52	7.25	7.10	7.24	7.45	7.59	7.48	5.39	5.59	5.35	160.20	160.65	161.51	83.12	83.00	45.43	43.31	9.37	9.15	9.27	9.36
98	Debrunner	Arcelor Mittal	IPE 180	7.57	7.88	7.78	7.56	7.87	8.07	7.85	7.76	5.89	6.01	5.89	180.52	180.62	180.95	91.81	91.58	49.54	48.38	8.99	8.94	9.01	9.08
99	Debrunner	Peiner	HEB 340	19.91	21.15	21.38	21.12	20.53	21.45	21.59	20.62	12.13	12.47	12.15	340.99	341.44	342.17	300.48	299.69	156.86	157.03	28.40	23.92	27.42	28.28
100	Debrunner	Arcelor Mittal	IPE 220	8.30	8.80	8.91	8.66	8.49	8.77	8.49	8.34	6.19	6.14	6.41	222.62	223.09	222.88	110.74	111.20	60.27	57.03	13.10	13.62	13.07	13.58
101	Debrunner	Arcelor Mittal	HEB 200	14.63	15.43	14.45	13.72	13.79	14.25	14.42	14.88	9.20	9.38	9.43	199.10	200.07	200.02	200.25	200.71	105.11	104.86	17.41	18.22	19.29	17.27
102	Debrunner	Peiner	HEB 220	14.80	15.26	15.15	14.68	14.75	15.82	14.84	14.57	9.61	9.60	9.34	223.55	221.52	219.57	221.18	219.69	113.61	116.56	25.22	24.30	25.18	23.37
103	Debrunner	Thüringen	HEB 240	16.51	16.97	16.93	16.79	16.71	17.00	17.13	16.78	10.05	10.21	10.01	238.96	239.76	239.04	241.02	240.81	125.07	125.36	20.19	23.49	23.01	20.72
104	Debrunner	Thüringen	HEB 240	16.58	16.96	17.57	16.76	16.60	16.99	17.15	16.75	10.01	10.21	10.00	238.74	240.14	239.54	240.96	240.94	125.52	125.97	21.33	22.78	23.45	20.41
105	Debrunner	Peiner	HEB 300	18.32	19.00	19.40	18.84	18.15	19.12	19.44	19.05	11.41	11.70	11.40	300.93	300.87	301.22	299.37	299.69	155.43	157.78	26.97	27.67	25.53	26.46
106	Debrunner	Celsa Compagnia	HEA 280	12.21	11.90	12.28	12.18	12.43	12.53	12.41	12.71	8.68	8.85	8.70	277.35	273.36	274.75	279.42	279.14	144.24	144.66	23.86	23.82	28.76	20.38
107	Debrunner	Arcelor Mittal	HEA 300	14.25	15.01	15.01	14.16	14.42	15.55	15.23	14.62	9.01	9.08	9.12	294.13	293.80	289.75	299.97	300.82	156.08	155.00	20.49	26.12	26.67	28.43
108	Debrunner	Thüringen	HEA 340	16.13	16.86	16.59	16.56	16.44	16.82	16.76	16.52	9.10	9.30	9.14	334.17	332.73	332.65	300.69	301.63	153.63	156.32	25.35	26.08	26.50	24.17
109	Debrunner	Arcelor Mittal	HEA 550	23.90	24.64	24.28	23.83	23.55	23.55	24.72	23.71	13.50	13.16	13.06	541.89	541.97	544.29	301.02	302.01	157.55	157.41	26.64	25.21	25.34	26.34
110	Debrunner	Peiner	HEB 320	18.94	20.13	20.32	19.63	18.72	19.97	20.41	19.40	12.51	12.20	12.20	323.16	322.65	320.82	300.53	298.93	153.94	158.88	26.74	27.40	25.86	27.46
111	Debrunner	Peiner	HEB 450	24.71	25.91	26.19	25.44	24.98	25.98	25.95	25.21	14.21	14.45	14.26	447.61	448.88	449.12	299.09	299.32	156.53	157.72	26.43	30.18	26.97	27.29
112	Ferroflex	Thüringen	HEA 300	13.60	14.11	14.25	13.96	13.74	14.24	14.19	13.75	8.20	8.35	8.41	292.94	292.30	293.95	299.84	300.50	155.97	153.07	26.74	27.18	28.40	26.42
113	Ferroflex	Peiner	IPE 600	18.30	18.66	18.86	18.44	17.92	18.48	18.59	18.66	11.63	11.76	12.02	602.89	603.35	605.21	218.22	219.34	115.57	114.99	23.23	24.25	24.03	23.90
114	Ferroflex	Thüringen	IPE 550	17.20	17.73	17.51	17.31	17.14	17.60	17.52	17.18	11.10	10.88	11.02	553.65	550.66	549.25	210.30	211.03	108.97	112.41	25.93	25.28	24.10	25.37
115	Ferroflex	Thüringen	IPE 500	15.79	16.20	15.98	15.80	16.71	16.81	16.88	16.55	10.14	10.05	10.26	499.23	499.38	500.37	200.74	202.47	106.08	105.74	22.90	23.78	24.52	22.75
116	Ferroflex	Thüringen	IPE 500	15.86	16.22	16.07	15.76	15.88	16.09	16.32	16.60	10.10	10.03	10.33	503.23	503.50	505.06	201.72	202.61	106.20	105.20	23.21	21.85	21.75	23.05
117	Ferroflex	Thüringen	IPE 500	15.77	16.21	16.00	15.81	15.55	15.48	15.52	15.53	10.39	10.52	10.54	500.67	501.30	502.28	199.98	200.40	105.00	105.90	22.82	22.67	23.49	22.20
118	Ferroflex	Thüringen	IPE 450	13.72	14.22	14.20	13.94	13.72	14.08	14.21	13.93	9.45	9.51	9.50	449.07	448.70	448.44	190.49	190.46	99.00	100.51	21.02	21.66	20.13	21.59
119	Ferroflex	-	IPE 450	13.74	14.11	14.14	13.85	13.54	13.88	13.83	13.62	9.05	9.00	9.12	450.75	450.48	450.58	191.50	190.62	99.85	100.34	25.20	20.19	21.82	21.36
120	Ferroflex	Peiner	IPE 400	12.98	13.04	12.78	12.76	12.59	12.80	13.25	12.89	8.61	8.47	8.36	402.77	402.93	400.56	180.70	181.52	93.10	96.87	21.36	21.21	21.30	21.59
121	Ferroflex	Thüringen	IPE 360	12.18	12.45	12.38	12.21	12.12	12.49	12.55	12.42	8.38	8.37	8.36	363.63	363.34	363.14	170.39	170.27	88.48	90.60	17.86	18.59	17.92	18.55
122	Ferroflex	Thüringen	IPE 360	12.64	12.93	12.80	12.61	12.70	12.90	13.00	12.81	8.13	8.13	8.10	361.84	360.94	361.07	170.60	169.72	88.81	90.37	17.77	18.99	17.88	18.87
123	Ferroflex	Thüringen	IPE 330	10.86	11.19	11.07	10.78	10.68	11.05	10.91	10.61	7.95	8.11	8.03	333.30	332.89	333.57	161.00	161.10	84.89	85.40	17.37	16.10	16.42	16.58
124	Ferroflex	-	IPE 330	10.81	11.31	11.18	11.03	11.00	11.21	11.46	11.19	7.93	8.03	7.88	330.83	330.47	330.69	159.79	160.20	83.30	84.66	15.94	16.51	16.29	16.8

#	Description			Measurements																					
	Steel trader	Producer	Type	$t_{r1,1}$	$t_{r1,2}$	$t_{r1,3}$	$t_{r1,4}$	$t_{r2,1}$	$t_{r2,2}$	$t_{r2,3}$	$t_{r2,4}$	t_{w1}	t_{w2}	t_{w3}	t_{heff}	t_{hmid}	t_{hight}	b_1	b_2	a_1	a_2	r_1	r_2	r_3	r_4
				[mm]	[mm]	[mm]	[mm]	[mm]	[mm]	[mm]	[mm]	[mm]	[mm]	[mm]	[mm]	[mm]	[mm]	[mm]	[mm]	[mm]	[mm]	[mm]	[mm]	[mm]	[mm]
161	Ferroflex	Thüringen	HEB 300	18.91	19.32	19.14	18.85	18.74	19.12	19.16	18.85	10.80	10.95	10.81	298.35	298.60	300.02	299.32	300.02	154.08	156.76	29.75	28.01	30.21	26.05
162	Ferroflex	-	HEB 280	12.34	12.93	13.43	12.46	12.32	13.48	12.84	12.30	7.94	8.05	7.84	266.71	267.70	267.27	280.17	280.33	145.77	143.38	27.55	22.10	29.89	34.43
163	Ferroflex	Peiner	HEA 220	9.69	9.90	9.91	9.72	10.13	10.09	10.06	9.66	7.01	7.27	7.06	212.52	212.08	213.75	218.09	217.38	113.59	111.75	24.12	25.62	25.47	24.43
164	Ferroflex	Thüringen	IPE 220	9.08	9.18	9.29	9.05	9.00	9.22	9.31	9.06	5.82	5.85	5.81	221.46	221.47	220.91	110.88	111.23	59.48	58.63	13.64	13.48	13.68	13.60
165	Ferroflex	-	HEB 280	17.81	18.17	18.11	17.81	17.80	18.06	18.12	17.52	9.97	10.19	10.06	281.84	281.40	281.33	280.69	279.79	146.01	145.18	20.64	28.10	24.34	25.47
166	Ferroflex	Peiner	HEB 220	15.00	15.35	15.31	15.07	15.36	15.08	15.13	15.09	8.89	9.12	8.98	224.86	224.35	223.65	219.57	219.71	113.77	114.77	27.86	22.82	25.62	23.99
167	Ferroflex	-	HEB 260	16.48	16.58	16.95	16.54	17.01	17.22	17.00	16.72	9.63	9.95	9.81	265.62	264.15	263.44	260.20	260.13	136.32	134.84	28.17	22.86	25.27	21.62
168	Ferroflex	-	HEA 260	12.31	13.12	12.94	12.55	12.50	13.00	13.04	12.48	7.16	7.25	7.25	250.39	250.99	250.69	260.83	261.04	133.80	134.61	23.49	27.20	26.25	24.25
169	Ferroflex	-	HEA 280	12.45	13.13	13.27	12.58	12.42	13.30	13.15	12.66	8.03	8.15	8.12	274.03	272.48	273.15	281.85	281.10	145.73	144.83	25.98	25.57	27.14	23.37
170	Ferroflex	-	HEB 240	15.73	15.61	16.12	15.46	15.46	15.91	15.95	15.45	9.75	9.75	9.49	241.42	242.31	242.97	239.59	240.72	126.26	123.86	31.93	22.60	24.84	25.94
171	Ferroflex	Thüringen	HEA 300	13.63	14.34	14.21	13.99	13.73	14.15	14.23	13.89	8.15	8.35	8.38	292.98	292.16	293.94	299.80	300.56	155.92	153.36	26.26	26.50	26.58	27.46
172	Ferroflex	Peiner	IPE 600	18.18	18.69	19.00	18.63	17.79	18.48	18.69	18.60	11.68	11.86	12.19	602.83	603.47	604.82	219.42	220.63	115.31	116.65	22.63	22.56	24.03	24.94
173	Ferroflex	SWT	IPE 550	17.15	17.58	17.54	17.26	17.23	17.47	17.74	17.17	11.10	10.91	10.99	553.78	550.44	549.30	210.25	211.61	109.21	112.44	25.88	24.70	24.90	26.03
174	Ferroflex	Thüringen	IPE 500	15.87	16.09	15.99	15.84	16.74	16.95	16.88	16.54	10.20	10.14	10.29	499.23	499.72	500.46	200.85	202.43	106.31	105.43	23.01	23.61	24.30	22.67
175	Ferroflex	Thüringen	IPE 500	15.88	16.11	16.31	15.68	15.98	16.18	16.24	15.71	10.22	10.13	10.33	503.31	503.58	505.06	201.80	200.55	106.16	105.39	23.61	22.41	24.31	23.05
176	Ferroflex	Peiner	IPE 500	16.55	16.78	16.28	16.14	15.05	15.32	16.15	16.04	10.17	10.02	10.17	500.01	499.89	500.29	200.70	200.68	106.41	104.88	20.93	20.99	21.08	20.78
177	Ferroflex	SWT	IPE 500	15.72	15.92	15.73	15.66	15.56	15.50	15.74	15.49	10.43	10.57	10.65	500.67	501.30	502.26	199.98	200.44	105.15	105.76	22.20	23.29	23.37	22.06
178	Ferroflex	Peiner	HEB 500	26.24	27.50	27.60	26.80	26.18	27.60	27.89	26.85	15.03	14.69	14.77	501.36	503.44	502.74	300.34	300.34	100.49	156.75	26.86	26.55	25.41	26.95
179	Ferroflex	-	IPE 330	11.08	11.17	11.28	10.92	11.17	11.45	11.21	11.01	7.87	8.00	7.81	331.35	330.44	330.53	160.18	160.25	84.84	83.71	19.24	17.11	18.99	17.98
180	Ferroflex	Arcelor Mittal	HEA 300	13.84	14.17	14.12	13.55	13.71	13.66	14.34	13.83	8.62	8.58	9.02	293.31	290.32	292.72	299.48	290.70	156.09	152.74	26.42	25.10	25.62	25.73
181	Ferroflex	Arcelor Mittal	HEA 300	13.94	14.25	14.22	13.58	13.75	13.63	13.23	13.72	8.72	8.64	9.04	292.98	290.39	291.51	299.20	299.51	155.22	153.20	25.01	25.67	25.34	26.47
182	Ferroflex	-	HEA 340	15.90	16.51	16.77	16.22	16.15	16.80	16.26	16.47	9.35	9.45	9.36	332.54	333.00	330.23	300.67	299.93	155.17	155.15	27.78	24.62	24.52	26.38
183	Ferroflex	-	HEA 340	16.08	16.51	16.54	16.13	16.16	16.60	16.68	16.31	9.60	9.59	9.54	328.81	329.59	326.66	299.86	299.62	152.09	157.93	26.64	26.64	26.43	26.80
184	Ferroflex	-	HEA 400	18.55	19.19	19.30	18.67	18.61	19.38	19.36	18.74	10.82	10.85	10.85	388.17	388.68	384.00	300.60	300.45	156.93	155.04	28.06	24.90	26.84	27.16
185	Ferroflex	-	HEB 360	22.14	22.71	22.59	22.41	22.11	22.52	22.52	22.26	12.41	12.43	12.55	364.56	363.39	362.93	301.36	300.36	157.66	155.69	27.85	27.38	27.62	23.91
186	Ferroflex	Arcelor Mittal	HEA 600	23.63	23.71	23.47	23.34	23.87	24.03	23.74	23.69	13.06	12.75	13.07	595.92	593.86	594.22	300.65	299.73	157.30	155.59	31.62	30.15	28.77	33.63
187	Ferroflex	-	HEA 450	19.67	20.88	21.15	20.65	19.78	20.85	20.19	20.52	12.20	12.11	12.00	445.56	445.29	444.87	299.55	299.58	156.44	155.35	28.11	26.70	28.23	26.97
188	Ferroflex	Peiner	HEA 450	19.13	20.33	20.39	19.88	19.38	20.45	21.10	19.97	12.58	12.11	12.38	441.94	442.57	443.82	299.76	299.12	155.34	156.33	26.12	26.97	26.14	26.92
189	Ferroflex	Peiner	HEA 500	21.43	22.97	22.45	22.13	21.50	23.04	23.77	22.24	12.59	12.55	12.51	490.92	492.24	493.88	299.90	298.55	155.84	156.31	27.60	26.74	25.06	26.26
190	Ferroflex	Peiner	HEA 550	22.63	23.61	23.85	22.80	22.49	23.54	23.77	22.88	12.72	12.76	12.80	540.28	540.32	540.87	298.97	298.92	155.54	156.62	25.58	29.64	26.47	27.12
191	Ferroflex	-	HEA 550	23.05	23.41	22.86	22.42	23.45	23.69	22.68	22.42	12.59	12.53	12.70	546.01	544.32	544.94	300.86	301.37	156.92	156.76	24.57	30.72	26.08	23.27
192	Ferroflex	Peiner	HEA 340	15.26	16.14	16.98	16.20	15.66	16.36	16.48	16.15	9.07	9.25	9.45	330.86	330.03	329.57	298.53	298.33	152.79	155.44	25.42	30.12	27.55	27.46
193	Ferroflex	SWT	HEA 360	17.87	18.05	18.01	17.64	17.72	18.10	17.90	17.61	9.71	10.01	10.02	354.25	354.66	355.94	300.62	301.12	156.17	155.13	25.42	26.66	26.51	25.69
194	Ferroflex	-	HEB 340	21.08	21.29	21.52	21.15	20.82	20.98	21.35	20.78	11.87	11.99	11.91	340.02	340.51	337.94	301.42	301.40	156.55	157.37	24.91	29.40	24.32	27.74
195	Ferroflex	Peiner	HEB 550	27.53	28.58	28.59	28.20	27.57	28.77	28.93	28.38	15.10	15.14	15.15	550.87	549.93	549.80	300.33	298.55	156.73	158.71	26.50	29.40	29.34	25.84
196	Ferroflex	Arcelor Mittal	HEB 600	29.50	29.51	29.57	29.57	28.83	29.51	29.88	29.42	15.48	15.26	15.27	602.61	602.46	605.28	298.98	298.52	155.74	158.19	32.33	31.46	30.50	35.39
197	Ferroflex	Arcelor Mittal	HEB 600	28.91	28.01	27.80	27.92	29.22	28.08	28.71	28.71	15.54	15.48	15.48	606.80	603.94	604.13	301.43	301.06	156.06	166.86	31.95	33.11	32.19	32.82
198	Ferroflex	ACS Transit	HEB 600	29.44	29.94	29.41	29.39	29.20	29.58	29.36	29.08	14.97	15.13	15.27	608.06	603.52	606.36	298.47	297.12	156.70	156.58	32.29	30.89	31.75	39.93
199	Ferroflex	Peiner	HEB 550	27.22	28.07	28.57	28.05	27.44	28.06	28.61	27.78	14.89	14.64	14.64	552.80	552.02	553.78	300.18	299.19	156.10	158.57	26.28	28.08	26.38	26.50
200	Ferroflex	-	HEB 500	27.71	28.72	28.54	28.82	27.37	28.34	28.54	28.36	13.43	13.35	13.73	497.11	498.52	499.76	298.21	298.73	154.55	157.73	26.51	28.35	25.64	28.52
201	Ferroflex	Peiner	HEB 450	24.37	25.68	25.89	25.27	24.24	25.31	26.10	25.20	10.42	10.41	14.51	452.32	452.67	455.24	301.96	301.36	157.83	158.76	26.95	29.32	27.33	28.06
202	Ferroflex	-	HEB 450	24.20	24.91	25.32	24.44	24.49	25.08	24.81	23.80	13.55	13.54	13.63	451.67	451.19	450.15	299.77	300.19	156.45	157.43	26.16	24.83	24.94	24.18
203	Ferroflex	-	HEB 360	22.15	22.31	22.37	22.01	21.93	22.27	22.29	22.11	12.27	12.51	12.42	357.77	360.51	362.27	300.78	300.78	156.90	156.46	28.62	24.96	26.47	29.42
204	Ferroflex	-	HEB 400	23.42	24.32	24.24	23.77	23.72	24.08	24.69	24.06	14.20	14.03	14.15	400.86	400.25	402.35	299.11	297.64	157.83					

#	Description			Measurements																					
	Steel trader	Producer	Type	t _{1,1}	t _{1,2}	t _{1,3}	t _{1,4}	t _{2,1}	t _{2,2}	t _{2,3}	t _{2,4}	t _{w1}	t _{w2}	t _{w3}	h _{eff}	h _{mid}	h _{right}	b ₁	b ₂	a ₁	a ₂	f ₁	f ₂	f ₃	f ₄
				[mm]	[mm]	[mm]	[mm]	[mm]	[mm]	[mm]	[mm]	[mm]	[mm]	[mm]	[mm]	[mm]	[mm]	[mm]	[mm]	[mm]	[mm]	[mm]	[mm]	[mm]	[mm]
241	Spaeter	-	IPE 400	13.08	13.07	13.25	13.44	12.93	13.28	13.44	13.25	8.22	8.14	8.42	400.77	400.15	400.13	179.66	179.42	93.75	94.11	22.45	21.46	19.74	22.16
242	Spaeter	-	HEB 600	27.97	29.23	30.35	28.84	28.35	29.56	29.88	28.65	15.73	15.37	15.61	596.58	598.40	598.34	298.44	298.44	156.87	156.86	26.90	29.53	27.97	28.35
243	Spaeter	-	HEB 600	28.08	29.19	29.86	28.79	28.60	29.84	30.17	29.00	15.85	15.88	15.91	598.31	599.14	598.64	299.23	299.55	157.38	157.88	26.74	30.12	27.62	29.34
244	Spaeter	-	HEB 600	27.96	29.31	29.72	28.85	28.50	29.65	29.64	28.79	15.83	15.91	16.02	598.20	598.71	597.85	299.23	299.47	156.60	158.51	27.83	29.40	28.01	28.47
245	Spaeter	-	HEA 340	16.07	16.76	16.82	16.39	16.44	16.95	17.00	16.53	9.28	9.33	9.33	334.26	332.38	334.65	300.41	300.65	154.80	155.17	25.51	26.26	29.21	23.51
246	Spaeter	-	IPE 400	13.07	13.58	13.63	13.32	13.27	13.64	13.70	13.29	8.51	8.48	8.40	402.78	401.32	401.21	180.39	181.00	94.90	94.16	21.56	22.27	20.41	22.10
247	Spaeter	-	HEB 340	22.41	21.64	20.70	20.07	21.07	21.09	21.18	21.14	12.37	12.58	12.55	343.48	343.13	343.14	299.58	298.65	156.74	155.57	27.92	25.99	26.78	25.97
248	Spaeter	Peiner	HEA 320	14.05	14.81	14.97	14.49	14.42	15.12	15.07	14.33	9.41	9.41	9.44	309.94	310.10	311.11	298.69	299.37	156.52	152.15	25.91	27.69	25.91	27.58
249	Spaeter	Arcelor Mittal	HEB 300	18.42	19.08	19.10	18.90	18.30	18.88	19.24	18.83	11.32	11.33	11.27	300.49	298.44	299.79	299.18	299.86	156.26	155.09	25.48	24.75	24.80	24.98
250	Spaeter	-	HEA 300	14.37	14.77	14.84	14.31	14.10	14.58	14.44	14.22	8.41	8.44	8.51	291.30	290.08	291.51	300.09	299.34	156.76	153.05	28.11	24.19	25.34	26.55
251	Spaeter	Peiner	HEA 280	12.21	13.06	12.86	12.34	12.48	12.54	13.08	12.81	8.68	8.75	8.65	270.63	271.70	272.09	280.17	280.47	146.11	143.56	23.82	23.61	23.82	24.03
252	Spaeter	-	HEB 260	17.35	18.05	17.82	16.95	17.21	17.79	17.94	17.38	9.55	9.53	9.72	261.93	261.66	262.05	260.37	260.74	134.91	135.41	19.73	22.27	22.45	19.32
253	Spaeter	-	HEB 360	20.50	22.05	22.40	21.77	21.66	22.40	22.27	21.88	11.54	12.24	12.08	362.05	362.31	360.59	300.42	300.26	156.52	156.25	28.18	23.10	25.15	25.15
254	Spaeter	-	HEB 360	21.60	22.17	22.54	22.03	21.50	22.18	22.20	21.98	12.30	12.50	12.36	361.61	362.93	361.08	300.73	299.95	157.10	156.17	28.72	24.31	26.30	25.91
255	Spaeter	-	HEA 450	24.61	25.72	26.10	25.12	24.27	25.27	25.05	24.40	13.46	13.70	13.68	451.27	450.50	449.81	298.74	299.27	154.33	159.19	26.22	29.70	27.67	28.52
256	Spaeter	Arcelor Mittal	HEA 320	15.41	16.03	15.35	15.00	15.09	15.60	15.92	15.24	9.23	9.52	9.35	310.30	309.11	309.99	296.30	296.48	152.51	154.38	26.88	24.32	24.90	26.58
257	Spaeter	Arcelor Mittal	HEA 360	16.89	17.71	17.37	16.75	16.79	17.89	17.47	16.47	10.59	10.35	10.30	352.54	352.92	352.76	298.55	298.41	153.32	155.51	25.77	24.13	23.44	26.97
258	Spaeter	-	HEA 260	12.32	12.86	12.97	12.38	12.27	12.82	12.96	12.45	7.32	7.43	7.40	250.07	248.88	250.32	260.54	259.97	133.72	135.11	24.85	21.95	23.78	24.70
259	Spaeter	Thüringen	IPE 450	13.83	14.28	14.19	13.93	13.74	14.11	14.46	14.03	9.68	9.48	9.55	453.78	453.03	453.26	191.04	191.31	100.42	100.88	20.78	22.52	21.65	22.31
260	Spaeter	Arcelor Mittal	IPE 300	9.90	10.36	11.00	10.63	10.56	10.95	10.26	9.83	7.32	7.09	7.12	302.17	301.69	301.31	151.99	151.97	79.55	80.20	13.54	13.16	14.36	13.31
261	Spaeter	Arcelor Mittal	HEA 500	22.19	22.82	23.02	22.67	22.28	22.62	22.88	22.16	12.19	12.31	12.64	493.53	493.40	494.02	299.14	299.91	156.54	155.11	26.60	24.70	25.34	23.31
262	Spaeter	Peiner	IPE 300	10.28	10.30	10.24	10.47	10.37	10.24	10.40	10.27	6.84	6.88	7.07	302.24	301.89	300.65	151.00	149.81	78.76	78.64	14.91	15.21	16.24	14.97
263	Spaeter	Thüringen	IPE 300	10.93	11.06	10.82	10.51	11.01	11.17	11.42	10.60	7.22	7.10	7.29	300.80	300.62	301.66	151.57	150.35	79.82	78.34	14.35	15.00	14.65	14.20
264	Spaeter	Arcelor Mittal	HEA 320	14.96	15.58	15.84	15.09	15.26	15.81	15.93	15.37	9.07	9.08	9.24	311.75	311.53	312.34	298.48	297.95	155.29	152.46	27.09	23.44	24.19	26.16
265	Spaeter	Thüringen	HEB 300	18.88	19.49	20.06	19.28	18.66	19.14	19.41	19.08	11.06	11.14	11.07	306.83	304.21	304.70	301.00	300.58	157.81	154.98	26.84	24.05	29.98	23.64
266	Spaeter	-	HEA 300	13.67	13.75	14.03	13.85	13.55	13.70	13.82	13.41	8.62	8.65	8.71	285.76	286.44	288.85	300.93	300.67	156.47	153.37	25.67	25.04	26.40	25.99
267	Spaeter	-	IPE 330	11.42	11.67	11.87	11.57	11.37	11.75	11.64	11.47	7.56	7.70	7.61	330.01	329.13	328.87	161.16	161.29	83.91	85.50	17.32	18.50	17.81	18.22
268	Spaeter	Peiner	HEB 340	20.77	21.60	21.64	21.25	21.01	21.83	22.12	21.67	11.24	11.20	11.13	339.85	340.04	341.24	299.18	298.85	152.68	158.31	26.56	27.44	27.07	28.52
269	Spaeter	Arcelor Mittal	HEB 300	18.69	19.10	18.74	18.30	18.33	18.83	18.92	18.38	10.89	10.75	10.73	302.52	302.40	299.58	299.47	299.30	154.29	156.86	26.74	24.62	24.88	26.72
270	Spaeter	-	IPE 360	12.01	12.64	12.78	12.21	12.03	12.52	12.49	11.92	8.49	8.16	8.00	363.25	362.60	363.49	170.21	169.55	88.79	89.86	15.28	15.10	15.46	15.01
271	Spaeter	-	IPE 600	17.88	18.26	18.68	18.28	17.74	18.00	18.19	17.76	12.04	12.00	12.37	603.84	604.06	605.37	220.05	220.70	117.17	114.32	23.23	24.52	23.90	24.84
272	Debrunner	Arcelor Mittal	IPE 160	6.98	7.05	7.18	7.10	7.31	7.48	7.25	7.18	5.48	5.73	5.71	160.38	160.38	160.68	83.96	84.03	45.78	43.35	9.27	9.15	9.05	8.77
273	Debrunner	Arcelor Mittal	IPE 180	8.00	8.28	7.72	7.58	7.35	7.48	7.42	7.95	5.72	5.54	5.55	180.31	180.41	180.46	92.02	92.46	47.98	51.34	9.59	10.28	9.74	10.48
274	Debrunner	Arcelor Mittal	IPE 200	8.29	8.53	8.45	8.16	8.08	8.54	8.67	8.40	5.72	5.61	5.70	197.26	198.10	198.41	101.61	101.48	54.52	53.38	12.60	12.81	12.57	13.11
275	Debrunner	Arcelor Mittal	IPE 220	8.75	9.16	8.51	8.04	8.31	8.64	9.32	8.85	6.14	6.31	6.32	222.77	222.80	222.55	110.83	111.11	60.73	56.60	13.08	13.27	13.18	13.13
276	Debrunner	CELSA	IPE 240	9.18	9.71	9.38	9.64	9.11	9.45	9.28	9.33	6.25	6.59	6.07	241.84	242.02	241.77	122.35	122.61	64.90	64.63	15.37	15.07	15.12	15.56
277	Debrunner	Arcelor Mittal	IPE 270	9.41	9.76	9.51	9.15	9.03	9.38	9.83	9.52	6.96	7.04	7.17	272.42	272.91	272.93	135.65	135.44	72.85	69.65	15.21	15.12	15.22	14.61
278	Debrunner	Peiner	IPE 300	9.64	9.63	9.75	9.63	9.50	9.52	9.52	9.65	7.52	7.58	7.51	303.79	303.88	304.28	151.31	152.76	79.31	80.52	15.21	15.28	15.24	15.24
279	Debrunner	Peiner	IPE 300	9.97	9.81	9.58	9.77	9.61	9.72	10.05	10.12	7.54	7.54	7.32	302.76	303.91	303.96	149.62	150.26	79.30	78.34	15.33	15.28	15.67	14.95
280	Debrunner	Arcelor Mittal	IPE 270	9.61	9.99	9.76	9.46	9.56	9.78	10.04	9.28	6.72	6.74	6.99	271.35	271.15	270.80	135.57	135.42	73.93	69.58	15.16	15.03	15.11	14.95
281	Debrunner	CELSA	IPE 500	15.65	15.87	16.02	16.20	15.16	15.23	15.58	15.74	10.04	10.44	10.12	505.05	504.37	504.55	202.71	201.83	105.14	107.77	23.01	20.00	21.02	23.49
282	Debrunner	Arcelor Mittal	IPE 450	14.98	15.37	14.78	14.58	14.53	14.72	15.35	14.90	9.13	9.05	9.14	450.55	450.99	451.79	190.65	190.57	100.56	99.84	19.74	20.75	22.93	20.84
283	Debrunner	Arcelor Mittal	IPE 400	13.36	13.69	13.36	13.16	13.35	13.54	13.43	13.45	8.50	8.51	8.40	404.27	404.13	403.98	181.18	181.23	94.05	95.69	21.08	21.08	20.69	23.33
284	Debrunner	Arcelor Mittal	IPE 550	16.01	16.50	16.93	16.59	15.95	16.33	16.21	15.87	11.31	11.35	11.56	553.11	553.46	555.57	210.46	210.00	111.05	112.08	23.53	26.52	25.88	25.13
285	Debrunner	Arcelor Mittal	IPE 600	18.71	18.91	18.90	18.21	18.35																	

#	Description			Measurements																					
	Steel trader	Producer	Type	t _{1,1}	t _{1,2}	t _{1,3}	t _{1,4}	t _{2,1}	t _{2,2}	t _{2,3}	t _{2,4}	t _{w1}	t _{w2}	t _{w3}	h _{eff}	h _{mid}	h _{light}	b ₁	b ₂	a ₁	a ₂	f ₁	f ₂	f ₃	f ₄
	[mm]	[mm]	[mm]	[mm]	[mm]	[mm]	[mm]	[mm]	[mm]	[mm]	[mm]	[mm]	[mm]	[mm]	[mm]	[mm]	[mm]	[mm]	[mm]	[mm]	[mm]	[mm]	[mm]	[mm]	[mm]
321	Debrunner	Arcelor Mittal	HEB 450	24.33	24.83	25.03	24.48	24.34	25.22	24.99	24.70	13.63	13.31	13.53	454.59	454.11	452.58	302.22	300.50	157.45	159.43	23.39	26.54	26.20	24.85
322	Debrunner	Arcelor Mittal	HEB 600	28.62	29.24	30.37	29.50	29.08	29.92	29.71	29.52	15.70	15.73	15.63	603.96	604.14	605.69	300.72	299.50	159.02	156.27	29.48	30.38	30.43	29.56
323	Debrunner	Arcelor Mittal	HEB 600	29.37	29.83	30.21	30.87	30.00	30.06	28.91	28.88	15.41	15.17	15.17	601.18	601.51	600.35	299.77	300.14	158.37	162.14	30.26	29.56	30.18	29.78
324	Debrunner	Arcelor Mittal	HEB 500	26.82	27.63	27.66	27.27	26.85	27.36	27.83	27.12	14.49	14.45	14.60	502.48	504.29	503.65	299.71	299.99	156.89	157.30	25.64	24.64	24.72	25.60
325	Debrunner	-	HEB 360	21.57	22.21	22.81	22.15	21.62	22.42	22.47	22.38	12.08	12.18	12.29	361.73	359.99	360.70	297.96	299.14	152.97	156.84	29.88	29.03	26.60	27.71
326	Debrunner	Arcelor Mittal	HEB 340	20.88	21.43	21.28	20.63	20.33	20.99	21.67	21.07	12.09	12.12	12.42	345.61	343.13	344.57	298.62	299.57	156.94	154.64	25.58	24.59	23.68	25.86
327	Debrunner	Arcelor Mittal	IPE 450	14.83	15.13	14.88	14.54	14.53	14.87	14.92	15.03	9.22	9.12	9.28	450.63	453.01	451.63	191.58	191.73	100.76	100.04	20.69	20.61	22.24	20.78
328	Debrunner	Arcelor Mittal	IPE 400	13.00	13.62	13.13	12.64	12.78	13.13	13.60	13.27	8.38	8.72	8.87	400.34	400.07	400.43	180.77	181.47	96.32	93.54	21.43	20.75	21.56	20.35
329	Debrunner	Arcelor Mittal	IPE 270	10.18	10.88	10.18	9.58	9.70	10.20	10.48	10.21	6.53	6.46	6.70	270.22	269.97	269.81	134.73	135.34	70.88	70.94	15.05	15.22	14.74	15.27
330	Debrunner	Peiner	HEB 450	24.19	25.02	25.57	24.70	25.08	25.13	25.71	25.07	14.51	14.46	14.31	450.35	451.52	451.13	299.38	299.82	157.19	156.94	27.67	28.75	27.27	29.75
331	Debrunner	Thüringen	HEA 340	16.17	16.69	16.57	16.52	16.27	16.68	16.66	16.43	9.26	9.37	9.21	333.65	332.26	333.59	300.81	300.42	155.01	155.27	26.08	26.32	29.00	24.94
332	Debrunner	Peiner	HEB 300	17.74	17.88	17.99	17.80	18.22	18.67	18.47	18.01	11.36	11.35	11.15	299.26	300.35	300.50	300.97	301.55	157.14	155.84	27.64	22.85	28.37	22.88
333	Debrunner	CELSA	HEA 300	13.48	13.20	13.90	13.85	13.96	14.00	13.15	13.24	8.72	9.15	8.80	292.86	293.42	296.95	298.82	298.17	154.78	153.15	27.01	24.13	25.78	28.47
334	Debrunner	Arcelor Mittal	HEB 360	21.90	22.57	22.30	21.62	21.63	22.03	22.11	21.61	12.48	12.78	12.62	361.90	362.48	360.88	297.78	298.21	154.78	155.80	22.64	27.33	26.70	23.73
335	Debrunner	CELSA	HEA 300	13.36	13.57	13.13	13.43	12.95	12.72	13.33	13.77	8.57	8.92	8.51	294.26	291.96	292.27	297.83	298.96	153.94	153.55	25.18	27.15	26.74	25.27
336	Debrunner	-	HEA 360	17.73	18.15	18.23	17.42	17.52	18.17	18.42	17.59	10.41	10.37	10.19	351.43	351.35	352.36	297.20	297.35	155.84	152.34	24.99	24.85	25.77	24.85
337	Debrunner	Arcelor Mittal	HEA 360	16.65	17.37	17.60	16.72	16.75	17.52	16.96	16.25	10.16	10.22	10.27	353.81	352.55	352.51	298.40	297.83	153.45	156.04	24.28	25.21	25.66	23.91
338	Debrunner	Arcelor Mittal	HEA 360	17.18	17.80	17.65	17.06	17.12	17.71	18.01	17.18	10.70	10.96	10.90	356.49	356.21	357.21	298.80	299.16	158.22	154.26	26.43	24.76	25.41	26.18
339	Debrunner	CELSA	HEA 400	18.51	18.65	18.12	18.32	18.46	18.27	18.15	17.84	11.27	11.73	11.47	394.34	393.69	393.05	298.91	299.63	156.22	155.10	28.97	25.47	27.62	25.84
340	Debrunner	Arcelor Mittal	HEB 340	20.71	21.32	21.48	21.19	20.33	21.30	21.26	21.03	12.72	12.47	12.56	340.48	341.33	341.82	299.91	299.30	153.67	153.79	25.99	24.68	24.32	26.18
341	Debrunner	Peiner	HEA 360	16.34	17.13	17.44	16.69	16.38	17.27	17.20	16.54	9.97	10.02	9.98	350.42	350.99	352.20	298.70	299.07	156.52	153.31	24.43	28.08	25.99	28.28
342	Debrunner	Thüringen	HEA 260	11.93	12.54	12.41	12.13	12.02	12.49	12.60	12.11	7.36	7.06	7.29	250.12	250.42	250.42	261.15	261.07	135.26	133.54	24.34	24.80	24.40	24.14
343	Debrunner	Arcelor Mittal	HEB 340	21.02	21.89	22.37	21.91	21.61	21.81	22.00	21.30	12.61	12.52	12.74	345.84	343.35	344.86	298.53	300.56	157.99	154.47	25.99	25.00	24.68	25.61
344	Debrunner	Arcelor Mittal	HEB 320	20.45	21.28	21.02	20.68	20.74	21.12	20.83	20.01	11.76	11.66	11.60	323.19	322.09	320.98	299.38	298.43	153.65	158.03	25.66	25.04	24.75	27.01
345	Debrunner	Arcelor Mittal	HEA 360	16.73	17.55	17.01	16.27	16.71	17.45	18.30	17.00	10.22	9.96	10.20	352.29	351.92	350.92	297.69	298.17	152.21	156.31	26.42	24.49	23.98	26.28
346	Debrunner	Peiner	HEA 550	23.12	23.47	23.95	23.92	23.30	24.38	23.72	23.92	12.98	12.63	13.24	537.88	539.89	540.31	300.17	300.29	153.04	158.57	26.36	28.59	26.86	28.13
347	Debrunner	CELSA	HEA 280	12.21	12.05	12.31	12.40	12.85	12.61	12.42	12.58	8.55	8.30	8.45	275.40	272.70	273.32	280.73	281.11	144.92	144.28	22.10	23.37	26.25	23.21
348	Debrunner	Arcelor Mittal	IPE 400	12.20	12.79	12.70	12.40	12.47	12.85	12.97	12.67	9.00	8.86	8.80	402.24	401.68	402.11	180.75	180.61	95.31	94.79	22.10	21.13	21.75	20.99
349	Debrunner	-	HEA 340	15.41	15.92	15.44	14.78	15.42	16.05	15.45	14.86	9.95	10.13	10.22	330.36	330.00	330.13	297.81	298.02	153.24	154.95	24.13	26.48	25.58	24.78
350	Debrunner	Arcelor Mittal	IPE 180	7.94	8.16	7.62	7.45	7.28	7.37	7.90	7.67	5.48	5.31	5.48	180.06	180.30	180.31	92.31	92.10	47.96	49.88	10.04	10.13	9.96	10.38
351	Debrunner	Arcelor Mittal	IPE 220	9.24	9.46	8.31	8.03	8.36	8.55	9.40	9.25	5.75	5.67	5.94	221.55	221.50	221.18	113.09	112.80	61.09	58.87	12.01	12.01	11.86	11.69
352	Debrunner	Celsa	IPE 240	8.38	9.31	9.54	8.85	8.61	9.21	9.21	9.06	6.19	6.57	6.48	242.18	242.05	241.14	122.23	122.84	65.10	64.87	15.06	15.27	14.92	15.42
353	Debrunner	Arcelor Mittal	IPE 240	9.17	9.71	9.72	9.51	9.24	9.64	9.95	9.44	6.33	6.35	6.63	242.29	242.63	242.87	120.98	121.09	64.68	65.63	15.01	15.22	15.17	15.21
354	Debrunner	Arcelor Mittal	IPE 270	9.60	10.05	9.71	9.44	9.46	9.70	9.63	9.33	6.84	6.78	7.02	271.25	271.04	270.89	135.62	136.45	72.95	70.35	14.79	15.15	15.05	15.21
355	Debrunner	Arcelor Mittal	IPE 270	9.36	9.72	9.49	9.18	9.04	9.30	9.72	9.51	6.93	6.99	7.22	272.44	272.53	272.93	135.68	135.91	72.93	68.73	15.02	15.40	15.42	14.63
356	Debrunner	Peiner	IPE 200	8.18	8.22	8.09	8.13	7.94	8.17	8.08	8.06	6.11	5.78	5.78	199.69	200.13	200.88	100.13	101.43	52.93	54.58	13.25	12.31	12.43	12.85
357	Debrunner	Arcelor Mittal	IPE 360	12.18	12.62	12.68	11.95	12.12	12.79	12.60	12.15	8.47	8.21	8.21	362.40	362.17	362.08	171.57	172.30	88.75	91.66	14.94	15.31	15.06	15.19
358	Debrunner	Peiner	IPE 500	16.00	16.24	16.10	15.73	15.63	15.80	16.20	15.90	10.02	10.13	10.25	498.65	498.70	499.85	200.04	200.56	106.46	103.73	21.18	21.52	21.30	21.27
359	Debrunner	Celsa	IPE 500	15.67	15.88	16.16	16.27	15.16	15.24	15.73	15.75	10.07	10.21	10.06	505.08	504.39	504.60	202.72	202.59	105.07	107.50	23.17	20.19	20.75	23.57
360	Debrunner	Celsa	IPE 450	14.02	14.28	14.65	14.36	14.04	14.28	14.37	14.22	9.06	9.05	9.21	452.03	452.46	453.08	190.70	191.23	99.68	100.49	21.36	20.02	21.48	21.62
361	Debrunner	Arcelor Mittal	IPE 400	12.77	12.83	13.52	13.31	12.82	12.75	12.42	12.32	8.54	8.58	8.63	404.52	403.07	402.78	180.77	181.23	93.54	96.41	19.01	23.82	25.52	25.94
362	Debrunner	Arcelor Mittal	IPE 550	16.01	16.51	16.83	16.64	15.91	16.33	16.26	15.84	11.36	11.41	11.53	552.80	553.45	555.55	210.50	211.00	111.16	110.89	22.22	27.80	24.84	24.79
363	Debrunner	Peiner	IPE 600	18.11	18.24	19.16	18.48	18.12	18.33	18.33	18.33	12.17	12.13	12.41	605.08	605.75	606.79	218.84	219.15	115.54	115.54	23.69	25.93	25.98	25.27
364	Debrunner	Arcelor Mittal	IPE 500	15.08	15.35	16.23	15.92	15.72	16.10	15.56	15.32	10.48	10.35	10.37	502.78	501.67	501.91	200.88	199.85	105.58	105.21	17.96	21.27	21.75	20.61
365	Debrunner	Celsa	IPE 360	11.73	11.58	11.80	12.06	11.91	11.88	11.90	12.14														

#	Description			Measurements																					
	Steel trader	Producer	Type	$t_{f1,1}$	$t_{f1,2}$	$t_{f1,3}$	$t_{f1,4}$	$t_{f2,1}$	$t_{f2,2}$	$t_{f2,3}$	$t_{f2,4}$	t_{w1}	t_{w2}	t_{w3}	t_{heff}	t_{mid}	t_{height}	b_1	b_2	a_1	a_2	r_1	r_2	r_3	r_4
				[mm]	[mm]	[mm]	[mm]	[mm]	[mm]	[mm]	[mm]	[mm]	[mm]	[mm]	[mm]	[mm]	[mm]	[mm]	[mm]	[mm]	[mm]	[mm]	[mm]	[mm]	[mm]
401	Debrunner	Peiner	HEB 360	20.87	21.71	21.84	21.10	21.00	21.77	21.95	21.45	12.82	12.94	12.92	361.15	360.20	360.68	299.80	299.61	157.40	155.92	26.88	26.35	27.62	29.48
402	Debrunner	Arcelor Mittal	HEB 340	20.82	21.55	21.41	20.65	20.31	21.03	21.69	21.08	12.00	12.23	12.31	345.96	342.89	344.52	299.72	299.72	156.74	154.87	26.40	25.53	24.43	27.03
403	Debrunner	Arcelor Mittal	HEB 320	19.39	19.98	20.22	19.57	19.72	20.26	20.31	19.87	11.60	11.59	11.84	323.15	321.65	319.39	300.51	299.16	156.26	155.25	28.18	25.23	25.60	27.87
404	Debrunner	Arcelor Mittal	HEB 260	17.54	18.09	18.70	17.97	17.66	18.52	18.54	17.75	9.23	9.06	9.07	263.44	262.71	262.99	255.79	259.00	133.45	135.21	24.16	18.46	17.53	26.80
405	Debrunner	Peiner	HEB 240	15.72	15.88	16.21	15.85	15.53	16.03	16.53	15.93	10.49	10.21	10.15	237.88	237.17	238.75	241.14	241.23	127.37	124.68	22.97	24.61	24.25	23.69
406	Debrunner	Arcelor Mittal	IPE 500	15.14	15.56	15.13	14.75	14.71	15.11	15.85	15.41	10.51	10.67	10.65	503.27	503.51	504.10	203.39	202.72	108.25	105.62	20.05	21.11	21.79	21.11
407	Debrunner	Peiner	HEA 260	11.69	12.55	12.43	11.86	11.67	12.33	12.76	12.14	7.99	8.02	8.14	250.64	250.94	252.95	261.35	262.07	136.20	133.85	20.55	21.33	22.86	19.03
408	Debrunner	Arcelor Mittal	HEA 400	18.76	18.98	20.13	19.35	19.24	19.81	19.55	19.05	11.00	10.83	10.86	392.30	391.15	393.01	296.48	296.42	155.64	152.24	24.67	25.82	25.64	24.62
409	Debrunner	Peiner	HEB 450	24.22	25.18	25.78	24.80	23.95	25.11	25.68	25.13	14.44	14.37	14.22	450.15	451.13	451.25	299.42	299.74	157.19	156.97	27.62	28.72	26.97	30.21
410	Debrunner	Arcelor Mittal	HEB 360	21.94	22.35	22.84	22.01	22.04	22.87	22.57	22.08	12.78	12.69	12.58	362.04	363.16	362.50	298.66	298.58	156.47	155.24	24.67	26.99	26.22	24.28
411	Debrunner	Celsa	HEA 220	10.27	10.46	10.42	10.34	10.69	10.63	10.81	10.69	7.18	7.16	7.17	213.10	212.15	213.76	218.37	218.40	112.44	114.06	17.20	17.84	18.76	17.44
412	Debrunner	Celsa	HEA 300	13.33	13.51	13.26	13.48	12.93	12.68	13.42	13.67	8.66	8.77	8.66	294.08	292.69	292.68	297.92	298.96	154.29	153.73	25.73	26.58	27.18	25.66
413	Debrunner	Arcelor Mittal	HEA 320	14.58	15.24	15.10	14.45	14.65	15.03	14.89	14.42	9.09	9.08	9.37	314.68	312.21	314.94	296.77	296.74	152.30	154.06	24.01	26.40	26.64	23.95
414	Debrunner	Peiner	HEA 400	17.83	18.84	18.65	18.20	17.98	18.72	19.27	18.06	11.37	11.44	11.30	391.68	392.95	392.71	300.52	300.48	155.20	156.91	27.69	28.04	28.92	1.00
415	Debrunner	Arcelor Mittal	IPE 400	12.29	12.80	12.77	12.37	12.48	12.92	12.97	12.68	9.01	8.83	8.72	402.23	401.83	402.23	180.88	180.67	95.17	94.97	21.46	21.78	22.86	20.41
416	Debrunner	Arcelor Mittal	HEB 340	21.38	22.00	22.29	22.02	21.65	21.80	22.10	21.56	12.55	12.51	12.72	346.04	343.26	345.00	298.38	300.63	157.93	154.29	25.95	24.75	24.25	25.88
417	Debrunner	Peiner	HEA 280	12.48	12.44	12.31	12.52	12.32	12.17	12.44	12.28	8.50	8.55	8.52	276.22	273.42	275.46	279.28	279.33	144.76	143.47	24.83	22.75	24.88	23.05
418	Debrunner	Arcelor Mittal	HEA 360	16.67	17.52	17.00	16.40	16.39	17.39	17.65	16.80	10.27	9.96	10.04	352.34	351.77	351.07	297.79	298.68	153.25	155.96	26.16	24.29	25.31	26.07
419	Debrunner	Peiner	HEB 260	16.67	16.87	16.62	16.48	16.32	16.47	16.65	16.45	9.88	10.07	9.84	266.53	265.25	262.90	260.59	260.23	135.20	135.56	23.38	22.78	25.51	21.69
420	Debrunner	Peiner	HEA 400	19.00	19.48	19.26	18.91	18.50	19.08	19.32	19.55	10.79	10.97	11.03	390.42	390.22	391.68	299.32	299.57	155.33	155.43	26.74	29.40	27.53	28.87
421	Debrunner	Arcelor Mittal	IPE 300	10.06	10.54	10.34	9.90	9.82	10.18	10.56	10.15	7.82	8.15	7.81	303.03	302.68	303.36	150.91	151.14	80.93	79.24	13.46	13.25	14.00	13.25
422	Debrunner	-	HEA 340	15.35	15.85	15.37	14.86	15.12	16.02	15.49	14.84	9.91	10.12	10.14	330.42	329.64	330.17	297.86	297.78	153.12	155.28	24.16	26.84	25.95	24.65
423	Debrunner	Celsa	IPE 300	10.01	9.88	10.51	10.59	10.68	9.93	9.81	10.13	7.08	7.39	7.25	303.51	303.84	304.40	151.89	152.27	79.91	79.88	15.34	15.21	15.07	14.69
424	Debrunner	Arcelor Mittal	IPE 240	9.00	9.59	9.08	8.70	8.69	9.06	9.68	9.33	6.35	6.56	6.54	239.43	239.28	239.19	122.17	122.88	64.91	64.52	15.12	15.24	14.82	14.76
425	Debrunner	Peiner	IPE 220	8.90	8.93	9.14	9.05	8.87	8.97	8.82	8.81	6.21	6.07	5.84	219.19	219.62	220.15	110.73	111.38	59.29	58.72	13.21	13.03	12.98	13.05
426	Debrunner	Peiner	IPE 220	8.83	8.82	8.93	9.01	8.73	8.85	8.74	8.76	6.17	5.92	5.85	218.94	219.09	219.61	110.86	111.84	58.89	58.37	13.25	13.01	13.37	13.36
427	Debrunner	Celsa	IPE 200	8.31	8.57	8.55	8.02	8.18	8.36	8.67	8.18	5.87	5.92	5.91	200.09	200.00	199.69	101.31	101.24	53.27	54.73	12.93	13.62	12.98	13.30
428	Debrunner	Arcelor Mittal	IPE 160	7.04	7.12	7.08	7.07	7.36	7.26	7.26	7.14	5.42	5.42	5.48	160.76	160.59	160.69	82.79	82.88	44.94	43.85	8.91	9.72	8.51	
429	Ferroflex	Peiner	HEA 300	13.71	14.47	14.91	14.38	13.95	14.78	14.90	14.23	9.03	8.96	9.11	289.43	290.14	290.39	299.83	299.12	152.27	156.18	24.96	29.75	25.95	30.32
430	Ferroflex	Peiner	HEA 300	13.36	13.76	14.17	13.62	13.71	13.83	13.97	13.34	9.06	9.11	9.08	290.46	290.88	291.52	300.83	300.19	156.47	153.55	25.28	28.47	28.57	26.80
431	Ferroflex	Peiner	HEA 300	12.32	12.61	14.00	13.62	12.94	13.71	13.93	13.45	8.93	9.09	9.02	290.99	291.11	291.56	300.61	300.37	156.98	152.50	27.01	26.90	28.85	26.50
432	Ferroflex	Peiner	IPE 600	18.22	18.60	19.14	18.73	18.94	18.50	18.62	18.51	11.70	11.83	11.23	602.67	603.06	605.02	219.37	220.95	115.53	116.15	24.08	24.21	24.43	24.08
433	Ferroflex	Thüringen	IPE 500	15.80	16.03	16.30	15.67	16.12	16.42	16.23	15.94	10.15	10.06	10.30	503.22	503.80	504.51	201.18	201.43	106.84	105.11	22.97	22.31	23.61	22.91
434	Ferroflex	Thüringen	IPE 400	13.28	13.72	13.46	13.05	13.15	13.41	13.30	13.01	8.63	8.52	8.46	402.83	402.12	403.65	180.22	180.65	94.42	94.22	22.10	20.61	21.65	21.79
435	Ferroflex	Thüringen	IPE 360	12.65	12.76	12.81	12.60	12.72	12.90	13.00	12.81	8.07	8.20	8.22	361.60	360.70	361.25	170.24	170.19	89.24	89.80	17.58	18.76	17.79	18.53
436	Ferroflex	Peiner	IPE 300	9.71	9.90	10.10	9.55	9.32	9.55	9.89	8.68	7.54	7.46	7.51	299.16	301.46	304.33	150.21	151.87	81.44	77.49	15.17	15.78	15.12	14.79
437	Ferroflex	Peiner	IPE 300	9.92	10.21	10.11	9.77	9.60	9.66	9.90	9.88	8.00	7.80	7.87	300.87	301.91	303.12	150.76	152.56	80.28	79.53	15.50	15.48	14.73	15.48
438	Ferroflex	Thüringen	IPE 500	14.94	15.21	16.53	14.99	15.71	16.00	16.16	15.85	10.27	10.21	10.39	499.03	498.44	498.07	200.50	202.14	107.53	107.53	23.01	22.56	23.17	22.97
439	Ferroflex	Thüringen	IPE 550	17.12	17.53	17.58	17.28	17.74	17.44	17.63	17.28	11.12	10.85	10.91	553.75	551.42	549.17	210.27	210.93	109.04	112.38	25.32	24.56	24.84	26.19
440	Ferroflex	Thüringen	IPE 400	13.01	13.16	13.07	12.78	13.11	13.37	13.14	12.88	8.52	8.54	8.42	400.81	399.98	400.24	181.33	180.97	94.46	95.11	23.09	20.52	22.82	22.33
441	Ferroflex	-	IPE 330	10.38	10.61	10.54	10.40	10.11	10.42	10.59	10.10	8.11	7.98	8.10	331.13	332.38	334.50	160.38	161.45	85.31	81.12	18.65	18.04	16.38	18.53
442	Ferroflex	-	IPE 300	9.99	9.76	9.96	10.14	10.57	10.22	9.57	9.57	7.48	7.46	7.55	302.45	301.07	301.38	151.45	151.71	79.81	79.83	15.89	15.23	15.16	15.93
443	Ferroflex	-	IPE 300	10.40	10.81	10.78	10.75	10.27	10.56	11.02	10.95	6.85	7.07	7.12	299.57	299.77	300.20	150.58	151.03	79.38	79.84	15.54	14.59	14.41	14.78
444	Ferroflex	Arcelor Mittal	HEA 300	13.90	14.15	14.22	13.65	13.60	13.69	14.47	13.74	8.66	8.62	9.03	292.88	290.17	292.34	299.21	299.39	155.58	152.86	25.95	25.88	24.75	25.95
445	Ferroflex	Arcelor Mittal	HEA 300	13.9																					

#	Description			Measurements																					
	Steel trader	Producer	Type	t _{1,1}	t _{1,2}	t _{1,3}	t _{1,4}	t _{2,1}	t _{2,2}	t _{2,3}	t _{2,4}	t _{w1}	t _{w2}	t _{w3}	h _{eff}	h _{mid}	h _{light}	b ₁	b ₂	a ₁	a ₂	r ₁	r ₂	r ₃	r ₄
				[mm]	[mm]	[mm]	[mm]	[mm]	[mm]	[mm]	[mm]	[mm]	[mm]	[mm]	[mm]	[mm]	[mm]	[mm]	[mm]	[mm]	[mm]	[mm]	[mm]	[mm]	[mm]
481	Ferroflex	Peiner	HEB 500	27.74	28.85	29.03	28.66	28.26	29.08	29.05	28.26	13.77	13.79	13.64	502.57	502.04	501.75	299.98	298.95	155.06	158.03	26.62	28.08	26.64	27.94
482	Ferroflex	Thüringen	HEA 360	16.82	17.22	17.18	16.78	16.98	17.36	17.39	16.95	9.55	9.81	9.70	351.62	352.91	351.76	300.33	299.83	157.32	152.62	26.26	25.44	27.83	25.97
483	Ferroflex	-	HEB 450	24.39	25.66	25.79	24.82	24.10	25.40	25.71	24.96	14.34	14.35	14.21	448.79	450.40	451.43	299.15	299.32	157.47	156.14	26.47	26.62	28.40	27.17
484	Ferroflex	-	HEB 340	20.86	21.43	21.41	21.06	20.29	21.13	21.94	21.42	12.31	12.28	12.33	341.77	341.25	340.86	299.89	300.05	155.46	157.18	26.76	27.74	27.80	27.92
485	Ferroflex	Thüringen	HEA 240	11.71	12.19	11.99	11.67	11.80	12.00	12.17	12.81	7.47	7.40	7.39	229.85	230.56	230.01	240.57	241.67	125.44	124.80	21.08	22.27	21.72	21.21
486	Ferroflex	Peiner	HEA 550	22.22	23.21	23.53	23.01	22.62	23.47	23.66	22.84	12.82	12.77	12.82	542.54	542.27	543.23	299.63	299.58	155.06	157.95	25.01	29.42	25.44	28.18
487	Ferroflex	-	HEA 500	21.33	22.97	23.29	21.06	21.33	22.67	22.81	21.85	12.08	12.27	12.41	493.76	494.72	494.82	298.21	299.16	156.32	154.62	25.41	27.44	26.55	27.33
488	Ferroflex	Peiner	HEA 450	19.63	20.52	20.58	19.92	19.12	20.04	20.26	19.91	11.97	11.75	11.90	443.79	444.11	443.35	299.33	299.39	156.61	155.50	24.54	28.95	26.16	26.68
489	Ferroflex	Thüringen	HEA 240	11.76	12.07	12.22	11.90	11.88	12.27	12.63	11.95	7.34	7.30	7.39	232.81	233.57	234.79	240.98	240.04	123.51	124.91	21.46	22.34	21.56	23.57
490	Ferroflex	-	HEA 220	10.58	10.82	10.79	10.35	10.78	11.06	10.87	10.48	6.88	6.84	6.88	210.36	210.62	210.39	220.70	220.54	114.36	113.73	20.10	21.92	20.32	21.08
491	Ferroflex	-	IPE 240	9.76	10.06	10.14	9.95	9.75	10.00	10.10	9.93	6.20	6.13	6.05	243.26	243.21	243.02	119.45	119.84	62.56	63.66	15.17	15.24	14.98	15.24
492	Ferroflex	-	HEA 220	10.70	11.22	11.10	10.83	10.72	11.10	11.05	10.98	6.90	6.77	6.98	211.56	210.78	210.60	220.46	220.41	113.98	113.72	20.38	21.06	20.32	21.08
493	Ferroflex	-	HEA 240	11.75	12.05	11.96	11.62	11.57	11.97	12.12	11.68	7.29	7.42	7.35	229.82	230.08	230.70	241.30	241.58	125.01	124.43	21.18	22.71	21.69	21.99
494	Ferroflex	-	HEA 400	17.61	18.38	18.82	18.03	17.63	18.45	18.96	18.37	11.45	11.59	11.30	392.58	392.30	392.53	300.18	299.82	156.57	155.52	27.51	27.05	28.75	26.26
495	Ferroflex	-	HEA 400	18.73	19.12	19.41	19.19	19.00	19.40	19.25	18.86	11.27	11.23	11.27	390.63	391.30	390.68	300.76	300.81	156.22	156.25	27.38	24.45	26.36	25.13
496	Ferroflex	CELSA	HEA 280	12.21	12.05	12.31	12.40	12.85	12.42	12.58	8.55	8.30	8.45	275.40	272.70	273.32	280.73	281.11	144.92	144.28	22.10	23.37	26.25	23.21	
497	Ferroflex	Arcelor Mittal	IPE 400	12.20	12.79	12.70	12.40	12.47	12.85	12.97	12.67	9.00	8.86	8.80	402.24	401.68	402.11	180.75	180.61	95.31	94.79	22.10	21.18	21.75	20.99
498	Ferroflex	-	HEA 340	15.41	15.92	15.44	14.78	15.42	16.05	15.45	14.86	9.95	10.13	10.22	330.36	330.00	330.13	297.81	298.02	153.24	154.95	24.13	26.43	25.58	24.78
499	Spaeter	-	IPE 200	8.27	8.30	8.18	8.21	8.33	8.43	8.13	8.25	5.45	5.29	5.45	198.19	198.85	200.00	102.61	102.04	53.30	55.12	13.62	13.13	13.03	13.40
500	Spaeter	-	IPE 200	8.25	8.50	8.63	8.32	8.53	8.76	8.16	7.93	5.57	5.52	5.75	200.58	200.20	199.81	101.27	102.31	53.63	54.16	12.66	12.57	12.58	13.05
501	Spaeter	-	IPE 200	8.45	8.60	8.76	8.52	8.80	8.99	8.37	8.11	5.65	5.62	5.75	201.34	201.01	200.22	101.18	101.96	52.94	54.71	12.51	12.61	12.59	12.57
502	Spaeter	-	HEA 240	10.87	10.84	10.91	10.67	10.86	11.18	11.05	10.83	7.90	7.81	7.61	232.09	230.19	229.32	241.00	240.72	124.11	124.83	25.47	25.22	24.84	26.92
503	Spaeter	-	IPE 220	8.85	8.87	8.83	8.66	8.80	8.90	8.85	8.72	5.67	5.62	5.77	222.90	223.45	223.86	110.17	110.76	58.94	57.41	14.03	14.12	13.80	13.50
504	Spaeter	-	HEA 220	10.44	11.13	10.92	10.58	10.65	10.96	11.37	10.91	7.21	7.21	7.37	210.29	210.84	211.58	221.40	222.40	115.73	113.65	17.29	13.79	19.92	18.04
505	Spaeter	-	HEA 200	10.03	10.53	10.44	10.16	10.18	10.47	10.31	9.95	6.35	6.32	6.26	189.29	189.67	190.18	199.74	200.75	103.52	103.32	17.64	18.11	16.94	18.81
506	Spaeter	Peiner	HEA 200	9.23	9.45	9.21	9.24	9.10	9.35	9.71	9.47	6.61	6.78	6.37	193.75	193.34	194.66	199.70	200.35	103.42	103.46	20.19	20.66	19.76	20.99
507	Spaeter	-	HEB 240	15.58	16.10	15.87	15.74	15.77	15.85	15.88	15.70	10.21	10.32	10.32	241.59	240.64	240.69	240.00	239.89	124.77	125.65	24.00	22.38	23.95	26.41
508	Spaeter	ACS Transit	HEB 240	16.80	17.02	17.10	16.73	16.71	17.03	16.57	16.29	9.78	9.79	9.96	242.27	242.48	243.51	240.78	240.97	124.50	126.75	22.03	21.65	21.18	21.36
509	Spaeter	-	HEB 220	15.68	16.01	16.05	15.60	15.77	16.08	15.81	15.33	9.74	9.62	9.71	221.88	221.87	221.66	220.90	221.00	115.50	115.62	19.87	20.58	20.84	19.92
510	Spaeter	-	HEB 220	15.47	16.30	15.76	15.25	15.23	15.56	16.42	15.78	9.31	9.33	9.50	220.76	220.74	220.33	221.38	221.42	116.13	115.22	16.35	20.81	19.71	16.99
511	Spaeter	-	HEB 220	16.01	16.64	16.09	15.66	15.59	15.93	16.50	16.12	9.23	9.27	9.35	222.08	221.88	220.96	221.84	221.73	115.78	115.61	16.75	18.85	19.59	17.77
512	Spaeter	-	HEB 200	14.20	14.79	14.64	14.12	14.09	14.61	15.05	14.78	9.06	8.98	9.21	198.98	199.34	200.08	200.65	202.92	105.55	105.23	17.15	18.06	18.23	17.13
513	Spaeter	-	IPE 240	9.82	10.05	10.10	9.88	9.97	10.23	10.21	10.01	6.03	5.88	5.93	242.97	241.87	241.21	120.98	120.92	63.58	63.75	14.79	14.92	15.08	14.95
514	Spaeter	-	IPE 240	9.87	10.19	10.16	9.95	9.95	10.18	10.21	9.98	6.11	5.93	5.89	243.10	242.15	241.37	121.27	120.75	63.40	63.68	15.03	15.07	15.15	15.07
515	Spaeter	-	HEA 220	10.53	11.11	10.63	10.48	10.68	10.62	10.83	10.56	7.46	7.43	7.58	212.81	211.25	211.12	218.86	219.92	113.07	113.91	17.07	18.39	17.13	16.95
516	Spaeter	Peiner	HEA 200	9.01	9.12	9.12	9.05	8.92	9.00	9.67	8.86	6.89	6.68	6.58	193.03	192.11	192.71	200.97	200.89	103.09	105.00	20.19	21.56	21.75	20.05
517	Spaeter	-	HEB 220	15.30	15.62	16.30	16.03	16.10	16.11	15.69	15.25	9.93	9.75	9.88	218.15	218.79	219.63	219.46	219.44	115.75	113.88	18.68	17.57	17.18	18.11
518	Spaeter	-	IPE 360	12.08	12.54	12.48	12.34	12.60	12.11	12.67	12.23	8.42	8.34	8.31	361.11	360.68	360.51	171.11	171.04	89.34	90.59	18.04	18.53	18.55	18.32
519	Spaeter	-	IPE 300	9.63	9.90	10.22	10.20	10.20	10.54	9.96	9.96	7.15	7.12	7.20	301.35	301.39	300.69	151.22	151.52	80.62	78.38	15.42	15.62	15.73	15.13
520	Spaeter	-	IPE 330	11.56	11.82	11.66	11.33	11.51	11.58	11.71	11.31	7.59	7.71	7.92	329.03	329.41	330.11	161.03	161.30	84.53	84.32	18.87	17.90	18.81	17.90
521	Spaeter	-	HEB 280	17.95	18.43	18.41	17.96	17.59	18.07	18.24	17.80	10.08	10.21	9.98	283.82	282.81	282.33	280.48	281.70	146.40	144.68	29.10	22.35	24.89	25.72
522	Spaeter	-	HEA 260	12.18	13.00	12.27	11.75	11.88	12.27	12.80	12.09	7.99	8.06	8.03	250.89	250.36	251.28	259.21	259.87	136.51	131.52	19.61	22.78	24.98	19.89
523	Spaeter	Peiner	HEA 280	12.28	13.08	12.87	12.21	12.47	12.50	13.07	12.84	8.54	8.71	8.64	270.74	271.54	272.14	280.55	280.68	146.00	143.57	24.25	24.70	25.27	25.13
524	Spaeter	-	HEA 300	14.32	14.75	14.35	14.41	14.12	14.60	14.47	14.23	8.36	8.36	8.31	291.20	290.10	291.57	300.12	299.78	155.14	152.93	28.23	24.64	26.95	25.62
525	Spaeter	Arcelor Mittal	HEB 300	18.41	19.18	19.07	18.91	18.31	18.83	19.26	18.55	11.37	11.28	11.23											

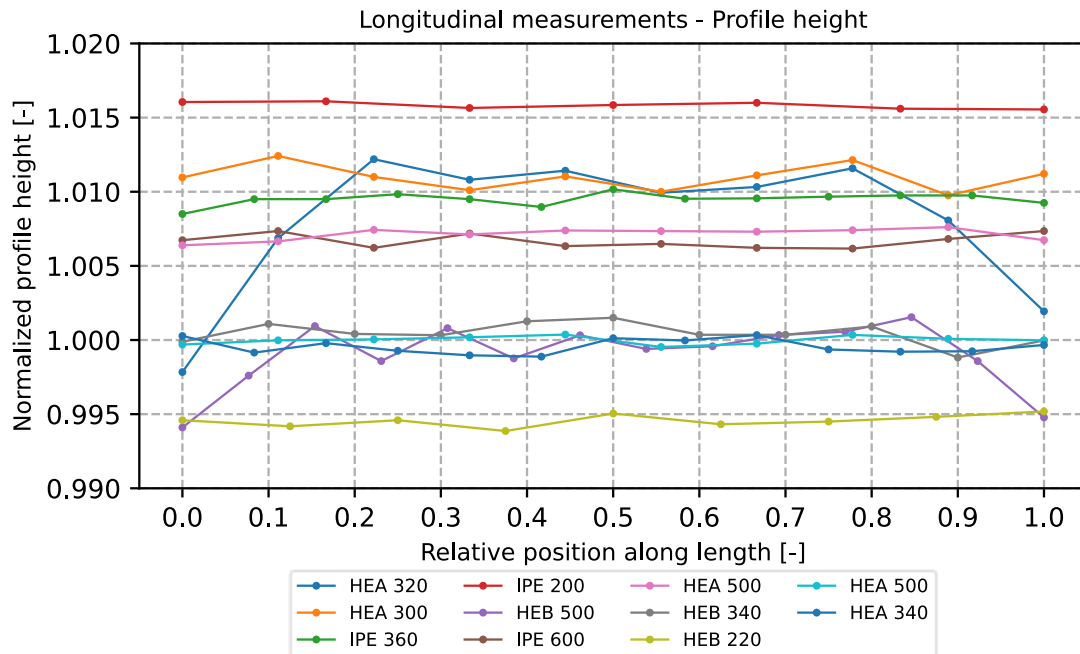
A.2.2 Longitudinal measurements

#	x [m]	L [m]	Profile	t _f [mm]	h [mm]	b [mm]	r [mm]
1	0.0	18.0	HEA 320	14.87	309.33	-	26.41
1	2.0	18.0	HEA 320	14.80	312.13	-	27.02
1	4.0	18.0	HEA 320	14.83	313.78	-	26.97
1	6.0	18.0	HEA 320	14.77	313.35	-	27.80
1	8.0	18.0	HEA 320	14.91	313.54	-	27.55
1	10.0	18.0	HEA 320	14.89	313.08	-	26.80
1	12.0	18.0	HEA 320	14.92	313.20	-	27.08
1	14.0	18.0	HEA 320	14.95	313.59	-	27.55
1	16.0	18.0	HEA 320	14.87	312.50	-	27.26
1	18.0	18.0	HEA 320	14.92	310.60	-	26.41
2	0.0	18.0	HEA 300	13.83	293.18	-	27.80
2	2.0	18.0	HEA 300	13.82	293.60	-	28.76
2	4.0	18.0	HEA 300	13.82	293.19	-	27.92
2	6.0	18.0	HEA 300	13.82	292.93	-	28.30
2	8.0	18.0	HEA 300	13.85	293.20	-	28.17
2	10.0	18.0	HEA 300	13.83	292.90	-	27.99
2	12.0	18.0	HEA 300	13.80	293.22	-	28.11
2	14.0	18.0	HEA 300	13.81	293.52	-	28.05
2	16.0	18.0	HEA 300	13.83	292.83	-	28.11
2	18.0	18.0	HEA 300	13.86	293.25	-	28.17
3	0.0	24.0	IPE 360	12.30	363.06	170.65	17.77
3	2.0	24.0	IPE 360	12.54	363.42	170.78	17.77
3	4.0	24.0	IPE 360	12.39	363.42	170.89	17.79
3	6.0	24.0	IPE 360	12.43	363.54	170.86	17.84
3	8.0	24.0	IPE 360	12.30	363.42	170.67	17.94
3	10.0	24.0	IPE 360	12.38	363.23	170.74	17.53
3	12.0	24.0	IPE 360	12.28	363.66	170.75	17.55
3	14.0	24.0	IPE 360	12.30	363.43	170.85	17.71
3	16.0	24.0	IPE 360	12.41	363.44	171.02	17.77
3	18.0	24.0	IPE 360	12.37	363.48	170.95	17.66
3	20.0	24.0	IPE 360	12.45	363.51	170.86	17.48
3	22.0	24.0	IPE 360	12.37	363.51	170.74	17.54
3	24.0	24.0	IPE 360	12.44	363.33	170.78	17.60
4	0.0	24.0	IPE 330	11.30	-	160.06	17.80
4	2.0	24.0	IPE 330	11.19	-	159.75	17.28
4	4.0	24.0	IPE 330	11.22	-	159.90	17.30
4	6.0	24.0	IPE 330	11.20	-	159.82	17.33
4	8.0	24.0	IPE 330	11.24	-	159.92	17.35
4	10.0	24.0	IPE 330	11.23	-	159.99	17.32
4	12.0	24.0	IPE 330	11.22	-	160.02	17.44
4	14.0	24.0	IPE 330	11.31	-	159.91	17.30
4	16.0	24.0	IPE 330	11.34	-	159.75	17.25
4	18.0	24.0	IPE 330	11.18	-	160.00	17.42
4	20.0	24.0	IPE 330	11.28	-	159.71	17.46
4	22.0	24.0	IPE 330	11.28	-	159.40	17.18
4	24.0	24.0	IPE 330	11.46	-	159.60	17.15
5	0.0	26.0	IPE 450	-	-	189.82	-
5	2.0	26.0	IPE 450	-	-	190.20	-
5	4.0	26.0	IPE 450	-	-	190.16	-
5	6.0	26.0	IPE 450	-	-	190.60	-
5	8.0	26.0	IPE 450	-	-	190.20	-
5	10.0	26.0	IPE 450	-	-	190.52	-
5	12.0	26.0	IPE 450	-	-	190.63	-
5	14.0	26.0	IPE 450	-	-	190.76	-
5	16.0	26.0	IPE 450	-	-	190.73	-
5	18.0	26.0	IPE 450	-	-	190.53	-
5	20.0	26.0	IPE 450	-	-	190.63	-
5	22.0	26.0	IPE 450	-	-	190.31	-
5	24.0	26.0	IPE 450	-	-	190.79	-
5	26.0	26.0	IPE 450	-	-	190.51	-
6	0.0	12.0	IPE 200	-	203.21	-	-
6	2.0	12.0	IPE 200	-	203.22	-	-
6	4.0	12.0	IPE 200	-	203.13	-	-
6	6.0	12.0	IPE 200	-	203.17	-	-
6	8.0	12.0	IPE 200	-	203.20	-	-
6	10.0	12.0	IPE 200	-	203.12	-	-
6	12.0	12.0	IPE 200	-	203.11	-	-

#	x [m]	L [m]	Profile	t _f [mm]	h [mm]	b [mm]	r [mm]
7	0.0	26.0	HEB 500	28.01	497.05	299.40	24.84
7	2.0	26.0	HEB 500	27.62	498.80	299.32	24.12
7	4.0	26.0	HEB 500	27.61	500.47	299.23	24.25
7	6.0	26.0	HEB 500	27.60	499.29	299.25	24.12
7	8.0	26.0	HEB 500	27.66	500.40	299.25	24.32
7	10.0	26.0	HEB 500	27.65	499.38	299.43	24.34
7	12.0	26.0	HEB 500	27.56	500.16	299.25	24.16
7	14.0	26.0	HEB 500	27.63	499.70	299.36	23.98
7	16.0	26.0	HEB 500	27.68	499.79	299.26	24.21
7	18.0	26.0	HEB 500	27.65	500.17	299.24	24.37
7	20.0	26.0	HEB 500	27.64	500.28	299.21	24.21
7	22.0	26.0	HEB 500	27.63	500.77	299.17	24.25
7	24.0	26.0	HEB 500	27.66	499.29	299.45	24.79
7	26.0	26.0	HEB 500	27.70	497.39	299.42	24.56
8	0.0	20.0	HEB 220	15.04	-	220.55	24.16
8	2.0	20.0	HEB 220	15.23	-	220.78	24.03
8	4.0	20.0	HEB 220	15.15	-	219.86	24.38
8	6.0	20.0	HEB 220	15.26	-	219.70	24.30
8	8.0	20.0	HEB 220	15.45	-	219.84	24.43
8	10.0	20.0	HEB 220	15.13	-	219.68	24.38
8	12.0	20.0	HEB 220	15.13	-	219.78	24.29
8	14.0	20.0	HEB 220	15.17	-	219.72	24.05
8	16.0	20.0	HEB 220	15.12	-	219.96	24.21
8	18.0	20.0	HEB 220	15.15	-	220.14	24.06
8	20.0	20.0	HEB 220	15.11	-	219.93	24.03
9	0.0	26.0	IPE 220	9.06	-	110.79	12.55
9	2.0	26.0	IPE 220	9.07	-	111.03	12.59
9	4.0	26.0	IPE 220	8.99	-	111.22	12.51
9	6.0	26.0	IPE 220	8.98	-	111.42	12.51
9	8.0	26.0	IPE 220	9.06	-	111.45	12.68
9	10.0	26.0	IPE 220	8.99	-	111.20	12.51
9	12.0	26.0	IPE 220	9.08	-	111.24	12.68
9	14.0	26.0	IPE 220	9.03	-	111.22	12.55
9	16.0	26.0	IPE 220	8.97	-	111.14	12.64
9	18.0	26.0	IPE 220	8.96	-	111.18	12.59
9	20.0	26.0	IPE 220	9.04	-	111.19	12.51
9	22.0	26.0	IPE 220	9.01	-	111.16	12.55
9	24.0	26.0	IPE 220	8.99	-	111.10	12.43
9	26.0	26.0	IPE 220	8.97	-	111.17	12.47
10	0.0	18.0	IPE 600	17.72	604.04	-	-
10	2.0	18.0	IPE 600	17.61	604.41	-	-
10	4.0	18.0	IPE 600	17.63	603.73	-	-
10	6.0	18.0	IPE 600	17.62	604.31	-	-
10	8.0	18.0	IPE 600	17.55	603.80	-	-
10	10.0	18.0	IPE 600	17.54	603.89	-	-
10	12.0	18.0	IPE 600	17.56	603.73	-	-
10	14.0	18.0	IPE 600	17.60	603.70	-	-
10	16.0	18.0	IPE 600	17.56	604.09	-	-
10	18.0	18.0	IPE 600	17.56	604.41	-	-
11	0.0	26.0	HEA 400	18.96	-	300.77	25.84
11	2.0	26.0	HEA 400	18.95	-	300.59	25.51
11	4.0	26.0	HEA 400	18.98	-	300.70	25.71
11	6.0	26.0	HEA 400	18.97	-	300.59	25.73
11	8.0	26.0	HEA 400	18.95	-	300.43	25.54
11	10.0	26.0	HEA 400	18.99	-	300.51	25.39
11	12.0	26.0	HEA 400	18.95	-	300.52	25.39
11	14.0	26.0	HEA 400	18.97	-	300.67	25.46
11	16.0	26.0	HEA 400	18.94	-	300.67	25.37
11	18.0	26.0	HEA 400	18.95	-	300.72	25.72
11	20.0	26.0	HEA 400	18.96	-	300.56	25.51
11	22.0	26.0	HEA 400	18.96	-	300.55	25.39
11	24.0	26.0	HEA 400	18.98	-	300.52	25.47
11	26.0	26.0	HEA 400	18.97	-	300.46	25.37

#	x [m]	L [m]	Profile	t _f [mm]	h [mm]	b [mm]	r [mm]
12	0.0	18.0	HEA 500	21.77	491.11	-	-
12	2.0	18.0	HEA 500	21.68	493.26	-	-
12	4.0	18.0	HEA 500	21.65	493.64	-	-
12	6.0	18.0	HEA 500	21.70	493.49	-	-
12	8.0	18.0	HEA 500	21.70	493.62	-	-
12	10.0	18.0	HEA 500	21.63	493.60	-	-
12	12.0	18.0	HEA 500	21.72	493.58	-	-
12	14.0	18.0	HEA 500	21.63	493.63	-	-
12	16.0	18.0	HEA 500	21.59	493.73	-	-
12	18.0	18.0	HEA 500	21.68	491.91	-	-
13	0.0	20.0	HEB 340	21.00	339.96	301.37	26.90
13	2.0	20.0	HEB 340	21.06	340.37	300.67	27.31
13	4.0	20.0	HEB 340	20.99	340.14	300.73	26.97
13	6.0	20.0	HEB 340	21.04	340.11	301.14	26.96
13	8.0	20.0	HEB 340	20.96	340.43	301.31	26.82
13	10.0	20.0	HEB 340	20.99	340.51	300.95	27.16
13	12.0	20.0	HEB 340	20.98	340.12	300.62	26.91
13	14.0	20.0	HEB 340	20.99	340.12	301.27	26.94
13	16.0	20.0	HEB 340	21.03	340.31	300.72	26.84
13	18.0	20.0	HEB 340	21.00	339.60	301.16	26.80
13	20.0	20.0	HEB 340	20.95	339.99	301.39	27.03
14	0.0	16.0	HEB 220	15.92	218.81	-	21.27
14	2.0	16.0	HEB 220	15.77	218.72	-	21.33
14	4.0	16.0	HEB 220	15.71	218.81	-	20.84
14	6.0	16.0	HEB 220	15.74	218.65	-	21.36
14	8.0	16.0	HEB 220	15.74	218.91	-	20.87
14	10.0	16.0	HEB 220	15.77	218.75	-	20.84
14	12.0	16.0	HEB 220	15.72	218.79	-	21.08
14	14.0	16.0	HEB 220	15.74	218.86	-	20.94
14	16.0	16.0	HEB 220	15.73	218.94	-	21.23
15	0.0	18.0	IPE 270	-	-	-	14.17
15	2.0	18.0	IPE 270	-	-	-	14.26
15	4.0	18.0	IPE 270	-	-	-	14.31
15	6.0	18.0	IPE 270	-	-	-	14.21
15	8.0	18.0	IPE 270	-	-	-	14.16
15	10.0	18.0	IPE 270	-	-	-	14.29
15	12.0	18.0	IPE 270	-	-	-	14.19
15	14.0	18.0	IPE 270	-	-	-	14.10
15	16.0	18.0	IPE 270	-	-	-	14.15
15	18.0	18.0	IPE 270	-	-	-	14.18
16	0.0	18.0	HEA 500	-	488.19	-	-
16	2.0	18.0	HEA 500	-	489.99	-	-
16	4.0	18.0	HEA 500	-	490.02	-	-
16	6.0	18.0	HEA 500	-	490.09	-	-
16	8.0	18.0	HEA 500	-	490.18	-	-
16	10.0	18.0	HEA 500	-	489.77	-	-
16	12.0	18.0	HEA 500	-	489.88	-	-
16	14.0	18.0	HEA 500	-	490.17	-	-
16	16.0	18.0	HEA 500	-	490.04	-	-
16	18.0	18.0	HEA 500	-	488.80	-	-
17	0.0	24.0	HEA 340	-	328.61	-	-
17	2.0	24.0	HEA 340	-	329.72	-	-
17	4.0	24.0	HEA 340	-	329.93	-	-
17	6.0	24.0	HEA 340	-	329.76	-	-
17	8.0	24.0	HEA 340	-	329.66	-	-
17	10.0	24.0	HEA 340	-	329.63	-	-
17	12.0	24.0	HEA 340	-	330.04	-	-
17	14.0	24.0	HEA 340	-	329.99	-	-
17	16.0	24.0	HEA 340	-	330.11	-	-
17	18.0	24.0	HEA 340	-	329.79	-	-
17	20.0	24.0	HEA 340	-	329.74	-	-
17	22.0	24.0	HEA 340	-	329.75	-	-
17	24.0	24.0	HEA 340	-	328.52	-	-

In section 3.2, it was shown that if the heights $h_{mid,0}$ and $h_{mid,1}$ would be plotted in Figure 17 instead of h_0 and h_1 for the three further investigated profiles, the pattern of reduced heights at the ends of the steel beams is not observed anymore. The corresponding plot is shown here:



It is pointed out that the two remaining profiles which still show this behaviour of reduced heights at the ends were not further investigated. The heights were not measured at the level of the webs for these two profiles, as this peculiarity of reduced heights at the ends was only observed during the evaluation after these two profiles were already measured.

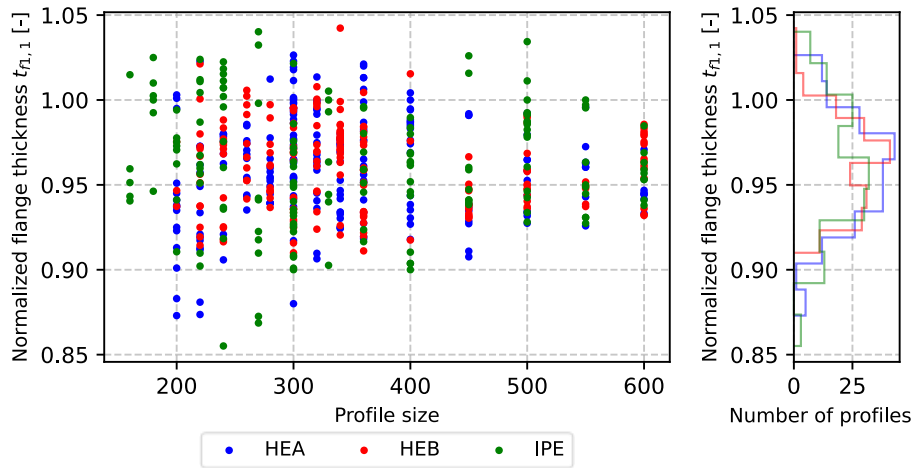
A.2.3 Repetitive measurements – uncertainty in measurement

Profile-Nr.	Measurement-Nr.	Profile	t_r [mm]	t_w [mm]	h [mm]	b [mm]	a [mm]	r [mm]
1	1	IPE 180	8.09	5.46	179.67	92.27	44.28	9.21
1	2	IPE 180	8.12	5.48	179.84	92.27	43.53	8.91
1	3	IPE 180	8.05	5.46	179.69	92.28	43.40	9.02
1	4	IPE 180	8.10	5.50	179.90	92.23	43.41	8.97
1	5	IPE 180	8.17	5.51	179.68	92.25	43.31	9.08
1	6	IPE 180	8.11	5.54	179.70	92.28	43.34	9.10
1	7	IPE 180	8.07	5.54	179.65	92.31	43.30	9.05
1	8	IPE 180	8.16	5.54	179.60	92.22	43.50	9.10
1	9	IPE 180	8.11	5.50	179.64	92.19	43.49	8.98
1	10	IPE 180	8.06	5.55	179.61	92.25	43.43	9.05
1	11	IPE 180	8.12	5.51	179.60	92.27	43.59	8.99
1	12	IPE 180	8.09	5.47	179.66	92.23	43.41	9.02
1	13	IPE 180	8.07	5.53	179.61	92.24	43.61	8.88
1	14	IPE 180	8.06	5.49	179.86	92.25	43.72	8.98
1	15	IPE 180	8.13	5.50	179.65	92.35	43.55	9.08
2	1	HEB 600	29.40	15.21	602.25	299.25	142.50	30.89
2	2	HEB 600	29.41	15.17	602.30	299.04	141.29	31.88
2	3	HEB 600	29.31	15.17	602.36	298.99	141.57	31.72
2	4	HEB 600	29.37	15.26	602.30	299.13	141.17	30.83
2	5	HEB 600	29.35	15.18	602.32	299.06	140.82	30.23
2	6	HEB 600	29.27	15.21	602.31	299.06	141.29	31.59
2	7	HEB 600	29.30	15.18	602.39	299.02	141.12	31.55
2	8	HEB 600	29.34	15.15	602.30	299.03	140.65	30.77
2	9	HEB 600	29.28	15.16	602.34	298.96	140.59	30.74
2	10	HEB 600	29.31	15.18	602.31	299.03	141.09	30.77
2	11	HEB 600	29.24	15.17	602.30	299.18	141.03	30.90
2	12	HEB 600	29.28	15.18	602.37	299.16	140.70	30.59
2	13	HEB 600	29.31	15.18	602.35	298.96	141.28	31.69
2	14	HEB 600	29.33	15.15	602.36	299.01	140.99	30.06
2	15	HEB 600	29.36	15.17	602.31	298.96	141.01	30.50
3	1	HEA 340	16.43	9.42	332.15	300.56	145.80	27.77
3	2	HEA 340	16.42	9.42	332.30	300.70	145.64	28.32
3	3	HEA 340	16.43	9.43	332.76	300.66	145.54	27.90
3	4	HEA 340	16.44	9.42	332.98	300.62	145.80	27.22
3	5	HEA 340	16.42	9.44	332.15	300.83	145.52	27.35
3	6	HEA 340	16.43	9.42	332.48	300.57	145.70	27.31
3	7	HEA 340	16.41	9.43	332.30	300.63	145.86	27.67
3	8	HEA 340	16.45	9.42	332.62	300.58	145.64	27.35
3	9	HEA 340	16.44	9.43	332.29	300.61	145.63	27.49
3	10	HEA 340	16.44	9.43	332.53	300.62	146.10	27.01
3	11	HEA 340	16.42	9.42	332.46	300.66	145.81	27.44
3	12	HEA 340	16.42	9.42	332.66	300.61	145.50	27.40
3	13	HEA 340	16.43	9.42	332.46	300.69	145.62	27.14
3	14	HEA 340	16.41	9.42	332.67	300.59	145.83	27.25
3	15	HEA 340	16.43	9.42	332.40	300.63	145.68	27.58

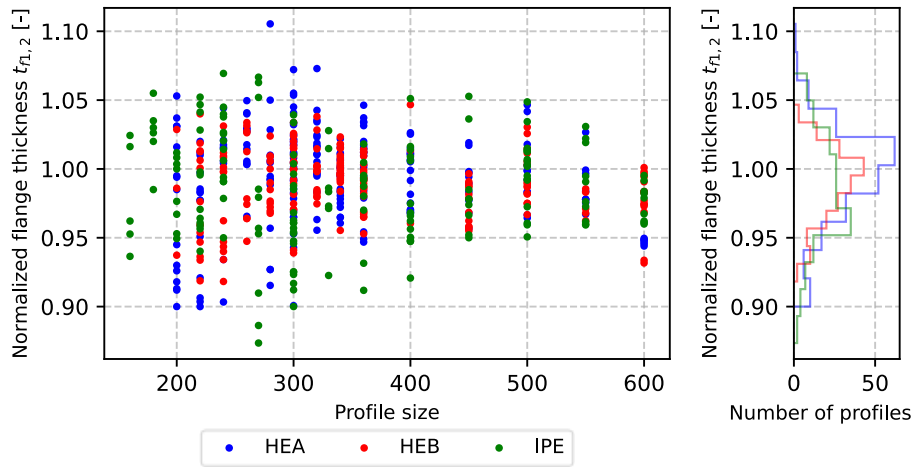
A.3 Investigation of the flange thicknesses

A.3.1 Visualization of the measurement results

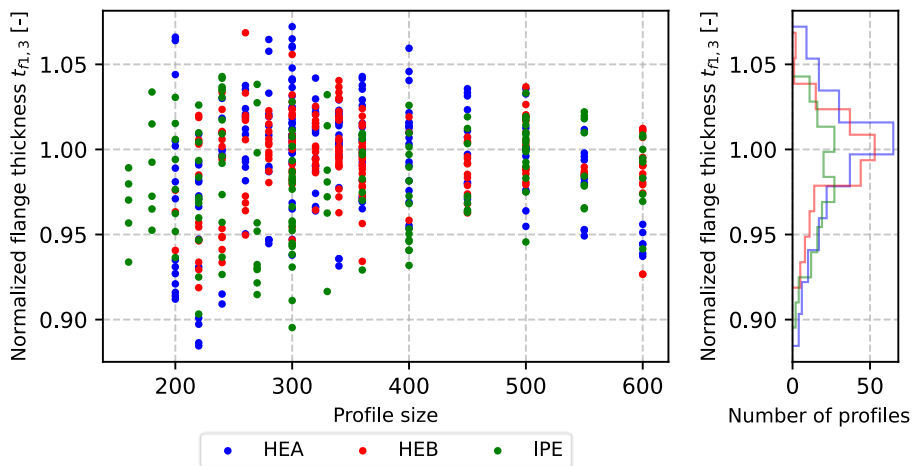
$t_{f1,1}$:



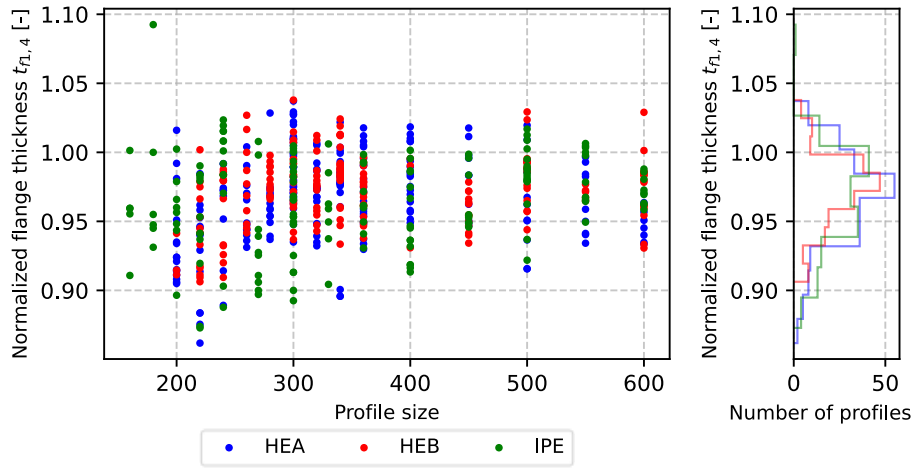
$t_{f1,2}$:



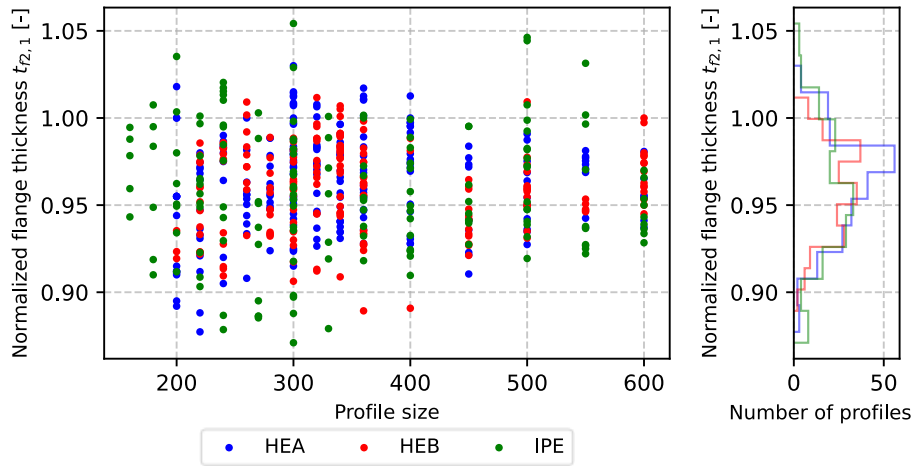
$t_{f1,3}$:



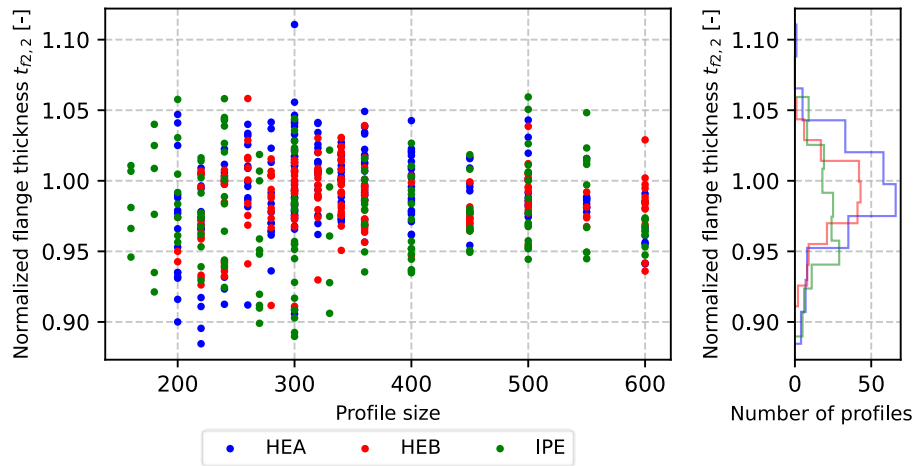
$t_{r1,4}$:



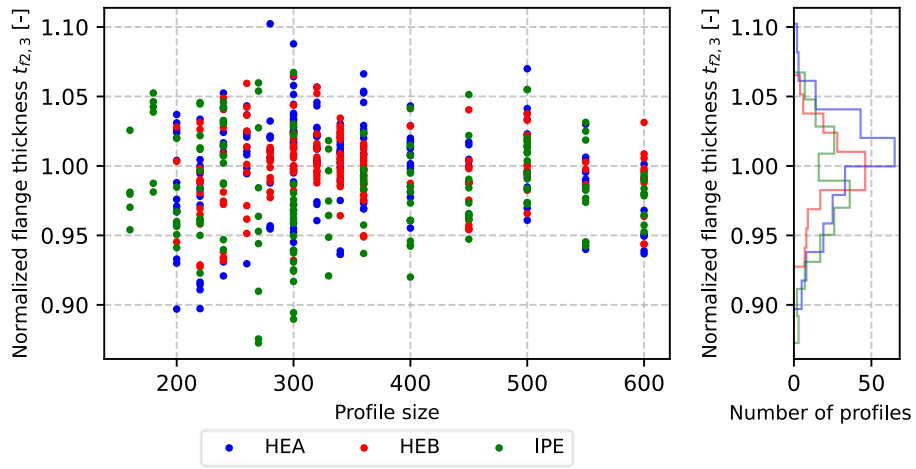
$t_{r2,1}$:



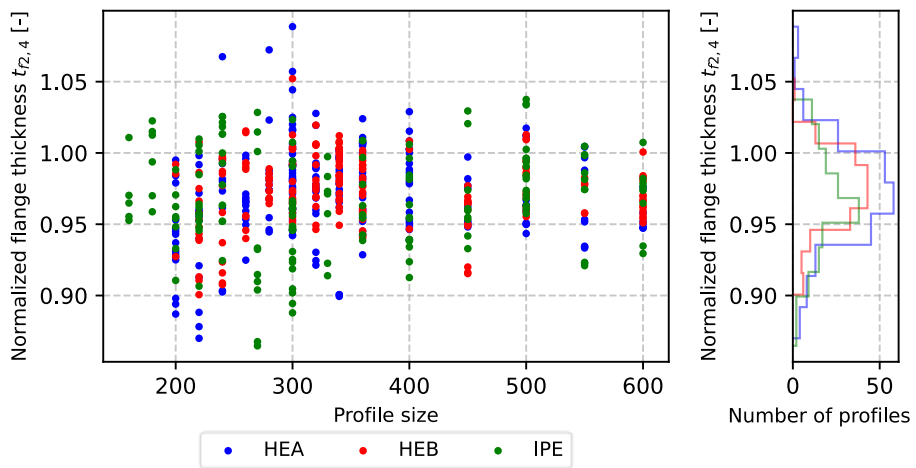
$t_{r2,2}$:



$t_{2,3}$:



$t_{2,4}$:



A.3.2 Correlation matrices

Category "Total":

	$t_{f1,1}$	$t_{f1,2}$	$t_{f1,3}$	$t_{f1,4}$	$t_{f2,1}$	$t_{f2,2}$	$t_{f2,3}$	$t_{f2,4}$
$t_{f1,1}$	1							
$t_{f1,2}$	0.806	1						
$t_{f1,3}$	0.593	0.746	1					
$t_{f1,4}$	0.601	0.608	0.808	1				
$t_{f2,1}$	0.723	0.593	0.635	0.680	1			
$t_{f2,2}$	0.595	0.700	0.805	0.699	0.799	1		
$t_{f2,3}$	0.636	0.818	0.744	0.621	0.574	0.724	1	
$t_{f2,4}$	0.688	0.725	0.691	0.729	0.606	0.649	0.838	1

Category "Small":

	$t_{f1,1}$	$t_{f1,2}$	$t_{f1,3}$	$t_{f1,4}$	$t_{f2,1}$	$t_{f2,2}$	$t_{f2,3}$	$t_{f2,4}$
$t_{f1,1}$	1							
$t_{f1,2}$	0.817	1						
$t_{f1,3}$	0.605	0.752	1					
$t_{f1,4}$	0.579	0.595	0.826	1				
$t_{f2,1}$	0.710	0.596	0.680	0.711	1			
$t_{f2,2}$	0.610	0.703	0.832	0.728	0.821	1		
$t_{f2,3}$	0.673	0.840	0.775	0.651	0.577	0.724	1	
$t_{f2,4}$	0.690	0.737	0.716	0.735	0.588	0.638	0.866	1

Category "Large":

	$t_{f1,1}$	$t_{f1,2}$	$t_{f1,3}$	$t_{f1,4}$	$t_{f2,1}$	$t_{f2,2}$	$t_{f2,3}$	$t_{f2,4}$
$t_{f1,1}$	1							
$t_{f1,2}$	0.781	1						
$t_{f1,3}$	0.568	0.737	1					
$t_{f1,4}$	0.683	0.681	0.759	1				
$t_{f2,1}$	0.751	0.589	0.527	0.616	1			
$t_{f2,2}$	0.560	0.694	0.722	0.623	0.746	1		
$t_{f2,3}$	0.542	0.755	0.661	0.559	0.567	0.724	1	
$t_{f2,4}$	0.692	0.702	0.618	0.717	0.657	0.682	0.765	1

Category “HEA”:

	$t_{f1,1}$	$t_{f1,2}$	$t_{f1,3}$	$t_{f1,4}$	$t_{f2,1}$	$t_{f2,2}$	$t_{f2,3}$	$t_{f2,4}$
$t_{f1,1}$	1							
$t_{f1,2}$	0.792	1						
$t_{f1,3}$	0.646	0.793	1					
$t_{f1,4}$	0.649	0.622	0.822	1				
$t_{f2,1}$	0.820	0.652	0.651	0.688	1			
$t_{f2,2}$	0.676	0.772	0.833	0.699	0.763	1		
$t_{f2,3}$	0.616	0.799	0.800	0.691	0.630	0.775	1	
$t_{f2,4}$	0.664	0.694	0.733	0.812	0.656	0.677	0.797	1

Category “HEB”:

	$t_{f1,1}$	$t_{f1,2}$	$t_{f1,3}$	$t_{f1,4}$	$t_{f2,1}$	$t_{f2,2}$	$t_{f2,3}$	$t_{f2,4}$
$t_{f1,1}$	1							
$t_{f1,2}$	0.726	1						
$t_{f1,3}$	0.471	0.743	1					
$t_{f1,4}$	0.492	0.681	0.855	1				
$t_{f2,1}$	0.772	0.613	0.588	0.653	1			
$t_{f2,2}$	0.567	0.731	0.825	0.760	0.756	1		
$t_{f2,3}$	0.487	0.778	0.727	0.661	0.450	0.670	1	
$t_{f2,4}$	0.590	0.703	0.691	0.741	0.529	0.618	0.835	1

Category “IPE”:

	$t_{f1,1}$	$t_{f1,2}$	$t_{f1,3}$	$t_{f1,4}$	$t_{f2,1}$	$t_{f2,2}$	$t_{f2,3}$	$t_{f2,4}$
$t_{f1,1}$	1							
$t_{f1,2}$	0.889	1						
$t_{f1,3}$	0.657	0.689	1					
$t_{f1,4}$	0.631	0.565	0.778	1				
$t_{f2,1}$	0.614	0.523	0.680	0.706	1			
$t_{f2,2}$	0.560	0.590	0.752	0.686	0.870	1		
$t_{f2,3}$	0.786	0.867	0.660	0.521	0.596	0.674	1	
$t_{f2,4}$	0.789	0.782	0.632	0.615	0.610	0.637	0.897	1

A.4 Statistical evaluation of the general measurements

A.4.1 Pre-investigation of the root fillet radii

Normalized mean values:

cat.	$\frac{r_1}{r_{nom}}$	$\frac{r_2}{r_{nom}}$	$\frac{r_3}{r_{nom}}$	$\frac{r_4}{r_{nom}}$
Total	1.0054	1.0164	1.0173	1.0111
Small	1.0085	1.0134	1.0210	1.0103
Large	1.0006	1.0210	1.0116	1.0124
HEA	0.9895	1.0008	1.0058	0.9930
HEB	1.0114	1.0272	1.0199	1.0180
IPE	1.0205	1.0251	1.0303	1.0282

Coefficients of variation (in %):

cat.	$\frac{r_1}{r_{nom}}$	$\frac{r_2}{r_{nom}}$	$\frac{r_3}{r_{nom}}$	$\frac{r_4}{r_{nom}}$
Total	9.569	8.757	8.671	10.092
Small	10.589	9.573	9.703	9.701
Large	7.709	7.348	6.725	10.685
HEA	9.526	8.810	8.781	11.811
HEB	11.512	10.205	10.104	10.365
IPE	6.164	6.078	6.122	6.244

Correlation matrices:

Category "Total":

	r_1	r_2	r_3	r_4
r_1	1			
r_2	0.571	1		
r_3	0.712	0.739	1	
r_4	0.655	0.630	0.531	1

Category "Small":

	r_1	r_2	r_3	r_4
r_1	1			
r_2	0.593	1		
r_3	0.733	0.767	1	
r_4	0.746	0.715	0.640	1

Category “Large”:

	r_1	r_2	r_3	r_4
r_1	1			
r_2	0.521	1		
r_3	0.646	0.675	1	
r_4	0.522	0.504	0.353	1

Category “HEA”:

	r_1	r_2	r_3	r_4
r_1	1			
r_2	0.550	1		
r_3	0.689	0.699	1	
r_4	0.616	0.552	0.506	1

Category “HEB”:

	r_1	r_2	r_3	r_4
r_1	1			
r_2	0.560	1		
r_3	0.740	0.766	1	
r_4	0.664	0.673	0.522	1

Category “IPE”:

	r_1	r_2	r_3	r_4
r_1	1			
r_2	0.622	1		
r_3	0.650	0.742	1	
r_4	0.776	0.764	0.624	1

A.4.2 Pre-investigation of the web thicknesses

Normalized mean values:

cat.	$\frac{t_{w1}}{t_{w,nom}}$	$\frac{t_{w2}}{t_{w,nom}}$	$\frac{t_{w3}}{t_{w,nom}}$
Total	1.0126	1.0137	1.0154
Small	1.0159	1.0194	1.0186
Large	1.0077	1.0050	1.0104
HEA	1.0195	1.0193	1.0227
HEB	1.0029	1.0081	1.0044
IPE	1.0150	1.0129	1.0186

Coefficients of variation (in %):

cat.	$\frac{t_{w1}}{t_{w,nom}}$	$\frac{t_{w2}}{t_{w,nom}}$	$\frac{t_{w3}}{t_{w,nom}}$
Total	3.750	3.776	3.654
Small	4.011	4.121	4.052
Large	3.248	2.960	2.864
HEA	3.774	3.726	3.732
HEB	3.658	3.632	3.454
IPE	3.599	3.933	3.482

Correlation matrices:

Category "Total":

	t_{w1}	t_{w2}	t_{w3}
t_{w1}	1		
t_{w2}	0.866	1	
t_{w3}	0.845	0.865	1

Category "Small":

	t_{w1}	t_{w2}	t_{w3}
t_{w1}	1		
t_{w2}	0.874	1	
t_{w3}	0.858	0.869	1

Category "Large":

	t_{w1}	t_{w2}	t_{w3}
t_{w1}	1		
t_{w2}	0.851	1	
t_{w3}	0.810	0.851	1

Category “HEA”:

	t_{w1}	t_{w2}	t_{w3}
t_{w1}	1		
t_{w2}	0.857	1	
t_{w3}	0.824	0.850	1

Category “HEB”:

	t_{w1}	t_{w2}	t_{w3}
t_{w1}	1		
t_{w2}	0.894	1	
t_{w3}	0.919	0.910	1

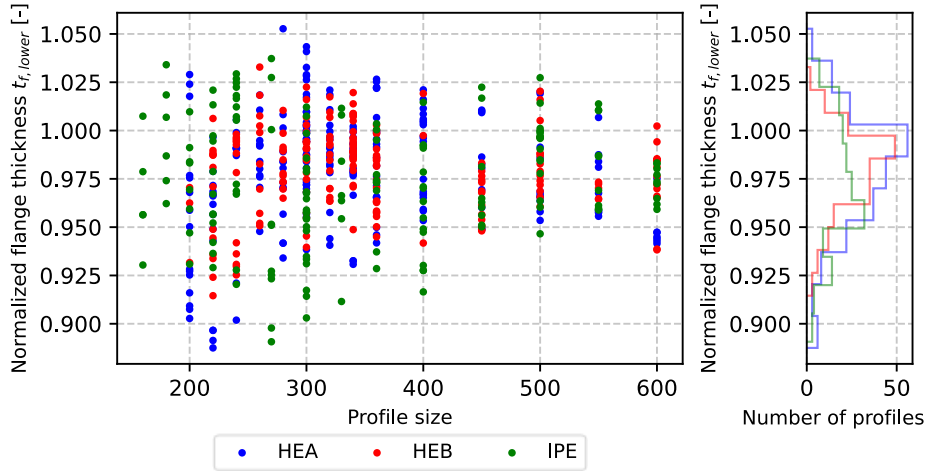
Category “IPE”:

	t_{w1}	t_{w2}	t_{w3}
t_{w1}	1		
t_{w2}	0.851	1	
t_{w3}	0.768	0.847	1

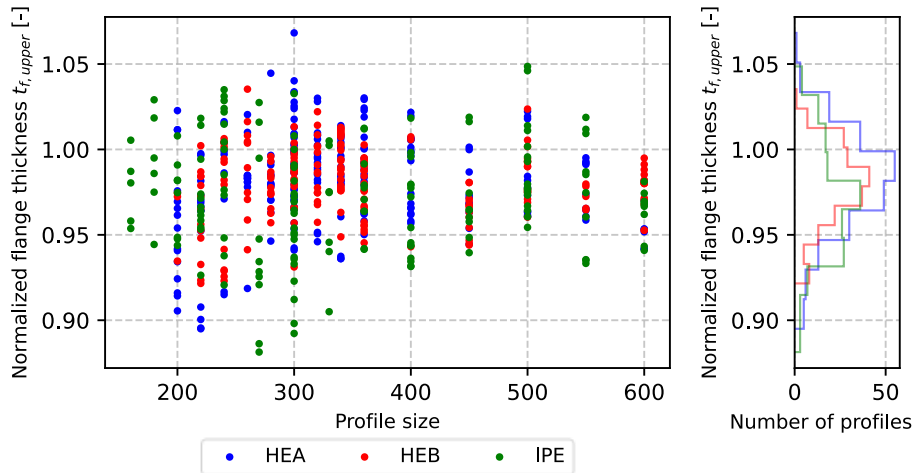
A.4.3 Visualization of the measurement results

The quantities introduced in section 3.5 are displayed in the following.

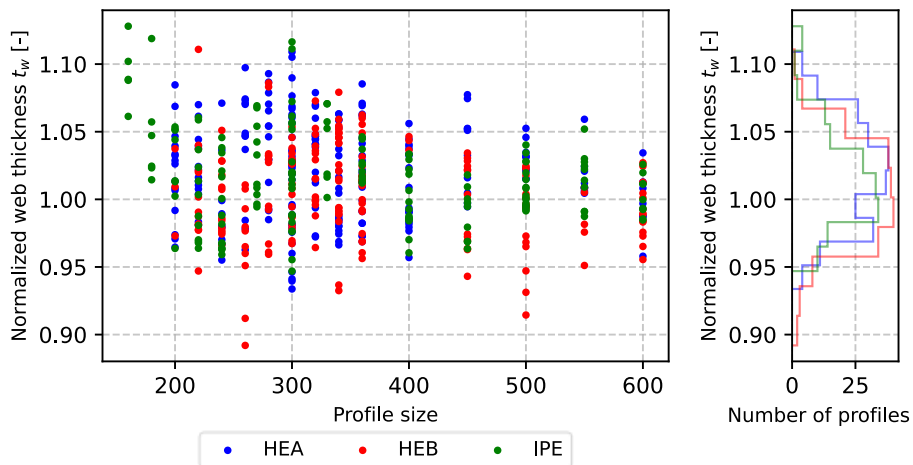
$t_{f,lower}$:



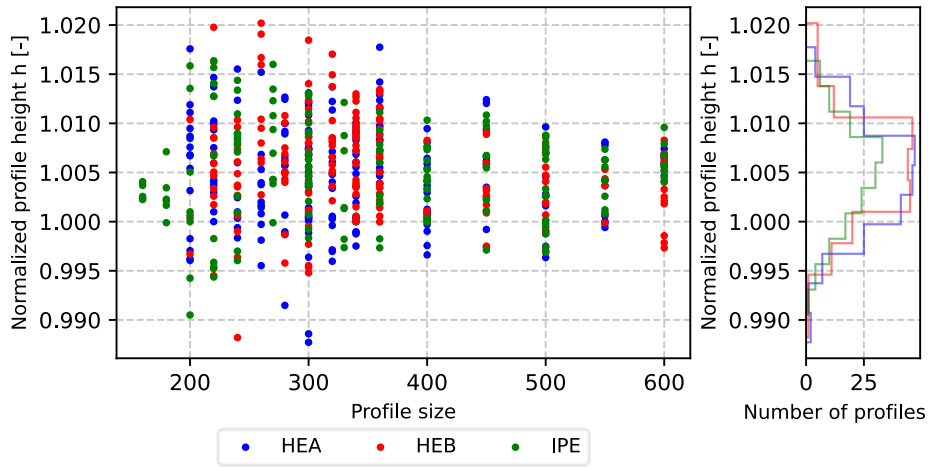
$t_{f,upper}$:



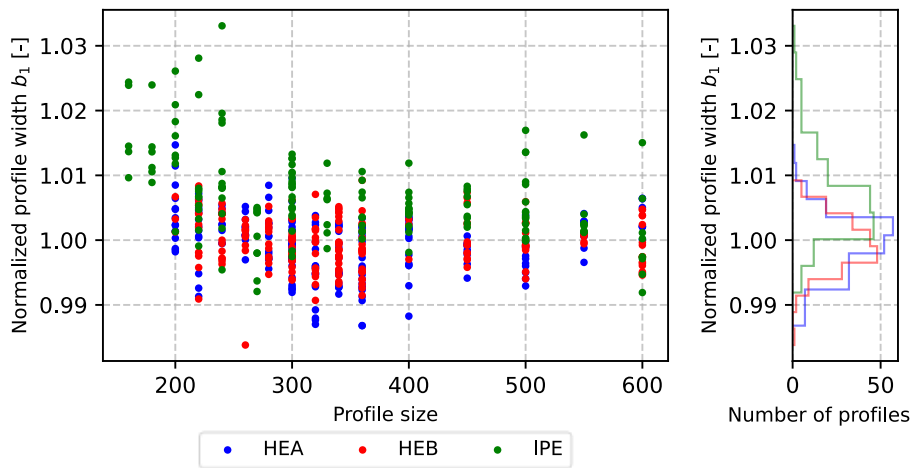
t_w :



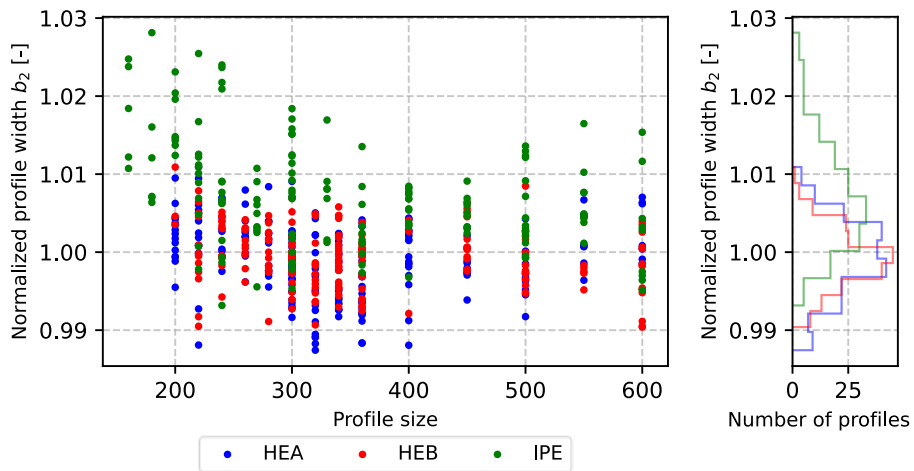
h:



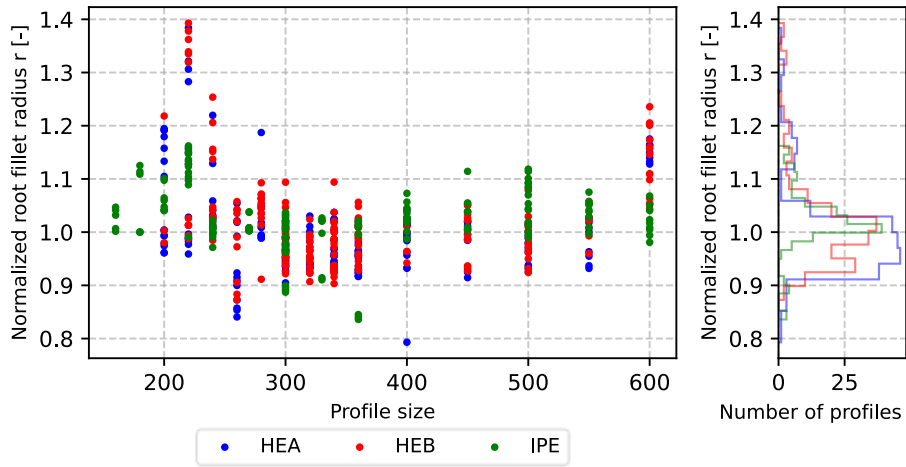
b₁:



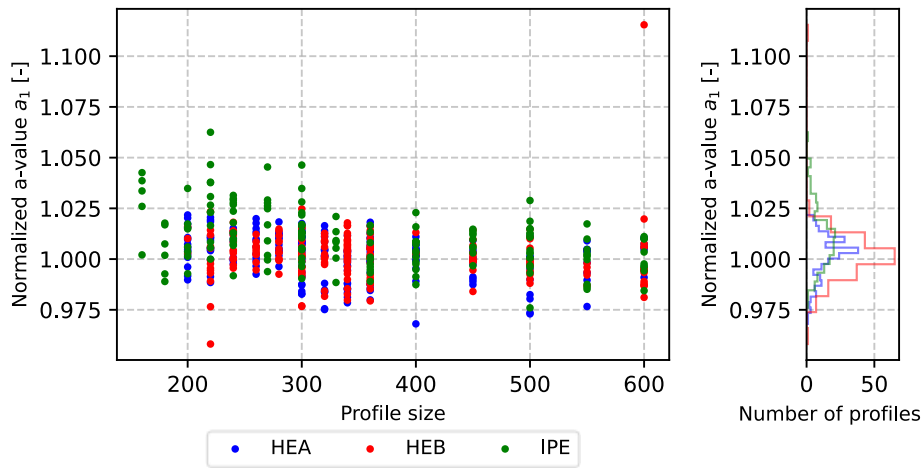
b₂:



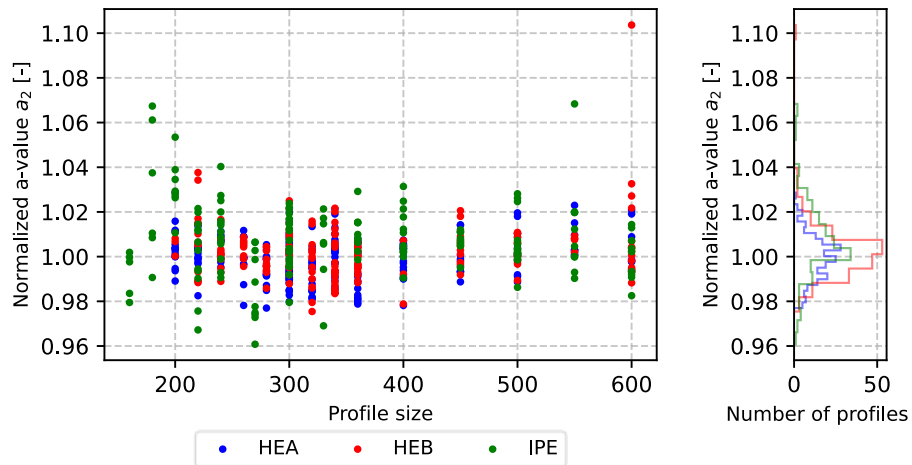
r:



a_1 :



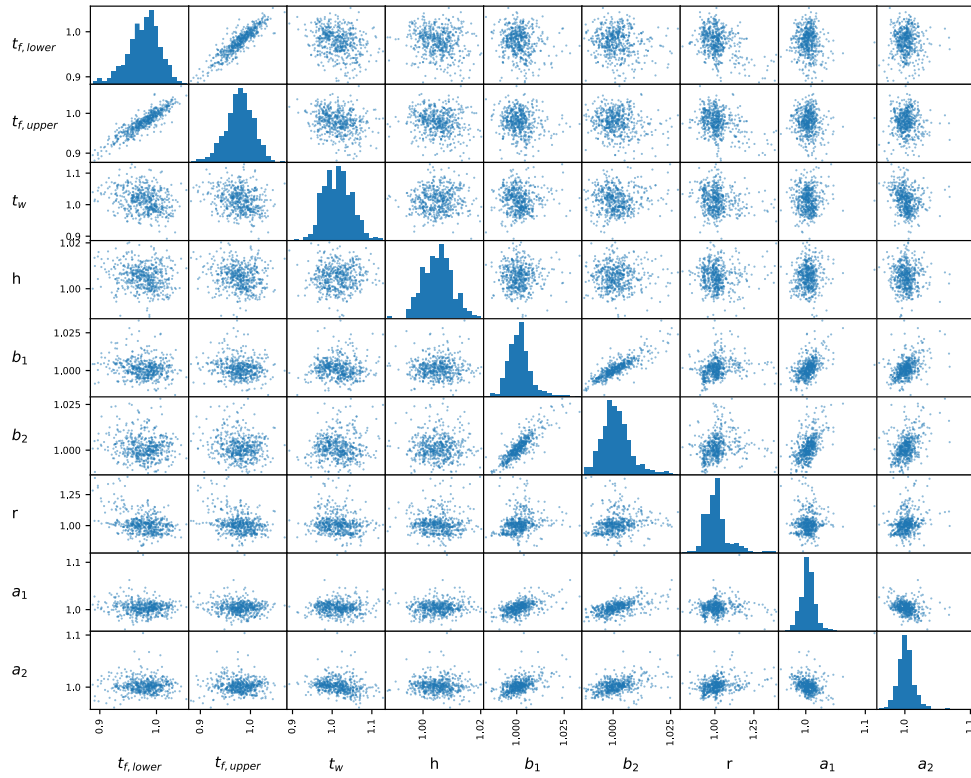
a_2 :



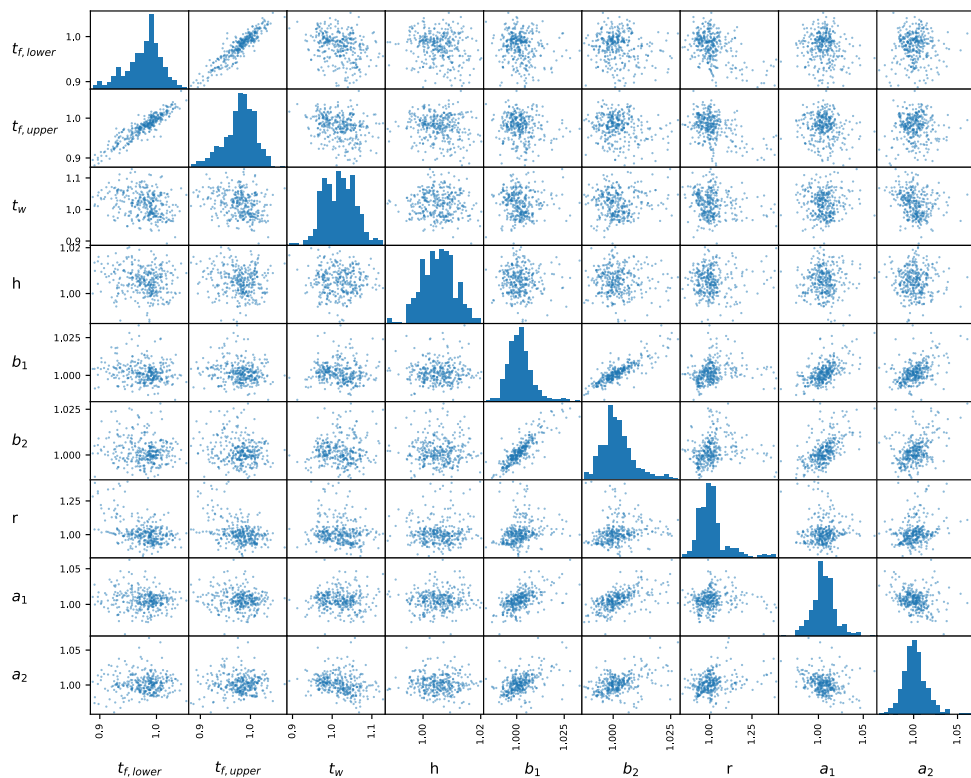
Correlation study – Scatter plot matrices:

Again, the quantities introduced in section 3.5 are displayed in the following.

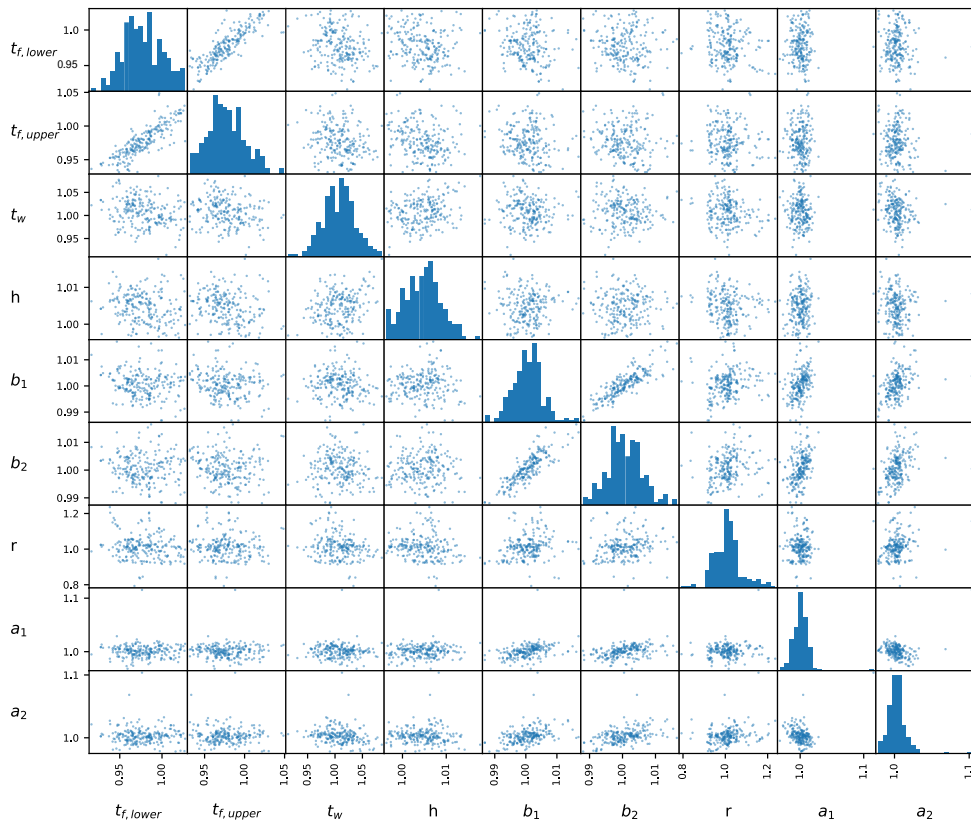
Category “Total”:



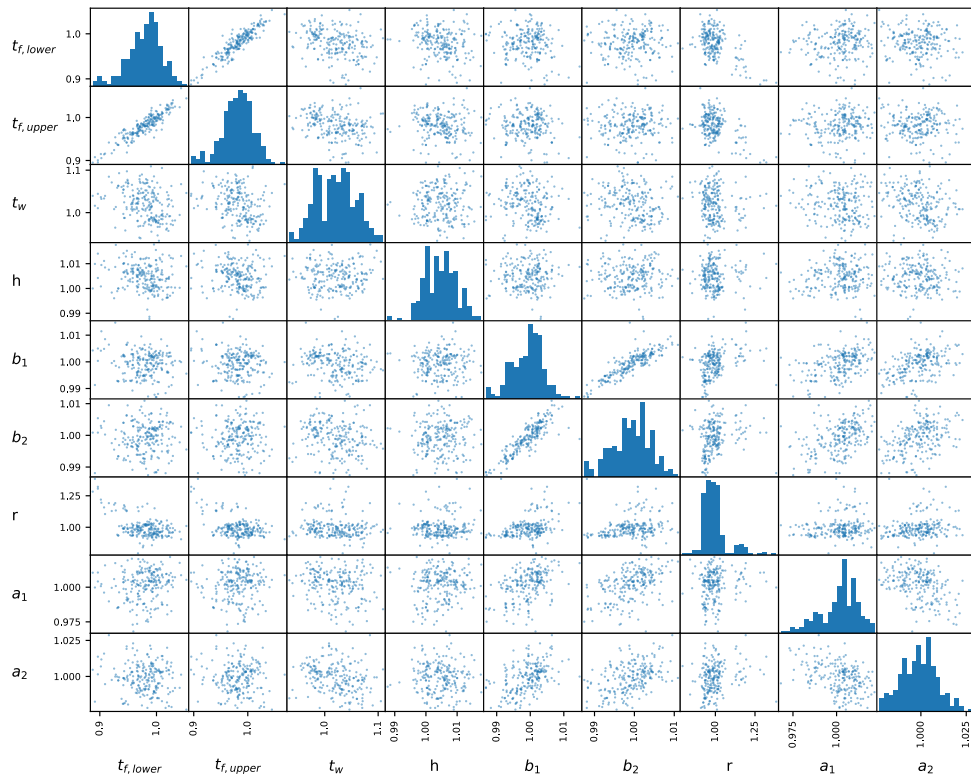
Category “Small”:



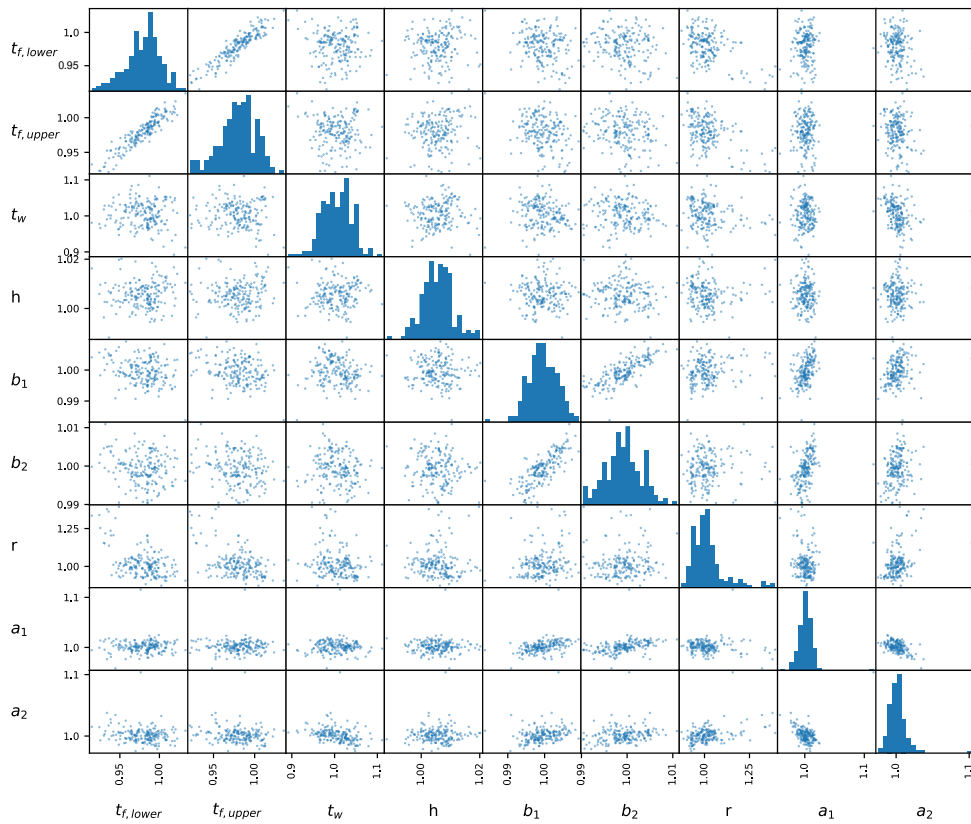
Category “Large”:



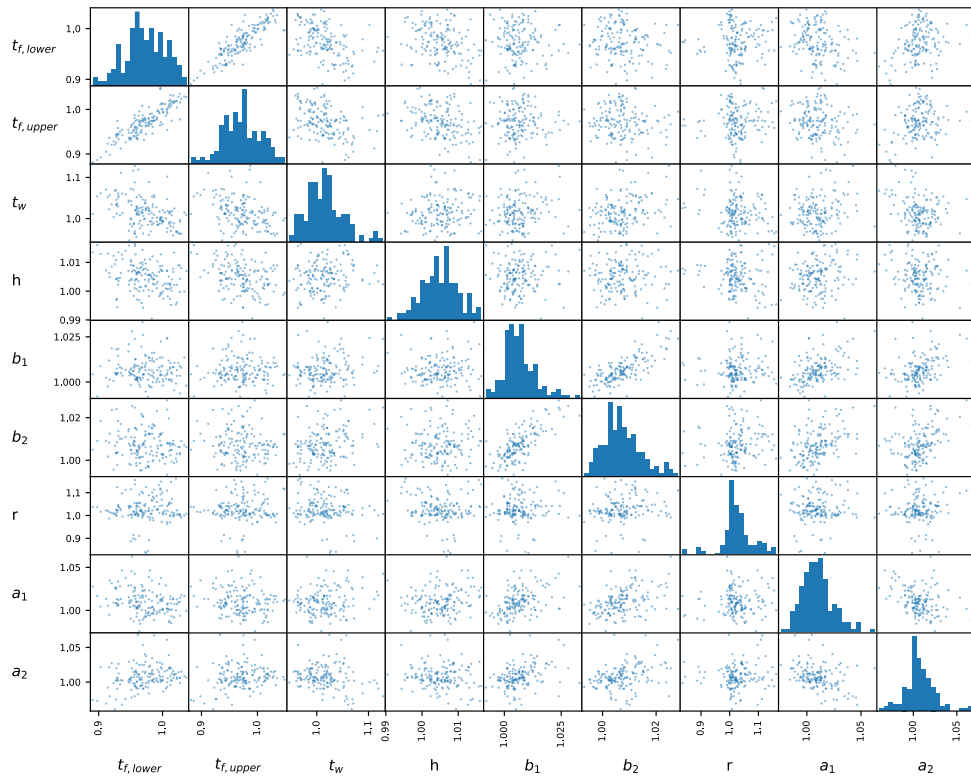
Category “HEA”:



Category “HEB”:



Category “IPE”:



A.4.4 Investigation excluding outliers of the root fillet radii

Mean values and coefficients of variation excluding outliers of the root fillet radii:

Whenever the value between the observed mean root fillet radius according to equation (15) deviates more than 2.5 mm from the recommended nominal value of the SZS C5/18 tables [7], it is defined as an outlier. This is based on the observation that the recommended root fillet radii size classes in the SZS C5/18 tables have size steps of 3 mm between each other.

cat.	$\left(\frac{r}{r_{nom}}\right)_{mean}$	$\left(\frac{r}{r_{nom}}\right)_{c.o.v.}$
Total	0.9990	4.924
Small	0.9972	5.218
Large	1.0018	4.442
HEA	0.9799	4.127
HEB	0.9928	4.501
IPE	1.0297	4.794

Correlation matrices excluding outliers of the root fillet radii:

Category "Total":

	$t_{f,lower}$	$t_{f,upper}$	t_w	h	b_1	b_2	r	a_1	a_2
$t_{f,lower}$	1								
$t_{f,upper}$	0.879	1							
t_w	-0.327	-0.294	1						
h	-0.176	-0.169	0.077	1					
b_1	-0.128	-0.131	-0.015	0.012	1				
b_2	-0.141	-0.173	0.022	0.006	0.865	1			
r	-0.134	-0.128	-0.109	-0.074	0.370	0.391	1		
a_1	-0.127	-0.127	0.007	0.109	0.559	0.569	0.163	1	
a_2	0.071	0.039	-0.260	-0.076	0.454	0.443	0.267	-0.242	1

Category "Small":

	$t_{f,lower}$	$t_{f,upper}$	t_w	h	b_1	b_2	r	a_1	a_2
$t_{f,lower}$	1								
$t_{f,upper}$	0.898	1							
t_w	-0.364	-0.339	1						
h	-0.196	-0.163	-0.004	1					
b_1	-0.139	-0.143	-0.013	0.008	1				
b_2	-0.184	-0.221	0.046	-0.002	0.866	1			
r	-0.156	-0.176	-0.122	0.002	0.382	0.399	1		
a_1	-0.196	-0.191	-0.014	0.082	0.584	0.605	0.235	1	
a_2	0.113	0.086	-0.253	-0.061	0.474	0.456	0.268	-0.213	1

Category “Large”:

	$t_{f,lower}$	$t_{f,upper}$	t_w	h	b_1	b_2	r	a_1	a_2
$t_{f,lower}$	1								
$t_{f,upper}$	0.834	1							
t_w	-0.274	-0.222	1						
h	-0.147	-0.204	0.265	1					
b_1	-0.126	-0.127	-0.079	-0.011	1				
b_2	-0.056	-0.083	-0.103	-0.006	0.854	1			
r	-0.082	-0.020	-0.063	-0.243	0.372	0.405	1		
a_1	-0.019	-0.037	-0.051	0.123	0.463	0.443	0.050	1	
a_2	-0.019	-0.058	-0.265	-0.103	0.434	0.443	0.258	-0.301	1

Category “HEA”:

	$t_{f,lower}$	$t_{f,upper}$	t_w	h	b_1	b_2	r	a_1	a_2
$t_{f,lower}$	1								
$t_{f,upper}$	0.882	1							
t_w	-0.384	-0.366	1						
h	-0.231	-0.169	0.049	1					
b_1	0.059	0.066	-0.192	0.015	1				
b_2	0.097	0.089	-0.209	0.011	0.898	1			
r	-0.152	-0.118	-0.065	0.018	0.383	0.369	1		
a_1	0.166	0.103	-0.145	0.114	0.471	0.503	0.151	1	
a_2	-0.003	0.061	-0.305	-0.082	0.437	0.414	0.174	-0.415	1

Category “HEB”:

	$t_{f,lower}$	$t_{f,upper}$	t_w	h	b_1	b_2	r	a_1	a_2
$t_{f,lower}$	1								
$t_{f,upper}$	0.896	1							
t_w	-0.147	-0.153	1						
h	0.105	0.095	0.098	1					
b_1	-0.187	-0.222	-0.111	-0.025	1				
b_2	-0.088	-0.171	-0.125	-0.046	0.776	1			
r	-0.161	-0.155	-0.103	-0.183	0.149	0.098	1		
a_1	-0.019	-0.080	-0.052	0.024	0.515	0.551	-0.124	1	
a_2	-0.057	-0.049	-0.411	-0.009	0.304	0.281	0.285	-0.461	1

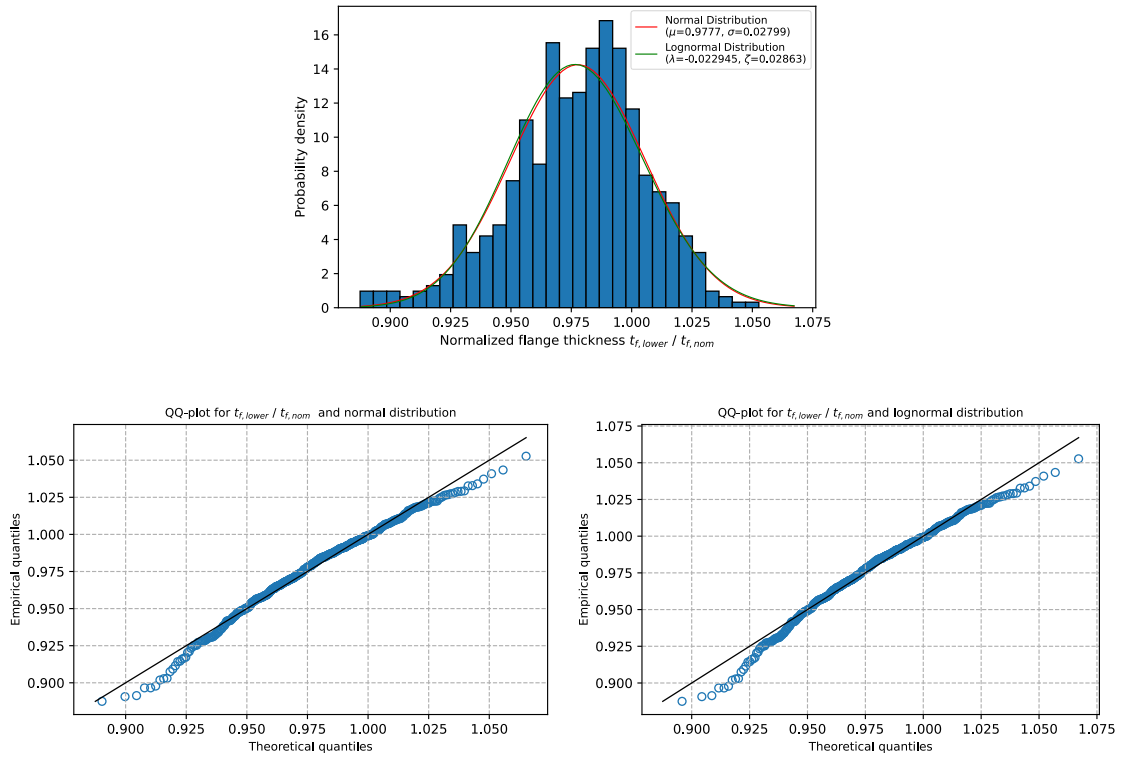
Category “IPE”:

	$t_{f,lower}$	$t_{f,upper}$	t_w	h	b_1	b_2	r	a_1	a_2
$t_{f,lower}$	1								
$t_{f,upper}$	0.862	1							
t_w	-0.437	-0.376	1						
h	-0.315	-0.345	0.132	1					
b_1	-0.034	0.016	0.172	0.048	1				
b_2	-0.117	-0.109	0.310	0.050	0.750	1			
r	0.061	0.084	-0.167	-0.102	0.072	0.141	1		
a_1	-0.269	-0.162	0.184	0.197	0.459	0.446	0.021	1	
a_2	0.276	0.193	-0.192	-0.132	0.354	0.343	0.103	-0.341	1

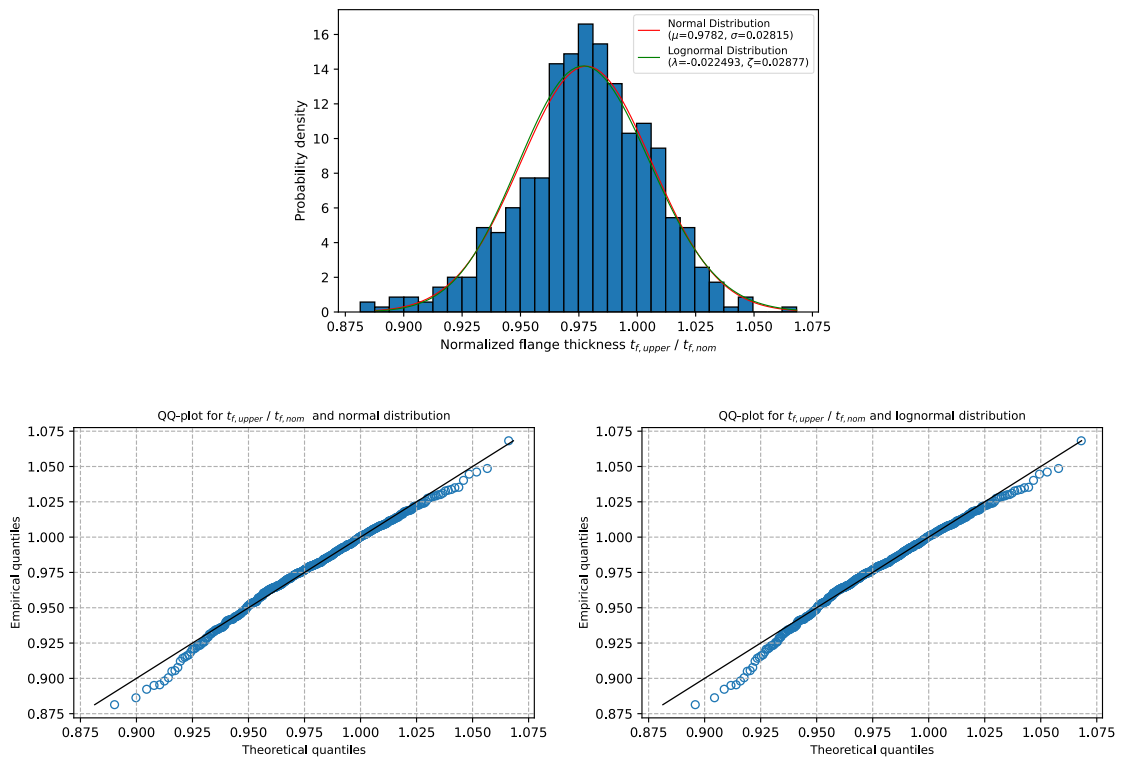
A.4.5 Choice of the probability distribution family

As mentioned in section 3.5.3, the histograms and QQ-plots are represented here for all dimensions introduced in section 3.5 except the a-values.

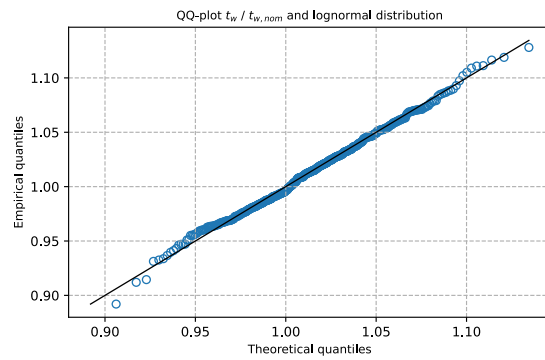
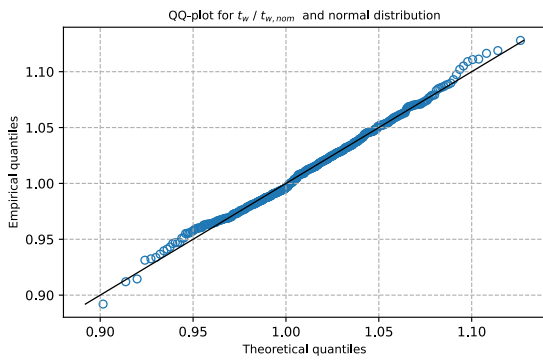
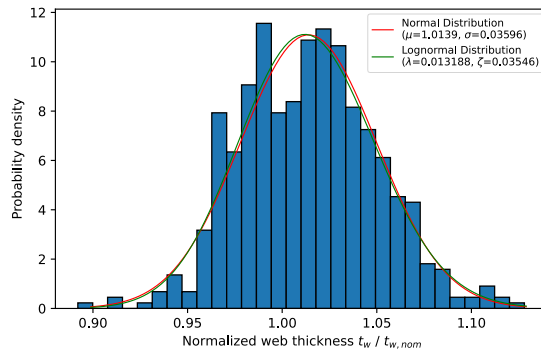
$t_{f,lower}$:



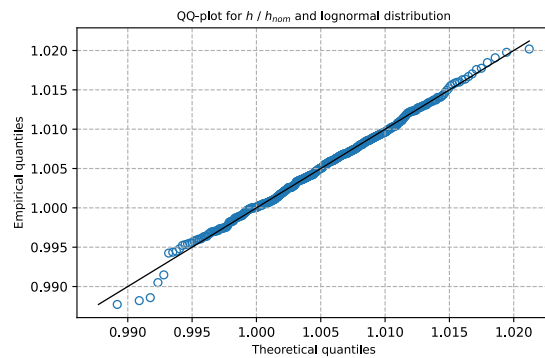
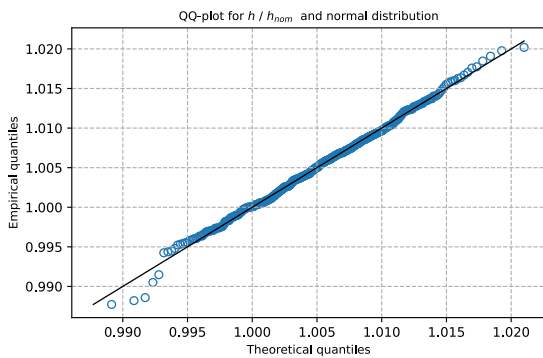
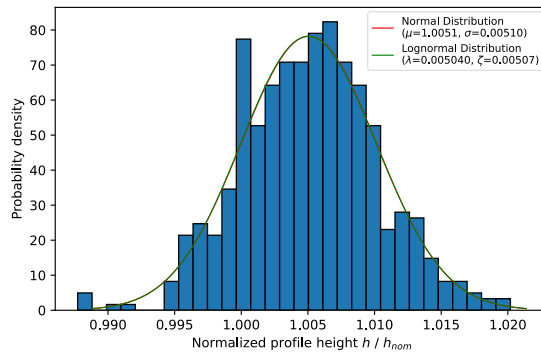
$t_{f,upper}$:



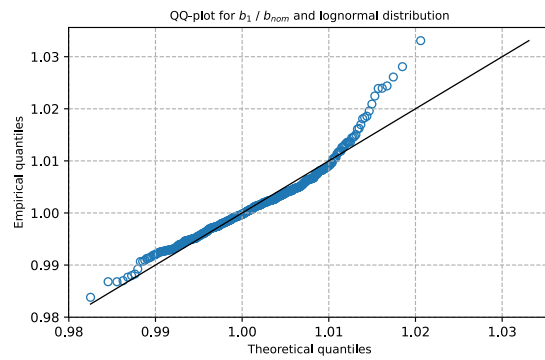
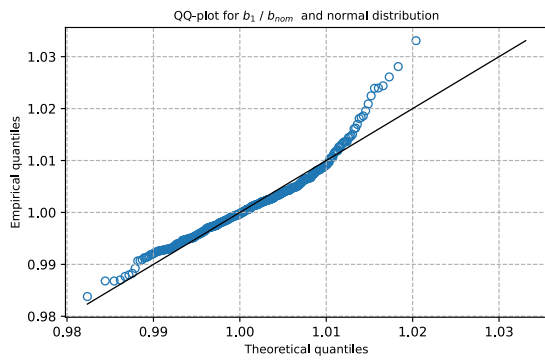
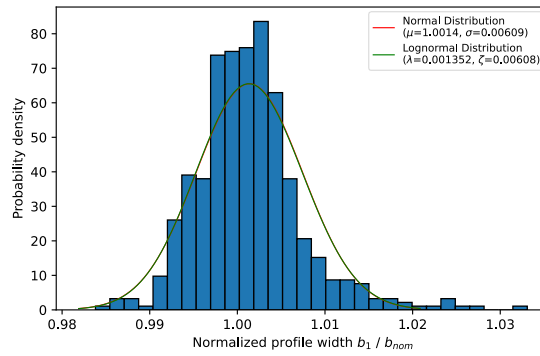
t_w:



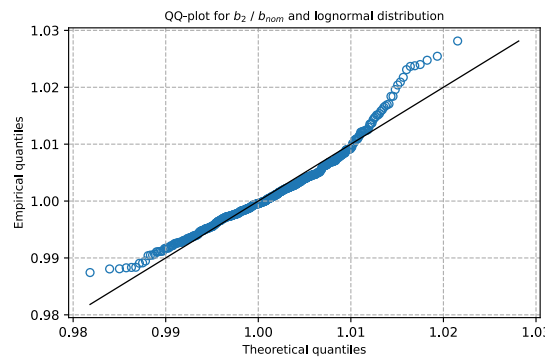
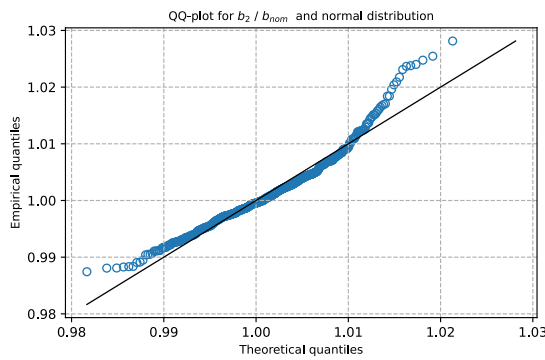
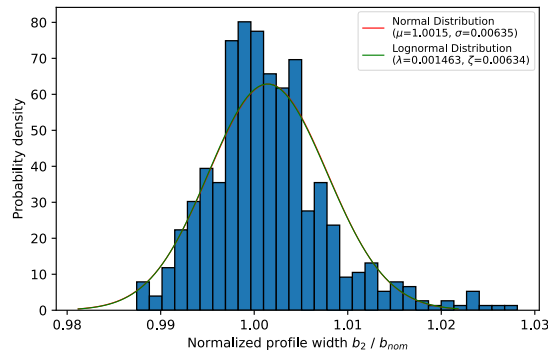
h:



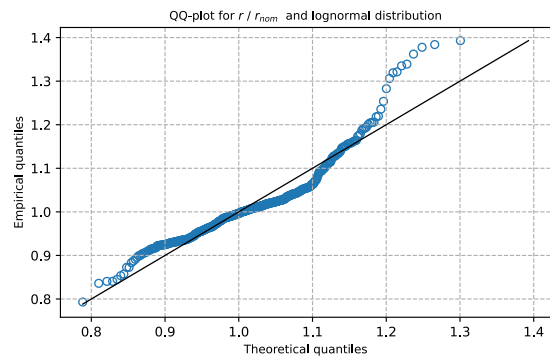
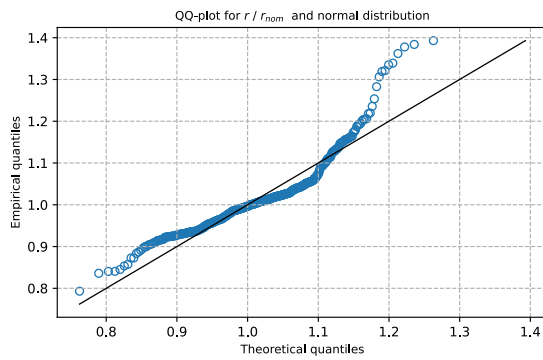
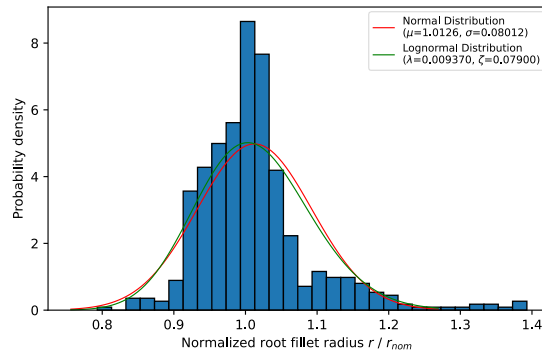
b₁:



b₂:



r:



Appendix B - Sectional properties

B.1 Real cross-sections

B.1.1 Calculated sectional properties

Profile #	Profile		Calculated quantity									
	A [mm ²]	I _y [mm ⁴]	W _{el,y,pos} [mm ³]	W _{el,y,neg} [mm ³]	W _{pl,y} [mm ³]	I _z [mm ⁴]	W _{el,z,pos} [mm ³]	W _{el,z,neg} [mm ³]	W _{pl,z} [mm ³]	e _{web} [mm]	Centroid_y [mm]	Centroid_z [mm]
1	6'250.1	52'300'000	495'283	493'549	549'432	17'700'000	158'903	161'273	247'159	-0.51	-0.840	0.2507
2	10'602.4	114'000'000	937'698	945'113	1'060'000	38'800'000	324'437	321'862	495'565	0.00	0.3194	-0.6068
3	7'461.0	74'100'000	645'594	642'375	713'813	25'300'000	210'417	211'306	324'523	0.11	-0.2438	0.3399
4	5'376.9	37'000'000	387'696	385'884	429'056	13'000'000	128'503	129'340	199'029	0.32	-0.5825	0.2915
5	3'414.5	29'100'000	263'423	258'799	296'220	2'120'000	37'343	37'722	59'516	0.42	-0.4273	1.0967
6	2'878.7	20'000'000	197'080	196'351	224'271	1'420'000	27'805	27'704	44'090	-0.33	0.4127	0.2098
7	8'591.6	103'000'000	816'272	819'858	904'522	35'800'000	274'675	271'440	420'814	2.05	-1.4126	-0.3427
8	6'202.0	51'500'000	488'630	491'030	542'787	17'500'000	158'516	158'019	244'762	0.31	-0.3246	-0.2920
9	5'216.6	35'300'000	373'240	369'839	412'448	12'300'000	122'532	123'042	189'283	0.02	0.0111	0.4354
10	3'915.5	29'100'000	327'704	322'850	367'912	2'840'000	47'449	46'897	74'036	1.10	-0.7382	0.9578
11	5'241.3	35'700'000	374'217	369'733	415'267	12'400'000	123'065	123'599	191'337	-0.95	0.6696	0.5906
12	8'927.7	80'700'000	722'153	726'354	817'501	26'400'000	238'819	241'951	372'439	-4.01	2.9836	-0.2836
13	8'836.7	79'400'000	717'576	715'060	806'576	26'500'000	238'914	239'929	369'045	-0.78	0.2813	0.1092
14	13'060.7	188'000'000	1'360'000	1'340'000	1'510'000	63'000'000	454'321	451'148	695'401	1.29	-0.8412	0.7023
15	21'127.5	783'000'000	3'460'000	3'480'000	3'890'000	114'000'000	761'973	753'966	1'170'000	0.95	-0.2981	-0.6552
16	17'664.0	621'000'000	2'830'000	2'830'000	3'160'000	89'300'000	599'606	594'955	923'961	0.62	-0.0568	0.3812
17	14'896.4	254'000'000	1'670'000	1'680'000	1'870'000	83'400'000	555'033	552'074	852'728	-0.65	1.0850	-0.4101
18	10'878.9	180'000'000	1'230'000	1'230'000	1'350'000	60'500'000	399'619	405'662	617'577	-0.94	-0.0771	-0.1383
19	10'847.1	179'000'000	1'230'000	1'210'000	1'350'000	60'000'000	397'075	402'001	612'627	-1.22	0.4990	1.2287
20	13'873.7	694'000'000	2'510'000	2'510'000	2'870'000	27'500'000	271'500	256'396	410'004	0.00	0.1724	0.1697
21	12'399.5	228'000'000	1'470'000	1'460'000	1'620'000	67'500'000	453'513	447'833	691'996	2.15	-1.3701	0.4854
22	5'270.7	82'700'000	550'721	545'576	618'693	5'860'000	77'181	77'732	121'443	-0.11	0.0859	0.7237
23	14'735.8	251'000'000	1'660'000	1'660'000	1'860'000	83'300'000	552'935	551'168	852'120	-0.39	0.8700	-0.2770
24	23'820.4	1'070'000'000	4'270'000	4'270'000	4'800'000	126'000'000	836'987	831'067	1'290'000	-0.06	0.6051	-0.0727
25	23'659.8	1'060'000'000	4'230'000	4'270'000	4'770'000	125'000'000	833'314	822'869	1'280'000	0.69	0.2651	-1.0965
26	11'577.3	484'000'000	1'940'000	1'910'000	2'200'000	20'800'000	207'947	207'478	328'448	0.14	0.0691	1.8306
27	5'344.6	83'500'000	548'506	553'621	624'737	6'060'000	78'612	79'076	124'153	-0.04	-0.0944	-0.6555
28	5'128.4	80'600'000	535'692	533'380	602'428	5'720'000	75'958	75'819	118'397	0.44	-0.1719	0.3418
29	5'189.7	81'700'000	543'536	540'642	610'545	5'840'000	77'252	77'032	120'627	-0.16	0.1528	0.4426
30	9'900.2	141'000'000	1'050'000	1'020'000	1'140'000	48'500'000	344'008	341'961	526'718	1.03	-0.6022	2.1063
31	5'336.8	83'400'000	555'347	549'938	624'448	5'970'000	78'755	79'177	123'689	-0.54	0.1524	0.7427
32	9'638.7	137'000'000	1'000'000	1'010'000	1'110'000	46'800'000	333'070	331'739	509'533	0.85	-0.7246	-0.7891
33	15'129.5	258'000'000	1'700'000	1'710'000	1'900'000	84'600'000	567'785	564'900	869'040	-0.78	1.3037	-0.2291
34	14'821.0	250'000'000	1'660'000	1'660'000	1'860'000	84'900'000	562'863	560'585	862'884	1.40	-0.8841	0.1543
35	5'338.5	82'200'000	546'026	538'414	617'408	5'620'000	74'051	74'382	117'887	-0.41	0.2269	1.1081
36	13'388.3	667'000'000	2'410'000	2'420'000	2'770'000	25'600'000	244'356	241'727	387'364	0.84	-0.2616	-0.2974
37	14'220.1	240'000'000	1'610'000	1'590'000	1'780'000	82'100'000	546'399	540'018	827'902	1.03	-0.0897	0.9131
38	12'398.1	229'000'000	1'450'000	1'460'000	1'620'000	66'700'000	442'473	446'589	686'276	-0.49	-0.0708	-0.5499
39	8'256.8	226'000'000	1'110'000	1'130'000	1'270'000	12'600'000	137'430	138'341	217'532	-1.14	0.6750	-1.2855
40	16'847.4	364'000'000	2'130'000	2'150'000	2'390'000	95'300'000	634'565	636'042	975'028	-2.50	2.2876	-0.9771
41	12'432.3	228'000'000	1'460'000	1'470'000	1'620'000	66'600'000	442'246	451'472	686'609	-2.12	0.8473	-0.2385
42	22'974.5	1'440'000'000	4'840'000	4'860'000	5'440'000	112'000'000	744'551	738'777	1'150'000	0.90	-0.4605	-0.8685
43	14'734.0	256'000'000	1'680'000	1'670'000	1'870'000	84'300'000	556'431	560'153	858'002	0.21	-0.6574	0.1785
44	16'702.1	359'000'000	2'110'000	2'100'000	2'350'000	92'700'000	617'405	616'544	948'381	1.09	-0.8732	0.6203
45	16'438.8	313'000'000	1'940'000	1'960'000	2'180'000	93'600'000	623'038	618'229	952'547	0.86	-0.2478	-0.7488
46	11'476.3	189'000'000	1'290'000	1'300'000	1'420'000	64'500'000	431'506	429'034	657'765	0.62	-0.2192	-0.3417
47	5'283.8	81'800'000	542'633	548'288	615'965	5'950'000	78'434	77'877	122'644	0.33	-0.0380	-0.7832
48	6'346.7	52'900'000	501'923	504'359	556'873	18'900'000	169'926	169'481	261'092	1.19	-0.9198	-0.2756
49	5'285.8	36'500'000	380'773	382'019	422'398	12'800'000	127'338	127'399	196'067	0.34	-0.3915	-0.1386
50	6'334.1	54'700'000	510'685	511'983	566'611	18'900'000	170'595	169'813	262'446	-0.51	0.7082	-0.0666
51	8'555.1	102'000'000	812'475	818'430	899'305	35'700'000	271'991	274'467	419'698	-0.61	0.1373	-0.5189
52	5'330.7	36'700'000	384'017	384'451	425'748	12'900'000	129'057	127'972	198'001	1.29	-0.8564	-0.1288
53	13'227.2	278'000'000	1'670'000	1'660'000	1'840'000	70'800'000	477'679	471'746	728'929	0.57	0.2328	0.2865
54	11'049.5	182'000'000	1'240'000	1'240'000	1'370'000	61'400'000	406'500	406'500	629'295	1.69	-0.4537	0.1210
55	12'596.0	232'000'000	1'490'000	1'490'000	1'650'000	68'500'000	459'638	452'009	701'749	1.36	-0.2406	0.3844
56	11'524.4	191'000'000	1'300'000	1'310'000	1'430'000	64'000'000	431'262	425'876	654'333	0.74	0.2534	-0.4582
57	13'172.4	275'000'000	1'660'000	1'640'000	1'830'000	72'100'000	479'605	474'396	735'174	-0.03	1.1275	1.1419
58	13'938.6	328'000'000	1'840'000	1'860'000	2'050'000	72'900'000	491'694	486'670	751'561	1.29	-0.6154	-1.0815
59	14'042.0	332'000'000	1'880'000	1'870'000	2'070'000	75'400'000	510'105	507'206	777'571	0.07	0.3683	0.2522
60	17'836.8	643'000'000	2'920'000	2'900'000	3'240'000	95'000'000	634'739	627'255	969'228	1.14	-0.2584	0.7368
61	19'532.5	856'000'000	3'480'000	3'490'000	3'890'000	99'500'000	663'461	665'176	1'020'000	0.08	-0.2755	-0.5324
62	22'028.0	1'390'000'000	4'640'000	4'730'000	5'230'000	108'000'000	714'874	714'832	1'110'000	-0.30	0.1868	-3.1771
63	15'369.8	907'000'000	3'030'000	2'980'000	3'450'000	32'000'000	292'560	288'989	462'875	0.66	-0.1817	2.3084
64	13'317.8	664'000'000	2'410'000	2'390'000	2'750'000	25'500'000	238'007	244'394	385'656	-3.16	1.8595	0.7926
65	6'248.2	120'000'000	722'683	709'701	810'069	7'940'000	97'603	96'593	152'943	0.14	0.0772	1.5996
66	5'460.2	85'700'000	556'561	570'358	639'449	6'130'000	80'315	79'716	126'395	0.98	-0.8305	-2.0450
67	7'196.9	162'000'000	892'875	889'433	1'010'000	10'300'000	119'946	118'970	187'114	0.73	-0.2901	0.3639
68	3'876.8	39'400'000	327'111	324'007	367'821	2'830'000	46'920	47'116	73'826	0.39	-0.2790	0.5829
69	3'961.1	39'900'000	331'257	332'055	374'537	2'940'000	48'750	48'231	76'105	0.12	0.1620	-0.1673
70	2'021.4	8'650'000	107'117	108'572	123'489	677'959	16'318	16'156	25'710	0.61	-0.4248	-0.5806
71	2'507.2	13'900'000	153'393	152'421	174'923	1'090'000	22'731	23'134	36'668	-1.27	0.7566	0.3097
72	7'122.6	161'000'000	884'189	882'984	1'000'000	9'850'000	115'973	114'902	181'092	0.23	0.1185	0.1748
73	15'033.0	262'000'000	1'700'000	1'700'000	1'910'000	84'600'00						

Profile #	Calculated quantity												
	A [mm ²]	I _y [mm ⁴]	W _{el,y,pos} [mm ³]	W _{el,y,neg} [mm ³]	W _{ply} [mm ³]	I _z [mm ⁴]	W _{el,z,pos} [mm ³]	W _{el,z,neg} [mm ³]	W _{pl,z} [mm ³]	E _{web} [mm]	Centroid_y [mm]	Centroid_z [mm]	
81	17'362.9	374'000'000	2'170'000	2'190'000	2'450'000	95'000'000	637'678	633'153	976'952	0.47	0.0404	-0.7699	
82	17'221.0	374'000'000	2'180'000	2'170'000	2'440'000	95'300'000	634'699	637'829	977'065	-0.33	-0.1880	0.3149	
83	16'684.9	359'000'000	2'100'000	2'090'000	2'350'000	89'900'000	606'525	595'835	925'676	1.21	0.0452	0.1661	
84	17'836.2	431'000'000	2'370'000	2'360'000	2'650'000	96'000'000	643'928	633'232	986'715	0.27	0.8669	0.4147	
85	17'719.5	428'000'000	2'350'000	2'360'000	2'640'000	99'700'000	661'932	655'809	1'010'000	1.46	-0.5619	-0.6764	
86	17'951.4	440'000'000	2'420'000	2'400'000	2'700'000	99'100'000	657'855	663'335	1'020'000	-1.23	0.8557	0.8238	
87	17'562.0	421'000'000	2'330'000	2'320'000	2'610'000	95'800'000	640'876	635'738	980'860	1.85	-1.1303	0.5590	
88	17'579.9	420'000'000	2'320'000	2'340'000	2'610'000	95'600'000	638'924	634'814	979'715	0.84	-0.4490	-0.7216	
89	23'726.5	1'060'000'000	4'260'000	4'230'000	4'780'000	123'000'000	820'979	815'332	1'260'000	-0.05	0.4826	0.8324	
90	17'807.8	428'000'000	2'370'000	2'370'000	2'650'000	98'000'000	656'653	654'947	1'010'000	-0.89	1.2448	-0.2264	
91	24'557.8	1'340'000'000	4'850'000	4'860'000	5'450'000	126'000'000	844'583	837'457	1'300'000	-0.30	0.7923	-0.2465	
92	26'974.3	1'720'000'000	5'710'000	5'720'000	6'450'000	134'000'000	890'321	885'507	1'380'000	1.88	-1.3972	-0.4058	
93	5'207.5	35'900'000	368'990	373'231	414'881	12'300'000	122'228	120'116	188'487	1.02	-0.5544	-0.5456	
94	11'313.9	184'000'000	1'250'000	1'270'000	1'390'000	63'400'000	421'638	413'340	640'116	0.03	1.4411	-1.0140	
95	6'420.8	54'800'000	513'495	515'675	571'312	19'000'000	171'686	170'996	264'121	0.61	-0.5258	-0.1786	
96	3'325.8	27'000'000	244'289	250'004	280'954	1'950'000	35'497	35'144	55'919	0.40	-0.2089	-1.3673	
97	2'098.5	8'970'000	110'976	112'188	128'081	702'329	17'011	16'653	26'799	1.06	-0.5857	-0.4630	
98	2'486.2	13'400'000	147'330	148'793	169'892	1'000'000	21'929	21'720	34'558	0.58	-0.4184	-0.5028	
99	17'013.7	366'000'000	2'130'000	2'140'000	2'400'000	94'000'000	625'733	620'935	962'211	-0.67	1.0950	-0.3075	
100	3'357.5	28'200'000	252'580	251'965	287'518	1'960'000	35'535	34'754	56'003	1.62	-0.8849	0.1742	
101	7'754.3	56'200'000	547'744	549'781	635'002	19'500'000	189'649	188'740	298'101	0.13	0.0079	-0.2522	
102	8'930.2	80'100'000	729'575	716'213	813'696	26'500'000	238'567	241'115	370'681	-1.47	0.8894	1.1289	
103	10'643.1	113'000'000	936'409	940'039	1'050'000	39'200'000	325'551	324'503	497'928	-0.14	0.2818	-0.2130	
104	10'689.7	113'000'000	943'944	940'730	1'060'000	39'300'000	326'066	324'581	499'715	-0.23	0.5018	0.3058	
105	15'033.4	253'000'000	1'680'000	1'680'000	1'880'000	84'300'000	564'463	559'647	863'150	-1.18	1.7430	0.0570	
106	9'591.9	136'000'000	981'814	1'000'000	1'100'000	44'900'000	321'464	320'785	491'424	-0.21	0.2850	-1.6567	
107	11'860.3	196'000'000	1'320'000	1'350'000	1'470'000	66'100'000	440'727	438'810	674'569	0.54	-0.2998	-1.9659	
108	13'329.2	282'000'000	1'690'000	1'700'000	1'870'000	75'000'000	497'119	498'601	761'272	-1.35	1.1281	-0.2673	
109	21'657.7	1'140'000'000	4'230'000	4'190'000	4'710'000	110'000'000	725'865	721'806	1'120'000	0.07	0.1568	1.3387	
110	16'000.3	307'000'000	1'910'000	1'890'000	2'130'000	87'700'000	583'841	583'841	901'460	-2.47	2.5787	0.8398	
111	21'717.6	786'000'000	3'510'000	3'500'000	3'940'000	113'000'000	756'708	755'643	1'170'000	-0.59	0.7541	0.3812	
112	11'277.4	186'000'000	1'270'000	1'270'000	1'400'000	62'800'000	417'734	415'312	639'782	1.45	-0.8484	-0.3986	
113	15'300.5	911'000'000	3'010'000	3'030'000	3'460'000	32'300'000	296'277	293'357	467'597	0.29	0.0989	-0.5967	
114	13'585.8	685'000'000	2'490'000	2'480'000	2'840'000	27'200'000	255'682	259'471	408'199	-1.72	0.9031	0.4059	
115	11'823.8	497'000'000	1'960'000	2'020'000	2'260'000	22'400'000	220'973	221'070	349'064	0.17	-0.1690	-4.0462	
116	11'710.3	498'000'000	1'970'000	1'980'000	2'250'000	21'900'000	217'076	216'589	342'309	0.52	-0.1282	-0.7703	
117	11'699.0	487'000'000	1'940'000	1'940'000	2'220'000	21'100'000	210'096	210'709	332'939	-0.45	0.1983	0.4521	
118	9'743.1	328'000'000	1'470'000	1'460'000	1'660'000	16'100'000	169'208	169'491	267'053	-0.51	0.4379	0.3662	
119	9'568.4	328'000'000	1'470'000	1'450'000	1'650'000	16'100'000	167'915	168'581	265'275	-0.24	0.1020	1.7530	
120	8'280.6	229'000'000	1'140'000	1'140'000	1'290'000	12'800'000	139'807	141'522	222'227	-1.89	1.1302	-0.0499	
121	7'352.5	165'000'000	906'894	910'970	1'030'000	10'200'000	119'116	120'303	187'847	-1.06	0.6673	-0.4322	
122	7'389.4	166'000'000	918'005	918'746	1'040'000	10'500'000	122'758	123'918	193'217	-0.78	0.5007	-0.0903	
123	6'264.0	117'000'000	703'684	700'038	797'162	7'580'000	93'772	94'369	147'930	-0.36	0.0941	0.4709	
124	6'266.1	116'000'000	698'524	703'130	794'949	7'610'000	94'938	95'021	149'280	-0.68	0.5430	-0.5808	
125	5'359.5	83'800'000	556'711	557'961	628'459	6'120'000	80'733	80'599	126'372	-0.66	0.6065	-0.1630	
126	11'239.2	181'000'000	1'240'000	1'240'000	1'380'000	62'100'000	412'037	411'353	633'556	0.20	-0.1583	0.1448	
127	11'288.3	183'000'000	1'250'000	1'250'000	1'390'000	62'900'000	416'593	414'706	640'537	1.43	-1.0758	-0.1509	
128	13'300.8	274'000'000	1'660'000	1'660'000	1'840'000	71'500'000	480'102	478'349	735'378	1.00	-0.5660	0.1849	
129	13'301.0	282'000'000	1'680'000	1'700'000	1'860'000	74'100'000	493'670	492'520	753'733	0.22	-0.0844	-0.9506	
130	13'303.9	281'000'000	1'680'000	1'700'000	1'860'000	74'000'000	493'182	490'344	752'535	1.07	-0.5899	-0.7929	
131	14'416.2	334'000'000	1'900'000	1'900'000	2'100'000	76'400'000	513'789	507'174	785'608	1.10	-0.1650	-0.0646	
132	15'931.1	453'000'000	2'320'000	2'330'000	2'570'000	86'600'000	574'574	575'548	880'959	0.01	-0.0774	-0.2819	
133	15'768.4	448'000'000	2'280'000	2'290'000	2'540'000	82'300'000	546'403	548'409	843'772	-1.96	1.7000	-0.5410	
134	14'511.3	338'000'000	1'940'000	1'910'000	2'130'000	79'900'000	532'058	529'277	813'756	0.05	0.2796	1.0819	
135	16'218.9	316'000'000	1'960'000	1'940'000	2'180'000	93'700'000	621'336	620'382	949'296	0.51	-0.2874	0.7708	
136	22'136.7	1'400'000'000	4'690'000	4'710'000	5'260'000	107'000'000	714'195	712'207	1'100'000	0.91	-0.7020	-0.7143	
137	17'844.4	635'000'000	2'860'000	2'890'000	3'210'000	92'600'000	617'027	609'956	951'992	0.40	0.5489	-0.7637	
138	19'028.9	839'000'000	3'410'000	3'420'000	3'800'000	96'700'000	645'114	652'851	997'053	-1.35	0.5519	-0.4363	
139	17'635.2	628'000'000	2'840'000	2'840'000	3'160'000	89'000'000	594'588	590'264	916'953	-0.74	1.1585	-0.0202	
140	19'959.7	876'000'000	3'540'000	3'620'000	3'990'000	104'000'000	690'916	687'027	1'060'000	-1.36	1.7044	-2.9581	
141	20'705.6	1'110'000'000	4'060'000	4'060'000	4'540'000	105'000'000	688'742	696'886	1'070'000	0.42	-1.1781	-0.1715	
142	11'345.3	187'000'000	1'280'000	1'280'000	1'410'000	64'100'000	425'997	425'985	651'646	0.25	-0.1708	0.0036	
143	13'107.1	272'000'000	1'630'000	1'660'000	1'820'000	70'900'000	474'292	472'864	729'410	-1.64	1.7823	-1.1493	
144	14'500.5	346'000'000	1'950'000	1'950'000	2'150'000	81'200'000	538'587	540'139	824'270	0.24	-0.3554	0.0876	
145	14'510.9	249'000'000	1'640'000	1'640'000	1'830'000	81'200'000	540'941	537'205	830'732	-1.50	1.8802	-0.3109	
146	14'639.1	250'000'000	1'650'000	1'650'000	1'840'000	80'200'000	537'092	537'098	828'670	-3.49	3.3941	-0.2651	
147	16'943.1	364'000'000	2'150'000	2'130'000	2'390'000	96'300'000	639'373	637'665	976'614	-0.10	0.2867	0.6638	
148	26'894.6	1'720'000'000	5'710'000	5'690'000	6'430'000	131'000'000	875'295	876'581	1'360'000	-1.36	1.3125	0.3028	
149	26'461.7	1'690'000'000	5'580'000	5'620'000	6'320'000	130'000'000	855'344	871'528	1'340'000	-2.87	1.5124	-1.1144	
150	26'614.6	1'710'000'000	5'690'000	5'650'000	6'390'000	130'000'000	870'025	873'350	1'350'000	-0.05	-0.1728	1.1846	
151	24'819.3	1'350'000'000	4'900'000	4'870'000	5'490'000	125'000'000	837'198	833'037	1'290'000	-0.87	1.0299	0.7252	
152	23'429.4	1'070'000'000	4'270'000	4'240'000	4'780'000	121'000'000	811'000	808'217	1'250'000</				

Profile #	Calculated quantity											Centroid_y [mm]	Centroid_z [mm]
	A [mm ²]	I _y [mm ⁴]	W _{el,y,pos} [mm ³]	W _{el,y,neg} [mm ³]	W _{ply} [mm ³]	I _z [mm ⁴]	W _{el,z,pos} [mm ³]	W _{el,z,neg} [mm ³]	W _{pl,z} [mm ³]	E _{web} [mm]			
161	14'973.2	250'000'000	1'680'000	1'670'000	1'870'000	85'200'000	566'580	568'466	869'200	-1.34	0.9147	0.2529	
162	9'868.6	136'000'000	996'770	1'030'000	1'120'000	46'400'000	330'401	328'929	510'893	1.19	-0.8456	-1.9657	
163	6'242.9	52'900'000	493'523	497'737	551'917	17'000'000	155'948	155'272	241'997	0.92	-0.8629	-0.5551	
164	3'387.4	28'600'000	258'147	258'751	292'572	2'090'000	37'784	37'458	59'098	0.42	-0.2068	-0.1386	
165	13'090.3	195'000'000	1'380'000	1'380'000	1'540'000	65'600'000	468'216	466'182	714'870	0.42	-0.3388	0.3107	
166	8'988.3	83'200'000	742'553	739'563	833'557	26'600'000	241'881	242'818	374'064	-0.50	0.1474	0.1591	
167	11'562.2	150'000'000	1'130'000	1'140'000	1'270'000	49'300'000	377'447	377'275	579'651	0.74	-0.7300	-0.5844	
168	8'881.1	108'000'000	860'065	861'581	947'570	37'500'000	286'693	286'960	440'681	-0.41	0.4021	-0.1144	
169	9'863.7	141'000'000	1'030'000	1'030'000	1'140'000	47'500'000	337'754	335'601	517'444	0.45	-0.1866	0.1034	
170	10'234.3	111'000'000	917'277	910'877	1'030'000	36'200'000	302'094	299'925	464'340	1.20	-0.9724	0.4496	
171	11'269.5	186'000'000	1'270'000	1'280'000	1'400'000	63'000'000	420'539	417'239	641'274	1.28	-0.6514	-0.2577	
172	15'402.0	917'000'000	3'030'000	3'050'000	3'480'000	32'900'000	298'606	297'761	473'434	-0.67	0.7246	-1.1293	
173	13'597.1	685'000'000	2'480'000	2'490'000	2'840'000	27'300'000	256'239	259'261	409'113	-1.61	0.9191	-0.4503	
174	11'862.3	498'000'000	1'960'000	2'030'000	2'270'000	22'400'000	221'551	221'514	349'820	0.44	-0.3433	-4.1168	
175	11'753.1	499'000'000	1'980'000	1'980'000	2'250'000	21'700'000	215'843	215'231	340'928	0.39	-0.2937	0.0390	
176	11'563.3	484'000'000	1'960'000	1'910'000	2'200'000	21'700'000	214'957	212'643	338'611	0.77	-0.2280	3.2953	
177	11'699.9	486'000'000	1'940'000	1'940'000	2'210'000	21'000'000	209'692	210'056	331'779	-0.30	0.1373	0.2499	
178	23'610.5	1'070'000'000	4'240'000	4'240'000	4'770'000	122'000'000	810'743	808'650	1'250'000	-0.86	1.0169	-0.0567	
179	6'327.9	117'000'000	708'886	711'361	804'916	7'660'000	95'618	95'443	150'477	0.56	-0.4695	-0.3305	
180	11'228.9	182'000'000	1'240'000	1'250'000	1'380'000	62'100'000	413'525	410'077	633'988	1.68	-1.1035	-0.0435	
181	11'156.6	181'000'000	1'250'000	1'230'000	1'370'000	61'700'000	411'728	411'947	629'010	1.01	-1.1282	1.3860	
182	13'331.0	282'000'000	1'690'000	1'860'000	1'700'000	73'900'000	493'153	490'361	753'048	0.01	0.4008	-0.4122	
183	13'316.8	275'000'000	1'670'000	1'670'000	1'840'000	73'300'000	486'428	490'947	749'408	-2.92	2.2867	-0.3299	
184	15'883.3	448'000'000	2'300'000	2'310'000	2'550'000	85'400'000	569'727	567'046	872'244	0.94	-0.5771	-0.4572	
185	18'110.4	441'000'000	2'440'000	2'420'000	2'710'000	102'000'000	675'903	672'367	1'030'000	0.98	-0.6514	0.8090	
186	22'155.7	1'390'000'000	4'680'000	4'710'000	5'250'000	107'000'000	711'667	711'899	1'100'000	0.86	-0.7633	-0.9836	
187	17'864.1	647'000'000	2'920'000	2'890'000	3'240'000	91'400'000	601'598	605'330	939'152	0.55	0.1116	1.1644	
188	17'669.1	630'000'000	2'840'000	2'850'000	3'170'000	89'200'000	596'826	593'840	920'190	-0.50	1.0249	-0.7307	
189	19'736.3	866'000'000	3'510'000	3'520'000	3'930'000	99'400'000	662'678	661'670	1'030'000	-0.22	0.6735	-0.6990	
190	20'889.0	1'100'000'000	4'060'000	4'050'000	4'530'000	103'000'000	687'554	686'332	1'060'000	-0.54	0.6855	0.3865	
191	20'709.4	1'110'000'000	4'060'000	4'060'000	4'530'000	105'000'000	688'037	697'057	1'070'000	0.08	-0.9363	-0.4117	
192	13'118.4	272'000'000	1'640'000	1'650'000	1'820'000	71'100'000	476'209	471'042	731'661	-1.32	2.0758	-0.0550	
193	14'538.2	346'000'000	1'950'000	1'950'000	2'160'000	80'900'000	537'175	538'016	821'929	0.52	-0.6098	-0.1395	
194	16'945.1	365'000'000	2'150'000	2'130'000	2'390'000	96'300'000	639'431	637'998	976'602	-0.41	0.5743	0.9580	
195	25'160.8	1'350'000'000	4'900'000	4'900'000	5'520'000	126'000'000	841'430	841'430	1'310'000	-0.99	1.0658	-0.0705	
196	26'904.2	1'720'000'000	5'710'000	5'700'000	6'430'000	131'000'000	875'287	878'071	1'360'000	-1.22	1.0723	0.1855	
197	26'482.4	1'690'000'000	5'580'000	5'620'000	6'320'000	130'000'000	854'327	870'883	1'340'000	-2.89	1.5351	-1.1153	
198	26'584.5	1'710'000'000	5'680'000	5'620'000	6'370'000	130'000'000	869'292	871'872	1'350'000	0.06	-0.2987	1.6807	
199	24'746.4	1'340'000'000	4'870'000	4'840'000	5'460'000	125'000'000	835'857	832'506	1'290'000	-1.24	1.3581	0.7043	
200	23'542.3	1'060'000'000	4'270'000	4'260'000	4'780'000	125'000'000	840'063	837'401	1'290'000	-1.59	1.7549	0.4876	
201	21'809.5	803'000'000	3'550'000	3'540'000	3'990'000	115'000'000	764'169	758'991	1'180'000	-0.47	1.1338	0.5088	
202	20'831.5	768'000'000	3'410'000	3'390'000	3'820'000	110'000'000	730'544	734'254	1'130'000	-0.49	0.2148	0.5598	
203	17'929.8	430'000'000	2'380'000	2'380'000	2'670'000	100'000'000	666'588	666'588	1'020'000	0.22	-0.1154	0.0497	
204	19'922.6	577'000'000	2'880'000	2'880'000	3'240'000	106'000'000	712'365	706'930	1'090'000	1.75	-0.9202	-0.1419	
205	18'005.7	435'000'000	2'390'000	2'380'000	2'680'000	97'600'000	646'485	646'485	999'804	0.42	0.4131	0.2117	
206	16'980.6	369'000'000	2'160'000	2'150'000	2'410'000	96'200'000	641'750	637'164	978'190	1.69	-1.3003	0.1705	
207	15'769.8	305'000'000	1'890'000	1'890'000	2'110'000	87'700'000	590'213	585'236	900'289	0.78	-0.0528	-0.2011	
208	13'488.2	680'000'000	2'430'000	2'470'000	2'810'000	26'500'000	251'262	248'257	397'245	1.35	-0.5256	-2.6190	
209	7'719.5	78'100'000	675'299	680'139	748'703	27'800'000	230'391	229'210	352'412	0.61	-0.5356	-0.4114	
210	7'581.8	76'700'000	670'060	660'179	735'478	27'100'000	225'058	224'834	345'395	-0.65	0.7736	0.8597	
211	3'927.0	39'100'000	328'492	325'685	369'290	2'890'000	47'524	48'026	75'195	0.02	-0.2974	0.6245	
212	11'699.1	149'000'000	1'130'000	1'150'000	1'270'000	50'000'000	382'554	383'429	586'584	-0.14	-0.0647	-1.3470	
213	11'854.8	151'000'000	1'150'000	1'160'000	1'290'000	51'200'000	393'401	392'448	602'383	-0.63	0.9289	-0.2989	
214	9'023.8	80'300'000	722'559	733'799	820'140	27'000'000	242'789	246'467	378'080	-3.22	2.2872	-0.9204	
215	2'472.6	13'600'000	150'771	150'896	171'906	1'070'000	23'452	23'041	36'415	0.18	0.0806	0.1024	
216	2'465.0	13'600'000	150'801	150'092	171'357	1'050'000	22'792	22'848	35'835	-0.06	0.0827	0.1951	
217	7'731.7	80'200'000	689'120	688'785	760'048	27'600'000	230'386	229'154	352'427	1.07	-0.6114	0.0779	
218	10'600.5	114'000'000	941'030	944'288	1'060'000	38'800'000	324'891	322'378	495'707	0.24	0.1380	-0.2468	
219	10'596.7	113'000'000	935'721	941'560	1'060'000	38'600'000	323'516	320'283	493'869	0.30	0.1283	-0.4574	
220	7'678.9	78'800'000	673'622	680'386	751'194	27'700'000	228'147	228'257	352'438	0.08	-0.0792	-0.6540	
221	2'863.4	19'700'000	194'351	194'773	222'023	1'400'000	27'175	27'640	43'498	-0.48	0.0176	-0.1674	
222	3'299.3	28'400'000	253'114	254'703	287'407	2'000'000	36'132	35'918	56'745	0.84	-0.5903	-0.3621	
223	5'324.5	37'200'000	389'019	385'473	428'507	12'900'000	128'368	128'975	197'720	0.02	-0.2422	0.5136	
224	3'383.3	28'200'000	256'310	257'492	290'663	2'100'000	37'830	37'861	59'604	0.15	-0.1573	-0.2478	
225	3'385.8	28'200'000	257'022	257'638	291'148	2'080'000	37'537	37'712	59'360	-0.30	0.1264	-0.1171	
226	10'683.6	115'000'000	943'495	949'927	1'070'000	39'600'000	325'988	324'680	502'432	0.72	-0.4095	-0.4646	
227	9'249.7	81'100'000	735'469	736'571	831'895	27'800'000	252'488	253'208	388'370	0.23	-0.3092	-0.0822	
228	9'052.8	80'800'000	736'292	725'127	823'373	27'700'000	251'109	249'746	385'407	1.80	-1.4194	0.9329	
229	5'291.8	37'000'000	383'559	387'069	426'197	12'800'000	125'761	126'376	195'575	0.84	-0.9724	-0.4642	
230	3'979.3	40'800'000	336'978	336'684	379'817	2'980'000	49'300	49'060	77'039	0.12	-0.0251	0.0153	
231	3'962.5	40'600'000	334'820	335'561	377'879	2'970'000	49'025	49'188	76'839	0.08	-0.1511	-0.1363	
232	5'480.9	37'400'000	395'245	391'563	436'421	13'600'000	135'547	134'791	208'453	1.58	-1.2563	0.4227	
233	5'456.8	37'200'000	393'784	391'									

Profile #	Calculated quantity											
	A [mm ²]	I _y [mm ⁴]	W _{el,y,pos} [mm ³]	W _{el,y,neg} [mm ³]	W _{ply} [mm ³]	I _z [mm ⁴]	W _{el,z,pos} [mm ³]	W _{el,z,neg} [mm ³]	W _{pl,z} [mm ³]	E _{web} [mm]	Centroid_y [mm]	Centroid_z [mm]
241	8'241.8	228'000'000	1'140'000	1'140'000	1'280'000	12'800'000	142'681	142'185	223'098	-0.18	0.3776	-0.0874
242	26'551.2	1'670'000'000	5'570'000	5'570'000	6'290'000	128'000'000	860'723	854'014	1'340'000	0.00	0.5639	0.1839
243	26'857.0	1'680'000'000	5'590'000	5'640'000	6'350'000	130'000'000	869'259	865'547	1'350'000	-0.25	0.6509	-1.5113
244	26'782.5	1'670'000'000	5'580'000	5'610'000	6'320'000	129'000'000	862'755	863'086	1'340'000	-0.96	0.9906	-0.6986
245	13'417.7	283'000'000	1'690'000	1'710'000	1'880'000	74'900'000	497'258	496'825	761'634	-0.19	0.3139	-0.9755
246	8'460.5	234'000'000	1'170'000	1'170'000	1'320'000	13'200'000	146'374	145'664	229'619	0.37	-0.0836	-0.0410
247	17'057.8	370'000'000	2'130'000	2'130'000	2'410'000	94'600'000	618'588	628'415	966'868	0.59	-1.5602	0.4140
248	12'087.6	221'000'000	1'410'000	1'430'000	1'570'000	64'900'000	434'226	430'039	666'566	2.19	-1.2952	-0.7290
249	14'818.9	246'000'000	1'650'000	1'650'000	1'840'000	84'100'000	563'947	557'453	858'133	0.59	0.1097	0.1024
250	11'501.2	187'000'000	1'300'000	1'280'000	1'420'000	64'600'000	431'371	429'839	658'976	1.85	-1.4228	1.0129
251	9'775.0	137'000'000	1'000'000	1'010'000	1'110'000	46'300'000	330'451	326'548	506'114	1.28	-0.5160	-0.3019
252	11'747.3	151'000'000	1'150'000	1'150'000	1'280'000	51'500'000	393'017	393'556	603'121	-0.25	0.0682	-0.1717
253	17'595.1	427'000'000	2'340'000	2'370'000	2'630'000	98'200'000	653'116	647'711	1'000'000	0.13	0.4540	-1.0800
254	17'831.6	433'000'000	2'390'000	2'380'000	2'670'000	99'200'000	662'141	657'324	1'010'000	0.46	0.0410	0.5952
255	21'433.7	788'000'000	3'490'000	3'500'000	3'920'000	113'000'000	752'359	748'111	1'160'000	-2.43	2.7255	-0.7413
256	12'389.0	225'000'000	1'440'000	1'450'000	1'610'000	66'700'000	445'064	447'916	689'175	-0.93	0.4088	-0.2369
257	14'256.1	333'000'000	1'870'000	1'890'000	2'090'000	76'600'000	509'172	509'960	785'842	-1.10	1.0237	-0.8673
258	8'760.1	105'000'000	839'252	840'539	924'830	36'900'000	282'531	283'041	434'008	-0.70	0.7251	-0.1188
259	9'882.2	339'000'000	1'500'000	1'500'000	1'700'000	16'400'000	171'462	170'944	270'706	-0.23	0.3077	-0.1354
260	5'358.3	83'800'000	555'317	552'093	627'426	6'100'000	78'733	79'241	125'175	-0.32	0.1699	0.4588
261	19'655.3	870'000'000	3'530'000	3'520'000	3'930'000	101'000'000	673'284	671'289	1'030'000	0.72	-0.3047	0.3521
262	5'258.9	82'800'000	547'141	549'101	618'233	5'880'000	77'987	77'701	121'604	0.06	0.0018	-0.2450
263	5'505.8	86'000'000	569'881	573'878	645'483	6'260'000	82'477	82'670	129'432	0.74	-0.6825	-0.6161
264	12'394.3	230'000'000	1'470'000	1'480'000	1'630'000	68'000'000	457'486	453'834	697'842	1.42	-0.8115	-0.7184
265	15'173.0	263'000'000	1'730'000	1'720'000	1'930'000	87'000'000	581'089	573'884	884'074	1.41	-0.5747	0.8311
266	11'102.8	175'000'000	1'220'000	1'220'000	1'350'000	62'200'000	413'818	410'330	631'212	1.55	-0.9750	0.4675
267	6'373.5	119'000'000	723'377	722'292	816'048	8'100'000	100'022	100'651	157'349	-0.80	0.5795	0.1533
268	16'885.0	365'000'000	2'130'000	2'160'000	2'390'000	95'400'000	636'289	638'121	977'873	-2.82	2.6887	-0.9682
269	14'650.1	252'000'000	1'660'000	1'660'000	1'850'000	83'200'000	551'094	555'131	849'029	-1.12	0.6122	0.3138
270	7'185.1	161'000'000	895'064	879'953	1'000'000	10'000'000	117'663	117'721	184'554	-0.54	0.3557	1.6084
271	15'392.2	912'000'000	3'020'000	3'020'000	3'470'000	32'300'000	295'091	291'120	466'044	1.43	-0.5196	0.4061
272	2'108.8	8'920'000	110'060	112'266	127'826	713'731	17'107	16'722	26'955	1.22	-0.7232	-0.8535
273	2'464.5	13'500'000	149'068	148'446	170'548	1'030'000	21'684	22'104	35'285	-1.68	1.1180	0.1959
274	2'885.4	19'300'000	194'703	195'505	221'761	1'470'000	28'872	28'570	45'513	0.57	-0.2682	-0.2398
275	3'383.4	28'300'000	251'253	254'504	288'986	1'980'000	35'727	34'570	56'736	2.07	-1.2066	-0.7373
276	3'928.5	39'400'000	327'054	323'379	368'444	2'880'000	47'108	46'953	73'975	0.13	-0.0063	0.7461
277	4'565.6	57'300'000	419'448	419'409	477'361	3'920'000	58'010	56'749	91'370	1.60	-0.7965	-0.0178
278	5'275.9	81'700'000	538'189	537'202	611'164	5'650'000	73'804	74'121	116'611	-0.60	0.4044	0.1540
279	5'280.6	82'000'000	537'283	539'365	612'835	5'550'000	74'015	73'082	116'041	0.48	-0.1603	-0.3315
280	4'553.6	57'200'000	420'778	421'889	477'512	4'010'000	59'813	58'461	93'519	2.18	-1.3671	-0.1924
281	11'618.9	491'000'000	1'960'000	1'930'000	2'220'000	21'700'000	213'684	215'251	338'176	-1.32	1.0873	2.0164
282	9'923.5	344'000'000	1'520'000	1'530'000	1'730'000	17'200'000	179'656	179'215	282'893	0.36	-0.2202	-0.4355
283	8'484.1	238'000'000	1'170'000	1'180'000	1'330'000	13'300'000	146'182	147'547	230'788	-0.82	0.3857	-0.3706
284	13'393.3	668'000'000	2'420'000	2'410'000	2'770'000	25'400'000	240'273	240'905	384'779	-0.51	0.4576	0.9761
285	15'551.1	930'000'000	3'080'000	3'090'000	3'530'000	34'200'000	306'856	305'137	486'199	-0.17	0.1165	-0.5057
286	15'590.5	923'000'000	3'050'000	3'050'000	3'510'000	32'400'000	294'043	295'994	469'443	-1.00	0.7621	-0.0133
287	11'563.3	487'000'000	1'920'000	1'940'000	2'200'000	20'800'000	208'237	206'795	328'425	0.08	0.3484	-1.0889
288	3'964.8	40'400'000	332'755	330'406	375'870	2'980'000	48'184	47'937	75'838	0.82	-0.2636	0.3554
289	2'101.7	8'970'000	112'973	110'437	128'221	719'987	17'055	17'065	27'074	0.05	-0.0529	1.0217
290	6'230.4	53'400'000	493'003	494'554	554'161	17'700'000	158'578	157'947	247'246	0.48	-0.5328	-0.1620
291	6'320.3	53'700'000	497'255	499'733	560'656	18'900'000	167'401	170'199	262'143	0.38	-1.2680	-0.1078
292	8'600.6	104'000'000	831'511	825'447	912'622	36'000'000	276'542	274'637	422'846	0.84	-0.4701	0.4724
293	9'934.4	138'000'000	1'010'000	1'010'000	1'130'000	46'800'000	333'241	327'045	514'351	1.84	-0.5129	0.1464
294	10'871.2	182'000'000	1'230'000	1'240'000	1'360'000	59'600'000	402'066	397'656	612'516	0.89	-0.0922	-0.8411
295	12'710.0	233'000'000	1'490'000	1'490'000	1'660'000	69'900'000	465'572	464'995	717'524	1.60	-1.4268	-0.1791
296	11'342.6	186'000'000	1'270'000	1'270'000	1'400'000	62'600'000	413'436	421'838	640'555	-1.11	-0.2474	-0.1991
297	17'780.9	643'000'000	2'920'000	2'890'000	3'230'000	94'300'000	622'395	629'385	963'751	-1.93	1.3650	1.1898
298	14'549.6	342'000'000	1'930'000	1'930'000	2'140'000	78'500'000	529'074	526'155	808'567	1.66	-1.2983	-0.0788
299	13'136.6	274'000'000	1'650'000	1'650'000	1'820'000	70'800'000	477'425	471'524	728'161	0.38	0.4061	-0.0149
300	21'127.0	1'110'000'000	4'090'000	4'160'000	4'600'000	107'000'000	711'156	707'591	1'090'000	-0.26	0.6433	-2.2391
301	22'276.0	1'400'000'000	4'720'000	4'710'000	5'270'000	109'000'000	716'714	722'959	1'110'000	-2.02	1.3451	0.3376
302	15'984.9	454'000'000	2'330'000	2'320'000	2'580'000	86'500'000	576'258	571'614	879'773	0.23	0.3097	0.1246
303	13'975.4	326'000'000	1'850'000	1'840'000	2'040'000	73'800'000	495'614	488'638	757'369	1.79	-0.7802	0.3758
304	14'233.1	330'000'000	1'880'000	1'870'000	2'080'000	76'100'000	509'386	505'110	782'516	1.82	-1.1592	0.2735
305	11'287.9	183'000'000	1'250'000	1'260'000	1'390'000	62'800'000	414'438	416'290	640'189	-1.24	1.0969	-0.4721
306	8'964.7	79'900'000	704'647	707'780	813'391	27'100'000	240'153	244'068	378'542	0.20	-0.8838	-0.0756
307	10'383.2	112'000'000	923'927	926'178	1'040'000	38'000'000	318'129	315'214	484'522	1.11	-0.7339	-0.1732
308	11'533.6	151'000'000	1'140'000	1'140'000	1'270'000	49'500'000	379'331	381'134	581'288	0.43	-0.6665	0.3369
309	13'034.2	192'000'000	1'370'000	1'370'000	1'530'000	65'200'000	464'607	461'865	710'146	1.15	-0.6788	-0.2079
310	13'231.7	194'000'000	1'370'000	1'370'000	1'540'000	64'200'000	458'369	452'540	701'905	0.33	0.5600	0.0206
311	17'335.0	378'000'000	2'190'000	2'200'000	2'460'000	96'800'000	645'814	642'198	988'955	0.42	0.0912	-0.3407
312	17'201.0	372'000'000	2'170'000	2'170'000	2'430'000	95'600'000	642'600	633'608	978'116	2.00	-0.9862	-0.2173
313	16'102.8	312'000'000	1'930'000	1'920'000	2							

Profile	Calculated quantity											
#	A [mm ²]	I _y [mm ⁴]	W _{el,y,pos} [mm ³]	W _{el,y,neg} [mm ³]	W _{ply} [mm ³]	I _z [mm ⁴]	W _{el,z,pos} [mm ³]	W _{el,z,neg} [mm ³]	W _{pl,z} [mm ³]	E _{web} [mm]	Centroid_y [mm]	Centroid_z [mm]
321	20'958.2	785'000'000	3'460'000	3'460'000	3'870'000	113'000'000	744'913	745'103	1'150'000	-0.99	0.8717	-0.0582
322	27'097.9	1'730'000'000	5'730'000	5'730'000	6'470'000	133'000'000	889'096	874'362	1'370'000	1.38	-0.4263	0.1140
323	26'914.9	1'720'000'000	5'730'000	5'660'000	6'440'000	134'000'000	882'915	892'206	1'380'000	-1.88	1.1887	1.9847
324	23'500.1	1'070'000'000	4'250'000	4'240'000	4'770'000	122'000'000	818'137	814'840	1'260'000	-0.21	0.4429	-0.0074
325	17'853.3	427'000'000	2'370'000	2'370'000	2'650'000	98'300'000	657'221	656'566	1'010'000	-1.94	2.0869	0.0950
326	16'857.7	366'000'000	2'130'000	2'130'000	2'390'000	93'400'000	623'832	616'593	956'454	1.15	-0.5068	-0.1877
327	9'986.9	349'000'000	1'540'000	1'540'000	1'740'000	74'400'000	496'134	496'134	544'272	0.36	-0.2098	-0.3537
328	8'415.8	229'000'000	1'140'000	1'150'000	1'300'000	60'400'000	494'583	498'112	545'721	1.39	-0.7779	-1.1691
329	4'601.3	58'100'000	429'325	429'511	485'709	41'600'000	60'916	60'849	68'224	-0.03	-0.0851	-0.0039
330	21'561.5	789'000'000	3'480'000	3'510'000	3'930'000	112'000'000	749'161	745'531	1'150'000	0.13	0.3436	-0.9728
331	13'349.8	281'000'000	1'690'000	1'700'000	1'870'000	74'600'000	496'134	494'711	577'654	-0.13	0.2485	-0.1950
332	14'487.2	244'000'000	1'610'000	1'640'000	1'810'000	82'300'000	544'272	545'721	835'300	0.65	-0.7103	-1.5650
333	11'111.1	183'000'000	1'220'000	1'230'000	1'370'000	60'400'000	399'155	398'502	618'170	0.81	-0.8542	-0.3184
334	17'717.6	428'000'000	2'360'000	2'350'000	2'640'000	96'600'000	648'793	648'224	993'068	-0.51	0.2371	0.5665
335	10'832.7	177'000'000	1'200'000	1'190'000	1'330'000	59'100'000	394'120	389'147	603'395	0.19	0.4789	0.6693
336	14'502.1	337'000'000	1'910'000	1'920'000	2'120'000	78'000'000	524'983	521'531	803'652	1.75	-1.2958	-0.1561
337	13'964.0	326'000'000	1'850'000	1'840'000	2'050'000	74'400'000	494'583	498'112	765'761	-1.30	0.6201	0.8144
338	14'558.3	344'000'000	1'930'000	1'940'000	2'140'000	77'400'000	518'519	513'938	794'867	1.98	-1.4036	-0.5651
339	15'714.6	449'000'000	2'280'000	2'270'000	2'530'000	81'800'000	544'568	548'054	838'845	0.56	-0.9765	0.5625
340	16'991.1	364'000'000	2'140'000	2'130'000	2'390'000	94'200'000	627'211	629'460	964'609	-2.56	2.3888	0.7187
341	13'964.1	324'000'000	1'850'000	1'850'000	2'040'000	74'600'000	500'487	495'639	766'529	1.61	-0.7882	0.1647
342	8'634.0	104'000'000	832'833	834'677	917'086	36'400'000	278'875	277'198	426'293	0.86	-0.4880	-0.1536
343	17'406.0	378'000'000	2'190'000	2'190'000	2'460'000	97'100'000	645'806	642'990	992'342	1.76	-0.9233	-0.0431
344	16'306.0	314'000'000	1'960'000	1'940'000	2'180'000	92'100'000	610'941	616'059	942'413	-2.19	1.3286	0.6482
345	14'034.5	327'000'000	1'830'000	1'870'000	2'060'000	74'900'000	496'457	499'335	771'758	-2.05	1.5084	-1.7629
346	21'167.0	1'120'000'000	4'120'000	4'130'000	4'610'000	107'000'000	708'287	713'107	1'100'000	-2.77	2.2894	-0.2011
347	9'567.6	136'000'000	977'366	1'000'000	1'100'000	46'100'000	325'871	326'067	500'283	0.32	-0.2893	-1.8934
348	8'338.5	227'000'000	1'130'000	1'130'000	1'280'000	12'400'000	137'679	137'159	217'194	0.26	-0.0539	-0.3617
349	12'807.3	262'000'000	1'580'000	1'590'000	1'760'000	67'500'000	449'354	457'018	695'548	-0.85	-0.3574	-0.3999
350	2'402.1	13'200'000	146'929	144'639	166'707	1'000'000	21'262	21'689	34'301	-0.96	0.5433	0.7756
351	3'301.1	27'900'000	249'367	251'247	285'249	2'120'000	36'653	36'387	58'776	1.11	-0.8213	-0.4171
352	3'876.1	38'600'000	317'616	319'699	361'815	2'760'000	45'057	44'655	71'243	0.11	0.2384	-0.3134
353	3'965.1	39'900'000	327'652	330'544	373'317	2'820'000	46'597	46'547	73'556	-0.47	0.4763	-0.5934
354	4'556.9	57'100'000	421'058	420'602	477'052	4'030'000	59'550	58'699	93'398	1.30	-0.9074	0.1742
355	4'555.1	57'100'000	418'136	418'660	475'992	3'930'000	58'459	56'608	91'532	2.10	-1.0567	-0.1196
356	2'855.5	19'300'000	192'623	192'168	219'372	1'390'000	27'270	27'581	43'603	-0.81	0.4421	0.1478
357	7'275.0	163'000'000	898'914	899'308	1'020'000	10'400'000	120'253	122'097	189'982	-1.46	0.7691	-0.0671
358	11'538.2	480'000'000	1'920'000	1'920'000	2'190'000	21'400'000	214'588	211'231	335'943	1.36	-0.6952	0.0368
359	11'602.0	493'000'000	1'970'000	1'940'000	2'220'000	21'900'000	215'688	216'294	340'125	-1.22	1.1090	2.0854
360	9'718.4	337'000'000	1'490'000	1'490'000	1'690'000	16'600'000	173'428	173'722	272'704	-0.40	0.4381	-0.2972
361	8'329.0	230'000'000	1'150'000	1'130'000	1'290'000	12'800'000	138'334	140'522	221'751	-1.44	0.8687	1.4914
362	13'399.4	668'000'000	2'420'000	2'400'000	2'770'000	25'500'000	241'117	240'326	384'849	0.13	0.1711	1.3579
363	15'588.0	928'000'000	3'060'000	3'060'000	3'520'000	32'300'000	293'385	293'385	468'797	0.17	0.2059	0.1329
364	11'585.3	483'000'000	1'930'000	1'920'000	2'200'000	21'000'000	209'012	206'975	330'863	0.19	0.0494	0.5613
365	7'083.5	156'000'000	860'656	873'759	981'195	10'000'000	117'169	116'348	182'426	0.28	0.0633	-1.3202
366	4'431.6	56'600'000	411'069	414'215	468'267	3'870'000	57'153	56'774	89'938	0.33	-0.2766	-0.5419
367	6'355.6	54'700'000	511'229	515'574	567'311	18'900'000	172'072	169'551	262'171	0.92	-0.1820	-0.5142
368	8'692.8	104'000'000	832'167	828'514	915'991	36'000'000	275'140	277'470	424'543	-0.78	0.2279	0.2452
369	8'718.0	104'000'000	828'368	822'989	915'427	36'100'000	274'936	274'810	424'770	0.63	-0.6487	0.4611
370	8'654.4	105'000'000	834'729	828'095	916'282	36'000'000	275'117	275'058	423'684	0.40	0.0006	0.5136
371	11'563.4	189'000'000	1'280'000	1'280'000	1'420'000	62'900'000	420'462	416'534	643'906	1.86	-1.1471	-0.0437
372	10'218.0	145'000'000	1'050'000	1'050'000	1'170'000	48'700'000	347'739	340'543	536'381	1.93	-0.4445	0.0627
373	11'323.3	184'000'000	1'250'000	1'260'000	1'390'000	60'600'000	409'187	398'143	622'359	2.48	-0.5091	-0.4548
374	11'033.6	182'000'000	1'240'000	1'240'000	1'370'000	61'600'000	414'030	407'224	631'003	1.47	-0.1967	0.0262
375	14'001.8	332'000'000	1'880'000	1'870'000	2'070'000	74'700'000	501'147	504'797	772'202	-0.54	0.1199	0.6866
376	17'659.1	640'000'000	2'920'000	2'860'000	3'210'000	93'600'000	616'763	624'310	955'958	-1.82	1.1106	2.5011
377	12'544.2	238'000'000	1'510'000	1'520'000	1'670'000	71'000'000	471'824	471'018	720'509	1.30	-1.0538	-0.1561
378	12'683.1	233'000'000	1'500'000	1'500'000	1'650'000	70'300'000	470'356	468'571	718'950	1.26	-0.9124	-0.2131
379	14'004.8	328'000'000	1'840'000	1'860'000	2'050'000	73'300'000	493'174	487'569	754'740	1.14	-0.3393	-1.2223
380	13'190.3	274'000'000	1'650'000	1'650'000	1'830'000	70'700'000	477'490	469'691	727'544	1.01	0.0938	-0.0773
381	21'145.7	1'110'000'000	4'110'000	4'150'000	4'610'000	107'000'000	713'824	709'083	1'100'000	0.29	0.2283	-1.3812
382	22'246.0	1'400'000'000	4'710'000	4'700'000	5'270'000	109'000'000	717'594	722'256	1'110'000	-1.84	1.3511	0.3642
383	15'998.0	453'000'000	2'330'000	2'320'000	2'580'000	86'500'000	576'494	571'138	880'551	0.27	0.5042	0.7505
384	15'650.9	440'000'000	2'260'000	2'250'000	2'510'000	80'900'000	542'692	536'308	832'750	0.81	0.0556	0.4813
385	15'749.3	448'000'000	2'280'000	2'280'000	2'530'000	82'000'000	546'223	547'616	840'087	0.85	-0.8858	0.1226
386	12'542.1	231'000'000	1'480'000	1'480'000	1'640'000	68'000'000	454'233	449'430	695'870	0.30	0.5173	-0.1419
387	5'383.0	36'900'000	379'012	386'710	427'484	12'700'000	125'214	125'343	194'711	-1.88	1.6819	-1.0705
388	10'273.7	108'000'000	898'564	897'425	1'010'000	36'800'000	303'874	304'440	469'337	0.63	-0.7053	0.0163
389	10'398.7	110'000'000	921'204	906'196	1'030'000	36'500'000	304'157	303'836	467'887	0.67	-0.5390	1.0520
390	8'857.1	81'100'000	723'101	727'153	815'694	26'400'000	237'804	239'622	368'146	-1.09	0.7805	-0.4552
391	13'096.1	192'000'000	1'360'000	1'340'000	1'520'000	63'200'000	405'889	444'213	692'392	-0.79	1.7945	0.8615
392	17'383.3	379'000'000	2'200'000	2'200'000	2'470'000	96'600'000	645'451	640'570	988'429	0.85	-0.2340	0.0310
393	17'285.6</											

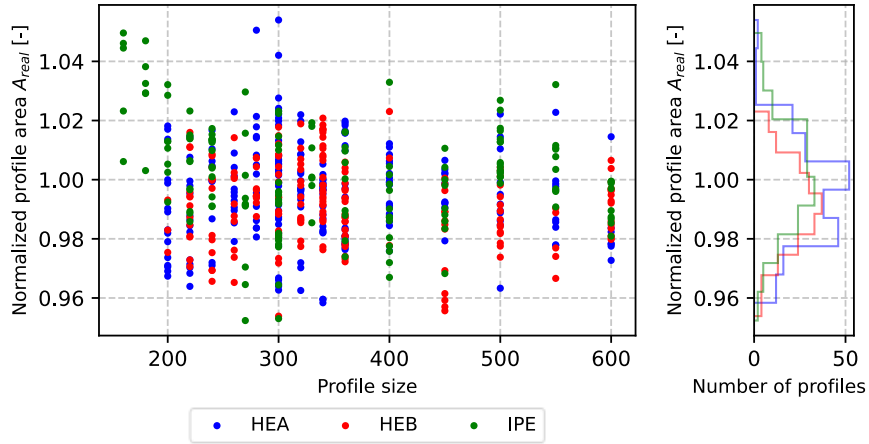
Profile #	Calculated quantity											Centroid_y [mm]	Centroid_z [mm]
	A [mm ²]	I _y [mm ⁴]	W _{el,y,pos} [mm ³]	W _{el,y,neg} [mm ³]	W _{ply} [mm ³]	I _z [mm ⁴]	W _{el,z,pos} [mm ³]	W _{el,z,neg} [mm ³]	W _{pl,z} [mm ³]	E _{web} [mm]			
401	17'676.7	420'000'000	2'320'000	2'340'000	2'610'000	95'900'000	641'312	637'029	983'325	0.74	-0.1889	-0.8401	
402	16'904.5	367'000'000	2'130'000	2'130'000	2'390'000	93'600'000	625'041	617'575	958'588	0.94	-0.3039	-0.0789	
403	15'900.1	306'000'000	1'900'000	1'910'000	2'120'000	89'200'000	594'793	591'995	910'459	0.50	-0.1634	-0.5238	
404	11'849.4	154'000'000	1'160'000	1'180'000	1'310'000	51'100'000	394'664	394'665	606'675	-0.88	1.1268	-0.8741	
405	10'337.1	107'000'000	897'390	899'036	1'010'000	37'200'000	310'357	306'057	474'276	1.35	-0.5289	-0.2137	
406	11'612.9	484'000'000	1'910'000	1'930'000	2'200'000	21'200'000	208'708	206'322	330'520	1.32	-0.5620	-0.8564	
407	8'620.1	104'000'000	819'814	825'375	909'294	36'000'000	276'079	272'140	422'130	1.17	-0.4022	-0.5349	
408	15'907.2	454'000'000	2'310'000	2'310'000	2'570'000	83'800'000	564'151	557'334	865'716	1.70	-0.8082	-0.2538	
409	21'495.2	785'000'000	3'480'000	3'480'000	3'910'000	111'000'000	747'404	738'070	1'150'000	0.11	0.7533	0.0951	
410	17'997.5	436'000'000	2'400'000	2'400'000	2'690'000	98'800'000	660'903	658'500	1'010'000	0.61	-0.3573	-0.0625	
411	6'259.7	53'400'000	497'467	508'487	555'544	18'300'000	167'275	167'653	255'856	-0.81	0.6796	-1.2498	
412	10'856.9	178'000'000	1'210'000	1'200'000	1'340'000	59'100'000	394'879	389'294	603'619	0.28	0.5275	0.6613	
413	11'970.9	222'000'000	1'430'000	1'420'000	1'570'000	64'100'000	429'801	432'882	661'288	-0.88	0.3407	0.2221	
414	15'706.3	448'000'000	2'300'000	2'260'000	2'530'000	82'800'000	549'848	551'041	847'143	-0.86	0.6882	1.4126	
415	8'339.9	227'000'000	1'130'000	1'130'000	1'280'000	12'500'000	137'958	137'785	217'806	0.10	-0.0161	-0.4234	
416	17'445.5	379'000'000	2'200'000	2'210'000	2'470'000	97'700'000	651'503	647'751	997'564	1.82	-0.9993	-0.0731	
417	9'538.0	136'000'000	994'978	989'947	1'090'000	45'000'000	322'399	321'507	492'226	0.64	-0.4593	0.3974	
418	13'946.2	325'000'000	1'840'000	1'850'000	2'040'000	74'700'000	497'342	499'388	768'124	-1.36	0.8330	-0.7790	
419	11'432.8	150'000'000	1'130'000	1'120'000	1'260'000	48'700'000	373'826	373'826	572'033	-0.18	0.0330	0.4835	
420	16'032.5	455'000'000	2'330'000	2'320'000	2'590'000	85'600'000	569'843	566'126	875'969	-0.05	0.4805	0.0200	
421	5'501.8	83'900'000	554'003	553'721	631'555	5'830'000	77'313	76'275	121'556	0.85	-0.3938	0.0344	
422	12'791.8	261'000'000	1'580'000	1'590'000	1'750'000	67'500'000	448'812	456'205	695'160	-1.08	-0.1598	-0.4927	
423	5'353.3	84'300'000	553'999	550'659	627'271	6'030'000	78'461	78'399	123'298	0.02	0.1079	0.4379	
424	3'888.8	37'900'000	314'753	317'279	359'492	2'800'000	45'404	44'857	72'161	0.20	0.0012	-0.5466	
425	3'358.5	27'600'000	253'094	249'907	285'564	2'050'000	36'756	36'772	57'856	0.29	-0.1389	0.7371	
426	3'326.8	27'300'000	250'114	248'559	282'861	2'040'000	36'552	36'500	57'504	0.26	-0.1048	0.4019	
427	2'939.9	19'900'000	198'653	198'175	226'270	1'450'000	28'603	28'663	45'353	-0.73	0.4260	0.0961	
428	2'055.8	8'780'000	108'462	110'056	125'376	682'504	16'497	16'381	26'032	0.55	-0.3822	-0.6592	
429	11'725.9	189'000'000	1'290'000	1'300'000	1'430'000	64'100'000	427'700	424'538	658'017	-1.96	2.3378	-0.5000	
430	11'329.0	183'000'000	1'250'000	1'250'000	1'390'000	61'800'000	410'649	406'613	630'776	1.46	-0.8732	-0.0340	
431	11'082.8	179'000'000	1'200'000	1'230'000	1'360'000	59'900'000	400'036	387'536	611'824	2.24	0.0920	-1.7243	
432	15'434.9	919'000'000	3'040'000	3'050'000	3'490'000	33'000'000	299'012	298'180	474'567	-0.31	0.5284	-0.3508	
433	11'743.4	500'000'000	1'970'000	1'990'000	2'260'000	21'900'000	217'498	216'398	342'320	0.87	-0.5529	-1.4535	
434	8'433.6	233'000'000	1'160'000	1'160'000	1'310'000	13'000'000	144'513	143'976	226'963	0.59	-0.5298	0.7122	
435	7'390.5	165'000'000	912'780	920'309	1'040'000	10'500'000	123'439	123'622	193'051	-0.28	0.2298	-0.7967	
436	5'263.4	80'500'000	536'450	531'556	606'712	5'580'000	74'735	72'135	116'268	1.98	-0.9070	0.7064	
437	5'435.0	82'800'000	551'318	544'513	624'415	5'750'000	75'973	74'834	119'461	0.38	-0.1305	0.9580	
438	11'580.4	479'000'000	1'910'000	1'940'000	2'190'000	21'000'000	207'708	210'530	332'456	-2.31	1.5649	-1.9739	
439	13'580.1	687'000'000	2'490'000	2'500'000	2'840'000	27'300'000	256'383	260'828	409'104	-1.67	0.8867	-0.4912	
440	8'363.0	229'000'000	1'140'000	1'150'000	1'290'000	13'000'000	142'497	143'693	225'056	-0.33	-0.0497	-0.5672	
441	6'169.4	114'000'000	687'754	688'785	782'732	7'270'000	91'418	88'789	142'792	1.70	-0.7856	-0.1469	
442	5'339.7	82'000'000	541'565	542'674	617'203	5'830'000	75'659	76'507	120'274	-0.01	-0.3536	-0.2605	
443	5'376.1	83'600'000	555'412	558'711	628'403	6'110'000	81'153	80'238	126'233	-0.23	0.5479	-0.5393	
444	11'241.9	182'000'000	1'250'000	1'240'000	1'380'000	62'000'000	413'368	409'551	633'451	1.36	-0.7081	0.2766	
445	11'309.5	183'000'000	1'260'000	1'260'000	1'390'000	62'700'000	417'369	415'601	639'766	1.21	-0.9551	-0.0679	
446	16'072.9	462'000'000	2'360'000	2'360'000	2'610'000	87'500'000	583'496	580'110	891'595	-0.03	0.4525	0.3413	
447	12'353.2	234'000'000	1'490'000	1'490'000	1'640'000	69'600'000	462'311	460'690	705'680	-0.86	1.0436	-0.4149	
448	13'344.6	276'000'000	1'670'000	1'660'000	1'840'000	71'800'000	482'711	479'218	737'415	0.87	-0.3292	0.6293	
449	13'315.3	281'000'000	1'680'000	1'700'000	1'860'000	74'000'000	492'084	492'000	753'346	0.05	0.1366	-0.7808	
450	13'370.6	276'000'000	1'670'000	1'670'000	1'850'000	73'400'000	491'527	750'249	985'961	-2.95	2.3002	-0.1767	
451	14'191.7	332'000'000	1'890'000	1'890'000	2'090'000	78'400'000	521'658	521'673	797'740	-0.58	0.6201	0.0047	
452	15'882.0	452'000'000	2'320'000	2'320'000	2'570'000	85'900'000	569'820	570'475	874'390	-0.06	-0.1066	-0.0350	
453	15'870.1	449'000'000	2'310'000	2'310'000	2'560'000	85'500'000	568'479	570'128	873'749	-0.31	0.2832	0.0038	
454	15'514.7	443'000'000	2'260'000	2'250'000	2'500'000	80'800'000	544'445	537'182	832'821	1.08	-0.2055	0.4495	
455	15'888.2	452'000'000	2'310'000	2'320'000	2'570'000	85'700'000	568'648	569'835	873'351	-0.28	0.0626	-0.4833	
456	22'152.4	1'400'000'000	4'690'000	4'720'000	5'260'000	107'000'000	714'234	714'193	1'100'000	0.63	-0.5350	-1.0828	
457	15'673.0	443'000'000	2'260'000	2'270'000	2'520'000	81'400'000	542'618	542'202	836'342	-1.21	1.3963	-0.4739	
458	17'919.4	650'000'000	2'930'000	2'900'000	3'250'000	91'500'000	614'657	606'777	941'721	0.39	0.5420	0.8889	
459	19'546.5	852'000'000	3'450'000	3'510'000	3'880'000	99'000'000	660'351	663'994	1'020'000	-3.20	2.9072	-2.0547	
460	19'590.4	862'000'000	3'500'000	3'500'000	3'910'000	100'000'000	663'432	662'306	1'030'000	0.54	-0.4394	-0.0082	
461	20'835.1	1'110'000'000	4'060'000	4'120'000	4'570'000	105'000'000	693'231	703'416	1'080'000	-1.32	0.2655	-1.9709	
462	11'487.3	185'000'000	1'260'000	1'260'000	1'400'000	62'200'000	419'109	407'224	640'407	-1.51	3.7577	-0.6086	
463	12'462.4	235'000'000	1'500'000	1'500'000	1'650'000	69'700'000	463'273	464'009	708'943	-0.11	-0.1462	0.2862	
464	13'111.2	273'000'000	1'640'000	1'650'000	1'820'000	71'300'000	475'792	472'387	733'266	-1.76	2.2370	-0.6280	
465	14'440.1	344'000'000	1'920'000	1'950'000	2'140'000	80'300'000	534'378	531'254	817'083	0.76	-0.5167	-1.4442	
466	11'588.7	483'000'000	1'950'000	1'910'000	2'200'000	21'200'000	210'753	210'425	334'381	-0.42	0.5412	2.5166	
467	26'450.3	1'690'000'000	5'630'000	5'640'000	6'340'000	132'000'000	876'323	875'437	1'360'000	0.13	0.0415	-0.2395	
468	25'122.9	1'350'000'000	4'890'000	4'910'000	5'520'000	127'000'000	843'800	843'189	1'310'000	-1.51	1.6701	-0.5919	
469	26'800.5	1'720'000'000	5'690'000	5'700'000	6'430'000	130'000'000	871'983	875'333	1'360'000	-0.41	0.3845	-0.5674	
470	23'352.3	1'060'000'000	4'240'000	4'240'000	4'750'000	114'000'000	831'251	827'841	1'280'000	-0.88	1.2155	-0.0915	
471	21'765.7	801'000'000	3'540'000	3'530'000	3'980'000	125'000'000	765'744	758'369	1'180'000	-0.56	1.2505	0.4103	
472	20'908.8	770'000'000	3'420'000	3'410'000	3'830'000	111'000'000	733'395	735'337	1'130'000	-0.34	0.2217		

Profile #	Calculated quantity											
	A [mm ²]	I _y [mm ⁴]	W _{el,y,pos} [mm ³]	W _{el,y,neg} [mm ³]	W _{ply} [mm ³]	I _z [mm ⁴]	W _{el,z,pos} [mm ³]	W _{el,z,neg} [mm ³]	W _{pl,z} [mm ³]	E _{web} [mm]	Centroid_y [mm]	Centroid_z [mm]
481	23'962.2	1'090'000'000	4'360'000	4'350'000	4'890'000	128'000'000	851'296	849'798	1'310'000	-1.49	1.3651	0.1234
482	13'990.2	330'000'000	1'860'000	1'880'000	2'070'000	76'700'000	512'828	509'181	782'953	2.35	-1.7877	-0.8784
483	21'467.7	782'000'000	3'470'000	3'470'000	3'900'000	111'000'000	747'531	740'435	1'150'000	0.67	0.0021	0.1496
484	17'102.8	368'000'000	2'140'000	2'150'000	2'410'000	95'100'000	631'924	627'361	971'807	-0.86	1.3695	-0.2503
485	7'763.5	78'900'000	672'803	679'544	755'206	28'100'000	232'594	229'239	356'411	0.32	0.2998	-0.8530
486	20'871.7	1'100'000'000	4'060'000	4'070'000	4'540'000	103'000'000	686'098	685'883	1'060'000	-1.44	1.4506	-0.4520
487	19'478.9	866'000'000	3'490'000	3'510'000	3'900'000	97'400'000	654'000	647'550	1'010'000	0.85	-0.3458	-0.4389
488	17'434.7	629'000'000	2'850'000	2'820'000	3'150'000	89'000'000	596'358	590'592	915'352	0.56	0.1519	1.3843
489	7'811.8	81'500'000	693'409	701'042	769'806	27'900'000	231'614	231'340	355'383	-0.70	0.8730	-0.7657
490	6'431.1	54'400'000	514'100	517'494	570'070	19'100'000	172'562	173'205	265'678	0.32	-0.5663	-0.4335
491	3'964.2	40'600'000	334'319	333'124	377'241	2'850'000	47'490	47'619	74'728	-0.55	0.4605	0.2265
492	6'527.6	55'300'000	524'490	524'056	579'688	19'500'000	176'988	176'383	271'126	0.13	0.0715	0.0274
493	7'681.3	77'700'000	673'694	674'454	745'339	27'700'000	228'725	228'021	350'749	0.29	-0.1739	-0.0493
494	15'759.6	447'000'000	2'270'000	2'280'000	2'530'000	81'800'000	547'579	541'861	839'763	0.52	0.3588	-0.3465
495	16'091.2	458'000'000	2'330'000	2'340'000	2'600'000	86'600'000	573'849	573'036	881'733	-0.02	0.1389	-0.0373
496	9'567.6	136'000'000	977'366	1'000'000	1'100'000	46'100'000	325'871	326'067	500'283	0.32	-0.2803	-1.8934
497	8'338.5	227'000'000	1'130'000	1'130'000	1'280'000	12'400'000	137'679	137'159	217'194	0.26	-0.0539	-0.3617
498	12'807.3	262'000'000	1'580'000	1'590'000	1'760'000	67'500'000	449'354	457'018	695'548	-0.85	-0.3574	-0.3999
499	2'826.8	19'300'000	194'140	194'046	219'741	1'480'000	28'691	29'174	45'498	-0.91	0.4280	-0.0176
500	2'885.2	19'800'000	196'894	197'749	224'369	1'480'000	28'404	29'063	45'657	-0.27	-0.0598	-0.2696
501	2'929.7	20'200'000	200'371	201'207	228'549	1'500'000	28'798	29'703	46'480	-0.89	0.2895	-0.2777
502	7'468.4	74'800'000	646'269	652'500	718'552	25'400'000	210'149	211'167	324'731	-0.36	0.1397	-0.5568
503	3'289.8	28'300'000	252'930	253'789	286'620	1'990'000	38'048	35'719	56'490	0.77	-0.5434	-0.1928
504	6'483.0	54'600'000	508'678	523'501	572'656	19'700'000	173'043	175'082	271'212	1.04	-0.5329	-1.6352
505	5'475.0	37'500'000	394'987	394'181	437'449	13'700'000	135'470	136'391	208'861	0.10	-0.1879	0.0916
506	5'270.2	37'100'000	379'424	382'351	425'050	12'500'000	124'052	122'977	191'565	-0.02	0.3005	-0.4336
507	10'273.3	109'000'000	903'016	908'728	1'020'000	36'400'000	302'894	303'654	465'890	-0.44	0.3173	-0.3250
508	10'567.6	115'000'000	948'287	938'193	1'060'000	39'000'000	320'909	324'227	495'349	-1.13	0.5577	0.6585
509	9'205.4	82'900'000	746'260	743'330	841'123	28'300'000	254'537	255'936	392'699	-0.06	-0.2188	0.1774
510	9'065.9	81'100'000	728'452	728'953	826'749	28'300'000	253'564	251'955	391'064	0.45	-0.1025	-0.1121
511	9'203.4	83'400'000	744'903	744'176	844'965	29'100'000	259'814	259'495	400'966	0.08	0.0162	0.0285
512	7'675.0	55'500'000	550'862	554'922	628'510	19'500'000	193'497	191'850	297'975	0.16	0.2099	-0.5108
513	3'950.2	40'400'000	333'117	335'247	376'661	2'960'000	48'973	48'955	76'560	-0.09	0.0862	-0.4179
514	3'971.3	40'700'000	336'823	335'274	378'865	2'970'000	49'040	49'084	76'888	-0.14	0.1123	0.2753
515	6'403.9	53'900'000	508'084	509'596	564'286	18'700'000	170'267	170'427	261'444	-0.42	0.1036	-0.1656
516	5'227.0	36'300'000	375'688	377'279	418'396	12'300'000	121'871	121'853	188'835	-0.95	0.9786	-0.1961
517	9'050.9	79'100'000	716'254	712'299	814'201	27'600'000	249'738	247'762	385'318	0.94	-0.4989	0.4086
518	7'343.4	163'000'000	904'416	901'742	1'020'000	10'300'000	120'171	120'481	188'860	-0.63	0.5370	0.2346
519	5'280.5	82'100'000	540'399	546'715	615'816	5'830'000	76'756	75'882	120'551	1.12	-0.6112	-0.8813
520	6'381.1	119'000'000	724'538	723'227	817'395	8'070'000	99'969	100'067	156'864	0.11	-0.2170	0.1770
521	13'235.2	199'000'000	1'410'000	1'390'000	1'570'000	66'300'000	472'049	469'871	722'118	0.86	-0.5944	0.8514
522	8'645.2	103'000'000	814'994	818'508	909'645	35'500'000	271'863	269'401	420'363	2.50	-2.0656	-0.2465
523	9'807.2	138'000'000	1'000'000	1'010'000	1'120'000	46'400'000	330'025	326'792	507'391	1.21	-0.5437	-0.4539
524	11'460.4	187'000'000	1'290'000	1'280'000	1'410'000	64'700'000	430'428	430'298	658'156	1.11	-1.0030	0.4450
525	14'815.5	247'000'000	1'650'000	1'650'000	1'840'000	84'100'000	563'506	557'210	858'223	0.27	0.3585	0.0905
526	12'321.9	223'000'000	1'440'000	1'440'000	1'590'000	66'000'000	441'529	444'911	683'034	-1.63	1.0925	-0.3301
527	12'066.5	220'000'000	1'420'000	1'420'000	1'570'000	64'800'000	434'969	430'051	665'876	2.26	-1.3035	-0.2491
528	8'724.4	241'000'000	1'200'000	1'200'000	1'360'000	13'600'000	149'762	149'765	236'243	-0.48	0.3862	0.1512
529	5'444.1	86'000'000	564'596	568'579	640'732	6'130'000	80'773	79'735	126'288	0.81	-0.3389	-0.5823
530	9'863.0	342'000'000	1'490'000	1'510'000	1'710'000	16'300'000	170'275	169'636	268'847	0.19	-0.1108	-1.0353
531	15'579.5	929'000'000	3'070'000	3'090'000	3'530'000	34'500'000	308'181	308'891	488'318	-0.15	0.2100	-0.9103
532	19'449.0	850'000'000	3'460'000	3'460'000	3'860'000	98'400'000	651'834	661'097	1'010'000	-3.36	2.4207	-0.1238
533	23'327.6	1'050'000'000	4'200'000	4'220'000	4'720'000	123'000'000	826'461	813'537	1'260'000	1.54	-0.4843	-0.5234
534	11'677.7	150'000'000	1'140'000	1'140'000	1'280'000	50'300'000	389'022	383'931	590'926	0.51	0.1767	-0.3112
535	12'471.0	226'000'000	1'450'000	1'460'000	1'620'000	67'300'000	448'583	450'037	695'075	-0.74	0.4194	-0.4451
536	9'683.1	135'000'000	1'000'000	998'438	1'100'000	46'000'000	330'866	326'397	504'483	0.89	0.0465	0.1103
537	9'744.9	136'000'000	1'010'000	1'010'000	1'110'000	46'200'000	332'535	327'420	506'939	1.36	-0.3139	-0.4201
538	11'513.9	186'000'000	1'280'000	1'290'000	1'410'000	65'600'000	432'177	434'968	664'140	-2.39	1.9878	-0.5678
539	20'191.8	881'000'000	3'610'000	3'600'000	4'020'000	104'000'000	694'748	696'395	1'070'000	-2.15	1.9980	0.2302
540	13'064.5	193'000'000	1'360'000	1'370'000	1'530'000	63'600'000	455'777	450'905	696'918	0.26	0.5805	-0.1748
541	13'062.6	192'000'000	1'370'000	1'360'000	1'530'000	63'500'000	456'131	450'036	695'501	0.50	0.4059	0.3938
542	13'055.4	192'000'000	1'360'000	1'370'000	1'520'000	63'500'000	457'169	451'073	696'060	0.42	0.5180	-0.5222
543	13'282.2	274'000'000	1'670'000	1'660'000	1'840'000	72'800'000	487'907	484'059	744'868	-0.39	1.0154	0.1049
544	8'167.4	225'000'000	1'130'000	1'120'000	1'270'000	12'600'000	139'439	138'729	218'816	0.21	-0.0740	0.8457
545	8'209.6	224'000'000	1'130'000	1'120'000	1'270'000	12'600'000	138'811	138'396	218'643	-0.02	0.0673	0.9379
546	13'193.6	198'000'000	1'400'000	1'380'000	1'560'000	65'700'000	466'229	464'288	715'160	0.28	-0.0183	0.9996
547	15'799.4	302'000'000	1'840'000	1'840'000	2'100'000	87'300'000	580'206	566'305	896'445	2.42	-0.9238	-0.2523
548	12'373.0	229'000'000	1'470'000	1'480'000	1'620'000	67'800'000	455'976	452'310	695'843	1.45	-0.8039	-0.4224
549	13'064.7	192'000'000	1'370'000	1'370'000	1'530'000	65'000'000	464'509	459'439	709'122	1.43	-0.6353	0.0785
550	14'934.2	255'000'000	1'680'000	1'680'000	1'880'000	82'800'000	550'411	553'580	850'811	-3.21	2.9896	-0.0079
551	11'134.8	176'000'000	1'230'000	1'220'000	1'350'000	62'000'000	412'922	409'673	629'689	1.22	-0.7005	1.1046
552	11'001.1	178'000'000	1'250'000	1'210'000	1'350'000	61'000'000	406'305	405'615	622'265	1.53	-1.3640	2.3782
553	20'233.4	588'000'000	2'940'000	2'910'000	3'300'000	110'000'000	730'075	723'919	1'1			

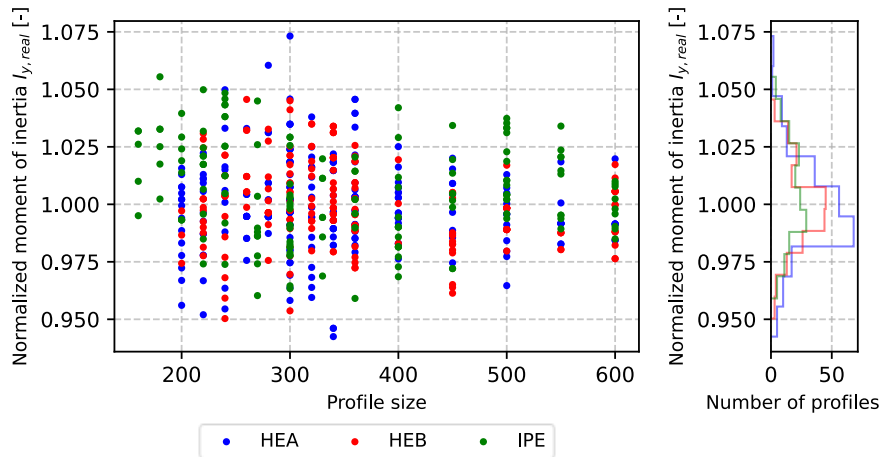
B.1.2 Visualization of the sectional properties

The real sectional properties are normalized with respect to the nominal sectional properties.

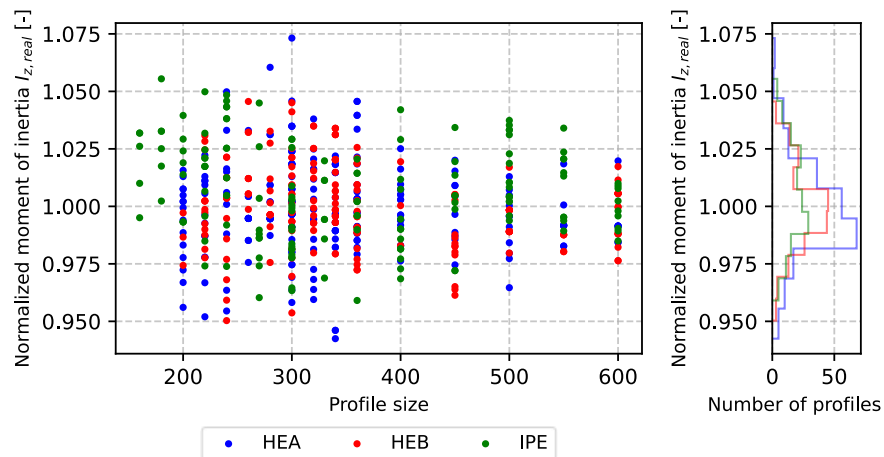
A_{real} :



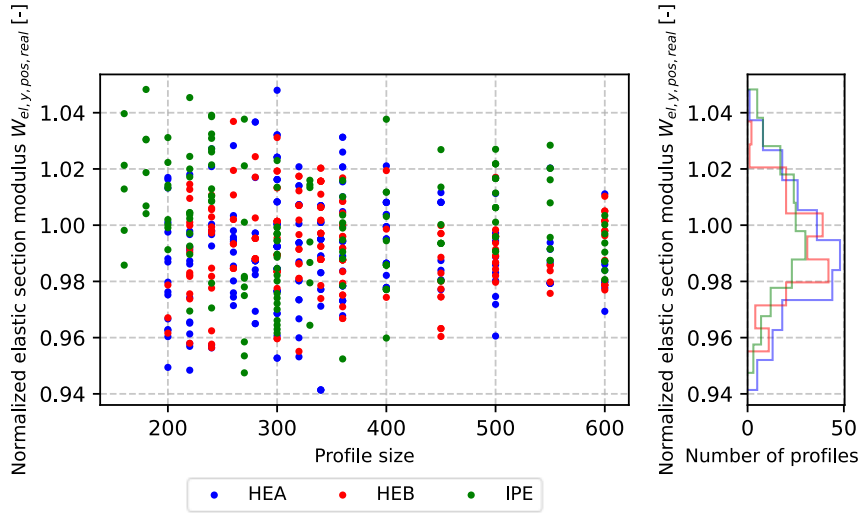
$I_{y,real}$:



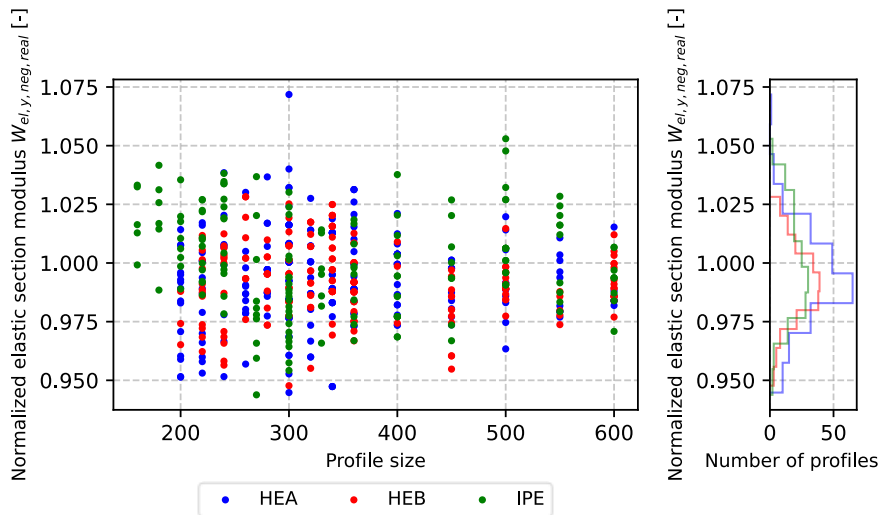
$I_{z,real}$:



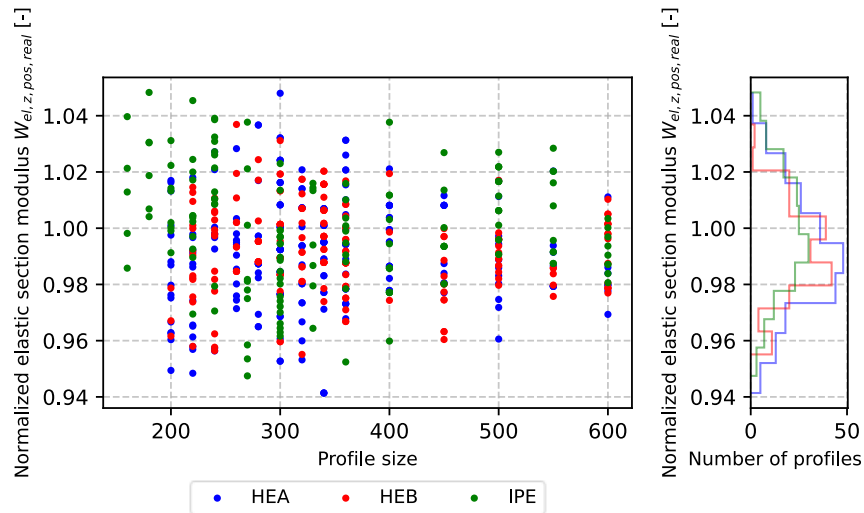
$W_{el,y,real}$:



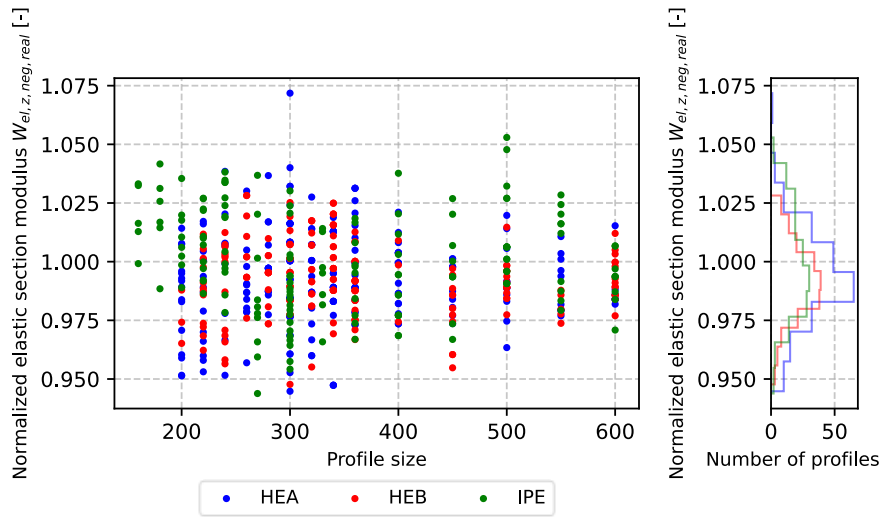
$W_{el,y,neg,real}$:



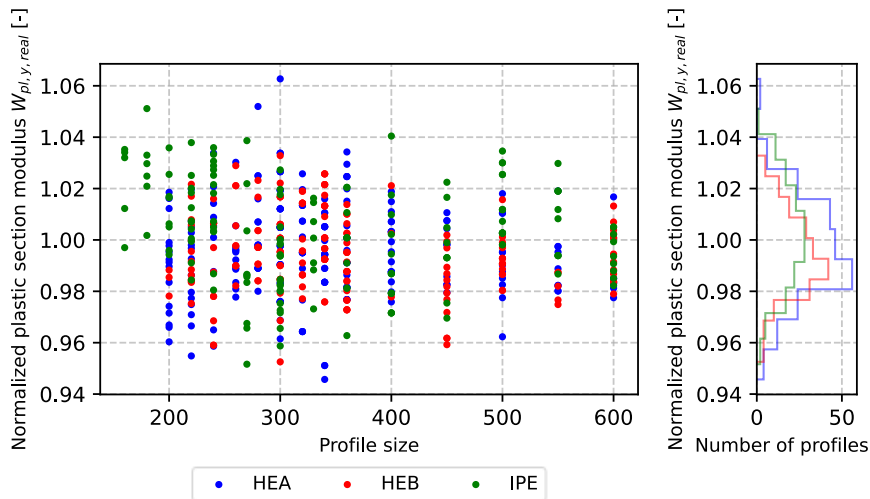
$W_{el,z,real}$:



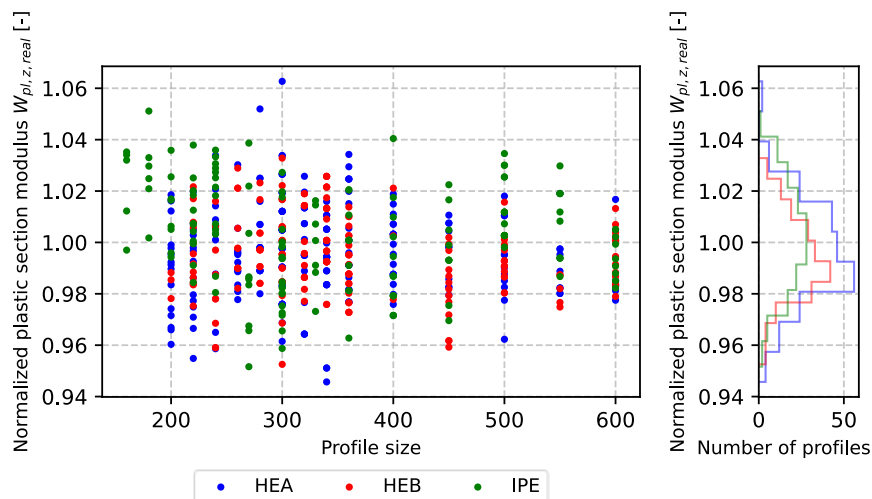
$W_{el,z,real}$:



$W_{pl,y,real}$:



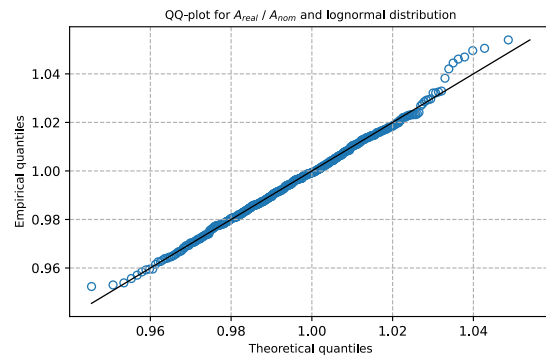
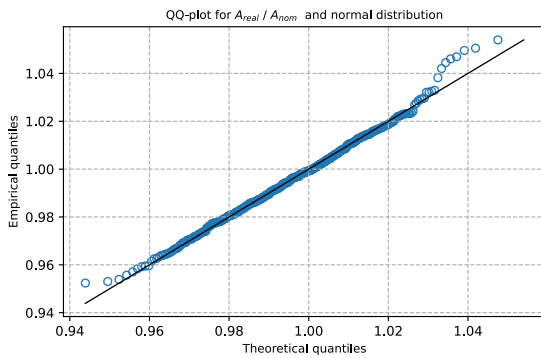
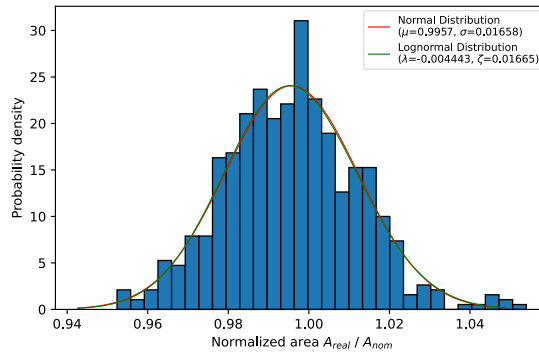
$W_{pl,z,real}$:



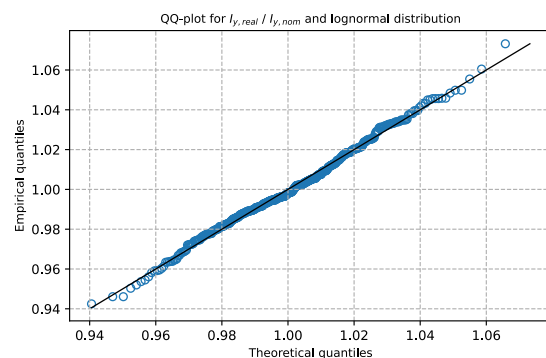
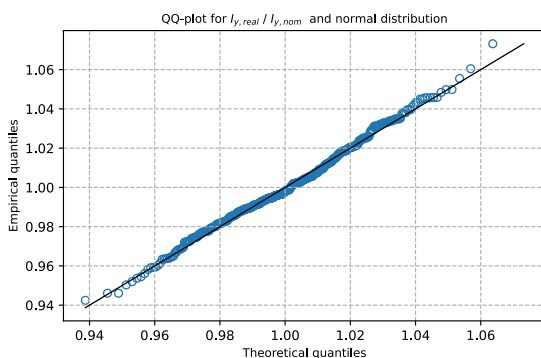
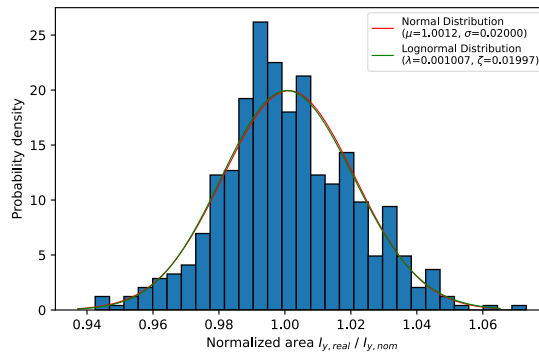
B.1.3 Further statistical evaluation of the results

Analogously to section 3.5.3, the histograms and the QQ-plots are constructed for the obtained normalized sectional properties of the real cross-sections.

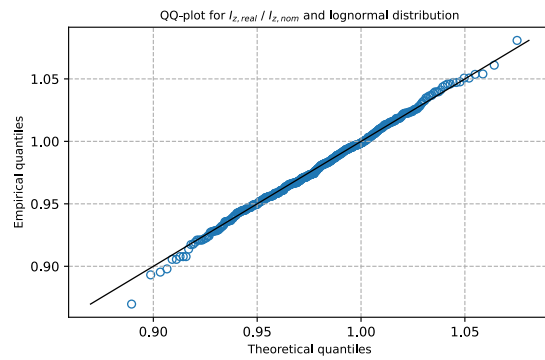
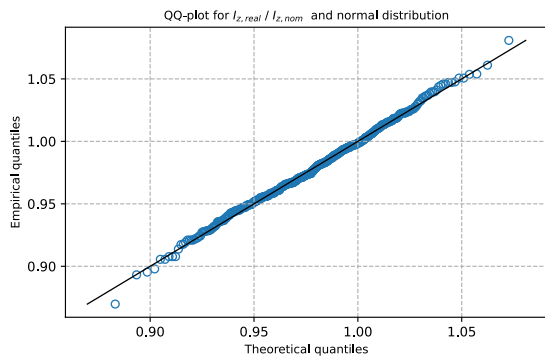
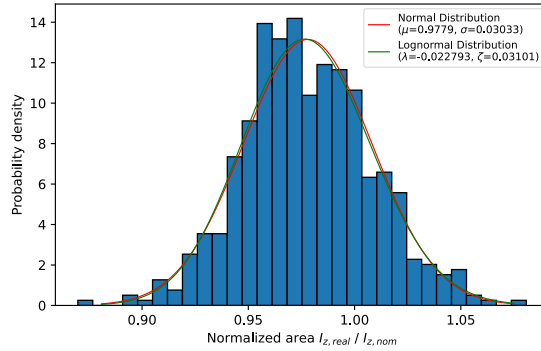
A_{real}:



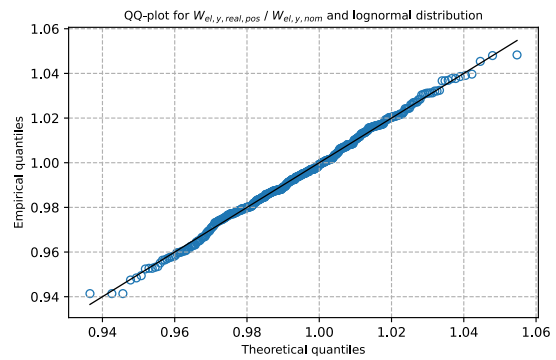
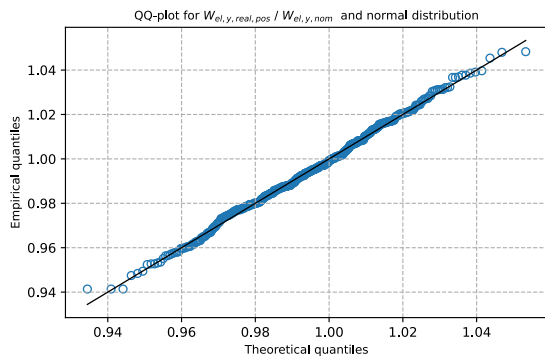
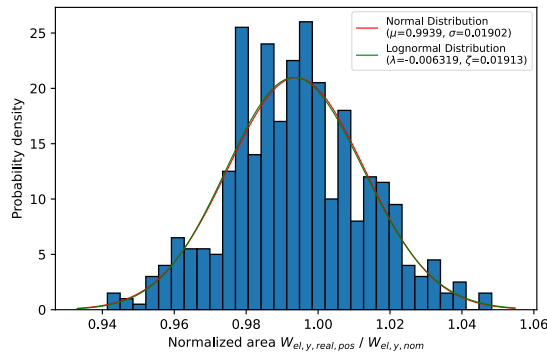
I_{y,real}:



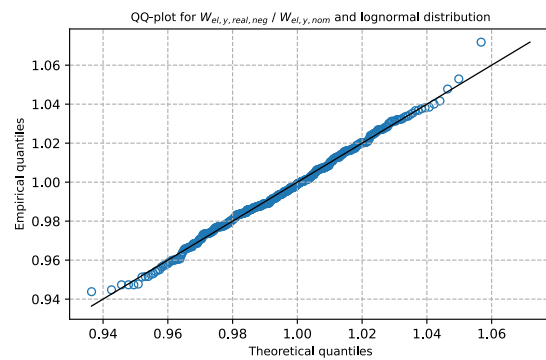
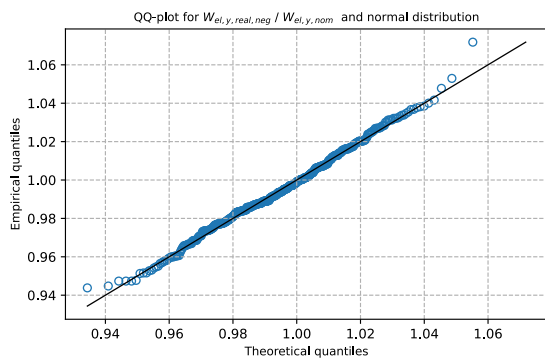
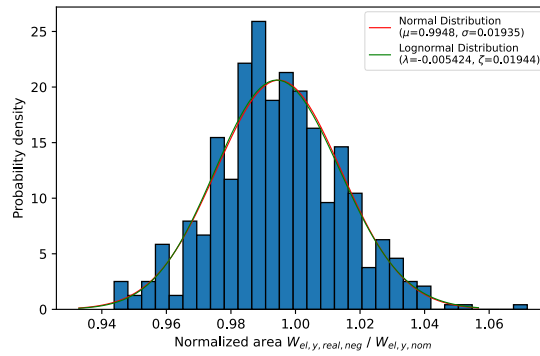
$I_{z,real}$:



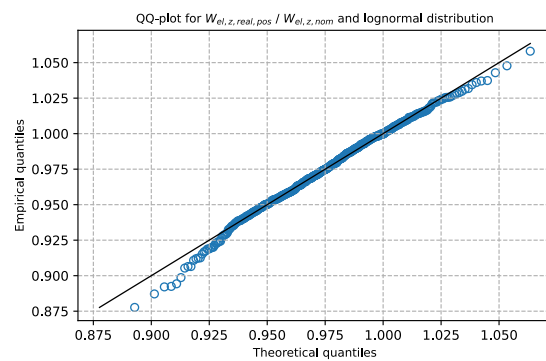
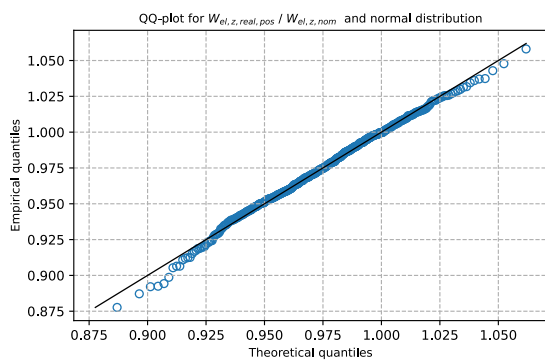
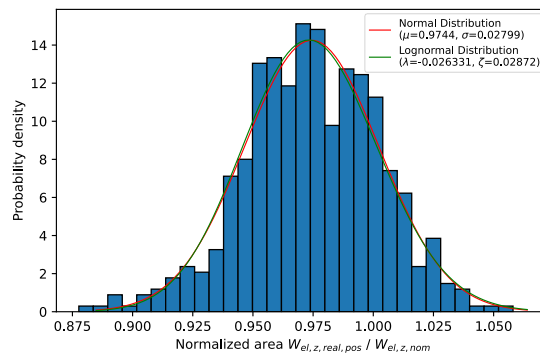
$W_{el,y,real,pos}$:



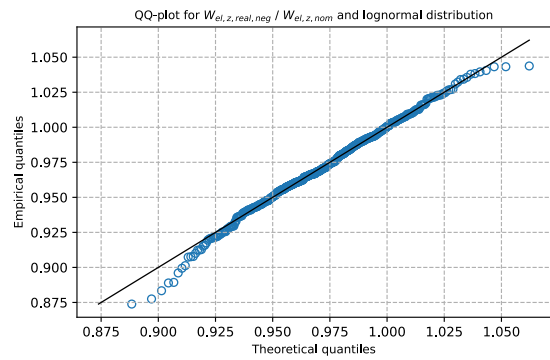
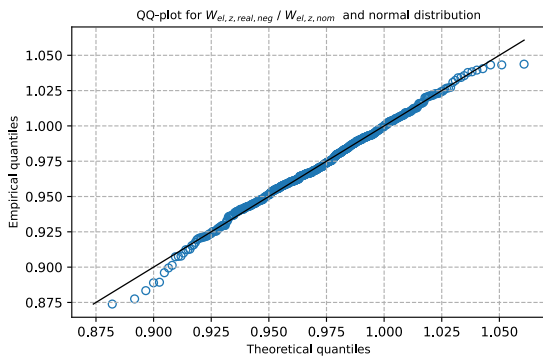
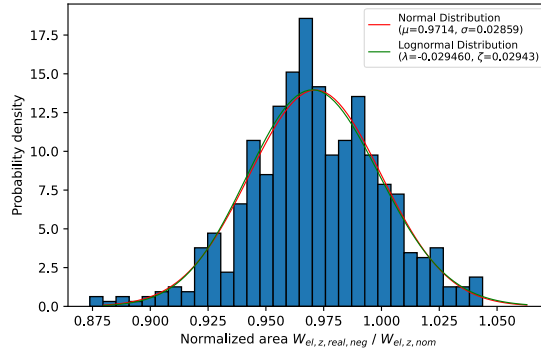
$W_{el,y,real,neg}$:



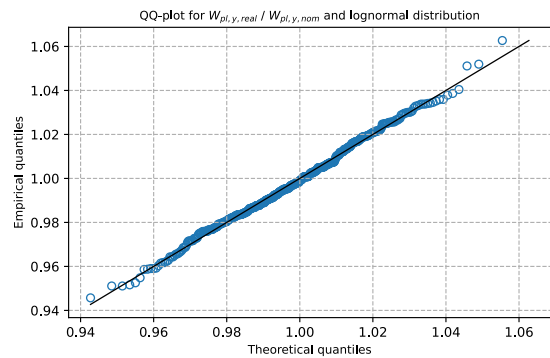
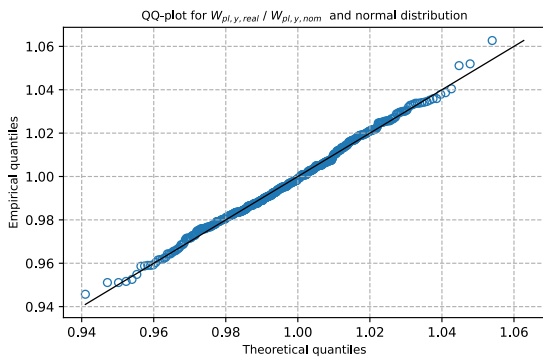
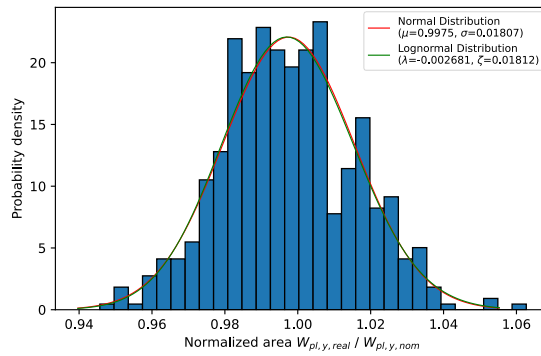
$W_{el,z,real,pos}$:



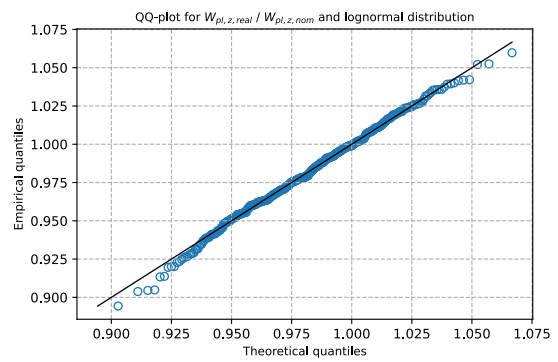
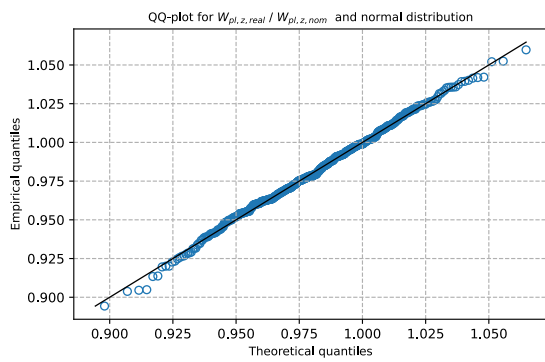
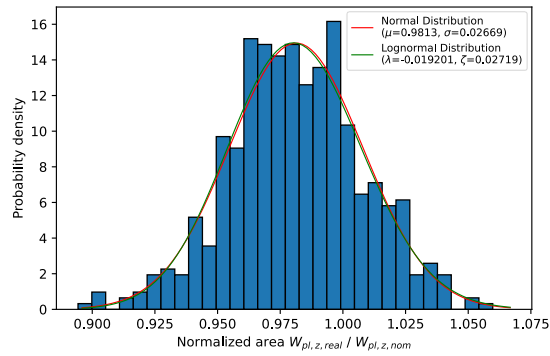
$W_{el,z,real,neg}$:



$W_{pl,y,real}$:



$W_{pl,z,real}$:



B.2 Idealized cross-sections

B.2.1 Calculated sectional properties

Profile #	Calculated quantity						
	A [mm ²]	I _y [mm ⁴]	W _{el,y} [mm ³]	W _{pl,y} [mm ³]	I _z [mm ⁴]	W _{el,z} [mm ³]	W _{pl,z} [mm ³]
1	6'226.4	52'171'619	494'776	547'421	17'690'652	160'350	246'673
2	10'609.8	113'750'906	944'422	1'059'646	39'191'244	327'207	498'884
3	7'455.1	73'979'857	644'368	713'048	25'385'873	211'858	324'939
4	5'370.8	37'133'397	388'282	429'432	13'276'619	132'224	201'924
5	3'401.1	29'083'026	261'057	295'384	2'138'424	38'217	59'784
6	2'874.7	19'988'729	196'769	224'093	1'433'314	28'165	44'359
7	8'593.8	103'031'032	822'603	905'664	36'367'773	279'215	425'010
8	6'188.3	51'448'540	489'986	541'945	17'666'767	160'192	246'154
9	5'212.9	35'209'690	372'097	411'896	12'291'210	123'171	189'225
10	3'882.2	38'857'685	323'517	365'273	2'838'710	47'233	73'798
11	5'230.8	35'749'310	375'124	415'121	12'628'929	126'441	193'259
12	8'909.3	80'666'134	726'362	816'496	26'527'098	242'667	371'999
13	8'834.4	79'426'318	717'816	806'431	26'629'737	241'310	370'177
14	13'113.2	189'111'650	1'356'514	1'515'707	63'887'946	459'592	701'401
15	21'095.1	783'138'601	3'474'670	3'883'855	115'206'000	765'031	1'170'734
16	17'638.9	621'999'259	2'834'678	3'154'986	90'723'205	608'472	933'115
17	14'887.5	254'943'448	1'684'407	1'876'846	84'823'183	564'979	861'783
18	10'847.6	179'893'454	1'232'316	1'349'119	61'204'177	408'791	622'086
19	10'759.5	178'646'017	1'222'975	1'338'602	60'596'136	404'784	615'963
20	13'831.9	692'496'082	2'504'190	2'867'181	27'779'308	260'301	411'893
21	12'374.9	227'963'546	1'465'768	1'615'699	68'305'869	457'278	696'962
22	5'243.8	82'421'549	546'471	615'885	5'860'828	78'004	121'351
23	14'758.1	252'160'901	1'673'264	1'861'657	84'622'879	565'075	861'053
24	23'777.6	1'068'409'027	4'278'171	4'800'674	127'206'089	845'841	1'296'869
25	23'629.9	1'063'253'715	4'252'675	4'772'047	125'948'228	837'450	1'284'336
26	11'534.9	483'016'325	1'919'893	2'190'461	21'016'358	209'859	329'889
27	5'329.0	83'355'825	551'861	623'259	6'089'727	80'086	124'462
28	5'112.0	80'292'876	533'366	600'397	5'699'684	75'920	118'067
29	5'164.6	81'389'136	540'343	607'917	5'844'651	77'629	120'578
30	9'857.7	140'815'166	1'037'121	1'137'762	49'296'728	349'173	531'866
31	5'366.5	83'652'605	555'407	627'133	5'998'306	79'775	124'160
32	9'619.7	137'227'235	1'009'803	1'107'882	47'344'076	337'004	513'209
33	15'107.2	257'841'477	1'766'599	1'903'073	85'616'699	573'704	874'888
34	14'812.9	249'865'018	1'606'545	1'855'411	85'650'917	569'620	867'675
35	5'320.7	82'165'500	542'831	616'176	5'699'812	76'145	118'886
36	13'340.5	665'424'950	2'409'694	2'759'009	25'824'220	245'641	388'775
37	14'185.6	239'073'183	1'597'495	1'774'661	81'847'871	542'093	826'180
38	12'373.8	228'897'654	1'467'105	1'618'124	67'338'007	452'571	690'314
39	8'242.6	225'248'522	1'119'275	1'269'650	12'619'208	138'810	217'877
40	16'839.7	364'662'869	2'143'878	2'388'656	96'197'410	642'945	979'735
41	12'389.1	227'867'252	1'465'007	1'615'830	67'543'502	454'272	692'688
42	22'889.7	1'436'721'738	4'841'359	5'419'799	112'552'832	745'852	1'151'596
43	14'718.1	255'699'900	1'684'009	1'872'024	84'833'435	565'688	861'436
44	16'677.3	359'727'359	2'108'725	2'353'300	93'678'315	625'439	954'188
45	16'451.0	313'503'094	1'955'239	2'185'526	94'412'767	628'580	957'952
46	11'465.0	188'821'190	1'294'937	1'421'285	65'287'356	435'351	662'485
47	5'266.7	81'617'738	545'027	614'271	5'980'919	79'039	122'944
48	6'332.5	52'957'892	503'857	556'504	19'164'454	172'785	263'480
49	5'277.0	36'560'391	382'251	422'367	13'014'338	129'806	198'151
50	6'293.9	54'627'062	512'738	564'672	19'259'363	174'112	265'059
51	8'553.4	102'122'288	818'517	900'405	36'376'397	279'335	425'065
52	5'316.8	36'773'421	385'002	425'436	13'125'016	131'080	200'082
53	13'212.4	278'093'718	1'668'629	1'841'397	71'884'114	482'298	735'764
54	11'020.0	181'895'998	1'248'771	1'367'989	61'980'962	416'217	633'027
55	12'606.9	232'991'461	1'495'980	1'649'787	69'816'062	465'254	710'270
56	11'472.6	190'789'270	1'300'053	1'427'972	64'142'156	430'253	655'099
57	13'149.2	274'990'398	1'658'517	1'828'494	72'480'058	482'895	737'156
58	13'872.6	327'421'110	1'844'782	2'040'591	73'593'487	494'215	755'273
59	13'985.5	330'967'977	1'873'156	2'066'857	75'811'873	511'776	779'778
60	17'707.5	641'089'800	2'903'881	3'219'453	95'549'769	636'638	972'089
61	19'445.6	854'622'885	3'482'642	3'877'371	100'461'020	671'060	1'028'498
62	22'089.4	1'392'114'668	4'697'060	5'246'041	108'044'377	720'776	1'111'050
63	15'340.6	906'415'595	3'004'112	3'447'632	32'270'740	293'571	464'754
64	13'268.6	662'673'786	2'394'658	2'743'804	25'678'552	243'710	385'657
65	6'238.6	119'656'162	716'504	808'636	7'943'058	97'875	152'907
66	5'485.4	85'895'003	566'945	641'581	6'122'108	80'927	126'220
67	7'175.0	161'517'921	890'347	1'006'095	10'362'212	121'061	188'142
68	3'855.0	39'232'368	324'637	366'005	2'834'829	47'310	73'737
69	3'944.3	39'849'290	331'208	373'411	2'967'455	49'089	76'524
70	2'014.4	8'627'857	107'606	123'114	679'292	16'300	25'692
71	2'508.8	13'930'153	153'687	175'069	1'096'937	23'497	36'800
72	7'111.8	160'780'991	883'412	998'555	9'942'312	116'619	182'063
73	15'038.0	262'435'221	1'717'845	1'914'128	85'529'842	570'427	870'093
74	15'081.6	257'590'996	1'702'574	1'899'230	85'036'079	570'119	869'653
75	15'903.1	305'928'716	1'901'064	2'121'815	89'043'901	598'092	911'918
76	17'382.1	379'862'482	2'206'450	2'468'032	97'723'801	652'340	995'572
77	17'256.6	374'691'260	2'184'279	2'442'573	96'911'346	647'717	988'290
78	16'140.2	316'586'558	1'951'889	2'176'812	92'129'984	614'548	936'697
79	16'040.3	309'748'118	1'919'609	2'143'654	89'857'031	602'340	899'869
80	17'388.8	378'301'436	2'200'834	2'462'688	97'551'355	651'472	994'355

Profile #	Calculated quantity						
	A [mm ²]	I _y [mm ⁴]	W _{el,y} [mm ³]	W _{pl,y} [mm ³]	I _z [mm ⁴]	W _{el,z} [mm ³]	W _{pl,z} [mm ³]
81	17'378.9	375'133'014	2'186'154	2'449'298	95'789'065	643'031	982'353
82	17'216.1	374'805'257	2'181'764	2'439'775	96'134'951	643'861	982'580
83	16'673.5	359'146'623	2'097'513	2'345'896	90'659'405	607'983	930'332
84	17'849.1	432'186'599	2'376'218	2'659'898	97'762'640	652'186	998'079
85	17'740.7	427'710'041	2'360'626	2'639'422	99'228'892	657'232	1'004'667
86	17'930.5	440'246'731	2'413'369	2'696'695	99'705'194	667'639	1'018'980
87	17'580.8	421'393'956	2'333'041	2'608'638	96'660'341	644'682	986'247
88	17'581.1	420'894'248	2'331'759	2'607'355	96'447'991	643'652	984'944
89	23'682.3	1'064'089'440	4'248'625	4'774'069	123'785'024	826'694	1'269'787
90	17'824.3	429'055'312	2'378'421	2'657'090	98'878'348	663'101	1'012'702
91	24'466.4	1'339'438'312	4'849'523	5'436'564	126'643'247	845'557	1'298'072
92	26'912.9	1'720'300'957	5'722'129	6'440'582	135'115'455	900'650	1'389'358
93	5'229.7	35'997'945	375'742	416'219	12'419'655	123'652	189'806
94	11'273.7	183'785'832	1'261'096	1'386'302	63'665'526	420'526	641'301
95	6'408.5	54'804'851	517'124	570'707	19'178'103	173'872	265'530
96	3'305.5	26'959'396	246'475	279'726	1'972'099	35'811	56'191
97	2'117.1	9'032'486	112'449	129'059	709'883	17'093	26'992
98	2'497.1	13'425'531	148'661	170'558	1'011'216	22'055	34'760
99	17'066.4	367'017'689	2'149'822	2'403'754	95'238'359	634'563	970'171
100	3'338.2	28'089'108	251'819	286'323	1'982'858	35'737	56'185
101	7'759.4	56'367'832	563'481	636'046	19'723'946	196'767	300'804
102	8'934.2	80'173'618	723'850	814'316	26'716'709	242'394	372'229
103	10'655.8	112'688'107	940'008	1'055'865	39'453'077	327'520	499'918
104	10'707.5	113'585'262	945'992	1'062'754	39'678'605	329'351	502'724
105	15'073.6	253'852'264	1'687'455	1'883'570	85'278'844	569'418	868'969
106	9'585.8	135'792'900	993'510	1'094'886	44'801'275	320'834	490'280
107	11'849.7	196'184'067	1'335'494	1'469'858	67'306'566	448'113	681'950
108	13'345.8	282'494'688	1'698'042	1'869'800	75'452'864	501'848	764'113
109	21'616.8	1'141'230'706	4'211'417	4'706'550	110'413'063	732'134	1'124'817
110	15'993.6	307'642'134	1'906'971	2'			

Profile #	Calculated quantity						
	A [mm ²]	I _y [mm ⁴]	W _{el,y} [mm ³]	W _{pl,y} [mm ³]	I _z [mm ⁴]	W _{el,z} [mm ³]	W _{pl,z} [mm ³]
161	14'973.4	250'363'129	1'676'913	1'868'820	85'633'475	571'519	871'885
162	9'869.1	136'041'902	1'016'376	1'118'110	47'392'150	338'213	517'347
163	6'254.4	52'894'845	498'820	552'464	17'147'702	157'506	242'833
164	3'388.1	28'636'128	258'601	292'624	2'108'214	37'965	59'360
165	13'099.6	194'817'148	1'384'628	1'541'851	66'043'383	471'334	717'919
166	8'991.6	83'217'287	741'852	833'665	26'733'455	244'431	375'063
167	11'575.1	150'615'798	1'140'381	1'272'695	49'541'953	380'843	581'350
168	8'873.7	108'191'228	862'116	947'588	38'029'587	291'481	444'512
169	9'864.5	140'870'779	1'033'990	1'136'322	48'249'472	342'827	522'975
170	10'229.4	110'904'774	915'396	1'025'959	36'529'447	304'209	466'479
171	11'269.4	186'094'919	1'273'925	1'397'934	63'565'095	423'513	645'166
172	15'368.4	915'751'701	3'034'954	3'474'207	33'134'286	301'180	474'994
173	13'546.9	683'250'075	2'482'560	2'828'159	27'461'451	260'384	410'123
174	11'822.2	497'107'592	1'989'545	2'259'121	22'522'077	223'389	350'445
175	11'708.1	497'593'450	1'976'224	2'246'547	21'932'730	218'041	342'395
176	11'513.8	482'856'369	1'931'850	2'194'783	21'729'569	216'549	339'012
177	11'693.1	485'363'870	1'936'421	2'210'927	21'087'848	210'657	332'180
178	23'567.9	1'068'628'905	4'245'300	4'769'644	123'379'383	821'379	1'261'857
179	6'349.4	117'625'938	711'935	807'050	7'720'315	96'371	151'194
180	11'178.0	181'616'238	1'251'145	1'373'988	62'602'113	417'919	636'563
181	11'096.3	180'130'897	1'240'614	1'362'616	61'787'298	412'796	628'915
182	13'335.1	281'976'732	1'693'554	1'866'071	74'705'917	497'542	758'045
183	13'303.8	274'945'423	1'668'409	1'840'021	73'850'108	492'761	751'431
184	15'879.4	448'368'590	2'307'135	2'555'495	86'403'026	575'004	878'496
185	18'084.7	441'119'297	2'427'801	2'712'670	102'098'569	678'711	1'036'249
186	22'023.4	1'389'126'601	4'678'297	5'228'496	107'121'508	713'691	1'101'065
187	17'856.2	647'313'351	2'907'379	3'236'578	92'251'504	615'893	944'837
188	17'587.9	629'242'384	2'843'584	3'165'543	90'643'729	605'422	928'556
189	19'742.7	868'573'623	3'529'066	3'935'156	101'141'285	676'010	1'037'165
190	20'888.9	1'097'798'706	4'063'513	4'537'459	104'131'468	696'648	1'070'964
191	20'662.0	1'104'607'315	4'058'669	4'526'477	105'016'023	697'503	1'070'569
192	13'105.3	272'562'807	1'651'746	1'819'641	72'600'389	483'011	736'819
193	14'546.3	346'491'871	1'953'938	2'157'696	81'361'748	540'843	824'483
194	16'943.7	364'768'107	2'142'481	2'391'033	96'758'842	642'041	979'585
195	25'158.9	1'348'602'546	4'904'633	5'520'264	127'550'667	851'928	1'312'397
196	26'841.6	1'716'627'063	5'698'725	6'420'396	131'690'381	881'462	1'363'292
197	26'402.8	1'687'500'010	5'588'304	6'300'997	129'127'866	857'280	1'328'281
198	26'550.8	1'704'730'412	5'649'292	6'361'765	130'430'907	875'963	1'351'815
199	24'707.0	1'341'036'154	4'858'651	5'458'299	126'223'140	842'358	1'295'770
200	23'470.8	1'062'349'483	4'262'013	4'769'438	125'929'769	843'835	1'291'486
201	21'790.2	803'774'962	3'551'262	3'987'046	116'492'993	772'346	1'185'993
202	20'820.0	769'253'566	3'409'887	3'816'154	111'484'788	743'281	1'138'210
203	17'940.6	430'211'003	2'386'713	2'667'536	100'882'667	670'919	1'024'769
204	19'888.1	576'911'943	2'882'758	3'236'222	106'974'287	717'034	1'098'085
205	18'003.7	435'309'000	2'393'320	2'680'639	98'755'622	658'108	1'007'346
206	16'993.9	368'858'188	2'157'065	2'407'684	96'504'540	642'122	979'688
207	15'791.7	306'058'568	1'897'508	2'115'752	88'718'478	594'867	907'065
208	13'397.9	677'451'598	2'445'453	2'793'698	26'656'187	252'402	398'214
209	7'702.8	78'055'614	678'066	747'733	28'008'226	232'318	354'146
210	7'573.0	76'652'547	666'950	734'902	27'307'051	227'341	346'605
211	3'923.1	39'136'466	327'433	369'169	2'922'073	48'560	75'753
212	11'716.6	148'872'572	1'138'344	1'272'534	50'291'101	385'446	588'785
213	11'857.9	150'910'960	1'157'692	1'292'801	51'725'321	397'749	606'380
214	9'017.4	80'398'446	729'006	820'168	27'264'002	247'001	379'066
215	2'487.5	13'642'783	151'603	172'631	1'073'006	23'339	36'448
216	2'473.5	13'609'508	150'898	171'863	1'058'749	23'066	36'039
217	7'730.1	80'339'733	690'085	760'423	27'988'093	232'982	355'113
218	10'603.0	113'977'619	945'206	1'060'337	39'218'959	327'357	499'009
219	10'600.0	113'277'992	941'551	1'056'691	39'034'110	326'018	497'217
220	7'671.9	78'964'998	682'557	751'454	28'191'530	233'838	356'055
221	2'863.3	19'744'525	194'806	222'094	1'410'185	27'760	43'782
222	3'286.1	28'331'432	253'412	286'491	2'011'242	36'347	56'845
223	5'321.2	37'296'059	387'975	428'653	13'064'534	130'593	199'458
224	3'369.9	28'105'935	256'734	289'834	2'122'520	38'396	59'893
225	3'366.3	28'129'161	256'899	289'932	2'103'473	38'248	59'665
226	10'675.8	115'192'263	954'131	1'070'024	40'072'638	332'222	506'416
227	9'246.1	81'267'079	737'518	832'420	28'093'287	255'696	390'825
228	9'049.7	81'069'356	733'294	824'467	28'079'064	254'836	388'690
229	5'271.6	36'893'886	385'013	425'023	12'879'713	127'927	196'171
230	3'965.7	40'740'873	336'507	378'951	3'008'571	49'770	77'502
231	3'944.8	40'467'505	330'539	367'653	3'002'190	49'615	77'218
232	5'476.3	37'421'201	395'072	436'559	13'832'817	137'798	210'121
233	5'459.2	37'290'554	394'025	435'247	13'811'194	137'521	209'703
234	5'226.4	36'114'422	376'584	417'059	12'355'945	122'713	188'784
235	4'365.2	55'491'979	405'584	459'559	3'785'102	55'815	87'574
236	4'448.9	56'277'029	410'302	466'372	3'765'342	55'750	87'731
237	4'728.6	60'557'040	445'469	502'590	4'382'082	64'785	100'907
238	4'670.0	59'478'100	438'694	494'917	4'287'609	63'629	99'108
239	7'630.3	56'879'695	562'942	634'073	19'271'969	191'038	293'088
240	9'791.9	338'973'665	1'491'338	1'695'034	16'406'920	171'621	269'664

Profile #	Calculated quantity						
	A [mm ²]	I _y [mm ⁴]	W _{el,y} [mm ³]	W _{pl,y} [mm ³]	I _z [mm ⁴]	W _{el,z} [mm ³]	W _{pl,z} [mm ³]
241	8'187.4	226'364'629	1'131'399	1'275'136	12'815'388	142'758	222'921
242	26'476.1	1'666'806'767	5'570'878	6'278'194	130'229'034	872'586	1'347'122
243	26'868.7	1'686'220'415	5'628'803	6'354'376	131'747'306	880'105	1'360'736
244	26'783.5	1'677'036'514	5'602'166	6'325'352	130'980'083	875'097	1'353'322
245	13'407.0	283'058'131	1'703'220	1'876'119	75'602'536	503'128	766'361
246	8'460.2	234'137'394	1'166'836	1'317'352	13'353'761	147'800	231'085
247	17'053.5	369'828'949	2'155'620	2'410'648	94'541'200	632'129	966'000
248	12'077.0	220'975'202	1'425'187	1'570'555	65'838'376	440'346	672'248
249	14'811.4	246'593'784	1'652'552	1'841'799	84'753'624	565'930	862'180
250	11'483.7	186'866'655	1'288'380	1'414'885	65'197'958	435'059	662'228
251	9'778.6	137'412'410	1'011'501	1'114'140	46'803'895	333'932	509'592
252	11'726.4	150'734'286	1'152'139	1'284'526	52'063'710	399'629	607'497
253	17'671.4	429'218'172	2'369'342	2'644'526	99'389'424	661'846	1'101'062
254	17'847.6	433'661'411	2'389'780	2'670'021	99'897'011	665'226	1'105'969
255	21'465.6	790'197'586	3'508'091	3'931'241	114'372'414	765'007	1'172'871
256	12'412.8	225'554'130	1'459'378	1'609'937	67'444'316	455'105	693'928
257	14'225.4	333'229'408	1'888'413	2'088'167	77'264'163	517'718	789'868
258	8'758.1	104'711'812	841'464	925'248	37'371'325	287'185	437'604
259	9'841.9	338'591'559	1'494'786	1'698'828	16'542'157	173'053	271'879
260	5'339.3	83'735'410	555'109	626'017	6'183'365	81'264	126'113
261	19'620.9	870'203'391	3'527'375	3'928'793	101'601'918	678'409	1'039'326
262	5'236.8	82'477'042	546'405	613'707	5'864'577	77'986	121'309
263	5'481.0	85'839'904	571'086	643'449	6'325'121	83'799	130'086
264	12'372.7	230'011'806	1'476'659	1'625'355	68'867'175	461'855	703'249
265	15'167.1	263'036'678	1'729'310	1'926'395	87'749'488	583'460	888'909
266	11'082.3	175'166'285	1'223'057	1'343'420	62'456'559	415'270	632'650
267	6'388.4	119'201'484	724'343	817'611	8'169'771	101'343	158'131
268	16'872.8	365'146'133	2'147'666	2'393'029	96'257'943	643'823	981'231
269	14'626.2	251'651'021	1'664'359	1'850'657	83'838'176		

Profile #	Calculated quantity						
	A [mm ²]	I _y [mm ⁴]	W _{el,y} [mm ³]	W _{pl,y} [mm ³]	I _z [mm ⁴]	W _{el,z} [mm ³]	W _{pl,z} [mm ³]
321	20'884.5	784'314'302	3'454'292	3'861'785	113'344'683	752'221	1'151'238
322	27'108.9	1'734'039'452	5'740'522	6'476'365	133'710'790	891'079	1'377'901
323	26'845.6	1'715'480'024	5'703'912	6'421'477	134'205'178	894'820	1'381'015
324	23'469.9	1'070'714'234	4'246'423	4'766'928	123'329'724	822'609	1'262'203
325	17'839.0	427'639'412	2'375'841	2'654'360	99'030'393	663'409	1'013'615
326	16'853.4	366'993'615	2'139'094	2'388'690	94'317'846	630'678	962'232
327	9'945.3	347'789'364	1'535'460	1'736'872	17'525'529	182'881	285'634
328	8'429.6	229'841'297	1'149'005	1'300'318	13'158'708	145'304	227'538
329	4'580.0	58'018'524	429'815	484'302	4'230'721	62'659	97'529
330	21'561.9	789'593'508	3'497'491	3'928'736	112'970'452	754'142	1'159'071
331	13'354.7	281'491'111	1'694'403	1'866'699	74'996'450	498'945	760'394
332	14'482.5	244'216'208	1'626'211	1'810'301	82'779'279	549'554	837'985
333	11'145.3	183'004'358	1'247'388	1'373'143	60'338'948	404'281	617'256
334	17'751.5	428'430'927	2'363'887	2'643'855	97'398'830	653'683	998'551
335	10'865.6	177'109'575	1'213'245	1'334'023	58'811'818	394'181	601'643
336	14'508.2	337'095'478	1'918'859	2'123'051	78'877'326	530'660	809'262
337	13'958.6	326'559'968	1'852'560	2'047'202	75'479'194	506'368	772'472
338	14'580.5	345'008'617	1'937'108	2'147'284	78'291'902	523'727	800'393
339	15'761.0	449'124'864	2'281'617	2'536'588	81'857'934	547'051	838'763
340	16'951.4	364'441'299	2'135'419	2'386'651	94'942'441	633'774	967'426
341	13'965.3	324'796'992	1'850'748	2'044'226	75'686'839	506'453	773'499
342	8'625.0	104'475'665	834'404	916'748	36'787'662	281'488	429'274
343	17'369.3	377'795'668	2'200'645	2'461'237	97'843'507	653'270	996'810
344	16'297.3	314'848'145	1'955'032	2'182'352	92'931'196	621'801	947'483
345	13'983.4	327'341'902	1'860'320	2'053'974	76'085'597	510'762	778'838
346	21'140.0	1'114'186'665	4'127'458	4'604'389	107'411'655	715'529	1'099'004
347	9'513.2	135'534'711	994'021	1'092'273	45'917'586	326'909	498'511
348	8'323.7	226'469'062	1'127'609	1'279'640	12'556'769	138'995	218'512
349	12'805.1	262'316'704	1'589'798	1'756'450	68'365'803	458'954	700'935
350	2'385.5	13'145'538	185'819	165'852	1'011'985	21'950	34'373
351	3'278.3	27'831'689	251'302	283'703	2'135'205	37'808	58'821
352	3'910.1	38'884'643	321'294	364'798	2'821'778	46'055	72'431
353	3'948.9	39'896'255	328'865	372'388	2'863'956	47'322	74'160
354	4'532.0	56'882'603	419'736	475'033	4'074'596	59'003	93'686
355	4'540.9	57'006'184	418'348	474'900	3'970'793	58'480	91'767
356	2'833.5	19'154'416	191'420	217'931	1'393'259	27'650	43'532
357	7'253.3	162'761'471	898'813	1'015'677	10'592'560	123'212	191'481
358	11'527.5	479'699'893	1'923'801	2'187'749	21'513'791	214'816	336'768
359	11'620.6	493'077'924	1'955'146	2'225'088	21'925'353	216'376	339'678
360	9'687.6	336'420'989	1'487'075	1'683'846	16'684'401	174'742	273'311
361	8'307.9	229'715'474	1'139'829	1'289'966	12'781'732	141'196	221'516
362	13'377.3	666'787'083	2'949'566	2'762'916	25'683'244	243'732	386'539
363	15'524.2	925'346'740	3'055'210	3'505'674	32'465'374	296'447	469'634
364	11'555.8	482'373'746	1'923'072	2'192'451	21'151'840	211'128	331'870
365	7'106.8	155'884'910	868'343	982'849	9'965'969	116'323	181'852
366	4'412.1	56'337'275	412'244	466'311	3'864'982	57'369	89'746
367	6'332.2	54'669'826	513'621	566'309	19'175'402	173'400	264'338
368	8'702.7	104'283'137	833'598	917'889	36'773'335	282'296	430'177
369	8'740.2	104'077'613	833'854	918'083	36'727'757	281'914	429'789
370	8'661.4	104'785'356	833'847	917'771	36'597'113	281'159	428'249
371	11'533.3	188'888'145	1'288'723	1'419'982	63'351'743	423'474	646'114
372	10'248.6	145'544'642	1'068'570	1'177'060	49'639'350	356'144	542'797
373	11'349.3	184'172'559	1'260'808	1'389'773	61'512'654	411'030	628'145
374	11'012.6	181'645'470	1'248'251	1'367'020	62'117'342	417'217	634'349
375	13'965.6	331'869'468	1'874'916	2'068'354	75'690'328	510'938	778'529
376	17'607.1	639'501'169	2'887'921	3'203'397	94'170'516	627'322	958'677
377	12'570.6	238'566'193	1'518'321	1'669'933	71'495'683	474'960	723'249
378	12'688.9	232'837'625	1'501'355	1'655'483	70'832'584	474'304	722'384
379	13'951.4	327'834'018	1'849'505	2'047'118	73'816'626	495'813	757'982
380	13'201.0	274'894'402	1'656'839	1'829'288	71'691'953	481'526	734'429
381	21'082.5	1'113'023'142	4'124'752	4'598'240	107'522'103	716'217	1'099'669
382	22'161.0	1'393'830'107	4'693'189	5'249'624	108'510'376	718'826	1'109'367
383	15'966.9	453'148'564	2'326'105	2'576'494	87'145'061	578'710	884'438
384	15'664.2	441'098'510	2'259'842	2'509'559	81'828'870	547'717	839'253
385	15'722.3	447'535'120	2'276'663	2'529'993	81'830'432	547'123	838'615
386	12'535.1	231'593'257	1'485'143	1'638'575	68'974'386	459'906	702'232
387	5'387.9	36'878'202	385'272	427'611	12'753'020	126'518	194'720
388	10'295.6	107'994'242	603'226	1'014'179	37'081'664	307'681	471'370
389	10'437.2	110'306'565	915'977	1'030'655	36'662'005	305'848	469'659
390	8'881.7	81'305'032	727'301	817'394	26'547'820	240'873	369'715
391	13'117.5	192'406'357	1'364'923	1'526'110	63'468'573	453'477	693'615
392	17'410.3	380'012'415	2'206'680	2'469'479	97'461'375	651'175	994'051
393	17'292.0	374'263'855	2'182'806	2'442'451	96'650'891	646'170	986'432
394	15'925.5	307'205'009	1'905'266	2'127'276	88'508'864	593'203	906'220
395	16'280.0	320'104'965	1'967'153	2'196'377	92'146'380	614'945	938'166
396	17'810.6	430'258'563	2'381'132	2'659'781	98'704'186	661'933	1'011'055
397	23'223.1	1'057'106'756	4'208'646	4'716'189	124'849'822	826'382	1'266'502
398	23'898.4	1'073'790'391	4'286'760	4'818'549	125'108'319	835'587	1'283'490
399	23'419.7	1'064'603'222	4'226'964	4'746'800	122'198'879	816'401	1'253'377
400	27'098.3	1'741'649'982	5'757'806	6'492'161	134'120'423	892'233	1'380'015

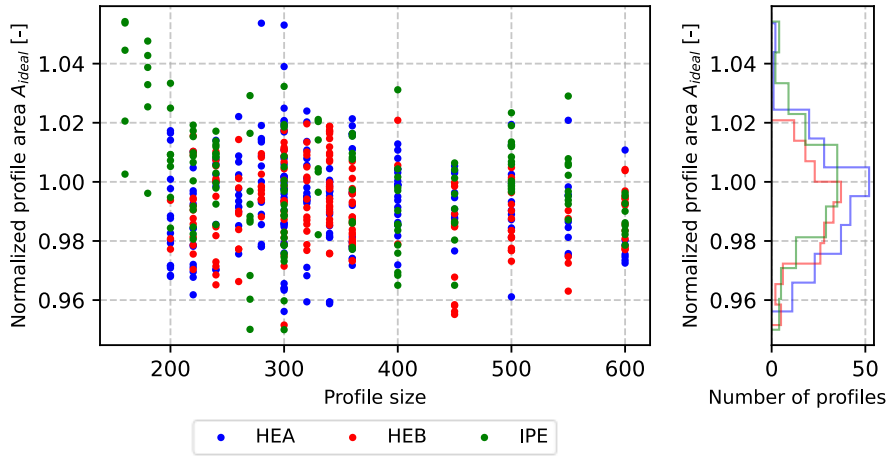
Profile #	Calculated quantity						
	A [mm ²]	I _y [mm ⁴]	W _{el,y} [mm ³]	W _{pl,y} [mm ³]	I _z [mm ⁴]	W _{el,z} [mm ³]	W _{pl,z} [mm ³]
401	17'685.2	420'705'091	2'335'953	2'613'852	96'962'571	647'043	990'293
402	16'910.9	367'782'912	2'145'195	2'395'875	94'581'634	632'272	965'060
403	15'865.0	305'860'015	1'901'819	2'120'628	89'947'806	599'972	915'258
404	11'820.5	153'749'250	1'170'486	1'304'836	51'758'444	402'164	611'039
405	10'311.6	106'632'528	899'208	1'009'495	37'543'147	311'316	476'418
406	11'631.2	484'367'335	1'923'963	2'199'440	21'414'746	210'920	332'288
407	8'609.4	103'670'720	826'259	909'460	36'670'815	280'240	426'767
408	15'880.0	453'619'452	2'319'414	2'570'019	84'483'432	569'967	870'123
409	21'503.1	786'889'587	3'488'527	3'917'480	112'810'963	753'127	1'157'282
410	17'989.5	436'529'493	2'404'062	2'688'662	99'652'398	667'419	1'019'201
411	6'248.2	53'309'053	502'560	554'751	18'339'105	167'948	256'093
412	10'848.0	178'110'283	1'217'058	1'337'364	58'880'012	394'585	602'158
413	11'932.0	222'249'125	1'423'716	1'566'633	64'813'275	436'806	665'727
414	15'607.2	445'586'653	2'267'905	2'516'273	83'941'956	558'862	852'859
415	8'325.5	226'948'707	1'129'576	1'281'425	12'606'653	139'469	219'165
416	17'410.3	378'555'847	2'205'651	2'466'964	98'205'955	655'777	1'000'484
417	9'520.4	135'631'840	992'114	1'091'718	44'955'548	321'904	491'375
418	13'904.2	325'164'169	1'848'732	2'040'878	75'745'391	507'949	774'473
419	11'445.0	150'001'503	1'131'020	1'261'668	48'905'681	375'605	573'187
420	16'024.1	455'042'131	2'332'234	2'585'499	85'987'233	574'301	878'488
421	5'555.0	84'514'135	558'439	638'907	5'912'528	78'296	122'808
422	12'797.0	261'606'220	1'587'224	1'753'623	68'254'521	458'361	700'104
423	5'374.9	84'318'914	555'022	628'482	5'965'160	78'448	122'511
424	3'903.4	38'041'409	317'966	360'795	2'845'129	46'440	72'942
425	3'359.1	27'630'225	251'618	285'514	2'053'194	36'975	57'927
426	3'309.6	27'219'527	248'478	281'514	2'041'485	36'668	57'398
427	2'943.5	19'900'158	199'002	226'648	1'470'691	29'042	45'777
428	2'050.4	8'761'591	109'118	125'074	683'040	16'491	26'006
429	11'691.6	188'753'804	1'301'122	1			

Profile #	Calculated quantity						
	A [mm ²]	I _y [mm ⁴]	W _{el,y} [mm ³]	W _{pl,y} [mm ³]	I _z [mm ⁴]	W _{el,z} [mm ³]	W _{pl,z} [mm ³]
481	23'979.0	1'095'843'334	4'365'562	4'892'167	128'823'116	860'341	1'317'748
482	14'009.9	330'708'727	1'874'182	2'067'631	77'300'976	515'202	785'827
483	21'489.6	784'206'828	3'482'268	3'910'059	113'034'276	755'476	1'159'926
484	17'086.6	367'903'969	2'156'214	2'409'737	95'893'270	639'352	976'685
485	7'741.9	78'770'016	683'293	753'399	28'196'697	233'881	356'555
486	20'848.9	1'102'748'130	4'067'155	4'541'683	104'102'333	694'919	1'068'383
487	19'501.4	868'728'610	3'512'001	3'912'331	99'570'313	666'713	1'022'649
488	17'386.7	629'138'781	2'833'257	3'149'437	90'026'563	601'460	921'749
489	7'791.6	81'451'353	697'447	768'753	28'194'857	234'459	357'562
490	6'414.7	54'335'095	515'954	569'166	19'292'424	174'893	267'091
491	3'960.8	40'577'767	333'685	376'990	2'871'809	48'004	75'021
492	6'500.2	55'244'225	524'188	578'201	19'690'583	178'648	272'621
493	7'683.5	77'808'070	676'357	745'728	27'934'964	231'403	352'930
494	15'798.5	448'363'396	2'285'819	2'539'626	82'909'421	552'729	847'160
495	16'068.7	457'457'462	2'338'142	2'593'286	87'077'543	578'992	884'847
496	9'513.2	135'534'711	994'021	1'092'273	45'917'586	326'909	498'511
497	8'323.7	226'469'062	1'127'609	1'279'640	12'556'769	138'995	218'512
498	12'805.1	262'316'704	1'589'798	1'756'450	68'365'803	458'954	700'935
499	2'803.9	19'193'055	193'041	218'197	1'482'955	28'984	45'354
500	2'869.0	19'736'092	197'164	223'455	1'491'278	29'301	45'899
501	2'919.5	20'197'835	200'963	227'975	1'513'150	29'795	46'677
502	7'455.3	74'687'519	648'921	717'391	25'527'758	211'972	325'639
503	3'272.3	28'203'228	252'434	285'309	1'993'908	36'099	56'478
504	6'464.7	54'632'612	518'238	572'003	19'908'612	179'438	273'212
505	5'472.0	37'572'543	396'189	437'556	13'818'951	138'017	210'367
506	5'289.6	37'203'298	384'848	426'043	12'531'252	125'294	192'301
507	10'265.0	109'032'891	906'191	1'017'317	36'581'048	304'906	467'158
508	10'546.8	114'745'891	946'436	1'060'774	39'241'576	325'818	496'853
509	9'187.3	82'886'761	747'165	840'502	28'544'529	258'380	394'595
510	9'053.8	81'266'571	736'310	826'833	28'617'375	258'513	393'932
511	9'198.3	83'499'297	752'653	845'306	29'367'366	264'821	403'285
512	7'658.0	55'575'847	557'599	628'230	19'730'417	196'528	299'993
513	3'933.6	40'328'308	333'471	375'452	2'985'336	49'365	76'849
514	3'958.1	40'619'730	335'492	377'902	2'999'060	49'567	77'210
515	6'386.0	53'814'178	509'483	563'254	18'875'091	172'069	262'500
516	5'210.9	36'247'881	377'366	417'488	12'404'795	123'474	189'625
517	9'030.3	79'081'164	722'896	813'466	27'851'502	253'830	387'096
518	7'333.4	162'821'777	902'860	1'021'467	10'387'724	121'437	189'698
519	5'265.4	81'948'727	543'805	614'285	5'858'655	77'408	120'717
520	6'392.8	119'411'348	725'001	818'529	8'134'366	100'941	157'645
521	13'245.5	198'886'361	1'406'502	1'566'730	66'822'016	476'280	725'817
522	8'643.2	103'421'615	826'183	910'192	36'063'781	277'905	423'594
523	9'812.2	137'795'276	1'014'917	1'117'972	46'925'005	334'438	510'747
524	11'442.8	186'424'881	1'285'246	1'410'966	65'035'195	433'640	660'152
525	14'800.4	246'921'919	1'653'532	1'842'537	84'762'698	566'066	862'255
526	12'357.7	223'754'741	1'449'423	1'599'280	66'902'876	451'787	688'909
527	12'041.8	220'352'679	1'422'181	1'566'636	65'691'326	439'495	670'940
528	8'709.5	240'984'148	1'200'001	1'356'136	13'767'459	152'043	238'158
529	5'427.7	85'916'358	566'544	639'362	6'193'094	81'595	126'951
530	9'922.6	342'758'060	1'507'026	1'715'073	16'366'681	171'307	270'151
531	15'443.5	922'116'495	3'061'425	3'498'586	34'342'628	308'089	485'716
532	19'383.7	848'873'536	3'455'763	3'852'463	99'120'910	662'396	1'015'877
533	23'310.1	1'053'771'421	4'212'221	4'721'172	123'901'222	827'415	1'267'677
534	11'653.2	149'765'389	1'141'200	1'273'826	50'616'391	389'672	593'248
535	12'506.2	227'122'280	1'469'762	1'621'758	68'210'447	460'011	701'227
536	9'659.4	134'933'941	1'000'808	1'099'982	46'540'371	333'372	508'282
537	9'727.1	136'334'150	1'009'210	1'109'592	46'752'335	334'830	510'798
538	11'486.1	185'580'321	1'284'515	1'410'392	66'032'883	437'362	666'009
539	20'137.7	880'449'657	3'602'716	4'012'052	105'112'710	703'166	1'077'362
540	13'057.7	192'890'165	1'369'472	1'528'068	64'006'400	458'531	699'963
541	13'059.7	192'324'168	1'367'055	1'525'694	63'988'701	457'765	699'130
542	13'060.1	192'162'388	1'366'682	1'525'271	63'934'495	457'852	699'188
543	13'284.5	274'382'054	1'667'064	1'837'954	73'490'849	491'183	749'356
544	8'150.8	224'331'479	1'119'056	1'263'995	12'692'560	140'087	219'349
545	8'179.4	223'552'178	1'117'705	1'263'492	12'653'261	139'769	219'070
546	13'170.5	197'605'226	1'396'405	1'555'719	66'348'373	471'576	719'003
547	15'760.0	301'504'925	1'877'658	2'095'730	87'876'618	589'915	899'866
548	12'358.1	229'264'000	1'473'182	1'621'666	68'646'271	460'574	701'409
549	13'053.8	191'645'702	1'370'709	1'526'786	65'564'328	467'432	712'784
550	14'916.2	255'892'184	1'686'664	1'880'809	84'014'959	560'810	856'190
551	11'092.9	175'616'559	1'225'132	1'345'886	62'238'623	413'821	630'928
552	10'982.0	177'930'931	1'228'508	1'348'137	61'275'662	409'227	623'510
553	20'189.9	587'754'913	2'935'545	3'294'130	111'246'439	738'934	1'131'092
554	11'859.4	156'432'469	1'183'570	1'318'693	52'252'811	402'316	612'521
555	14'591.2	251'222'212	1'661'523	1'847'020	83'757'744	559'691	852'113
556	11'373.4	184'122'517	1'265'316	1'393'185	62'463'024	416'656	636'355
557	9'748.5	337'818'953	1'486'945	1'689'071	16'283'857	170'726	268'256
558	8'470.2	103'552'111	816'013	899'780	34'119'275	262'952	402'432
559	12'980.7	191'145'816	1'358'438	1'515'845	63'475'486	454'435	693'875
560	13'471.6	679'267'826	2'459'689	2'807'612	26'857'822	254'167	401'450
561	20'002.8	874'479'825	3'582'392	3'986'622	104'774'751	701'820	1'074'280

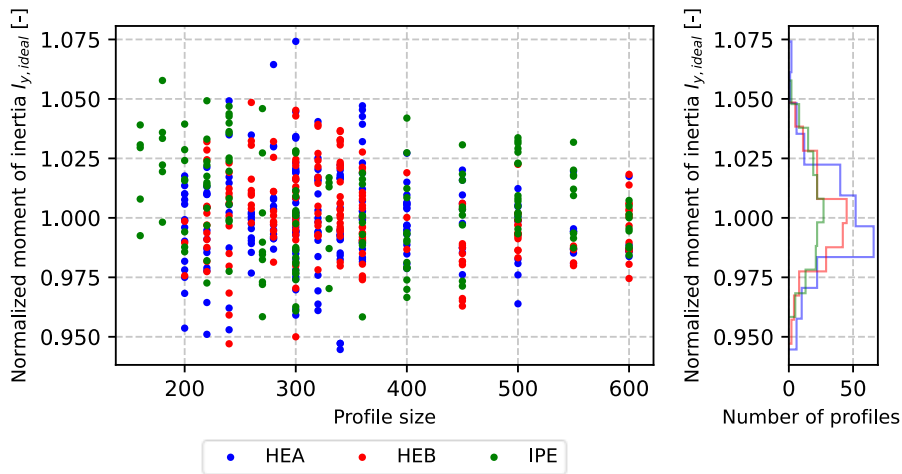
B.2.2 Visualization of the sectional properties

The idealized sectional properties are normalized with respect to the nominal sectional properties.

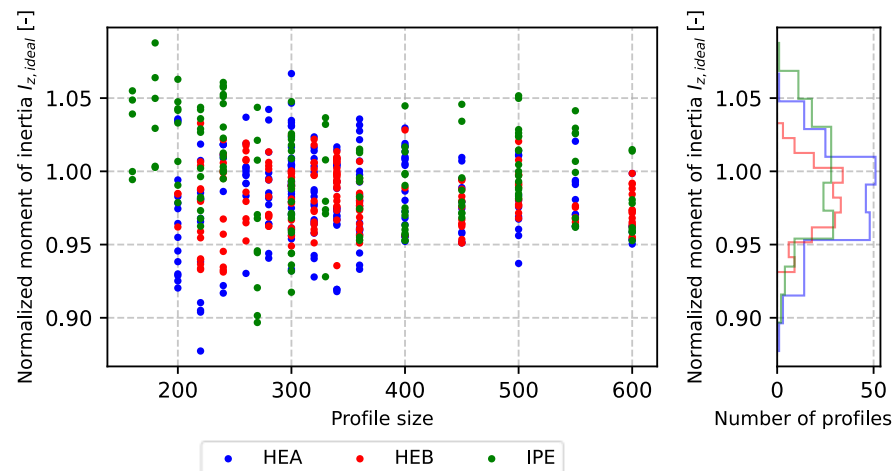
A_{ideal} :



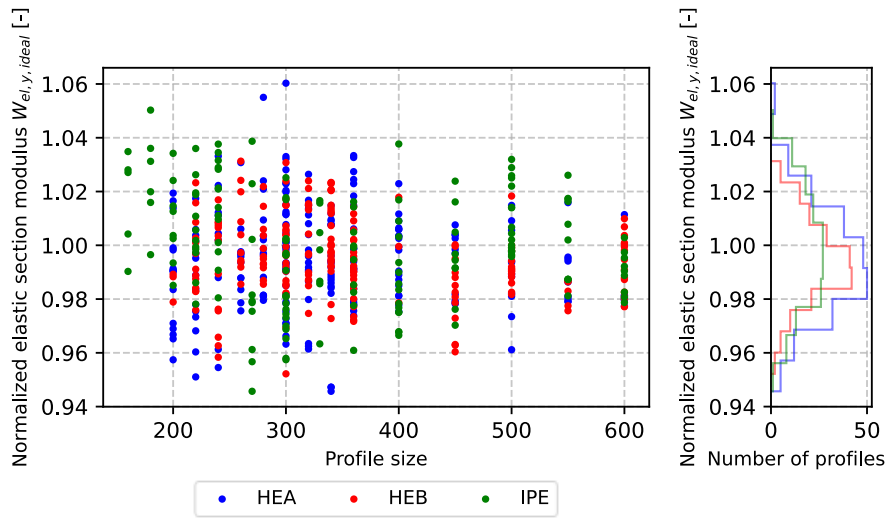
$I_{y,ideal}$:



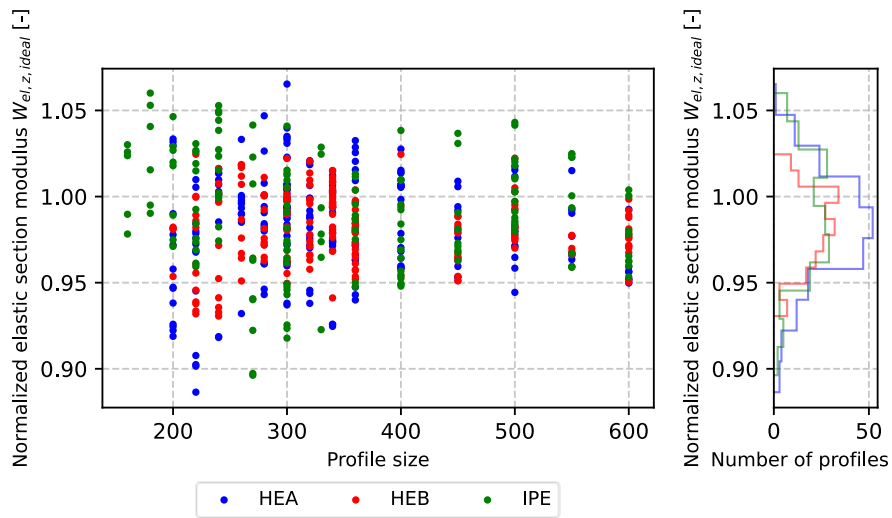
$I_{z,ideal}$:



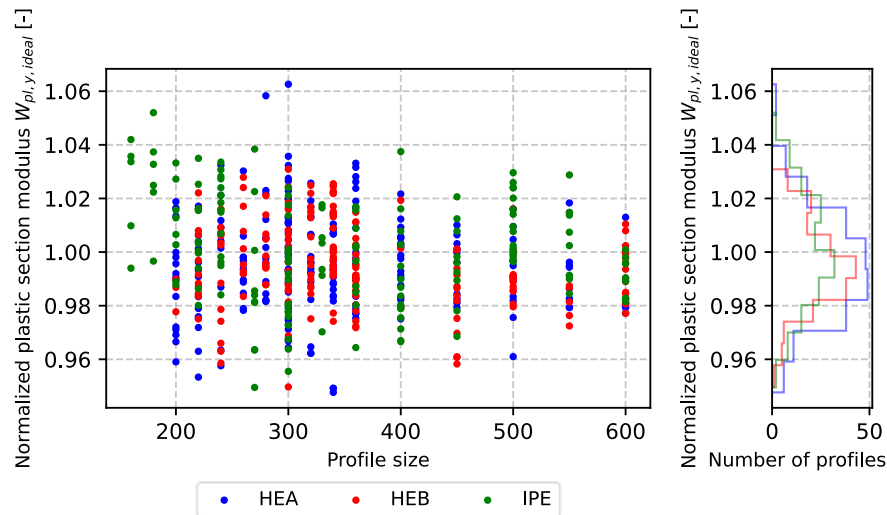
$W_{el,y,ideal}$:



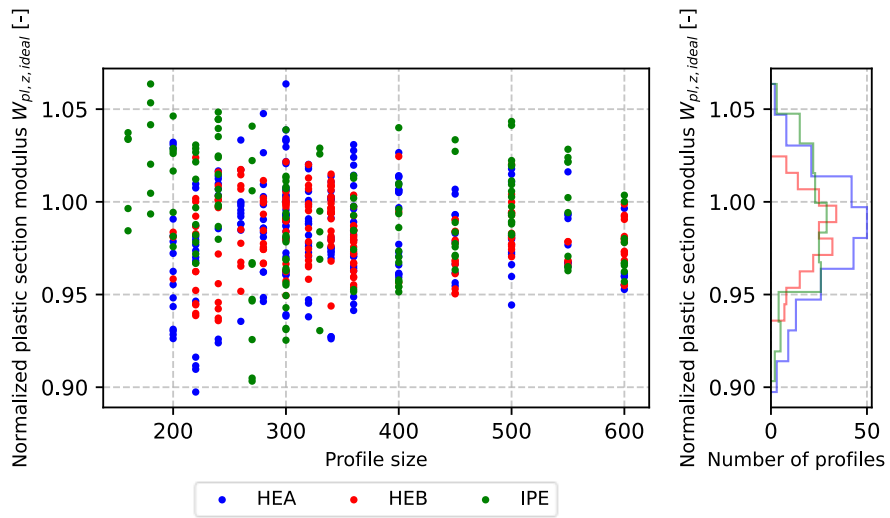
$W_{el,z,ideal}$:



$W_{pl,y,ideal}$:



$W_{pl,z,ideal}$:



B.2.3 Real vs. idealized cross-sections

The following tables show extensively the mean values and the coefficients of variation for the relation between the real and the idealized sectional properties for each category:

$$x_{real\ vs.\ ideal} = \frac{x_{real}}{x_{ideal}}$$

Mean values [-]:

cat.	$\frac{A_{real}}{A_{ideal}}$	$\frac{I_{y,real}}{I_{y,ideal}}$	$\frac{I_{z,real}}{I_{z,ideal}}$	$\frac{W_{el,y,real,pos}}{W_{el,y,ideal}}$	$\frac{W_{el,y,real,neg}}{W_{el,y,ideal}}$	$\frac{W_{el,z,real,pos}}{W_{el,z,ideal}}$	$\frac{W_{el,z,real,neg}}{W_{el,z,ideal}}$	$\frac{W_{pl,y,real}}{W_{pl,y,ideal}}$	$\frac{W_{pl,z,real}}{W_{pl,z,ideal}}$
Total	1.0011	0.9999	0.9916	0.9976	0.9985	0.9896	0.9865	1.0007	0.9954
Small	1.0009	0.9998	0.9915	0.9965	0.9976	0.9889	0.9852	1.0005	0.9952
Large	1.0015	1.0001	0.9919	0.9994	1.0000	0.9906	0.9885	1.0010	0.9956
HEA	1.0014	1.0000	0.9906	0.9964	0.9985	0.9885	0.9856	1.0009	0.9944
HEB	1.0002	0.9989	0.9915	0.9971	0.9970	0.9904	0.9864	0.9997	0.9951
IPE	1.0018	1.0010	0.9932	1.0000	1.0005	0.9901	0.9878	1.0015	0.9970

Coefficients of variation [%]:

cat.	$\frac{A_{real}}{A_{ideal}}$	$\frac{I_{y,real}}{I_{y,ideal}}$	$\frac{I_{z,real}}{I_{z,ideal}}$	$\frac{W_{el,y,real,pos}}{W_{el,y,ideal}}$	$\frac{W_{el,y,real,neg}}{W_{el,y,ideal}}$	$\frac{W_{el,z,real,pos}}{W_{el,z,ideal}}$	$\frac{W_{el,z,real,neg}}{W_{el,z,ideal}}$	$\frac{W_{pl,y,real}}{W_{pl,y,ideal}}$	$\frac{W_{pl,z,real}}{W_{pl,z,ideal}}$
Total	0.265	0.237	0.504	0.602	0.553	0.685	0.808	0.259	0.349
Small	0.281	0.237	0.512	0.642	0.586	0.759	0.833	0.272	0.352
Large	0.233	0.235	0.491	0.485	0.462	0.536	0.724	0.234	0.342
HEA	0.225	0.210	0.548	0.647	0.572	0.655	0.828	0.234	0.356
HEB	0.176	0.200	0.418	0.508	0.489	0.578	0.726	0.197	0.306
IPE	0.361	0.261	0.498	0.580	0.541	0.819	0.860	0.317	0.333

Appendix C - Abaqus investigation

C.1 Model verification GMNIA

Classification of the chosen cross-sections of section 5.2.9 according to prEN 1993-1-1 [9]:

	h [mm]	b [mm]	t _w [mm]	t _f [mm]	r [mm]	(c/t) _{flange}	(c/t) _{web}
<u>Pure compression:</u>							
CS 1	224	196	8	13	24	5.38	18.75
CS 1/2	255	244	8	13	24	7.23	22.63
CS 2/3	294	266	8	13	24	8.08	27.50
CS 3/4	320	350	8	13	24	11.31	30.75
CS 4	374	456	8	13	24	15.39	37.50
<u>Bending around strong axis:</u>							
CS 1	424	196	8	13	24	5.39	43.75
CS 1/2	540	244	8	13	24	7.23	58.25
CS 2/3	611	266	8	13	24	8.08	67.13
CS 3/4	858	350	8	13	24	11.31	98.00
CS 4	1074	456	8	13	24	15.39	125.00
<u>Bending around weak axis:</u>							
CS 1	224	196	8	13	24	5.39	18.75
CS 1/2	255	244	8	13	24	7.23	22.63
CS 2/3	294	266	8	13	24	8.08	27.50
CS 3/4	320	388	8	13	24	12.77	30.75
CS 4	374	496	8	13	24	16.92	37.50

The following table summarizes the threshold values of the slendernesses according to prEN 1993-1-1 [9]:

	Flange			Web		
	Class 1	Class 2	Class 3	Class 1	Class 2	Class 3
Pure compression	$9 \cdot \varepsilon$	$10 \cdot \varepsilon$	$14 \cdot \varepsilon$	$28 \cdot \varepsilon$	$34 \cdot \varepsilon$	$38 \cdot \varepsilon$
Bending strong axis	$9 \cdot \varepsilon$	$10 \cdot \varepsilon$	$14 \cdot \varepsilon$	$72 \cdot \varepsilon$	$83 \cdot \varepsilon$	$121 \cdot \varepsilon$
Bending weak axis	$9 \cdot \varepsilon / \alpha_c$	$10 \cdot \varepsilon / \alpha_c$	$21 \cdot \varepsilon \cdot \sqrt{k_\sigma}$	-	-	-

It is noted that for the load case "bending around the weak axis", it is assumed that the web will not buckle in any case.

The value $\varepsilon = 0.81$ is chosen, as recommended for a yield strength $f_y = 355 \text{ MPa}$.

For the factor α_c , the value 1.00 is chosen, as the whole decisive flange half is under compressive stresses for bending around the weak axis.

The factor $k_\sigma = 0.57$ is determined according to the table 6.2 of the standard prEN 1993-1-5 [22], assuming $\psi = 0$.

Inserting all these values gives the following threshold values for the slendernesses:

	Flange			Web		
	Class 1	Class 2	Class 3	Class 1	Class 2	Class 3
Pure compression	7.29	8.1	11.34	22.68	27.54	30.78
Bending strong axis	7.29	8.1	11.34	58.32	67.23	98.01
Bending weak axis	7.29	8.1	12.84	-	-	-

The following table shows the sectional properties used in the evaluation of these cross-sections:

	A [mm ²]	W _{pl,y} [mm ³]	W _{pl,z} [mm ³]
<u>Pure compression:</u>			
CS 1	7174		
CS 1/2	8670		
CS 2/3	9554		
CS 3/4	11946		
CS 4	15134		
<u>Bending around strong axis:</u>			
CS 1		1459780	
CS 1/2		2324458	
CS 2/3		2894308	
CS 3/4		5432236	
CS 4		8742654	
<u>Bending around weak axis:</u>			
CS 1			257500
CS 1/2			395276
CS 2/3			468830
CS 3/4			987868
CS 4			1609300

These sectional properties are calculated using the equations introduced in section 4.1.

C.2 Abaqus results – Nominal cross-sections

Profile Nr.	Profile	Pure Compression				Bending strong axis				Bending weak axis			
		N [kN]	A [mm ²]	N/(A*fy)	CS Class	My [kNm]	Wpl_y [mm ³]	My / (Wpl_y*fy)	CS Class	Mz [kNm]	Wpl_z [mm ³]	Mz / (Wpl_z*fy)	CS Class
1	IPE 160	710.55	2'009.1	0.9962	2	45.064	123'860	1.0249	1	10.009	26'100	1.0803	1
2	IPE 180	844.07	2'394.7	0.9929	3	60.293	166'415	1.0206	1	13.195	34'600	1.0743	1
3	IPE 200	1'003.77	2'848.4	0.9927	3	80.093	220'639	1.0226	1	17.028	44'612	1.0752	1
4	IPE 220	1'172.21	3'337.1	0.9895	3	103.211	285'406	1.0187	1	22.111	58'110	1.0718	1
5	IPE 240	1'374.50	3'911.6	0.9898	3	132.764	366'645	1.0200	1	28.138	73'924	1.0722	1
6	IPE 270	1'601.58	4'594.5	0.9819	4	174.626	483'997	1.0163	1	36.512	96'950	1.0609	1
7	IPE 300	1'861.84	5'381.2	0.9746	4	225.902	628'356	1.0127	1	46.792	125'219	1.0526	1
8	IPE 330	2'161.44	6'260.6	0.9725	4	289.477	804'331	1.0138	1	57.631	153'678	1.0564	1
9	IPE 360	2'500.54	7'272.9	0.9685	4	366.397	1'019'147	1.0127	1	71.878	191'099	1.0595	1
10	IPE 400	2'889.15	8'446.4	0.9635	4	470.212	1'307'148	1.0133	1	86.245	229'000	1.0609	1
11	IPE 450	3'341.75	9'882.1	0.9526	4	611.338	1'701'794	1.0119	1	104.266	276'380	1.0627	1
12	IPE 500	3'878.09	11'552.2	0.9456	4	786.843	2'194'118	1.0102	1	127.076	335'879	1.0657	1
13	IPE 550	4'495.23	13'441.6	0.9420	4	1'000.423	2'787'006	1.0112	1	152.148	400'536	1.0700	1
14	IPE 600	5'190.83	15'598.4	0.9374	4	1'260.037	3'512'400	1.0105	1	185.034	485'649	1.0733	1
15	HEA 180	1'616.72	4'525.1	1.0064	2	115.759	324'853	1.0038	2	56.446	156'494	1.0160	2
16	HEA 200	1'922.99	5'383.1	1.0063	2	153.059	429'485	1.0039	2	73.499	203'818	1.0158	2
17	HEA 220	2'294.87	6'434.1	1.0047	2	202.325	568'458	1.0026	2	97.412	270'594	1.0141	2
18	HEA 240	2'742.80	7'683.6	1.0055	2	265.199	744'624	1.0032	2	126.688	351'692	1.0147	2
19	HEA 260	3'098.45	8'681.9	1.0053	3	327.456	919'772	1.0029	3	154.710	430'168	1.0131	3
20	HEA 280	3'466.45	9'726.4	1.0039	3	395.569	1'112'224	1.0018	3	185.725	518'132	1.0097	3
21	HEA 300	4'012.64	11'252.8	1.0045	3	491.719	1'383'272	1.0013	3	230.004	641'165	1.0105	3
22	HEA 320	4'432.52	12'436.8	1.0040	2	580.270	1'628'090	1.0040	2	255.460	709'739	1.0139	2
23	HEA 340	4'753.67	13'347.3	1.0032	2	661.698	1'850'476	1.0073	1	273.717	755'947	1.0200	1
24	HEA 360	5'080.85	14'275.8	1.0026	2	748.674	2'088'474	1.0098	1	294.713	802'277	1.0348	1
25	HEA 400	5'646.45	15'897.8	1.0005	2	921.529	2'561'800	1.0133	1	320.574	872'863	1.0346	1
26	HEA 450	6'298.47	17'802.8	0.9966	3	1'159.819	3'215'868	1.0159	1	359.455	965'530	1.0487	1
27	HEA 500	6'956.72	19'753.8	0.9920	4	1'425.374	3'948'858	1.0168	1	399.937	1'058'512	1.0643	1
28	HEA 550	7'403.89	21'175.8	0.9849	4	1'668.055	4'621'818	1.0166	1	419.293	1'106'903	1.0670	1
29	HEA 600	7'851.61	22'645.8	0.9767	4	1'929.038	5'350'387	1.0156	1	438.164	1'155'656	1.0680	1
30	HEB 180	2'356.98	6'525.1	1.0175	1	173.014	481'448	1.0123	1	87.183	231'013	1.0631	1
31	HEB 200	2'818.51	7'808.1	1.0168	1	230.837	642'548	1.0120	1	115.030	305'812	1.0596	1
32	HEB 220	3'283.34	9'104.1	1.0159	1	296.644	827'048	1.0104	1	146.648	393'881	1.0488	1
33	HEB 240	3'818.79	10'598.6	1.0150	1	377.746	1'053'146	1.0104	1	186.081	498'418	1.0517	1
34	HEB 260	4'261.43	11'844.4	1.0135	1	459.825	1'282'912	1.0096	1	223.751	602'247	1.0466	1
35	HEB 280	4'715.37	13'136.4	1.0111	1	549.215	1'534'434	1.0082	1	264.063	717'571	1.0366	1
36	HEB 300	5'350.15	14'907.8	1.0109	1	669.071	1'868'675	1.0086	1	319.137	870'141	1.0331	1
37	HEB 320	5'775.35	16'134.3	1.0083	1	771.361	2'149'241	1.0110	1	349.338	939'096	1.0479	1
38	HEB 340	6'108.20	17'089.8	1.0068	1	866.823	2'408'107	1.0140	1	371.067	985'720	1.0604	1
39	HEB 360	6'449.28	18'063.3	1.0057	1	967.562	2'682'990	1.0159	1	390.930	1'032'489	1.0666	1
40	HEB 400	7'056.78	19'777.8	1.0051	1	1'170.333	3'231'740	1.0201	1	416.872	1'104'035	1.0636	1
41	HEB 450	7'749.94	21'797.8	1.0015	2	1'445.218	3'982'371	1.0223	1	458.378	1'197'656	1.0781	1
42	HEB 500	8'461.14	23'863.8	0.9988	2	1'751.799	4'814'568	1.0249	1	497.190	1'291'648	1.0843	1
43	HEB 550	8'975.29	25'405.8	0.9951	3	2'034.793	5'590'608	1.0253	1	516.067	1'341'142	1.0839	1
44	HEB 600	9'490.71	26'995.8	0.9903	3	2'338.663	6'425'137	1.0253	1	535.192	1'391'057	1.0838	1

It is noted that $f_y = 355$ MPa was inserted.

The following abbreviations are selected:

N : cross-sectional resistance for pure compression

M_y : cross-sectional resistance for bending around the strong axis

M_z : cross-sectional resistance for bending around the weak axis

C.3 Abaqus results – Real cross-sections

C.3.1 Obtained resistances

Profile Nr.	Pure Compression				Bending strong axis				Bending weak axis				
	N_real [kN]	N_real / N_nom [-]	A_real / A_nom [-]	My_real_pos [kNm]	My_real_neg [kNm]	My_real_pos / My_nom [-]	My_real_neg / My_nom [-]	Wpl_Y_real / Wpl_Y_nom [-]	Mz_real_pos [kNm]	Mz_real_neg [kNm]	Mz_real_pos / Mz_nom [-]	Mz_real_neg / Mz_nom [-]	Wpl_z_real / Wpl_z_nom [-]
1	2226.12	0.9700	0.9714	195.464	195.371	0.9661	0.9656	0.9665	88.092	88.645	0.9043	0.9100	0.9134
2	3812.46	0.9983	1.0004	378.959	379.437	1.0032	1.0045	1.0065	184.398	185.090	0.9910	0.9947	0.9943
3	2658.19	0.9692	0.9710	253.622	253.815	0.9563	0.9571	0.9586	116.404	115.953	0.9188	0.9153	0.9227
4	1917.09	0.9969	0.9988	152.580	152.620	0.9969	0.9971	0.9990	71.593	71.328	0.9741	0.9705	0.9765
5	1198.60	1.0225	1.0232	106.992	107.110	1.0366	1.0378	1.0379	22.641	22.541	1.0239	1.0195	1.0242
6	1012.38	1.0086	1.0106	80.922	80.904	1.0104	1.0101	1.0165	16.637	16.710	0.9771	0.9813	0.9883
7	3053.84	0.9856	0.9896	320.959	321.147	0.9802	0.9807	0.9834	151.478	149.762	0.9791	0.9680	0.9783
8	2212.82	0.9642	0.9639	192.961	192.958	0.9537	0.9537	0.9548	87.610	87.479	0.8994	0.8980	0.9045
9	1857.74	0.9661	0.9691	146.707	146.585	0.9585	0.9577	0.9603	67.851	67.997	0.9232	0.9251	0.9287
10	1372.94	0.9989	1.0010	132.942	133.171	1.0013	1.0031	1.0035	28.207	27.999	1.0024	0.9951	1.0015
11	1866.81	0.9708	0.9737	147.536	147.684	0.9639	0.9649	0.9669	68.218	68.804	0.9281	0.9361	0.9388
12	3198.57	0.9742	0.9806	292.836	292.997	0.9872	0.9877	0.9885	136.366	140.929	0.9299	0.9610	0.9456
13	1800.05	0.9685	0.9706	289.336	289.167	0.9754	0.9748	0.9752	137.416	136.844	0.9370	0.9331	0.9369
14	1682.89	0.9931	0.9942	539.589	539.535	0.9825	0.9824	0.9841	257.540	252.834	0.9753	0.9575	0.9691
15	7494.31	0.9670	0.9692	1405.056	1406.574	0.9722	0.9733	0.9768	443.934	443.949	0.9685	0.9685	0.9769
16	6248.32	0.9920	0.9922	1134.965	1135.080	0.9786	0.9787	0.9826	341.101	340.541	0.9489	0.9474	0.9569
17	5332.06	0.9966	0.9992	670.126	670.098	1.0016	1.0015	1.0007	312.333	312.299	0.9786	0.9786	0.9800
18	3869.02	0.9642	0.9668	479.666	479.211	0.9755	0.9746	0.9759	220.640	221.303	0.9593	0.9622	0.9632
19	3854.17	0.9605	0.9639	477.115	477.235	0.9703	0.9705	0.9759	217.891	219.914	0.9473	0.9561	0.9555
20	4655.56	1.0357	1.0321	1030.587	1031.070	1.0302	1.0306	1.0298	155.433	155.609	1.0216	1.0227	1.0236
21	4413.42	0.9957	0.9970	574.370	575.277	0.9898	0.9914	0.9950	250.580	248.511	0.9809	0.9728	0.9850
22	1814.62	0.9746	0.9795	221.773	221.654	0.9817	0.9812	0.9846	45.168	45.221	0.9653	0.9664	0.9699
23	5273.90	0.9857	0.9885	663.127	663.724	0.9920	0.9924	0.9954	310.720	314.033	0.9736	0.9840	0.9793
24	8436.90	0.9971	0.9982	1743.952	1744.705	0.9955	0.9960	0.9970	494.424	495.692	0.9944	0.9970	0.9987
25	8378.73	0.9903	0.9915	1731.217	1733.352	0.9883	0.9895	0.9907	490.044	491.394	0.9856	0.9883	0.9910
26	3876.87	0.9997	1.0022	785.892	787.559	0.9988	1.0009	1.0027	123.875	123.893	0.9748	0.9750	0.9779
27	1840.11	0.9883	0.9932	223.730	223.373	0.9904	0.9888	0.9942	45.926	45.998	0.9830	0.9830	0.9915
28	1759.11	0.9448	0.9530	215.694	215.639	0.9548	0.9546	0.9587	44.010	43.888	0.9406	0.9379	0.9455
29	1782.46	0.9574	0.9644	218.680	218.530	0.9680	0.9674	0.9717	44.799	44.829	0.9574	0.9581	0.9633
30	3523.32	1.0164	1.0179	404.297	404.666	1.0221	1.0230	1.0250	189.360	187.566	1.0196	1.0099	1.0166
31	1838.84	0.9876	0.9917	223.848	223.977	0.9909	0.9915	0.9938	46.001	46.114	0.9831	0.9855	0.9878
32	3430.54	0.9896	0.9910	393.780	393.516	0.9955	0.9948	0.9980	182.345	181.887	0.9818	0.9793	0.9834
33	5396.37	1.0086	1.0149	680.995	681.111	1.0178	1.0180	1.0168	318.872	319.309	0.9992	1.0005	0.9987
34	5309.87	0.9925	0.9942	662.441	662.857	0.9901	0.9907	0.9954	316.796	314.206	0.9927	0.9845	0.9917
35	1841.37	0.9890	0.9921	220.734	221.077	0.9771	0.9786	0.9826	43.759	43.450	0.9352	0.9286	0.9414
36	4467.49	0.9938	0.9960	991.564	991.006	0.9911	0.9906	0.9939	147.026	146.730	0.9663	0.9644	0.9671
37	5083.81	0.9502	0.9539	634.547	634.832	0.9488	0.9488	0.9525	303.162	300.454	0.9499	0.9415	0.9515
38	4413.77	0.9958	0.9969	576.605	576.150	0.9937	0.9929	0.9950	246.960	247.882	0.9667	0.9703	0.9669
39	2807.11	0.9716	0.9776	455.819	455.044	0.9694	0.9677	0.9716	80.751	81.005	0.9363	0.9392	0.9499
40	6000.10	0.9823	0.9858	857.973	860.038	0.9898	0.9922	0.9925	365.725	365.277	0.9856	0.9844	0.9872
41	4425.27	0.9984	0.9996	576.635	575.922	0.9937	0.9925	0.9950	246.793	248.756	0.9661	0.9738	0.9674
42	7983.90	1.0168	1.0145	1957.472	1956.943	1.0147	1.0145	1.0167	436.465	435.258	0.9961	0.9934	0.9951
43	5266.07	0.9843	0.9883	669.257	669.127	1.0003	1.0001	1.0007	314.749	313.192	0.9863	0.9814	0.9860
44	5956.40	0.9751	0.9773	844.810	844.318	0.9746	0.9740	0.9759	355.541	349.713	0.9582	0.9425	0.9621
45	5880.00	1.0181	1.0189	781.729	782.417	1.0143	1.0143	1.0143	351.745	353.028	1.0069	1.0106	1.0143
46	4082.81	1.0175	1.0199	504.843	505.103	1.0267	1.0272	1.0266	235.903	236.301	1.0256	1.0274	1.0259
47	1822.73	0.9790	0.9819	220.825	220.584	0.9775	0.9765	0.9803	45.586	45.501	0.9742	0.9724	0.9794
48	2260.18	0.9849	0.9864	197.866	197.940	0.9780	0.9783	0.9796	93.644	93.229	0.9613	0.9571	0.9649
49	1883.85	0.9796	0.9819	150.123	150.198	0.9808	0.9813	0.9835	70.436	70.412	0.9583	0.9580	0.9620
50	2254.25	0.9823	0.9844	201.267	201.221	0.9948	0.9945	0.9968	93.847	94.371	0.9634	0.9688	0.9699
51	3046.05	0.9831	0.9854	319.428	319.325	0.9755	0.9752	0.9777	150.194	150.103	0.9708	0.9702	0.9757
52	1899.59	0.9878	0.9903	151.324	151.180	0.9887	0.9873	0.9913	71.390	70.838	0.9713	0.9638	0.9715
53	4706.21	0.9900	0.9910	656.426	656.339	0.9920	0.9919	0.9943	265.070	264.162	0.9684	0.9651	0.9643
54	3928.26	0.9790	0.9819	486.010	486.293	0.9884	0.9890	0.9904	225.894	224.608	0.9821	0.9765	0.9815
55	4486.75	1.0122	1.0128	585.953	586.523	1.0098	1.0108	1.0135	254.166	252.691	0.9949	0.9892	0.9887
56	4099.45	1.0216	1.0241	109.044	109.216	1.0352	1.0356	1.0338	234.933	235.337	1.0214	1.0232	1.0205
57	4683.00	0.9851	0.9869	652.751	652.956	0.9865	0.9868	0.9889	266.233	266.258	0.9727	0.9727	0.9725
58	4950.93	0.9744	0.9764	730.634	730.795	0.9759	0.9761	0.9816	272.913	272.217	0.9260	0.9237	0.9368
59	4984.87	0.9811	0.9836	741.750	741.632	0.9908	0.9906	0.9912	285.144	282.820	0.9675	0.9596	0.9692
60	6298.01	0.9999	1.0019	1162.026	1161.954	1.0019	1.0018	1.0075	361.939	360.908	1.0069	1.0040	1.0038
61	6781.49	0.9877	0.9888	1400.460	1400.278	0.9825	0.9824	0.9851	384.915	384.053	0.9624	0.9603	0.9636
62	7606.15	0.9687	0.9727	1887.790	1881.690	0.9786	0.9755	0.9775	419.088	419.233	0.9565	0.9605	0.9605
63	5088.08	0.9802	0.9853	1233.135	1237.342	0.9787	0.9820	0.9822	175.672	175.917	0.9494	0.9507	0.9531
64	4433.78	0.9863	0.9908	984.630	985.249	0.9842	0.9848	0.9867	144.483	146.103	0.9496	0.9603	0.9628
65	2146.36	0.9930	0.9980	289.883	290.831	1.0014	1.0047	1.0071	56.916	56.824	0.9876	0.9860	0.9952
66	1885.18	1.0125	1.0147	229.210	228.839	1.0146	1.0130	1.0177	47.057	46.852	1.0057	1.0013	1.0094
67	2458.62	0.9832	0.9895	361.152	360.974	0.9857	0.9852	0.9910	69.876	69.682	0.9721	0.9694	0.9791
68	1355.91	0.9865	0.9911	132.981	133.062	1.0016	1.0022	1.0032	28.117	28.041	0.9992	0.9965	0.9987
69	1388.97	1.0105	1.0126	135.546	135.504	1.0210	1.0206	1.0215	28.947	28.989	1.0288	1.0302	1.0295
70	713.95	1.0048	1.0061	44.776	44.770	0.9936	0.9935	0.9970	9.795	9.739	0.9786	0.9730	0.9850
71	884.04	1.0474	1.0470	63.408	63.460	1.0517	1.0525	1.0511	13.855	14.009	1.0500	1.0617	1.0598
72	2434.25	0.9735	0.9793	358.273	358.276	0.9778	0.9778	0.9812	67.473	67.383	0.9387	0.9375	0.9476
73	3732.37	1.0042	1.0084	683.117	684.285	1.0210	1.0227	1.0221	317.129	318.232	0.9937	0.9972	0.9948
74	3383.80	1.0063	1.0121	679.231	678.986	1.0152	1.0148	1.0168	318.845	316.364	0.9991	0.9913	0.9932
75	5655.26												

Profile Nr.	Pure Compression			Bending strong axis					Bending weak axis				
	N_real [kN]	N_real / N_nom [-]	A_real / A_nom [-]	My_real_pos [kNm]	My_real_neg [kNm]	My_real_pos / My_nom [-]	My_real_neg / My_nom [-]	Wpl_y_real / Wpl_y_nom [-]	Mz_real_pos [kNm]	Mz_real_neg [kNm]	Mz_real_pos / Mz_nom [-]	Mz_real_neg / Mz_nom [-]	Wpl_z_real / Wpl_z_nom [-]
101	2794.05	0.9913	0.9931	227.592	227.995	0.9859	0.9877	0.9883	111.542	110.638	0.9697	0.9618	0.9748
102	3205.95	0.9764	0.9809	292.070	291.153	0.9846	0.9815	0.9839	136.151	139.500	0.9284	0.9513	0.9411
103	3831.23	1.0033	1.0042	377.709	378.005	0.9999	1.0007	0.9970	184.875	185.806	0.9935	0.9985	0.9990
104	3844.58	1.0068	1.0086	380.058	380.028	1.0061	1.0060	1.0065	185.213	186.718	0.9953	1.0034	1.0026
105	5363.07	1.0024	1.0084	671.315	671.712	1.0034	1.0039	1.0061	315.890	315.540	0.9898	0.9887	0.9920
106	3408.06	0.9832	0.9862	388.916	388.829	0.9832	0.9830	0.9890	174.347	175.708	0.9387	0.9461	0.9485
107	4219.66	1.0516	1.0540	522.125	521.996	1.0618	1.0616	1.0627	243.396	241.444	1.0582	1.0497	1.0521
108	4734.05	0.9959	0.9986	666.810	666.669	1.0077	1.0075	1.0106	276.483	275.967	1.0101	1.0082	1.0070
109	7580.95	1.0239	1.0228	1'698.342	1'698.865	1.0182	1.0185	1.0191	423.346	423.355	1.0097	1.0097	1.0118
110	5722.56	0.9909	0.9917	762.119	761.751	0.9880	0.9875	0.9910	331.662	335.200	0.9494	0.9595	0.9599
111	7718.02	0.9959	0.9963	1'429.065	1'429.219	0.9888	0.9889	0.9894	445.729	446.860	0.9724	0.9749	0.9769
112	4014.37	1.0004	1.0022	496.825	496.817	1.0104	1.0104	1.0121	228.864	228.961	0.9950	0.9955	0.9978
113	5056.55	0.9741	0.9809	1'238.380	1'237.008	0.9828	0.9817	0.9851	177.199	178.126	0.9577	0.9627	0.9628
114	4545.49	1.0112	1.0107	1'016.033	1'017.694	1.0156	1.0173	1.0190	154.466	155.535	1.0152	1.0223	1.0191
115	3979.35	1.0261	1.0235	812.639	807.941	1.0328	1.0268	1.0300	132.434	132.226	1.0422	1.0405	1.0393
116	3929.01	1.0131	1.0137	806.703	805.559	1.0252	1.0238	1.0255	129.637	129.506	1.0202	1.0191	1.0191
117	3933.29	1.0142	1.0127	794.256	794.645	1.0094	1.0099	1.0118	125.725	125.979	0.9894	0.9914	0.9912
118	3291.82	0.9851	0.9859	595.840	596.426	0.9746	0.9756	0.9754	100.041	100.203	0.9595	0.9610	0.9663
119	3218.89	0.9632	0.9683	591.119	592.622	0.9669	0.9694	0.9696	99.131	99.513	0.9508	0.9544	0.9598
120	2814.05	0.9740	0.9804	461.648	461.857	0.9822	0.9822	0.9869	82.530	83.300	0.9569	0.9659	0.9704
121	2525.87	1.0101	1.0109	369.594	369.411	1.0087	1.0082	1.0106	70.109	70.406	0.9754	0.9795	0.9830
122	2541.30	1.0163	1.0160	372.666	372.649	1.0171	1.0171	1.0205	72.545	72.679	1.0093	1.0111	1.0111
123	2155.02	0.9970	1.0005	284.995	285.263	0.9845	0.9854	0.9911	54.626	54.843	0.9479	0.9516	0.9626
124	2158.86	0.9988	1.0009	284.797	284.549	0.9838	0.9830	0.9883	55.358	55.566	0.9605	0.9642	0.9714
125	1847.64	0.9924	0.9960	225.373	225.197	0.9977	0.9969	1.0002	46.948	47.229	1.0033	1.0093	1.0092
126	3997.49	0.9962	0.9988	488.475	488.804	0.9934	0.9941	0.9976	226.986	226.459	0.9869	0.9846	0.9881
127	4014.05	1.0004	1.0032	491.697	491.930	1.0000	1.0004	1.0049	230.037	228.471	1.0001	0.9933	0.9990
128	4730.34	0.9951	0.9965	653.848	654.487	0.9881	0.9891	0.9943	267.702	266.288	0.9780	0.9728	0.9728
129	4727.26	0.9944	0.9965	664.195	664.414	1.0038	1.0041	1.0051	273.905	273.150	1.0007	0.9979	0.9971
130	4727.60	0.9945	0.9967	663.926	664.116	1.0034	1.0037	1.0051	273.980	272.838	1.0010	0.9968	0.9955
131	5125.29	1.0087	1.0098	751.614	751.767	1.0039	1.0041	1.0055	287.040	286.305	0.9740	0.9715	0.9792
132	5647.29	1.0001	1.0021	923.977	923.977	1.0027	1.0027	1.0032	322.249	322.666	1.0052	1.0065	1.0093
133	5591.37	0.9902	0.9919	908.608	908.636	0.9860	0.9860	0.9915	307.578	305.766	0.9595	0.9538	0.9667
134	5158.87	1.0154	1.0165	761.878	761.295	1.0176	1.0169	1.0199	297.440	296.363	1.0093	1.0056	1.0143
135	5791.08	1.0027	1.0052	781.932	781.313	1.0137	1.0129	1.0143	354.021	350.772	1.0134	1.0041	1.0109
136	7657.22	0.9752	0.9775	1'889.444	1'893.218	0.9795	0.9814	0.9831	417.752	416.507	0.9534	0.9506	0.9518
137	6309.31	1.0017	1.0023	1'155.565	1'155.943	0.9963	0.9967	0.9982	354.231	353.828	0.9855	0.9843	0.9860
138	6769.98	0.9598	0.9633	1'368.657	1'368.673	0.9602	0.9602	0.9623	373.764	375.305	0.9346	0.9384	0.9419
139	6235.37	0.9900	0.9906	1'137.145	1'137.295	0.9805	0.9806	0.9826	337.972	338.651	0.9402	0.9421	0.9497
140	7026.97	1.0101	1.0104	1'436.714	1'436.790	1.0080	1.0080	1.0104	400.249	402.104	1.0008	1.0054	1.0014
141	7211.86	0.9741	0.9778	1'632.603	1'632.439	0.9787	0.9786	0.9823	403.313	401.543	0.9619	0.9577	0.9667
142	4035.86	1.0058	1.0082	499.379	499.663	1.0162	1.0162	1.0193	233.966	233.234	1.0172	1.0140	1.0163
143	4659.63	0.9802	0.9820	648.702	648.806	0.9804	0.9805	0.9835	264.597	264.824	0.9667	0.9675	0.9649
144	5146.65	1.0130	1.0157	770.913	771.135	1.0297	1.0300	1.0295	304.313	299.414	1.0326	1.0160	1.0274
145	5170.47	0.9664	0.9734	653.648	653.900	0.9773	0.9793	0.9793	304.119	302.854	0.9529	0.9490	0.9547
146	5213.72	0.9745	0.9820	659.177	659.452	0.9852	0.9856	0.9847	302.564	302.949	0.9481	0.9493	0.9523
147	6037.93	0.9885	0.9914	858.173	857.322	0.9900	0.9890	0.9925	367.451	361.218	0.9903	0.9735	0.9908
148	9452.74	0.9960	0.9963	2'340.643	2'340.311	1.0008	1.0007	1.0008	522.638	525.824	0.9765	0.9825	0.9777
149	9291.39	0.9790	0.9802	2'296.799	2'294.998	0.9821	0.9813	0.9836	511.526	515.256	0.9558	0.9627	0.9633
150	9336.46	0.9837	0.9859	2'324.001	2'322.757	0.9937	0.9932	0.9945	521.267	520.566	0.9740	0.9727	0.9705
151	8750.14	0.9749	0.9769	1'995.507	1'995.233	0.9807	0.9806	0.9820	494.993	497.465	0.9592	0.9640	0.9619
152	8292.00	0.9800	0.9818	1'735.582	1'733.839	0.9907	0.9897	0.9928	479.695	482.698	0.9648	0.9709	0.9678
153	8314.16	0.9826	0.9841	1'727.528	1'727.931	0.9864	0.9864	0.9887	479.208	480.328	0.9638	0.9661	0.9678
154	7653.96	0.9876	0.9891	1'436.659	1'436.833	0.9941	0.9942	0.9969	446.415	446.525	0.9739	0.9741	0.9769
155	7400.51	0.9549	0.9570	1'381.294	1'381.479	0.9558	0.9559	0.9617	429.140	429.776	0.9362	0.9376	0.9435
156	6430.70	0.9971	0.9989	969.723	970.217	1.0022	1.0022	1.0026	382.843	380.088	0.9793	0.9723	0.9782
157	6480.52	1.0048	1.0060	974.484	975.184	1.0072	1.0079	1.0101	378.475	374.929	0.9681	0.9591	0.9782
158	6148.17	1.0065	1.0082	878.434	878.018	1.0134	1.0129	1.0132	373.324	369.099	1.0061	0.9947	1.0036
159	5402.42	1.0098	1.0118	678.918	678.923	1.0147	1.0147	1.0168	321.050	315.547	1.0060	0.9888	0.9981
160	5285.15	0.9879	0.9893	665.397	666.069	0.9945	0.9955	0.9954	303.495	304.525	0.9510	0.9542	0.9589
161	5364.82	1.0027	1.0044	667.854	667.979	0.9984	0.9984	1.0007	316.484	321.910	1.0087	1.0087	0.9989
162	3520.87	1.0157	1.0146	396.983	397.079	1.0036	1.0038	1.0070	183.125	182.388	0.9860	0.9820	0.9860
163	2223.66	0.9690	0.9703	196.581	196.521	0.9716	0.9713	0.9709	86.889	86.490	0.8920	0.8879	0.8943
164	1188.95	1.0143	1.0151	105.914	106.028	1.0262	1.0273	1.0251	22.511	22.438	1.0181	1.0148	1.0170
165	4664.86	0.9893	0.9965	550.975	550.691	1.0032	1.0027	1.0036	263.690	261.354	0.9986	0.9897	0.9962
166	3209.46	0.9775	0.9873	299.343	299.037	1.0091	1.0081	1.0079	139.874	139.593	0.9538	0.9519	0.9497
167	4144.00	0.9724	0.9762	454.803	455.151	0.9891	0.9898	0.9899	212.658	214.215	0.9504	0.9574	0.9625
168	3163.87	1.0211	1.0229	336.910	336.926	1.0289	1.0289	1.0302	158.188	158.742	1.0225	1.0261	1.0244
169	3509.80	1.0125	1.0141	403.222	403.262	1.0193	1.0194	1.0250	184.723	185.546	0.9946	0.9990	0.9987
170	3658.33	0.9580	0.9656	367.645	367.645	0.9733	0.9733	0.9780	173.210	171.134	0.9308	0.9197	0.9316
171	4011.28	0.9997	1.0015	496.450	496.483	1.0096	1.0097	1.0121	229.601	229.464	0.9982	0.9977	1.0002
172	5094.91	0.9815	0.9874	1'246.983	1'243.943	0.9896	0.9872	0.9908	179.385	180.634	0.9695	0.9762	0.9748
173	4549.90	1.0122	1.0116	1'017.459	1'017.316	1.0170	1.0169	1.0190	154.769	155.952	1.0172	1.0250	1.0214
174	3993.09	1.0297	1.026										

Profile Nr.	Pure Compression			Bending strong axis						Bending weak axis					
	N_real [kN]	N_real / N_nom [-]	A_real / A_nom [-]	My_real_pos [kNm]	My_real_neg [kNm]	My_real_pos / My_nom [-]	My_real_neg / My_nom [-]	Wpl_y_real / Wpl_y_nom [-]	Mz_real_pos [kNm]	Mz_real_neg [kNm]	Mz_real_pos / Mz_nom [-]	Mz_real_neg / Mz_nom [-]	Wpl_z_real / Wpl_z_nom [-]		
201	7748.15	0.9998	1.0005	1'443.098	1'442.407	0.9985	0.9981	1.0019	447.589	448.181	0.9765	0.9778	0.9853		
202	7389.83	0.9535	0.9557	1'380.790	1'380.782	0.9554	0.9554	0.9592	428.469	429.863	0.9348	0.9378	0.9435		
203	6390.02	0.9908	0.9926	960.411	960.691	0.9926	0.9929	0.9952	386.794	382.585	0.9894	0.9787	0.9879		
204	7103.22	1.0066	1.0073	1'170.635	1'170.354	1.0003	1.0000	1.0026	413.379	411.651	0.9916	0.9875	0.9873		
205	6417.99	0.9951	0.9968	963.142	963.156	0.9954	0.9954	0.9989	375.444	371.188	0.9604	0.9495	0.9683		
206	6055.21	0.9913	0.9936	864.188	863.924	0.9970	0.9967	1.0008	368.682	363.977	0.9936	0.9809	0.9924		
207	5628.48	0.9746	0.9774	756.269	756.517	0.9804	0.9808	0.9817	335.075	328.778	0.9592	0.9411	0.9587		
208	4498.70	1.0008	1.0035	1'007.969	1'004.324	1.0075	1.0039	1.0083	150.897	150.010	0.9918	0.9859	0.9918		
209	2748.28	1.0020	1.0047	266.071	266.225	1.0033	1.0039	1.0055	126.870	126.707	1.0014	1.0002	1.0020		
210	2699.17	0.9841	0.9868	261.455	261.556	0.9859	0.9863	0.9877	124.304	124.156	0.9812	0.9800	0.9821		
211	1377.17	1.0019	1.0039	133.472	133.361	1.0053	1.0045	1.0072	28.675	28.559	1.0191	1.0150	1.0172		
212	4172.82	0.9792	0.9877	454.287	455.034	0.9880	0.9896	0.9899	215.896	216.313	0.9649	0.9668	0.9740		
213	4245.36	0.9962	1.0009	462.014	462.376	1.0048	1.0055	1.0055	221.687	223.800	0.9908	1.0002	1.0002		
214	3220.60	0.9809	0.9912	293.918	294.827	0.9908	0.9939	0.9916	140.050	140.955	0.9550	0.9612	0.9599		
215	871.23	1.0322	1.0325	62.423	62.327	1.0337	1.0330	1.0330	13.894	13.921	1.0530	1.0550	1.0525		
216	868.78	1.0293	1.0294	61.177	62.169	1.0309	1.0311	1.0297	13.671	13.690	1.0361	1.0375	1.0357		
217	2745.16	1.0041	1.0063	270.234	270.386	1.0190	1.0196	1.0207	127.580	126.440	1.0070	0.9980	1.0021		
218	3810.54	0.9978	1.0002	379.195	379.717	1.0038	1.0052	1.0065	185.460	183.495	0.9967	0.9861	0.9946		
219	3814.35	0.9988	0.9998	377.954	378.644	1.0006	1.0024	1.0065	183.789	184.166	0.9877	0.9897	0.9909		
220	2736.35	0.9976	0.9994	267.122	267.093	1.0073	1.0071	1.0088	126.837	126.820	1.0012	1.0010	1.0021		
221	1'007.12	1.0033	1.0053	80.313	80.284	1.0027	1.0024	1.0063	16.436	16.469	0.9653	0.9672	0.9750		
222	1'154.80	0.9851	0.9887	103.763	103.774	1.0053	1.0055	1.0070	21.568	21.435	0.9754	0.9694	0.9765		
223	1'898.17	0.9871	0.9891	152.436	152.403	0.9959	0.9957	0.9977	70.941	71.038	0.9652	0.9665	0.9701		
224	1'188.78	1.0141	1.0139	105.425	105.318	1.0215	1.0204	1.0184	22.732	22.723	1.0281	1.0277	1.0257		
225	1'189.99	1.0152	1.0146	105.536	105.511	1.0225	1.0223	1.0201	22.681	22.699	1.0258	1.0266	1.0215		
226	3'817.84	0.9998	1.0080	383.087	383.624	1.0141	1.0156	1.0160	186.779	187.063	1.0037	1.0053	1.0081		
227	3'307.02	1.0072	1.0160	298.382	298.509	1.0059	1.0063	1.0059	144.457	145.127	0.9851	0.9896	0.9860		
228	3'254.03	0.9911	0.9944	295.108	294.702	0.9948	0.9935	0.9956	144.692	141.912	0.9867	0.9875	0.9885		
229	1'888.60	0.9821	0.9830	151.841	151.587	0.9920	0.9904	0.9923	69.989	70.156	0.9522	0.9545	0.9596		
230	1'393.85	1.0141	1.0173	137.507	137.498	1.0357	1.0357	1.0359	29.376	29.359	1.0440	1.0434	1.0421		
231	1'387.63	1.0096	1.0130	136.785	136.664	1.0303	1.0294	1.0306	29.285	29.215	1.0407	1.0383	1.0394		
232	1'953.54	1.0159	1.0182	155.208	155.277	1.0145	1.0145	1.0161	75.668	74.764	1.0295	1.0172	1.0227		
233	1'945.62	1.0118	1.0137	154.605	154.759	1.0101	1.0111	1.0122	75.255	74.624	1.0239	1.0153	1.0191		
234	1'859.88	0.9672	0.9705	148.252	148.364	0.9686	0.9693	0.9715	67.328	67.646	0.9160	0.9204	0.9257		
235	1'513.56	0.9450	0.9524	165.103	165.132	0.9455	0.9456	0.9516	32.557	32.254	0.8917	0.8834	0.9038		
236	1'546.38	0.9655	0.9705	167.669	167.705	0.9602	0.9604	0.9657	32.562	32.378	0.8918	0.8868	0.9049		
237	1'648.34	1.0292	1.0297	181.178	181.402	1.0375	1.0388	1.0386	37.910	37.951	1.0383	1.0394	1.0355		
238	1'624.57	1.0144	1.0157	178.227	178.290	1.0206	1.0210	1.0219	37.148	37.226	1.0174	1.0196	1.0169		
239	2'738.94	0.9718	0.9754	226.823	227.379	0.9826	0.9850	0.9854	109.580	108.549	0.9526	0.9437	0.9548		
240	3'295.10	0.9860	0.9903	306.210	306.904	0.9916	0.9927	0.9931	100.834	100.835	0.9671	0.9671	0.9729		
241	2'803.70	0.9704	0.9758	260.235	260.044	0.9788	0.9784	0.9792	83.764	83.869	0.9712	0.9725	0.9742		
242	9'330.48	0.9831	0.9835	2'285.536	2'286.289	0.9773	0.9776	0.9790	512.427	514.642	0.9575	0.9616	0.9633		
243	9'444.11	0.9951	0.9949	2'306.234	2'305.123	0.9861	0.9857	0.9883	517.942	520.233	0.9678	0.9720	0.9705		
244	9'418.01	0.9923	0.9921	2'295.874	2'296.111	0.9817	0.9818	0.9836	514.940	518.062	0.9622	0.9680	0.9633		
245	4'768.91	1.0032	1.0053	669.900	670.224	1.0124	1.0129	1.0160	277.039	276.691	1.0121	1.0109	1.0075		
246	2'886.73	0.9992	1.0017	472.720	473.398	1.0053	1.0068	1.0098	86.363	86.161	1.0014	0.9990	1.0027		
247	6'084.19	0.9961	0.9981	866.663	865.984	0.9998	0.9990	1.0008	361.271	358.749	0.9736	0.9668	0.9809		
248	4'300.00	0.9701	0.9719	558.698	558.960	0.9628	0.9633	0.9643	240.452	238.541	0.9412	0.9338	0.9392		
249	5'311.13	0.9927	0.9940	658.000	658.197	0.9835	0.9837	0.9847	315.836	313.264	0.9897	0.9816	0.9862		
250	4'093.37	1.0201	1.0221	502.866	503.000	1.0227	1.0229	1.0266	237.100	235.798	1.0309	1.0252	1.0278		
251	3'476.17	1.0028	1.0050	394.994	395.299	0.9985	0.9993	0.9980	181.345	180.124	0.9764	0.9698	0.9768		
252	4'208.89	0.9877	0.9918	459.246	459.661	0.9877	0.9897	0.9977	222.974	222.375	0.9965	0.9939	1.0015		
253	3'269.09	0.9721	0.9741	346.143	346.335	0.9801	0.9801	0.9802	177.134	177.886	0.9647	0.9564	0.9685		
254	6'354.23	0.9853	0.9872	959.891	959.080	0.9921	0.9912	0.9952	381.561	376.777	0.9760	0.9638	0.9782		
255	7'610.36	0.9820	0.9833	1'421.688	1'424.405	0.9837	0.9856	0.9843	442.094	445.771	0.9645	0.9725	0.9686		
256	4'409.54	0.9948	0.9962	572.240	571.905	0.9862	0.9856	0.9889	248.209	249.211	0.9716	0.9755	0.9710		
257	5'067.91	0.9975	0.9986	747.505	747.709	0.9987	0.9987	1.0007	287.304	284.976	0.9749	0.9795	0.9795		
258	3'118.99	1.0066	1.0090	328.773	328.773	1.0040	1.0040	1.0055	155.822	156.137	1.0072	1.0092	1.0089		
259	3'335.36	0.9981	1.0000	611.007	610.752	0.9995	0.9990	0.9989	101.559	101.602	0.9740	0.9745	0.9795		
260	1'846.43	0.9917	0.9957	224.489	224.728	0.9937	0.9948	0.9985	46.538	46.304	0.9946	0.9896	0.9997		
261	6'910.32	0.9933	0.9950	1'416.911	1'416.927	0.9941	0.9941	0.9952	389.041	389.330	0.9728	0.9735	0.9731		
262	1'809.26	0.9718	0.9773	221.745	221.394	0.9816	0.9800	0.9839	45.147	45.215	0.9648	0.9663	0.9711		
263	1'906.15	1.0238	1.0232	231.988	231.622	1.0269	1.0253	1.0273	48.436	48.257	1.0351	1.0313	1.0336		
264	4'408.98	0.9947	0.9966	578.554	578.642	0.9970	0.9972	1.0012	252.067	251.516	0.9867	0.9846	0.9832		
265	5'413.83	1.0119	1.0178	688.427	688.308	1.0289	1.0289	1.0328	325.102	324.300	1.0187	1.0187	1.0160		
266	3'948.18	0.9839	0.9867	477.242	477.138	0.9706	0.9703	0.9759	226.342	224.952	0.9841	0.9780	0.9845		
267	2'201.93	1.0187	1.0180	293.022	293.179	1.0122	1.0128	1.0146	58.786	58.873	1.0200	1.0215	1.0239		
268	6'013.73	0.9845	0.9880	860.065	861.853	0.9922	0.9943	0.9925	367.032	366.176	0.9891	0.9868	0.9920		
269	5'237.69	0.9790	0.9827	661.740	661.362	0.9890	0.9885	0.9900	309.861	312.202	0.9709	0.9783	0.9757		
270	2'456.34	0.9823	0.9879	359.427	360.294	0.9810	0.9833	0.9812	68.681	68.922	0.9550	0.9589	0.9658		
271	5'093.26	0.9812	0.9868	1'240.228	1'240.527	0.9843	0.9845	0.9879	177.457	176.831	0.9591	0.9557	0.9596		
272	745.48	1.0492	1.0496	46.399	46.341	1.0296	1.0283	1.0320	10.290	10.184	1.0281	1.0174	1.0328		
273	868.74	1.0292	1.0291	61.734	61.805	1.0239	1.0231	1.0248	13.264	13.450	1.0052	1.0193	1.0198		
274	1'017.06	1.0132	1.0130	80.436	80.384	1.0043									

Profile Nr.	Pure Compression			Bending strong axis						Bending weak axis					
	N_real [kN]	N_real / N_nom [-]	A_real / A_nom [-]	My_real_pos [kNm]	My_real_neg [kNm]	My_real_pos / My_nom [-]	My_real_neg / My_nom [-]	Wpl_y_real / Wpl_y_nom [-]	Mz_real_pos [kNm]	Mz_real_neg [kNm]	Mz_real_pos / Mz_nom [-]	Mz_real_neg / Mz_nom [-]	Wpl_z_real / Wpl_z_nom [-]		
301	7709.81	0.9819	0.9837	1'898.240	1'897.880	0.9840	0.9838	0.9850	418.731	420.811	0.9557	0.9604	0.9605		
302	5'668.45	1.0039	1.0055	926.147	926.433	1.0050	1.0053	1.0071	323.538	322.288	1.0092	1.0053	1.0079		
303	4'963.66	0.9769	0.9790	729.203	729.236	0.9740	0.9768	0.9768	274.562	273.846	0.9316	0.9292	0.9440		
304	5'055.75	0.9951	0.9970	742.843	743.159	0.9922	0.9926	0.9959	285.546	284.434	0.9689	0.9651	0.9754		
305	4'015.61	1.0007	1.0031	492.627	492.304	1.0018	1.0012	1.0049	228.868	229.251	0.9951	0.9967	0.9985		
306	3'223.69	0.9818	0.9847	291.473	291.534	0.9826	0.9828	0.9835	140.801	140.553	0.9601	0.9584	0.9611		
307	3'706.30	0.9705	0.9797	372.505	372.653	0.9861	0.9865	0.9875	180.504	179.682	0.9700	0.9656	0.9721		
308	4'115.95	0.9659	0.9738	455.561	455.289	0.9907	0.9901	0.9899	213.283	213.448	0.9532	0.9540	0.9652		
309	4'646.18	0.9853	0.9922	545.263	544.869	0.9928	0.9921	0.9971	259.932	260.248	0.9844	0.9856	0.9897		
310	4'745.67	1.0064	1.0073	550.919	551.083	1.0031	1.0034	1.0036	258.795	255.857	0.9800	0.9689	0.9782		
311	6'187.26	1.0129	1.0143	883.498	883.927	1.0192	1.0197	1.0215	371.288	369.271	1.0006	0.9952	1.0033		
312	6'136.73	1.0047	1.0065	871.548	871.393	1.0055	1.0053	1.0091	368.216	362.610	0.9923	0.9772	0.9923		
313	5'754.14	0.9963	0.9981	771.694	771.376	1.0004	1.0000	1.0004	341.988	338.541	0.9790	0.9691	0.9792		
314	5'800.91	1.0044	1.0070	785.186	785.505	1.0179	1.0183	1.0190	350.191	347.565	1.0024	0.9949	1.0022		
315	6'325.33	0.9808	0.9830	953.664	953.305	0.9856	0.9853	0.9877	380.966	377.230	0.9745	0.9650	0.9782		
316	6'397.88	0.9920	0.9936	958.465	959.418	0.9906	0.9916	0.9952	372.412	368.441	0.9526	0.9425	0.9630		
317	6'462.89	1.0021	1.0040	979.331	980.276	1.0122	1.0131	1.0138	386.106	383.954	0.9877	0.9822	0.9879		
318	6'287.91	0.9750	0.9774	942.593	942.893	0.9742	0.9745	0.9765	372.174	365.317	0.9520	0.9345	0.9551		
319	6'291.32	0.9755	0.9780	940.656	940.578	0.9722	0.9721	0.9765	369.618	364.214	0.9455	0.9317	0.9527		
320	8'463.65	1.0003	1.0012	1'747.629	1'747.626	0.9976	0.9976	0.9991	488.432	489.842	0.9824	0.9852	0.9832		
321	7'430.77	0.9588	0.9615	1'398.795	1'398.477	0.9679	0.9677	0.9718	434.675	435.835	0.9483	0.9508	0.9602		
322	9'524.28	1.0035	1.0038	2'353.394	2'353.414	1.0063	1.0063	1.0070	527.705	527.789	0.9860	0.9862	0.9849		
323	9'451.31	0.9958	0.9970	2'339.363	2'340.929	1.0003	1.0010	1.0023	530.766	533.477	0.9917	0.9968	0.9921		
324	8'315.48	0.9828	0.9848	1'725.633	1'730.363	0.9873	0.9878	0.9907	480.329	482.459	0.9661	0.9704	0.9755		
325	6'360.87	0.9863	0.9884	956.508	956.929	0.9886	0.9890	0.9877	381.051	378.155	0.9747	0.9673	0.9782		
326	6'012.06	0.9843	0.9864	856.755	857.805	0.9884	0.9896	0.9925	359.021	353.221	0.9675	0.9519	0.9703		
327	3'367.65	1.0078	1.0106	625.456	624.855	1.0231	1.0221	1.0225	107.514	107.477	1.0312	1.0308	1.0315		
328	2'872.40	0.9942	0.9964	466.026	465.122	0.9911	0.9922	0.9945	84.764	84.351	0.9828	0.9780	0.9875		
329	1'601.74	1.0001	1.0015	174.836	175.017	1.0012	1.0022	1.0035	36.272	36.293	0.9934	0.9940	0.9962		
330	7'658.17	0.9882	0.9892	1'419.168	1'422.162	0.9820	0.9840	0.9868	439.384	438.837	0.9586	0.9574	0.9602		
331	4'743.63	0.9979	1.0002	666.282	665.764	1.0069	1.0061	1.0106	275.634	274.234	1.0070	1.0019	1.0023		
332	5'183.68	0.9689	0.9718	646.178	646.721	0.9658	0.9666	0.9686	302.882	306.022	0.9491	0.9589	0.9600		
333	3'957.40	0.9862	0.9874	487.150	486.810	0.9907	0.9900	0.9904	220.965	220.491	0.9607	0.9586	0.9641		
334	6'308.93	0.9782	0.9809	949.535	949.138	0.9814	0.9810	0.9840	374.018	369.729	0.9567	0.9458	0.9618		
335	3'851.95	0.9600	0.9627	472.471	473.133	0.9609	0.9622	0.9615	215.670	215.141	0.9377	0.9354	0.9411		
336	5'151.59	1.0139	1.0159	758.962	759.166	1.0137	1.0140	1.0151	296.474	293.552	1.0060	0.9961	1.0017		
337	4'963.42	0.9769	0.9782	731.177	731.153	0.9766	0.9766	0.9816	279.511	278.864	0.9484	0.9462	0.9545		
338	5'171.48	1.0178	1.0198	765.623	765.395	1.0223	1.0223	1.0247	290.516	288.750	0.9858	0.9798	0.9908		
339	5'570.28	0.9865	0.9885	907.416	906.846	0.9847	0.9841	0.9876	305.036	305.663	0.9515	0.9535	0.9610		
340	6'057.16	0.9916	0.9942	859.217	858.189	0.9912	0.9900	0.9925	357.994	358.789	0.9648	0.9669	0.9786		
341	4'958.67	0.9760	0.9782	729.641	729.984	0.9746	0.9750	0.9768	281.979	278.595	0.9568	0.9453	0.9554		
342	3'073.58	0.9920	0.9945	325.694	325.771	0.9946	0.9949	0.9971	153.273	152.701	0.9907	0.9870	0.9910		
343	6'209.35	1.0166	1.0185	884.989	885.597	1.0210	1.0217	1.0215	374.358	368.960	1.0089	0.9943	1.0067		
344	5'833.69	1.0101	1.0106	783.061	782.221	1.0152	1.0141	1.0143	349.828	350.163	1.0014	1.0024	1.0035		
345	4'987.68	0.9817	0.9831	735.719	735.943	0.9827	0.9830	0.9864	281.704	281.539	0.9529	0.9553	0.9620		
346	7'397.17	0.9991	0.9996	1'661.985	1'661.462	0.9964	0.9960	0.9974	413.155	416.693	0.9854	0.9938	0.9938		
347	3'402.99	0.9817	0.9837	389.309	388.965	0.9842	0.9833	0.9890	178.362	178.301	0.9604	0.9600	0.9656		
348	2'844.84	0.9847	0.9872	459.501	459.482	0.9772	0.9772	0.9792	80.981	80.987	0.9390	0.9390	0.9484		
349	4'553.17	0.9578	0.9595	625.270	624.735	0.9449	0.9441	0.9511	250.884	251.081	0.9166	0.9173	0.9201		
350	846.09	1.0024	1.0031	60.347	60.400	1.0009	1.0018	1.0018	12.955	13.054	0.9958	0.9913	0.9914		
351	1'154.88	0.9852	0.9892	102.780	102.753	0.9958	0.9952	0.9994	22.163	21.997	1.0023	0.9948	1.0115		
352	1'358.01	0.9880	0.9909	130.529	130.093	0.9832	0.9830	0.9868	26.834	26.648	0.9537	0.9470	0.9637		
353	1'390.88	1.0119	1.0137	134.889	134.822	1.0160	1.0155	1.0182	27.773	27.888	0.9870	0.9911	0.9950		
354	1'585.70	0.9901	0.9918	171.457	171.401	0.9818	0.9815	0.9857	34.910	34.673	0.9561	0.9496	0.9634		
355	1'584.23	0.9892	0.9914	170.962	171.001	0.9790	0.9792	0.9835	34.175	33.729	0.9360	0.9238	0.9441		
356	1'005.12	1.0013	1.0025	79.399	79.444	0.9913	0.9919	0.9943	16.497	16.588	0.9688	0.9742	0.9774		
357	2'491.13	0.9962	1.0003	364.263	364.465	0.9942	0.9947	1.0008	70.444	70.951	0.9800	0.9871	0.9942		
358	3'870.77	0.9981	0.9988	784.591	784.673	0.9971	0.9971	0.9981	127.294	126.534	1.0017	0.9957	1.0002		
359	3'879.96	1.0005	1.0043	794.065	796.754	1.0092	1.0126	1.0118	127.603	128.646	1.0042	1.0126	1.0002		
360	3'270.01	0.9785	0.9834	604.792	604.477	0.9893	0.9888	0.9931	102.261	102.627	0.9808	0.9843	0.9867		
361	2'836.04	0.9816	0.9861	463.482	464.390	0.9857	0.9876	0.9869	82.347	83.064	0.9548	0.9631	0.9683		
362	4'469.01	0.9942	0.9969	989.860	991.739	0.9894	0.9913	0.9939	145.734	145.741	0.9578	0.9579	0.9608		
363	5'171.68	0.9963	0.9993	1'260.547	1'260.610	1.0004	1.0005	1.0022	178.315	178.884	0.9637	0.9668	0.9653		
364	3'884.91	1.0018	1.0029	786.726	787.364	0.9999	1.0007	1.0027	124.813	124.900	0.9822	0.9829	0.9851		
365	2'425.26	0.9699	0.9740	351.597	350.640	0.9596	0.9570	0.9628	68.037	67.867	0.9466	0.9442	0.9546		
366	1'534.27	0.9580	0.9645	168.170	168.037	0.9630	0.9623	0.9675	33.541	33.492	0.9186	0.9173	0.9277		
367	2'264.64	0.9868	0.9878	201.424	201.570	0.9955	0.9963	0.9980	94.106	93.940	0.9661	0.9644	0.9689		
368	3'096.92	0.9995	1.0013	325.454	325.556	0.9939	0.9942	0.9959	151.737	152.589	0.9808	0.9863	0.9869		
369	3'102.95	1.0015	1.0042	325.177	325.331	0.9930	0.9935	0.9953	152.948	151.407	0.9886	0.9786	0.9874		
370	3'081.42	0.9945	0.9968	325.513	325.549	0.9941	0.9942	0.9962	152.306	151.670	0.9845	0.9803	0.9849		
371	4'121.20	1.0271	1.0276	505.259	505.456	1.0275	1.0279	1.0266	230.865	229.815	1.0037	0.9992	1.0043		
372	3'640.40	1.0502	1.0505	417.075	417.138	1.0544	1.0545	1.0519	193.300	192.160	1.0408	1.0346	1.0352		
373	4'032.70	1.0050	1.0063	492.885	493.006	1.0024	1.0026	1.0049	223.466	221.804	0.9716	0.9644	0.9707		
374	3'923.13	0.977													

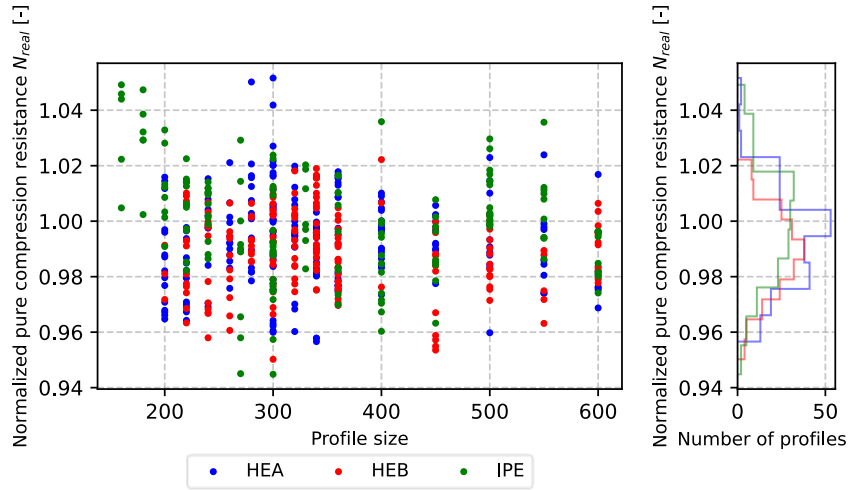
Profile Nr.	Pure Compression			Bending strong axis						Bending weak axis					
	N_real [kN]	N_real / N_nom [-]	A_real / A_nom [-]	My_real_pos [kNm]	My_real_neg [kNm]	My_real_pos / My_nom [-]	My_real_neg / My_nom [-]	Wpl_y_real / Wpl_y_nom [-]	Mz_real_pos [kNm]	Mz_real_neg [kNm]	Mz_real_pos / Mz_nom [-]	Mz_real_neg / Mz_nom [-]	Wpl_z_real / Wpl_z_nom [-]		
401	6'298.85	0.9767	0.9786	937.496	938.509	0.9689	0.9700	0.9728	369.233	364.857	0.9445	0.9333	0.9524		
402	6'028.95	0.9870	0.9892	859.247	859.822	0.9913	0.9919	0.9925	360.226	353.713	0.9708	0.9532	0.9725		
403	5'683.01	0.9840	0.9855	760.282	760.632	0.9861	0.9856	0.9864	335.796	335.707	0.9612	0.9610	0.9695		
404	4'238.55	0.9946	1.0004	467.227	468.711	1.0161	1.0193	1.0211	227.463	224.715	1.0166	1.0043	1.0074		
405	3'691.84	0.9668	0.9753	362.072	362.283	0.9585	0.9591	0.9590	175.493	174.891	0.9431	0.9399	0.9516		
406	3'889.53	1.0029	1.0053	786.031	784.242	0.9990	0.9967	1.0027	124.354	124.128	0.9786	0.9768	0.9840		
407	3'067.56	0.9900	0.9929	322.899	322.840	0.9861	0.9859	0.9886	151.027	151.027	0.9762	0.9762	0.9813		
408	5'639.00	0.9987	1.0006	923.998	924.289	1.0027	1.0030	1.0032	319.016	316.752	0.9951	0.9881	0.9918		
409	7'636.52	0.9854	0.9861	1'413.731	1'414.274	0.9782	0.9786	0.9818	436.843	437.193	0.9530	0.9538	0.9602		
410	6'409.91	0.9939	0.9964	967.432	967.464	0.9999	0.9999	1.0026	383.191	378.252	0.9802	0.9676	0.9782		
411	2'228.02	0.9709	0.9729	197.348	197.237	0.9754	0.9749	0.9773	91.630	91.916	0.9406	0.9436	0.9455		
412	3'861.04	0.9622	0.9648	474.803	475.490	0.9656	0.9670	0.9687	215.758	215.234	0.9381	0.9358	0.9414		
413	4'256.25	0.9602	0.9625	557.700	557.787	0.9611	0.9613	0.9643	237.114	238.435	0.9282	0.9334	0.9317		
414	5'558.25	0.9844	0.9880	906.125	907.073	0.9833	0.9843	0.9876	308.171	309.457	0.9613	0.9653	0.9705		
415	2'844.65	0.9846	0.9874	460.165	459.944	0.9786	0.9782	0.9792	81.089	81.308	0.9402	0.9428	0.9511		
416	6'224.14	1.0190	1.0208	887.107	888.006	1.0234	1.0244	1.0257	376.589	371.578	1.0149	1.0014	1.0120		
417	3'991.89	0.9785	0.9806	387.983	388.010	0.9808	0.9808	0.9800	175.746	175.400	0.9463	0.9444	0.9500		
418	4'954.63	0.9752	0.9769	730.742	730.639	0.9760	0.9759	0.9768	280.476	279.746	0.9517	0.9492	0.9574		
419	4'093.66	0.9606	0.9652	450.960	450.747	0.9807	0.9803	0.9821	209.327	210.881	0.9355	0.9425	0.9498		
420	5'685.73	1.0070	1.0085	929.500	929.885	1.0086	1.0091	1.0110	322.453	321.768	1.0059	1.0037	1.0036		
421	1'903.73	1.0225	1.0224	226.186	226.237	1.0013	1.0015	1.0051	44.808	45.082	0.9576	0.9634	0.9708		
422	4'547.37	0.9566	0.9584	624.101	623.195	0.9432	0.9418	0.9457	250.661	250.484	0.9158	0.9151	0.9196		
423	1'842.19	0.9894	0.9948	223.801	224.397	0.9907	0.9933	0.9983	45.683	45.696	0.9763	0.9766	0.9847		
424	1'364.43	0.9927	0.9942	129.681	129.708	0.9768	0.9770	0.9805	27.086	27.083	0.9626	0.9625	0.9761		
425	1'179.54	1.0063	1.0064	103.134	103.342	0.9993	1.0013	1.0006	21.951	21.918	0.9928	0.9913	0.9956		
426	1'168.34	0.9967	0.9969	102.088	102.256	0.9891	0.9907	0.9911	21.776	21.776	0.9848	0.9848	0.9896		
427	1'036.78	1.0329	1.0321	82.180	81.841	1.0261	1.0218	1.0255	17.218	17.293	1.0112	1.0156	1.0166		
428	726.40	1.0223	1.0232	45.534	45.471	1.0104	1.0090	1.0122	9.941	9.898	0.9932	0.9889	0.9974		
429	4'180.53	1.0418	1.0420	510.174	510.137	1.0375	1.0375	1.0338	236.183	236.038	1.0269	1.0262	1.0263		
430	4'030.86	1.0045	1.0068	492.479	492.428	1.0014	1.0014	1.0049	226.169	224.889	0.9833	0.9778	0.9838		
431	3'947.16	0.9837	0.9849	481.551	481.439	0.9793	0.9791	0.9832	219.235	217.171	0.9532	0.9442	0.9542		
432	5'112.02	0.9848	0.9895	1'248.516	1'248.516	0.9912	0.9909	0.9936	180.028	180.911	0.9729	0.9772	0.9772		
433	3'943.63	1.0169	1.0166	809.454	807.851	1.0287	1.0267	1.0300	129.803	129.277	1.0215	1.0173	1.0192		
434	2'876.40	0.9956	0.9985	470.786	471.342	1.0012	1.0024	1.0022	85.349	85.092	0.9896	0.9866	0.9911		
435	2'541.82	1.0165	1.0162	372.134	371.569	1.0157	1.0141	1.0205	72.508	72.565	1.0088	1.0096	1.0102		
436	1'815.64	0.9752	0.9781	216.600	217.302	0.9588	0.9619	0.9656	42.889	42.740	0.9166	0.9134	0.9285		
437	1'882.87	1.0113	1.0100	223.138	223.942	0.9878	0.9913	0.9937	44.069	43.853	0.9418	0.9372	0.9540		
438	3'896.91	1.0049	1.0024	786.377	784.659	0.9994	0.9972	0.9981	124.664	125.905	0.9810	0.9908	0.9898		
439	4'539.74	1.0099	1.0103	1'018.409	1'017.924	1.0180	1.0175	1.0190	154.851	155.926	1.0178	1.0248	1.0214		
440	2'853.45	0.9876	0.9901	464.722	464.371	0.9883	0.9876	0.9869	84.275	84.467	0.9772	0.9794	0.9828		
441	2'124.28	0.9828	0.9854	280.299	280.492	0.9683	0.9690	0.9731	52.795	52.409	0.9161	0.9094	0.9292		
442	1'844.80	0.9908	0.9923	221.040	220.910	0.9785	0.9779	0.9823	44.428	44.467	0.9495	0.9503	0.9605		
443	1'855.65	0.9967	0.9991	225.255	225.145	0.9971	0.9966	1.0001	47.037	47.082	1.0052	1.0062	1.0081		
444	3'998.09	0.9964	0.9990	488.812	489.278	0.9941	0.9950	0.9976	227.578	225.861	0.9895	0.9820	0.9880		
445	4'022.68	1.0025	1.0050	492.550	492.606	1.0017	1.0018	1.0049	229.622	227.522	0.9983	0.9892	0.9978		
446	5'697.52	1.0090	1.0110	939.135	939.232	1.0191	1.0192	1.0188	328.793	327.706	1.0256	1.0222	1.0215		
447	4'392.10	0.9909	0.9933	583.101	582.851	1.0049	1.0044	1.0073	254.379	254.242	0.9958	0.9952	0.9943		
448	4'744.10	0.9980	0.9998	656.276	656.762	0.9918	0.9925	0.9943	267.971	266.861	0.9790	0.9750	0.9755		
449	4'734.19	0.9959	0.9976	664.271	664.546	1.0039	1.0043	1.0051	273.303	272.805	0.9985	0.9967	0.9966		
450	4'752.14	0.9997	1.0017	659.409	659.267	0.9965	0.9963	0.9997	271.193	271.901	0.9908	0.9934	0.9925		
451	5'039.61	0.9919	0.9941	747.003	746.913	0.9976	0.9976	1.0007	292.881	290.594	0.9938	0.9860	0.9943		
452	5'630.12	0.9971	0.9990	920.960	921.387	0.9994	0.9998	1.0032	319.805	319.917	0.9976	0.9980	1.0017		
453	5'626.36	0.9964	0.9983	918.443	917.743	0.9967	0.9959	0.9993	320.364	321.099	0.9993	1.0016	1.0010		
454	5'496.55	0.9735	0.9759	898.256	898.203	0.9747	0.9747	0.9759	302.823	303.841	0.9446	0.9478	0.9541		
455	5'632.46	0.9975	0.9994	921.524	921.635	1.0001	1.0002	1.0032	319.493	319.805	0.9966	0.9976	1.0006		
456	7'662.58	0.9759	0.9782	1'890.876	1'893.593	0.9802	0.9816	0.9831	418.271	417.080	0.9546	0.9519	0.9518		
457	5'557.39	0.9842	0.9859	901.636	901.592	0.9784	0.9784	0.9837	305.446	305.885	0.9528	0.9542	0.9582		
458	6'334.31	1.0057	1.0066	1'168.345	1'168.836	1.0074	1.0078	1.0106	348.277	348.733	0.9689	0.9702	0.9753		
459	6'878.97	0.9888	0.9895	1'399.464	1'398.308	0.9818	0.9810	0.9826	382.021	386.312	0.9552	0.9659	0.9636		
460	6'892.49	0.9908	0.9917	1'407.064	1'407.924	0.9871	0.9878	0.9902	385.303	384.125	0.9634	0.9605	0.9731		
461	7'259.60	0.9805	0.9839	1'644.864	1'642.734	0.9861	0.9848	0.9888	405.099	406.002	0.9661	0.9683	0.9757		
462	4'077.59	1.0162	1.0208	497.141	498.306	1.0110	1.0114	1.0121	226.981	228.516	0.9869	0.9935	0.9988		
463	4'432.68	1.0000	1.0021	586.475	586.576	1.0107	1.0109	1.0135	256.106	255.720	1.0025	1.0010	0.9989		
464	4'661.03	0.9805	0.9823	650.800	650.634	0.9824	0.9833	0.9835	266.980	265.812	0.9754	0.9711	0.9700		
465	5'124.40	1.0086	1.0115	766.408	766.793	1.0237	1.0242	1.0247	300.928	296.230	1.0211	1.0211	1.0185		
466	3'888.55	1.0027	1.0032	786.916	790.031	1.0001	1.0041	1.0027	126.009	126.596	0.9916	0.9962	0.9955		
467	9'279.77	0.9778	0.9798	2'304.725	2'303.951	0.9855	0.9852	0.9867	521.991	522.756	0.9753	0.9768	0.9777		
468	8'866.23	0.9878	0.9889	2'003.327	2'004.769	0.9845	0.9852	0.9874	499.951	503.951	0.9688	0.9765	0.9768		
469	9'409.77	0.9915	0.9928	2'340.474	2'338.372	1.0008	0.9999	1.0008	522.498	524.506	0.9763	0.9800	0.9777		
470	8'261.13	0.9764	0.9786	1'722.908	1'724.779	0.9835	0.9846	0.9866	491.340	493.758	0.9631	0.9931	0.9910		
471	7'732.52	0.9978	0.9985	1'442.354	1'442.430	0.9980	0.9981	0.9994	446.999	448.169	0.9752	0.9777	0.9853		
472	7'418.37	0.9572	0.9592	1'384.537	1'384.532	0.9580	0.9580	0.9617	430.165	430.470	0.9385	0.9391	0.9435		
473	6'889.23	0.9763	0.9778	1'141.964	1'141.857	0.9758	0.9757	0.9778	390.314	389.502	0.9363	0.9343	0.9511		
474															

Profile Nr.	Pure Compression			Bending strong axis						Bending weak axis					
	N_real [kN]	N_real / N_nom [-]	A_real / A_nom [-]	My_real_pos [kNm]	My_real_neg [kNm]	My_real_pos / My_nom [-]	My_real_neg / My_nom [-]	Wpl_y_real / Wpl_y_nom [-]	Mz_real_pos [kNm]	Mz_real_neg [kNm]	Mz_real_pos / Mz_nom [-]	Mz_real_neg / Mz_nom [-]	Wpl_z_real / Wpl_z_nom [-]		
501	1'031.99	1.0281	1.0285	82.874	82.899	1.0347	1.0350	1.0359	17.658	17.767	1.0370	1.0434	1.0419		
502	2'661.67	0.9704	0.9720	255.465	255.396	0.9633	0.9630	0.9650	116.428	116.098	0.9190	0.9164	0.9233		
503	1'151.40	0.9823	0.9858	103.569	103.563	1.0035	1.0034	1.0043	21.484	21.332	0.9716	0.9647	0.9721		
504	2'308.67	1.0060	1.0076	203.555	203.569	1.0061	1.0061	1.0074	97.235	97.565	0.9982	1.0016	1.0023		
505	1'950.81	1.0145	1.0171	155.542	155.657	1.0162	1.0170	1.0185	75.443	75.422	1.0264	1.0262	1.0247		
506	1'878.43	0.9768	0.9790	151.204	151.243	0.9879	0.9881	0.9897	68.797	68.560	0.9360	0.9328	0.9399		
507	3'692.98	0.9671	0.9693	364.609	364.853	0.9652	0.9659	0.9685	172.882	171.803	0.9291	0.9233	0.9347		
508	3'798.51	0.9947	0.9971	380.645	380.127	1.0077	1.0063	1.0065	183.128	185.506	0.9841	0.9969	0.9938		
509	3'316.57	1.0101	1.0111	301.681	301.615	1.0170	1.0168	1.0170	146.101	147.108	0.9963	1.0031	0.9970		
510	3'260.34	0.9930	0.9958	296.058	296.286	0.9980	0.9988	0.9996	146.307	144.343	0.9977	0.9843	0.9928		
511	3'313.21	1.0091	1.0109	302.793	302.851	1.0207	1.0209	1.0217	149.911	149.208	1.0222	1.0175	1.0180		
512	2'765.03	0.9810	0.9830	225.147	225.699	0.9753	0.9777	0.9782	111.119	111.773	0.9660	0.9717	0.9744		
513	1'383.00	1.0062	1.0099	136.309	136.244	1.0267	1.0262	1.0273	29.173	29.171	1.0368	1.0367	1.0357		
514	1'390.86	1.0119	1.0153	137.022	137.053	1.0321	1.0323	1.0333	29.266	29.321	1.0401	1.0420	1.0401		
515	2'280.50	0.9937	0.9953	200.418	200.558	0.9906	0.9913	0.9927	93.629	94.131	0.9612	0.9663	0.9662		
516	1'861.19	0.9679	0.9710	148.823	148.759	0.9723	0.9719	0.9742	67.447	67.603	0.9177	0.9198	0.9265		
517	3'259.96	0.9929	0.9942	291.755	291.635	0.9835	0.9831	0.9845	144.346	143.006	0.9843	0.9752	0.9783		
518	2'526.51	1.0104	1.0097	366.857	367.284	1.0013	1.0024	1.0008	70.505	70.660	0.9809	0.9830	0.9883		
519	1'819.97	0.9775	0.9813	220.586	220.428	0.9765	0.9758	0.9800	44.680	44.437	0.9549	0.9497	0.9627		
520	2'205.29	1.0203	1.0193	293.633	293.655	1.0144	1.0144	1.0162	58.699	58.702	1.0185	1.0186	1.0207		
521	4'723.63	1.0018	1.0075	559.716	559.441	1.0191	1.0186	1.0232	266.704	265.267	1.0100	1.0046	1.0063		
522	3'074.60	0.9923	0.9958	323.298	323.355	0.9873	0.9875	0.9890	150.585	149.705	0.9733	0.9676	0.9772		
523	3'492.24	1.0074	1.0083	396.721	397.006	1.0029	1.0036	1.0070	181.659	180.896	0.9781	0.9740	0.9793		
524	4'079.16	1.0166	1.0184	501.847	501.599	1.0206	1.0201	1.0193	236.100	235.956	1.0265	1.0259	1.0265		
525	5'310.32	0.9926	0.9938	658.453	658.755	0.9841	0.9848	0.9847	315.695	313.365	0.9892	0.9819	0.9863		
526	4'390.94	0.9906	0.9908	567.928	568.021	0.9787	0.9789	0.9766	245.717	246.793	0.9619	0.9661	0.9624		
527	4'292.14	0.9683	0.9702	557.613	557.474	0.9610	0.9607	0.9643	239.966	238.444	0.9393	0.9334	0.9382		
528	2'992.83	1.0359	1.0329	488.291	488.834	1.0384	1.0396	1.0404	88.980	89.087	1.0317	1.0330	1.0316		
529	1'879.13	1.0093	1.0117	229.784	229.583	1.0172	1.0163	1.0197	46.998	46.813	1.0044	1.0004	1.0085		
530	3'329.28	0.9963	0.9981	611.703	611.419	1.0006	1.0001	1.0048	100.785	100.897	0.9666	0.9677	0.9727		
531	5'170.11	0.9960	0.9988	1'262.238	1'261.036	1.0017	1.0008	1.0050	185.524	185.645	1.0026	1.0033	1.0055		
532	6'841.00	0.9834	0.9846	1'389.349	1'388.954	0.9747	0.9744	0.9775	377.322	381.146	0.9435	0.9530	0.9542		
533	8'253.44	0.9755	0.9775	1'712.254	1'713.052	0.9774	0.9779	0.9804	485.041	484.813	0.9756	0.9751	0.9755		
534	4'186.59	0.9824	0.9859	456.089	456.415	0.9919	0.9926	0.9977	217.406	217.126	0.9716	0.9704	0.9812		
535	4'441.94	1.0021	1.0028	576.201	576.052	0.9930	0.9927	0.9950	250.538	251.491	0.9807	0.9845	0.9793		
536	3'445.49	0.9940	0.9955	390.835	391.046	0.9880	0.9886	0.9890	180.920	179.893	0.9741	0.9686	0.9737		
537	3'469.44	1.0009	1.0019	394.447	394.559	0.9972	0.9974	0.9980	181.680	181.238	0.9782	0.9758	0.9784		
538	4'093.51	1.0202	1.0232	501.584	501.875	1.0201	1.0207	1.0193	237.035	238.900	1.0306	1.0387	1.0358		
539	7'116.29	1.0229	1.0222	1'450.506	1'450.886	1.0176	1.0179	1.0180	403.575	406.638	1.0091	1.0168	1.0109		
540	4'682.70	0.9931	0.9945	546.366	546.592	0.9948	0.9952	0.9971	256.159	255.570	0.9701	0.9678	0.9712		
541	4'684.12	0.9934	0.9944	545.495	545.340	0.9932	0.9929	0.9971	256.505	253.100	0.9714	0.9585	0.9692		
542	4'659.59	0.9882	0.9938	544.987	545.285	0.9923	0.9928	0.9906	256.301	254.842	0.9706	0.9651	0.9700		
543	4'725.42	0.9941	0.9951	655.423	655.870	0.9905	0.9912	0.9943	271.476	270.556	0.9918	0.9885	0.9853		
544	2'774.45	0.9603	0.9670	453.380	454.417	0.9642	0.9664	0.9716	81.785	81.683	0.9483	0.9471	0.9555		
545	2'794.61	0.9673	0.9720	454.335	455.050	0.9662	0.9678	0.9716	81.661	81.619	0.9468	0.9464	0.9548		
546	4'721.93	1.0014	1.0044	556.790	556.348	1.0138	1.0130	1.0167	260.912	263.670	0.9881	0.9985	0.9966		
547	5'644.68	0.9774	0.9792	750.612	751.920	0.9731	0.9748	0.9771	332.655	326.755	0.9522	0.9354	0.9546		
548	4'403.00	0.9933	0.9949	576.814	577.055	0.9940	0.9945	0.9950	251.443	250.710	0.9843	0.9814	0.9804		
549	4'683.23	0.9932	0.9945	545.689	545.871	0.9936	0.9939	0.9971	261.879	258.324	0.9917	0.9783	0.9882		
550	5'319.03	0.9942	1.0018	672.977	672.775	1.0058	1.0055	1.0061	311.004	311.717	0.9745	0.9768	0.9778		
551	3'961.91	0.9874	0.9895	478.467	478.611	0.9730	0.9733	0.9759	225.517	224.096	0.9805	0.9743	0.9821		
552	3'913.75	0.9754	0.9776	478.866	478.893	0.9739	0.9739	0.9759	222.542	221.551	0.9676	0.9633	0.9705		
553	7'213.51	1.0222	1.0230	1'192.636	1'190.938	1.0191	1.0176	1.0211	426.156	424.073	1.0223	1.0173	1.0235		
554	4'234.79	0.9937	1.0024	472.980	472.768	1.0286	1.0281	1.0289	228.413	226.548	1.0208	1.0125	1.0127		
555	5'227.23	0.9770	0.9806	660.346	660.016	0.9870	0.9865	0.9900	308.864	311.142	0.9678	0.9749	0.9740		
556	4'058.50	1.0114	1.0133	495.864	495.964	1.0084	1.0086	1.0049	225.435	226.300	0.9801	0.9839	0.9855		
557	3'288.99	0.9842	0.9881	605.854	605.905	0.9910	0.9911	0.9931	100.610	100.154	0.9649	0.9606	0.9684		
558	3'023.46	0.9758	0.9791	320.202	320.485	0.9778	0.9787	0.9809	143.199	143.652	0.9256	0.9285	0.9337		
559	4'647.48	0.9856	0.9875	541.377	541.553	0.9857	0.9860	0.9841	254.842	250.866	0.9651	0.9500	0.9628		
560	4'530.92	1.0079	1.0078	1'012.299	1'009.874	1.0119	1.0094	1.0118	151.496	151.786	0.9957	0.9976	0.9970		
561	7'058.48	1.0146	1.0145	1'439.737	1'439.249	1.0101	1.0097	1.0104	402.912	402.481	1.0074	1.0064	1.0109		

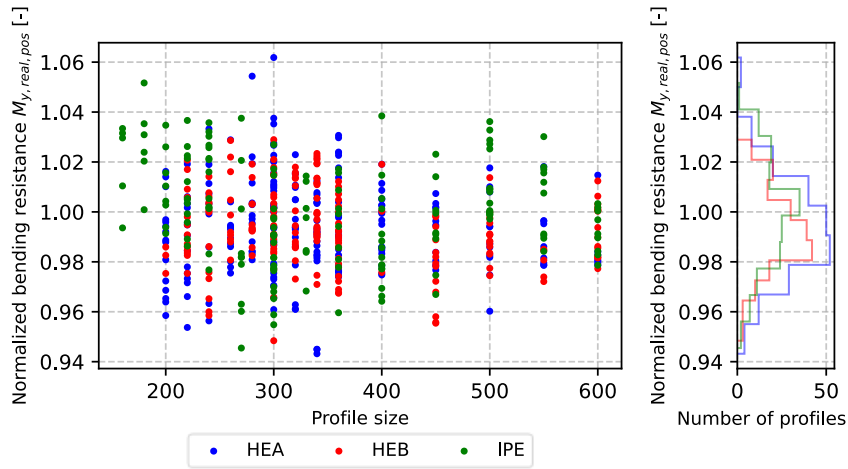
C.3.2 Visualization of the obtained cross-sectional resistances

The cross-sectional resistances are normalized with respect to the obtained nominal cross-sectional resistances.

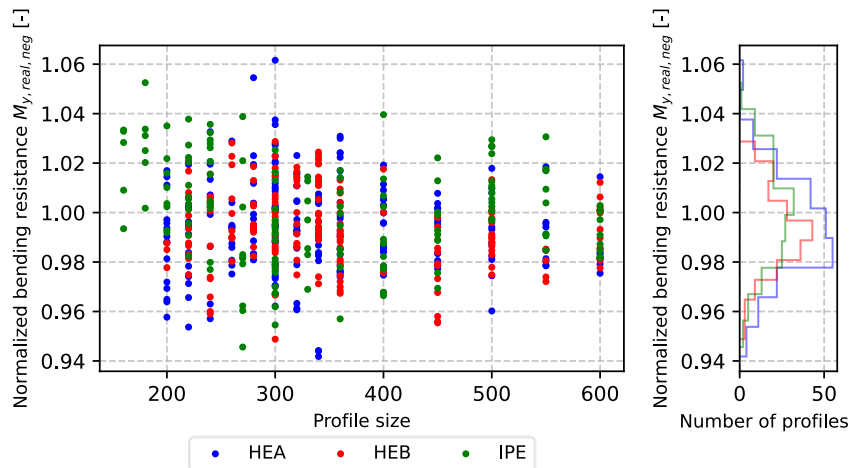
N_{real} :



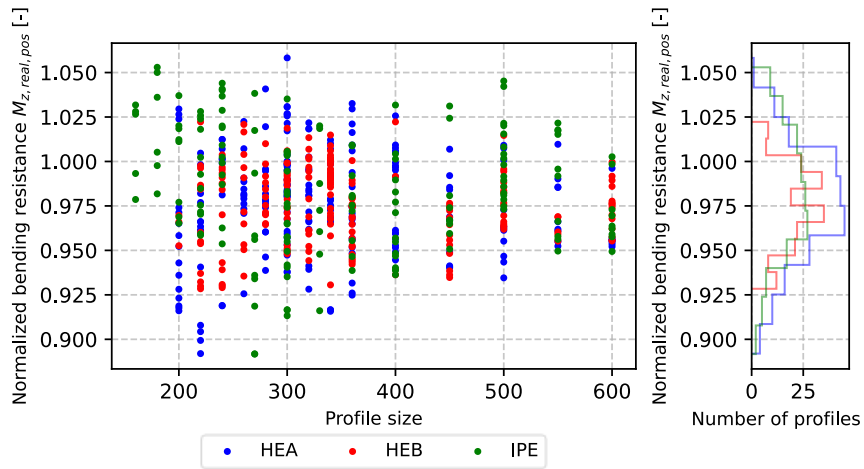
$M_{y,real,pos}$:



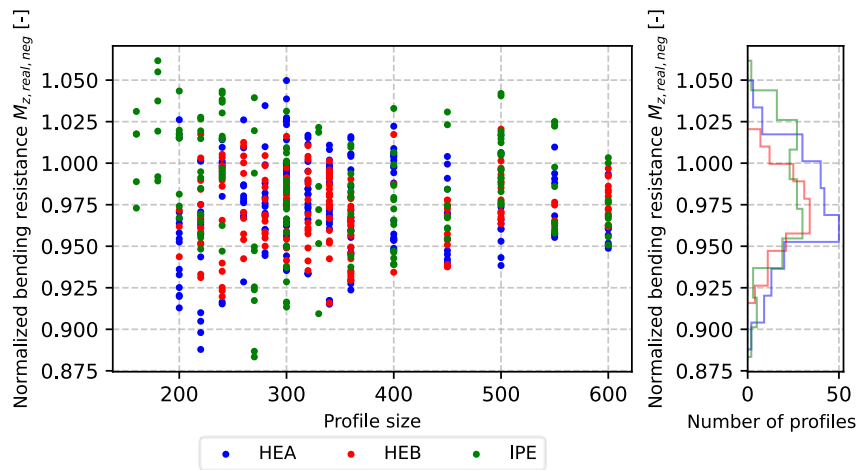
$M_{y,real,neg}$:



$M_{z,real,pos}$:



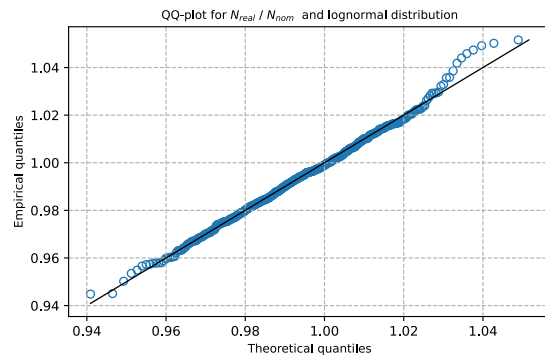
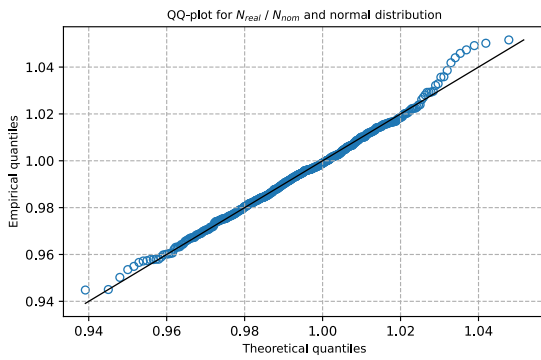
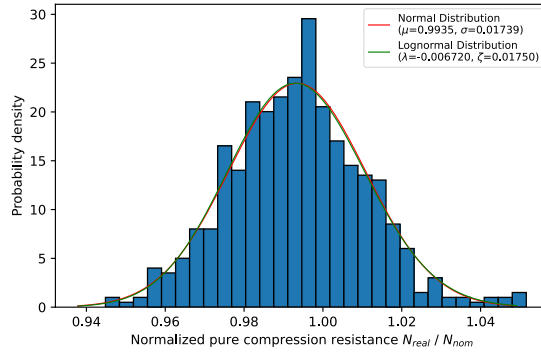
$M_{z,real,neg}$:



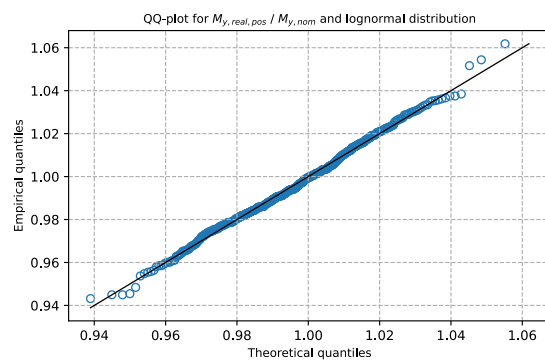
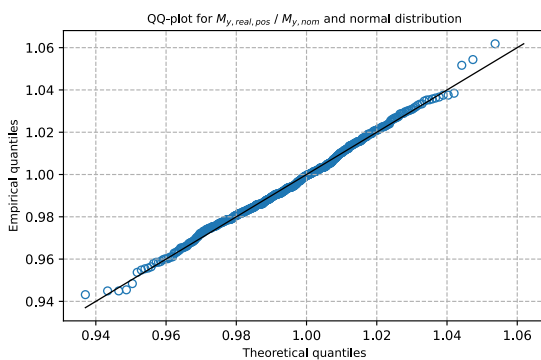
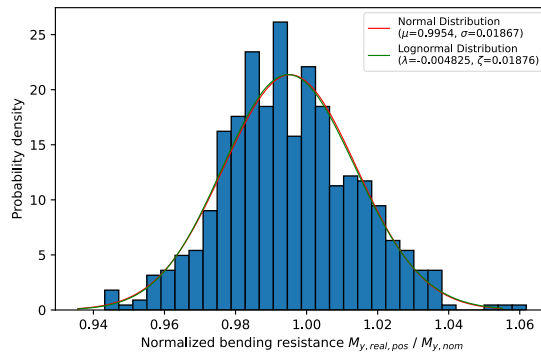
C.3.3 Further statistical evaluation of the results

In the following, some histograms including the fitted PDFs and some QQ-plots are shown using the procedure introduced in section 3.5.3.

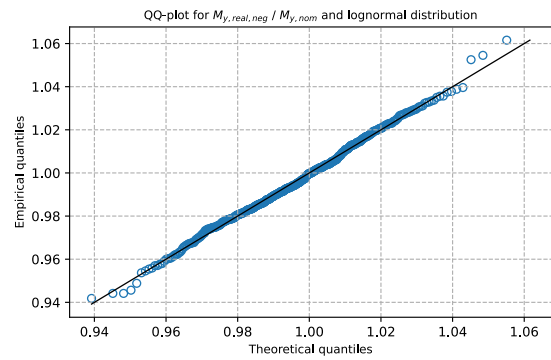
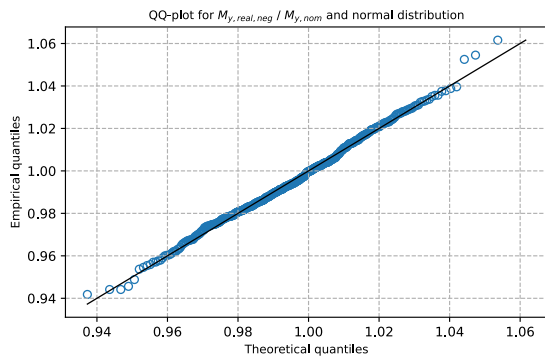
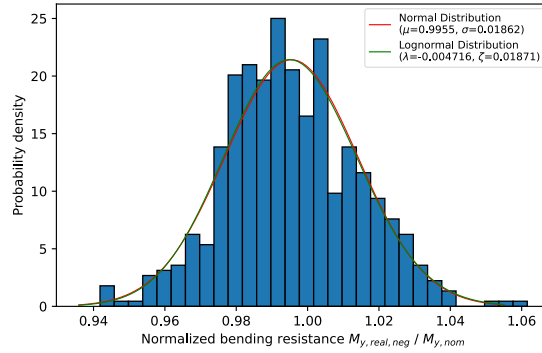
N_{real} :



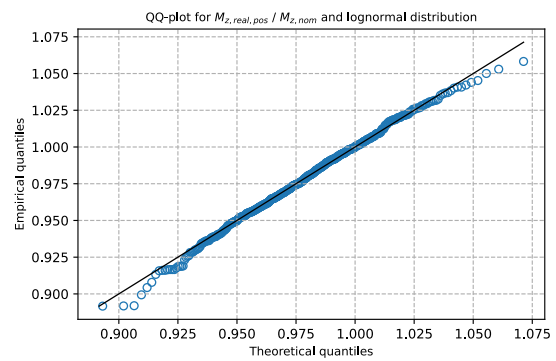
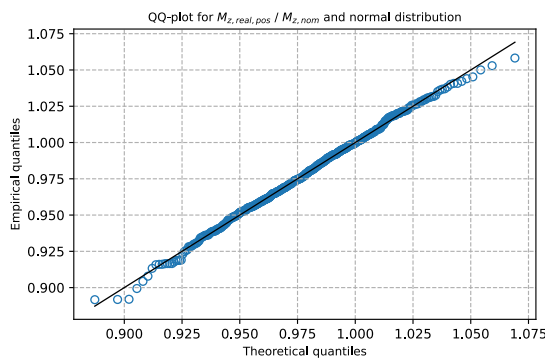
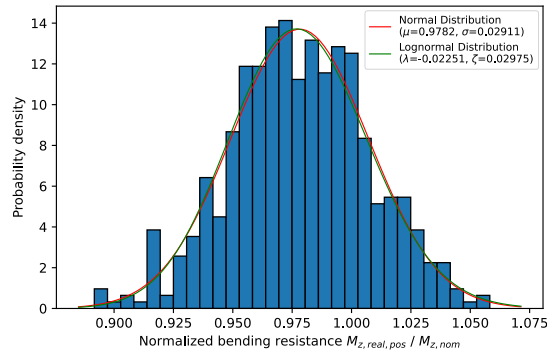
$M_{y,real,pos}$:



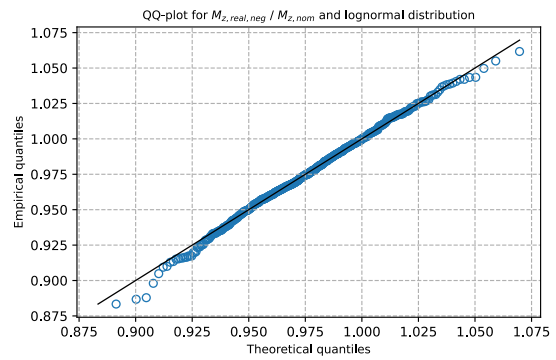
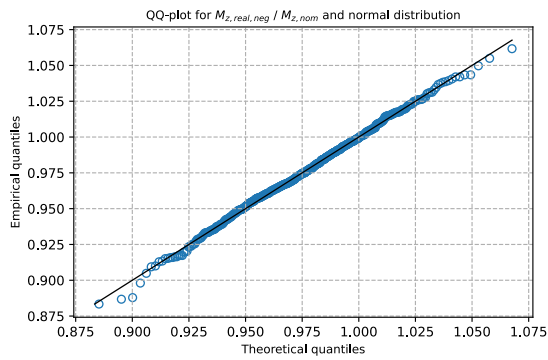
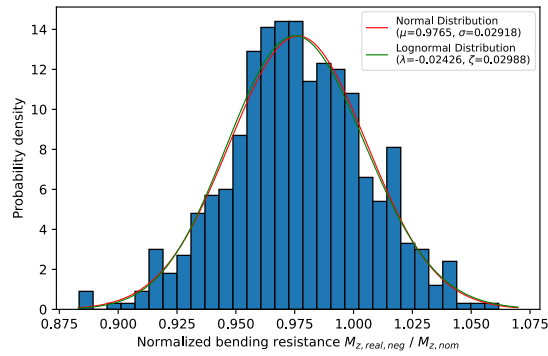
$M_{y,real,neg}$:



$M_{z,real,pos}$:



$M_{z,real,neg}$:



C.4 Abaqus results – Idealized cross-sections

C.4.1 Obtained resistances

Profile Nr.	Pure Compression			Bending strong axis			Bending weak axis		
	N_ideal [kN]	N_ideal / N_nom [-]	A_ideal / A_nom [-]	My_ideal [kNm]	My_ideal / My_nom [-]	WpLy_ideal / WpLy_nom [-]	Mz_ideal [kNm]	Mz_ideal / Mz_nom [-]	WpLz_ideal / WpLz_nom [-]
1	2'226.26	0.9701	0.9677	195.198	0.9648	0.9630	88.153	0.9050	0.9116
2	3'820.09	1.0003	1.0011	380.313	1.0068	1.0062	186.257	1.0009	1.0009
3	2'663.72	0.9712	0.9703	254.125	0.9582	0.9576	116.346	0.9184	0.9239
4	1'917.06	0.9969	0.9977	152.954	0.9993	0.9999	72.549	0.9871	0.9907
5	1'195.81	1.0201	1.0192	106.978	1.0365	1.0350	22.747	1.0288	1.0288
6	1'012.74	1.0089	1.0092	81.153	1.0132	1.0157	16.832	0.9885	0.9943
7	3'061.64	0.9881	0.9898	321.931	0.9831	0.9847	152.068	0.9829	0.9880
8	2'211.79	0.9638	0.9618	193.119	0.9545	0.9534	88.101	0.9044	0.9097
9	1'864.44	0.9696	0.9684	146.960	0.9601	0.9590	67.779	0.9222	0.9284
10	1'362.85	0.9915	0.9925	132.302	0.9965	0.9963	28.067	0.9975	0.9983
11	1'866.82	0.9708	0.9717	147.741	0.9652	0.9666	69.289	0.9427	0.9482
12	3'212.29	0.9784	0.9786	293.532	0.9895	0.9877	139.358	0.9503	0.9444
13	3'185.63	0.9702	0.9704	289.807	0.9770	0.9751	137.254	0.9359	0.9398
14	4'711.00	0.9991	0.9982	542.878	0.9885	0.9878	258.502	0.9789	0.9775
15	7'491.13	0.9666	0.9678	1'406.478	0.9732	0.9753	446.689	0.9745	0.9775
16	6'245.96	0.9917	0.9908	1'136.913	0.9803	0.9811	345.537	0.9613	0.9664
17	5'341.13	0.9983	0.9986	671.775	1.0040	1.0044	316.240	0.9909	0.9904
18	3'862.48	0.9626	0.9640	479.425	0.9750	0.9753	222.594	0.9678	0.9702
19	3'830.33	0.9546	0.9562	475.512	0.9670	0.9677	220.288	0.9578	0.9607
20	4'643.01	1.0329	1.0290	1'030.060	1.0296	1.0288	156.221	1.0268	1.0284
21	4'409.53	0.9948	0.9950	575.604	0.9920	0.9924	250.910	0.9822	0.9820
22	1'806.75	0.9704	0.9745	221.008	0.9783	0.9802	45.195	0.9659	0.9691
23	5'289.57	0.9887	0.9900	666.385	0.9960	0.9962	316.027	0.9903	0.9896
24	8'427.20	0.9960	0.9964	1'745.369	0.9963	0.9971	498.742	1.0031	1.0040
25	8'373.63	0.9897	0.9902	1'734.129	0.9899	0.9912	493.510	0.9926	0.9943
26	3'864.59	0.9965	0.9985	785.455	0.9982	0.9983	124.576	0.9803	0.9822
27	1'835.41	0.9858	0.9903	223.275	0.9884	0.9919	46.207	0.9875	0.9940
28	1'756.23	0.9433	0.9500	215.347	0.9533	0.9555	43.866	0.9375	0.9429
29	1'774.98	0.9533	0.9598	218.110	0.9655	0.9675	44.847	0.9584	0.9629
30	3'514.25	1.0138	1.0135	404.741	1.0232	1.0230	190.742	1.0270	1.0265
31	1'854.62	0.9961	0.9973	225.112	0.9965	0.9981	46.331	0.9902	0.9915
32	3'426.87	0.9886	0.9890	393.762	0.9954	0.9961	183.561	0.9883	0.9905
33	5'424.35	1.0139	1.0134	681.716	1.0189	1.0184	322.698	1.0112	1.0055
34	5'311.29	0.9927	0.9936	663.804	0.9921	0.9929	318.190	0.9970	0.9972
35	1'834.59	0.9854	0.9888	220.706	0.9770	0.9806	44.073	0.9419	0.9494
36	4'453.91	0.9908	0.9925	989.904	0.9895	0.9900	147.333	0.9684	0.9706
37	5'078.06	0.9491	0.9516	634.275	0.9480	0.9497	301.569	0.9450	0.9495
38	4'410.22	0.9950	0.9949	576.740	0.9939	0.9939	247.336	0.9682	0.9726
39	2'807.07	0.9716	0.9759	455.555	0.9688	0.9713	81.338	0.9431	0.9514
40	6'012.57	0.9843	0.9854	860.127	0.9923	0.9919	370.695	0.9990	0.9939
41	4'415.45	0.9961	0.9962	575.939	0.9925	0.9925	248.589	0.9731	0.9760
42	7'960.47	1.0139	1.0108	1'958.469	1.0153	1.0130	436.661	0.9966	0.9965
43	5'267.99	0.9846	0.9873	669.728	0.9873	1.0010	316.013	0.9902	0.9900
44	5'957.59	0.9753	0.9759	846.197	0.9762	0.9772	356.753	0.9614	0.9680
45	5'890.67	1.0200	1.0196	784.051	1.0165	1.0169	356.216	1.0197	1.0201
46	4'086.14	1.0183	1.0189	505.332	1.0277	1.0275	238.254	1.0359	1.0333
47	1'818.29	0.9766	0.9787	220.340	0.9754	0.9776	45.720	0.9771	0.9818
48	2'257.99	0.9839	0.9842	197.999	0.9786	0.9790	94.332	0.9684	0.9737
49	1'883.15	0.9793	0.9803	150.338	0.9822	0.9834	71.156	0.9681	0.9722
50	2'243.30	0.9775	0.9782	200.880	0.9929	0.9933	95.071	0.9760	0.9795
51	3'047.39	0.9835	0.9852	320.061	0.9774	0.9789	152.399	0.9847	0.9881
52	1'898.06	0.9870	0.9877	151.495	0.9898	0.9906	71.847	0.9775	0.9817
53	4'704.33	0.9896	0.9899	657.834	0.9942	0.9951	266.891	0.9751	0.9733
54	3'923.91	0.9779	0.9793	486.347	0.9891	0.9890	226.532	0.9849	0.9873
55	4'496.89	1.0145	1.0137	588.355	1.0139	1.0133	254.226	0.9952	1.0007
56	4'089.16	1.0191	1.0195	507.905	1.0329	1.0323	235.738	1.0249	1.0217
57	4'682.94	0.9851	0.9852	653.367	0.9874	0.9881	267.132	0.9759	0.9751
58	4'935.15	0.9713	0.9718	729.746	0.9747	0.9771	274.403	0.9311	0.9414
59	4'969.24	0.9780	0.9797	740.983	0.9897	0.9896	285.851	0.9699	0.9720
60	6'254.67	0.9930	0.9946	1'160.067	1.0002	1.0011	362.238	1.0077	1.0068
61	6'843.66	0.9837	0.9844	1'398.894	0.9814	0.9819	387.065	0.9678	0.9716
62	7'646.53	0.9739	0.9754	1'893.006	0.9813	0.9805	421.084	0.9610	0.9614
63	5'081.96	0.9790	0.9835	1'235.627	0.9806	0.9816	176.509	0.9539	0.9570
64	4'418.63	0.9830	0.9871	983.661	0.9832	0.9845	145.887	0.9588	0.9629
65	2'147.70	0.9936	0.9965	290.582	1.0038	1.0054	57.010	0.9892	0.9950
66	1'899.52	1.0202	1.0194	230.408	1.0199	1.0210	47.006	1.0046	1.0080
67	2'451.06	0.9802	0.9865	360.710	0.9845	0.9872	70.297	0.9780	0.9845
68	1'349.99	0.9822	0.9855	132.465	0.9978	0.9983	28.068	0.9975	0.9975
69	1'384.65	1.0074	1.0083	135.286	1.0190	1.0185	29.166	1.0365	1.0352
70	712.57	1.0028	1.0026	44.688	0.9917	0.9940	9.780	0.9771	0.9844
71	886.19	1.0499	1.0476	63.499	1.0532	1.0520	14.033	1.0635	1.0636
72	2'432.96	0.9730	0.9779	358.432	0.9783	0.9802	67.961	0.9455	0.9527
73	5'392.75	1.0080	1.0087	685.487	1.0245	1.0243	319.057	0.9997	0.9999
74	5'415.59	1.0122	1.0117	680.294	1.0168	1.0164	320.686	1.0049	0.9994
75	5'687.29	0.9848	0.9857	761.320	0.9870	0.9872	338.556	0.9691	0.9711
76	6'213.18	1.0172	1.0171	888.370	1.0249	1.0249	374.062	1.0081	1.0100
77	6'167.45	1.0097	1.0098	878.501	1.0135	1.0143	371.292	1.0006	1.0026
78	5'772.83	0.9996	1.0004	781.051	1.0126	1.0128	345.726	0.9897	0.9974
79	5'738.38	0.9936	0.9942	768.991	0.9969	0.9974	341.292	0.9770	0.9785
80	6'216.69	1.0178	1.0175	885.822	1.0219	1.0227	373.501	1.0066	1.0088
81	6'215.05	1.0175	1.0169	881.536	1.0170	1.0171	368.455	0.9930	0.9966
82	6'152.91	1.0073	1.0074	878.066	1.0130	1.0132	368.974	0.9944	0.9968
83	5'960.63	0.9758	0.9756	843.472	0.9731	0.9742	346.167	0.9329	0.9438
84	6'368.69	0.9875	0.9881	957.790	0.9899	0.9914	375.141	0.9596	0.9667
85	6'327.99	0.9812	0.9821	949.370	0.9812	0.9838	376.771	0.9638	0.9731
86	6'390.97	0.9910	0.9926	972.425	0.9950	1.0051	384.891	0.9846	0.9869
87	6'272.55	0.9726	0.9733	939.185	0.9707	0.9723	370.410	0.9475	0.9552
88	6'272.46	0.9726	0.9733	938.766	0.9702	0.9718	370.324	0.9473	0.9540
89	8'395.01	0.9922	0.9924	1'735.873	0.9909	0.9916	487.708	0.9809	0.9831
90	6'356.38	0.9856	0.9868	957.892	0.9900	0.9903	383.394	0.9807	0.9808
91	8'616.16	0.9600	0.9630	1'973.678	0.9700	0.9724	497.744	0.9645	0.9679
92	9'460.19	0.9968	0.9969	2'343.836	1.0022	1.0024	535.146	0.9999	0.9988
93	1'868.66	0.9717	0.9715	148.330	0.9691	0.9691	67.873	0.9235	0.9313
94	4'018.56	1.0015	1.0019	492.952	1.0025	1.0022	229.200	0.9965	1.0002
95	2'288.15	0.9971	0.9960	203.320	1.0049	1.0040	95.362	0.9790	0.9813
96	1'163.41	0.9925	0.9905	101.280	0.9813	0.9801	21.319	0.9642	0.9670
97	749.88	1.0554	1.0538	47.004	1.0431	1.0420	10.334	1.0325	1.0342
98	881.76	1.0446	1.0428	61.779	1.0246	1.0249	13.220	1.0019	1.0046
99	6'102.77	0.9991	0.9986	864.892	0.9978	0.9982	363.317	0.9791	0.9842
100	1'172.99	1.0007	1.0003	103.375	1.0016	1.0032	21.265	0.9617	0.9669

Profile Nr.	Pure Compression			Bending strong axis			Bending weak axis		
	N_ideal [kN]	N_ideal / N_nom [-]	A_ideal / A_nom [-]	My_ideal [kNm]	My_ideal / My_nom [-]	Wpl_y_ideal / Wpl_y_nom [-]	Mz_ideal [kNm]	Mz_ideal / Mz_nom [-]	Wpl_z_ideal / Wpl_z_nom [-]
101	2'801.38	0.9939	0.9938	228.544	0.9901	0.9899	112.850	0.9810	0.9836
102	3'222.54	0.9815	0.9813	292.815	0.9871	0.9846	138.224	0.9426	0.9450
103	3'843.11	1.0064	1.0054	378.768	1.0027	1.0026	184.976	0.9941	1.0030
104	3'861.85	1.0113	1.0103	381.279	1.0094	1.0091	186.370	1.0016	1.0086
105	5'409.58	1.0111	1.0111	674.509	1.0081	1.0080	319.774	1.0020	0.9987
106	3'415.87	0.9854	0.9855	389.192	0.9839	0.9844	174.609	0.9401	0.9462
107	4'223.24	1.0525	1.0530	522.753	1.0631	1.0626	245.526	1.0675	1.0636
108	4'749.37	0.9991	0.9999	668.739	1.0106	1.0104	277.457	1.0137	1.0108
109	7'573.09	1.0229	1.0208	1'697.323	1.0175	1.0183	425.538	1.0149	1.0162
110	5'731.48	0.9924	0.9913	764.607	0.9912	0.9915	336.879	0.9643	0.9684
111	7'744.29	0.9993	0.9985	1'433.127	0.9916	0.9915	450.612	0.9831	0.9842
112	4'018.05	1.0013	1.0015	497.183	1.0111	1.0109	230.864	1.0037	1.0038
113	5'047.27	0.9723	0.9786	1'236.904	0.9816	0.9827	178.503	0.9647	0.9657
114	4'528.27	1.0073	1.0062	1'014.890	1.0145	1.0138	155.680	1.0232	1.0218
115	3'970.19	1.0237	1.0190	809.458	1.0287	1.0259	132.716	1.0444	1.0413
116	3'910.33	1.0083	1.0084	803.482	1.0211	1.0201	129.784	1.0213	1.0200
117	3'941.40	1.0163	1.0127	795.531	1.0110	1.0094	126.166	0.9928	0.9927
118	3'292.83	0.9854	0.9861	597.449	0.9773	0.9781	100.891	0.9676	0.9712
119	3'211.39	0.9610	0.9650	591.374	0.9673	0.9685	99.939	0.9585	0.9633
120	2'814.27	0.9741	0.9786	462.009	0.9826	0.9836	83.183	0.9645	0.9703
121	2'526.11	1.0102	1.0096	369.769	1.0092	1.0088	70.518	0.9811	0.9846
122	2'543.89	1.0173	1.0155	372.891	1.0177	1.0169	72.954	1.0150	1.0141
123	2'165.53	1.0019	1.0034	286.694	0.9904	0.9935	55.334	0.9601	0.9690
124	2'171.66	1.0047	1.0044	286.449	0.9895	0.9913	55.921	0.9703	0.9767
125	1'852.67	0.9951	0.9968	225.774	0.9994	1.0007	47.361	1.0122	1.0131
126	3'994.27	0.9954	0.9960	488.656	0.9938	0.9932	228.282	0.9925	0.9933
127	4'000.08	0.9969	0.9976	491.039	0.9986	0.9982	230.596	1.0026	1.0027
128	4'726.10	0.9942	0.9943	654.786	0.9896	0.9907	268.567	0.9812	0.9793
129	4'733.68	0.9958	0.9965	666.022	1.0065	1.0068	274.197	1.0018	1.0022
130	4'736.92	0.9965	0.9970	666.169	1.0068	1.0067	273.849	1.0005	1.0011
131	5'140.47	1.0117	1.0110	754.951	1.0084	1.0090	290.642	0.9862	0.9892
132	5'661.77	1.0027	1.0031	925.780	1.0046	1.0052	323.653	1.0096	1.0141
133	5'618.05	0.9950	0.9950	913.321	0.9911	0.9928	309.498	0.9655	0.9729
134	5'159.24	1.0154	1.0156	762.744	1.0188	1.0190	301.073	1.0216	1.0198
135	5'798.97	1.0041	1.0050	782.470	1.0144	1.0147	354.434	1.0146	1.0128
136	7'630.89	0.9719	0.9735	1'890.397	0.9800	0.9793	417.983	0.9539	0.9552
137	6'326.50	1.0045	1.0037	1'159.428	0.9997	0.9998	356.983	0.9931	0.9931
138	6'666.09	0.9582	0.9611	1'368.011	0.9598	0.9610	376.039	0.9402	0.9444
139	6'221.77	0.9878	0.9875	1'136.656	0.9800	0.9825	342.144	0.9518	0.9564
140	6'971.18	1.0021	1.0025	1'432.631	1.0051	1.0047	404.405	1.0112	1.0108
141	7'194.65	0.9717	0.9750	1'629.858	0.9771	0.9793	403.340	0.9620	0.9670
142	4'016.36	1.0009	1.0018	497.864	1.0125	1.0128	234.716	1.0205	1.0206
143	4'665.17	0.9814	0.9812	649.594	0.9817	0.9817	264.772	0.9673	0.9696
144	5'157.45	1.0151	1.0161	772.967	1.0324	1.0316	305.042	1.0351	1.0309
145	5'210.44	0.9739	0.9751	656.188	0.9807	0.9814	306.063	0.9590	0.9623
146	5'258.38	0.9828	0.9830	660.679	0.9875	0.9875	305.277	0.9566	0.9574
147	6'049.95	0.9905	0.9906	858.670	0.9906	0.9914	367.917	0.9915	0.9940
148	9'431.82	0.9938	0.9930	2'336.564	0.9991	0.9977	525.543	0.9820	0.9793
149	9'277.95	0.9776	0.9773	2'294.356	0.9811	0.9809	511.032	0.9549	0.9556
150	9'349.42	0.9851	0.9857	2'324.122	0.9938	0.9936	521.740	0.9749	0.9733
151	8'736.33	0.9734	0.9747	1'994.787	0.9803	0.9814	499.101	0.9671	0.9684
152	8'255.01	0.9756	0.9767	1'731.618	0.9885	0.9888	484.187	0.9738	0.9743
153	8'294.02	0.9802	0.9810	1'727.105	0.9859	0.9871	484.255	0.9740	0.9761
154	7'627.81	0.9842	0.9851	1'433.411	0.9918	0.9938	449.283	0.9802	0.9839
155	7'400.30	0.9549	0.9561	1'384.876	0.9582	0.9607	433.119	0.9449	0.9507
156	6'427.87	0.9967	0.9977	970.401	1.0029	1.0027	384.763	0.9842	0.9850
157	6'494.28	1.0070	1.0070	978.365	1.0112	1.0112	383.668	0.9814	0.9847
158	6'164.78	1.0093	1.0091	880.393	1.0157	1.0151	374.272	1.0086	1.0064
159	5'409.66	1.0111	1.0107	680.331	1.0168	1.0159	320.796	1.0052	1.0004
160	5'289.71	0.9887	0.9887	667.020	0.9969	0.9966	308.379	0.9663	0.9665
161	5'374.75	1.0046	1.0044	669.355	1.0004	1.0001	321.274	1.0067	1.0020
162	3'524.99	1.0169	1.0147	398.336	1.0070	1.0053	185.858	1.0007	0.9985
163	2'238.75	0.9755	0.9721	197.329	0.9753	0.9719	87.329	0.8965	0.8974
164	1'191.71	1.0166	1.0153	106.025	1.0273	1.0253	22.611	1.0226	1.0215
165	4'697.01	0.9961	0.9972	551.993	1.0051	1.0048	262.730	0.9950	1.0005
166	3'241.02	0.9871	0.9876	299.809	1.0107	1.0080	140.932	0.9610	0.9522
167	4'154.95	0.9750	0.9773	456.191	0.9921	0.9920	214.830	0.9601	0.9653
168	3'168.01	1.0225	1.0221	337.714	1.0313	1.0302	159.087	1.0283	1.0333
169	3'517.54	1.0147	1.0142	403.898	1.0211	1.0217	187.354	1.0088	1.0093
170	3'684.39	0.9648	0.9652	368.393	0.9752	0.9742	172.410	0.9265	0.9359
171	4'016.42	1.0009	1.0015	497.438	1.0116	1.0106	231.510	1.0065	1.0062
172	5'086.23	0.9798	0.9853	1'244.929	0.9880	0.9891	180.701	0.9766	0.9781
173	4'537.99	1.0095	1.0078	1'016.256	1.0158	1.0148	155.992	1.0253	1.0239
174	3'989.49	1.0287	1.0234	812.411	1.0325	1.0296	132.990	1.0465	1.0434
175	3'935.29	1.0147	1.0135	806.796	1.0254	1.0239	129.768	1.0212	1.0194
176	3'860.63	0.9955	0.9967	787.350	1.0006	1.0003	128.227	1.0091	1.0093
177	3'939.55	1.0158	1.0122	794.025	1.0091	1.0077	125.693	0.9891	0.9890
178	8'351.74	0.9871	0.9876	1'732.231	0.9888	0.9907	484.095	0.9737	0.9769
179	2'199.56	1.0176	1.0142	290.470	1.0034	1.0034	56.488	0.9802	0.9838
180	3'983.73	0.9928	0.9934	488.710	0.9939	0.9933	228.255	0.9924	0.9928
181	3'953.90	0.9854	0.9861	484.529	0.9854	0.9851	225.269	0.9794	0.9809
182	4'746.80	0.9986	0.9991	667.269	1.0084	1.0084	274.549	1.0030	1.0028
183	4'739.00	0.9969	0.9967	657.696	0.9940	0.9943	272.677	0.9962	0.9940
184	5'638.93	0.9987	0.9988	919.101	0.9974	0.9975	321.501	1.0029	1.0065
185	6'448.42	0.9999	1.0012	978.192	1.0110	1.0111	391.906	1.0025	1.0036
186	7'623.28	0.9709	0.9725	1'885.873	0.9776	0.9772	416.306	0.9501	0.9528
187	6'319.66	1.0034	1.0030	1'166.080	1.0054	1.0064	349.935	0.9735	0.9786
188	6'223.17	0.9880	0.9879	1'138.095	0.9813	0.9844	344.489	0.9584	0.9617
189	6'955.77	0.9999	0.9994	1'419.865	0.9961	0.9965	390.656	0.9768	0.9798
190	7'304.80	0.9866	0.9865	1'636.902	0.9813	0.9817	404.772	0.9654	0.9675
191	7'199.26	0.9724	0.9757	1'630.724	0.9776	0.9794	403.243	0.9617	0.9672
192	4'667.61	0.9819	0.9819	650.686	0.9834	0.9833	266.951	0.9753	0.9747
193	5'173.46	1.0182	1.0190	773.901	1.0337	1.0331	303.192	1.0288	1.0277
194	6'055.28	0.9913	0.9915	859.743	0.9918	0.9929	367.281	0.9898	0.9938
195	8'889.15	0.9904	0.9903	2'008.972	0.9873	0.9874	504.822	0.9782	0.9786
196	9'443.62	0.9950	0.9943	2'340.106	1.0006	0.9993	525.868	0.9826	0.9800
197	9'283.79	0.9782	0.9780	2'292.642	0.9803	0.9807	510.451	0.9538	0.9549
198	9'321.19	0.9821	0.9835	2'316.495	0.9905	0.9901	520.292	0.9722	0.9718
199	8'714.31	0.9709	0.9725	1'982.901	0.9745	0.9763	497.235	0.9635	0.9662
200	8'312.18	0.9824	0.9835	1'735.408	0.9906	0.9906	497.190	1.0000	0.9999

Profile Nr.	Pure Compression			Bending strong axis			Bending weak axis		
	N_ideal / N_nom [kN] / [-]	N_ideal / N_nom [-]	A_ideal / A_nom [-]	My_ideal / My_nom [kNm] / [-]	My_ideal / My_nom [-]	Wpl_y_ideal / Wpl_y_nom [-]	Mz_ideal / Mz_nom [kNm] / [-]	Mz_ideal / Mz_nom [-]	Wpl_z_ideal / Wpl_z_nom [-]
201	7'749.32	0.9999	0.9997	1'445.782	1.0004	1.0012	452.096	0.9863	0.9903
202	7'391.26	0.9537	0.9551	1'379.581	0.9546	0.9583	432.463	0.9435	0.9504
203	6'405.85	0.9933	0.9932	961.803	0.9940	0.9942	387.641	0.9916	0.9925
204	7'097.77	1.0058	1.0056	1'171.656	1.0011	1.0014	414.371	0.9940	0.9946
205	6'425.61	0.9963	0.9967	965.324	0.9977	0.9991	378.781	0.9689	0.9756
206	6'070.87	0.9939	0.9944	866.158	0.9992	0.9998	368.211	0.9923	0.9939
207	5'648.10	0.9780	0.9788	759.013	0.9840	0.9844	336.754	0.9640	0.9659
208	4'466.85	0.9937	0.9968	1'001.844	1.0014	1.0024	150.988	0.9924	0.9942
209	2'749.39	1.0024	1.0025	266.319	1.0042	1.0042	127.703	1.0080	1.0070
210	2'703.24	0.9856	0.9856	261.704	0.9868	0.9869	124.848	0.9855	0.9855
211	1'378.57	1.0030	1.0029	133.919	1.0087	1.0069	28.905	1.0273	1.0247
212	4'217.34	0.9897	0.9892	456.258	0.9922	0.9919	217.843	0.9736	0.9776
213	4'259.95	0.9997	1.0011	463.479	1.0079	1.0077	224.328	1.0026	1.0069
214	3'253.24	0.9908	0.9905	294.851	0.9940	0.9917	141.988	0.9682	0.9624
215	878.21	1.0404	1.0387	62.667	1.0394	1.0374	13.937	1.0562	1.0534
216	872.92	1.0342	1.0329	62.360	1.0343	1.0327	13.771	1.0436	1.0416
217	2'759.66	1.0061	1.0061	270.936	1.0216	1.0212	127.873	1.0094	1.0097
218	3'815.79	0.9992	1.0004	380.342	1.0069	1.0068	186.182	1.0005	1.0012
219	3'817.87	0.9998	1.0001	379.284	1.0041	1.0034	185.626	0.9976	0.9976
220	2'737.71	0.9981	0.9985	267.570	1.0089	1.0092	128.129	1.0114	1.0124
221	1'008.73	1.0049	1.0052	80.409	1.0039	1.0066	16.589	0.9742	0.9814
222	1'151.76	0.9826	0.9847	103.603	1.0038	1.0038	21.571	0.9756	0.9782
223	1'899.47	0.9878	0.9885	152.690	0.9976	0.9981	71.659	0.9750	0.9786
224	1'185.90	1.0117	1.0099	105.206	1.0193	1.0155	22.886	1.0350	1.0307
225	1'184.44	1.0104	1.0088	105.374	1.0210	1.0159	22.842	1.0330	1.0268
226	3'843.36	1.0064	1.0073	383.791	1.0160	1.0160	189.185	1.0167	1.0160
227	3'337.14	1.0164	1.0156	298.940	1.0077	1.0065	145.324	0.9910	0.9922
228	3'263.65	0.9940	0.9940	295.706	0.9968	0.9969	144.209	0.9834	0.9868
229	1'885.19	0.9803	0.9793	151.611	0.9905	0.9896	70.484	0.9590	0.9625
230	1'391.00	1.0120	1.0138	137.392	1.0349	1.0336	29.593	1.0517	1.0484
231	1'382.81	1.0060	1.0085	136.399	1.0274	1.0273	29.448	1.0465	1.0446
232	1'956.79	1.0176	1.0173	155.559	1.0163	1.0165	75.522	1.0275	1.0309
233	1'950.72	1.0144	1.0141	155.087	1.0132	1.0134	75.358	1.0253	1.0289
234	1'868.75	0.9718	0.9709	148.729	0.9717	0.9711	67.452	0.9177	0.9262
235	1'512.41	0.9443	0.9501	165.157	0.9458	0.9495	32.545	0.8914	0.9033
236	1'545.31	0.9649	0.9683	167.710	0.9604	0.9636	32.618	0.8934	0.9049
237	1'650.11	1.0303	1.0292	181.493	1.0393	1.0384	38.134	1.0444	1.0408
238	1'628.81	1.0170	1.0164	178.666	1.0231	1.0226	37.482	1.0266	1.0223
239	2'752.69	0.9766	0.9772	227.832	0.9870	0.9868	109.895	0.9554	0.9584
240	3'304.14	0.9887	0.9909	608.285	0.9950	0.9960	101.317	0.9717	0.9757
241	2'786.39	0.9644	0.9693	458.597	0.9753	0.9755	83.896	0.9728	0.9735
242	9'304.21	0.9803	0.9807	2'285.385	0.9772	0.9771	517.927	0.9677	0.9684
243	9'456.38	0.9964	0.9953	2'312.735	0.9889	0.9890	523.131	0.9775	0.9782
244	9'426.06	0.9932	0.9921	2'301.388	0.9841	0.9845	519.970	0.9716	0.9729
245	4'772.65	1.0040	1.0045	670.944	1.0140	1.0139	278.812	1.0186	1.0138
246	2'891.65	1.0009	1.0016	474.303	1.0087	1.0078	87.079	1.0097	1.0091
247	6'095.99	0.9980	0.9979	867.273	1.0005	1.0011	361.642	0.9746	0.9800
248	4'304.56	0.9711	0.9711	559.437	0.9641	0.9647	241.939	0.9471	0.9472
249	5'314.21	0.9933	0.9935	658.802	0.9847	0.9856	316.179	0.9907	0.9909
250	4'094.17	1.0203	1.0205	503.214	1.0234	1.0229	238.252	1.0359	1.0329
251	3'485.32	1.0054	1.0054	396.262	1.0018	1.0017	181.979	0.9798	0.9835
252	4'203.19	0.9863	0.9900	459.950	1.0003	1.0013	224.347	1.0027	1.0087
253	6'297.88	0.9765	0.9783	952.700	0.9846	0.9857	381.081	0.9748	0.9783
254	6'363.88	0.9868	0.9881	962.180	0.9944	0.9952	383.658	0.9814	0.9840
255	7'630.58	0.9846	0.9848	1'426.668	0.9872	0.9872	448.594	0.9787	0.9793
256	4'424.04	0.9981	0.9981	573.892	0.9890	0.9888	249.808	0.9779	0.9777
257	5'060.93	0.9961	0.9965	747.596	0.9986	0.9999	289.562	0.9825	0.9845
258	3'125.80	1.0088	1.0088	329.451	1.0061	1.0060	157.597	1.0187	1.0173
259	3'119.30	0.9933	0.9959	609.625	0.9972	0.9983	102.259	0.9808	0.9837
260	1'839.20	0.9878	0.9922	224.363	0.9932	0.9963	46.884	1.0020	1.0071
261	9'602.19	0.9922	0.9933	1'416.871	0.9940	0.9949	391.225	0.9782	0.9819
262	1'803.52	0.9687	0.9732	220.882	0.9778	0.9799	45.157	0.9651	0.9688
263	1'897.66	1.0192	1.0186	231.394	1.0243	1.0240	48.717	1.0412	1.0389
264	4'407.04	0.9943	0.9948	579.013	0.9978	0.9983	253.143	0.9909	0.9909
265	5'437.21	1.0163	1.0174	689.769	1.0309	1.0309	325.381	1.0196	1.0216
266	3'949.88	0.9844	0.9849	477.652	0.9714	0.9712	226.365	0.9842	0.9867
267	2'212.12	1.0234	1.0204	294.172	1.0162	1.0165	59.269	1.0284	1.0290
268	6'024.38	0.9863	0.9873	861.901	0.9943	0.9938	371.689	1.0017	0.9954
269	5'236.74	0.9788	0.9811	662.030	0.9895	0.9904	312.718	0.9799	0.9803
270	2'451.11	0.9802	0.9860	360.139	0.9829	0.9850	69.674	0.9693	0.9743
271	5'069.43	0.9766	0.9822	1'236.802	0.9816	0.9828	177.646	0.9601	0.9623
272	750.06	1.0556	1.0542	46.613	1.0344	1.0357	10.281	1.0272	1.0337
273	867.16	1.0274	1.0254	61.710	1.0235	1.0224	13.466	1.0205	1.0203
274	1'014.85	1.0110	1.0092	80.350	1.0032	1.0027	17.487	1.0270	1.0275
275	1'194.23	1.0188	1.0173	104.806	1.0155	1.0162	21.618	0.9777	0.9821
276	1'399.46	1.0182	1.0171	134.453	1.0127	1.0149	28.143	1.0002	1.0068
277	1'588.31	0.9917	0.9924	171.588	0.9826	0.9855	34.303	0.9395	0.9474
278	1'820.72	0.9779	0.9811	218.773	0.9684	0.9727	42.828	0.9153	0.9311
279	1'825.80	0.9806	0.9829	219.856	0.9732	0.9760	42.838	0.9155	0.9254
280	1'579.32	0.9861	0.9872	171.582	0.9826	0.9839	35.132	0.9622	0.9672
281	3'926.10	1.0124	1.0121	799.649	1.0163	1.0159	127.538	1.0036	1.0057
282	3'336.88	0.9985	1.0013	618.812	1.0122	1.0124	107.292	1.0290	1.0272
283	2'895.99	1.0024	1.0044	477.926	1.0164	1.0161	87.057	1.0094	1.0099
284	4'460.81	0.9923	0.9938	990.512	0.9901	0.9910	146.307	0.9616	0.9645
285	5'140.63	0.9903	0.9927	1'260.635	1.0005	1.0009	185.106	1.0004	1.0036
286	5'158.75	0.9938	0.9962	1'254.324	0.9955	0.9957	178.758	0.9661	0.9667
287	3'861.57	0.9957	0.9974	788.354	1.0019	1.0015	124.616	0.9806	0.9829
288	1'385.42	1.0079	1.0094	135.109	1.0177	1.0211	28.614	1.0169	1.0239
289	743.22	1.0460	1.0445	46.558	1.0332	1.0337	10.335	1.0326	1.0373
290	2'229.81	0.9716	0.9695	197.651	0.9769	0.9753	88.606	0.9096	0.9162
291	2'245.16	0.9783	0.9787	198.692	0.9820	0.9834	93.992	0.9649	0.9682
292	3'066.67	0.9897	0.9914	325.030	0.9926	0.9938	153.332	0.9911	0.9938
293	3'336.02	1.0201	1.0191	400.299	1.0120	1.0122	185.954	1.0012	1.0028
294	3'859.90	0.9619	0.9634	481.531	0.9793	0.9791	220.224	0.9575	0.9606
295	4'538.82	1.0240	1.0240	591.431	1.0192	1.0191	261.278	1.0228	1.0202
296	4'041.73	1.0073	1.0079	498.599	1.0140	1.0131	231.633	1.0071	1.0063
297	6'267.06	0.9950	0.9963	1'162.094	1.0020	1.0031	360.696	1.0035	1.0042
298	5'159.89	1.0156	1.0163	767.115	1.0246	1.0238	300.458	1.0195	1.0143
299	4'668.16	0.9820	0.9826	651.867	0.9851	0.9860	266.953	0.9753	0.9730
300	7'370.55	0.9955	0.9953	1'657.875	0.9939	0.9944	415.059	0.9899	0.9910

Profile Nr.	Pure Compression				Bending strong axis			Bending weak axis		
	N_ideal [kN]	N_ideal / N_nom [-]	A_ideal / A_nom [-]	My_ideal [kNm]	My_ideal / My_nom [-]	Wpl_y_ideal / Wpl_y_nom [-]	Mz_ideal [kNm]	Mz_ideal / Mz_nom [-]	Wpl_z_ideal / Wpl_z_nom [-]	
301	7'690.45	0.9795	0.9802	1'895.024	0.9824	0.9825	418.877	0.9560	0.9597	
302	5'669.79	1.0041	1.0043	926.044	1.0049	1.0055	322.511	1.0060	1.0098	
303	4'947.79	0.9738	0.9741	728.378	0.9729	0.9753	275.770	0.9357	0.9487	
304	5'059.08	0.9957	0.9960	744.410	0.9943	0.9955	288.725	0.9797	0.9824	
305	4'001.45	0.9972	0.9979	491.535	0.9996	0.9992	230.741	1.0032	1.0033	
306	3'236.38	0.9857	0.9857	292.117	0.9847	0.9840	140.457	0.9578	0.9624	
307	3'747.01	0.9812	0.9818	373.507	0.9888	0.9884	180.602	0.9706	0.9719	
308	4'156.48	0.9754	0.9772	457.562	0.9951	0.9953	215.321	0.9623	0.9675	
309	4'689.33	0.9945	0.9959	547.868	0.9975	0.9985	263.130	0.9965	0.9995	
310	4'764.15	1.0103	1.0095	553.348	1.0075	1.0067	259.639	0.9832	0.9846	
311	6'196.84	1.0145	1.0146	884.830	1.0208	1.0218	373.500	1.0066	1.0085	
312	6'150.77	1.0070	1.0069	873.258	1.0074	1.0089	368.470	0.9930	0.9967	
313	5'782.50	1.0012	1.0016	775.233	1.0050	1.0057	343.662	0.9838	0.9857	
314	5'850.54	1.0130	1.0134	790.717	1.0251	1.0249	352.543	1.0092	1.0070	
315	6'336.53	0.9825	0.9838	955.827	0.9879	0.9877	382.799	0.9792	0.9795	
316	6'423.41	0.9960	0.9963	963.327	0.9956	0.9972	376.720	0.9636	0.9718	
317	6'469.92	1.0032	1.0045	981.954	1.0149	1.0149	389.452	0.9962	0.9974	
318	6'313.77	0.9790	0.9798	946.782	0.9785	0.9804	373.937	0.9565	0.9627	
319	6'321.62	0.9802	0.9806	944.945	0.9766	0.9780	372.203	0.9521	0.9596	
320	8'465.89	1.0006	1.0007	1'751.155	0.9996	1.0001	493.324	0.9922	0.9928	
321	7'410.41	0.9562	0.9581	1'395.955	0.9659	0.9697	437.209	0.9538	0.9612	
322	9'538.28	1.0050	1.0042	2'359.557	1.0089	1.0080	530.423	0.9911	0.9905	
323	9'437.06	0.9943	0.9944	2'339.403	1.0003	0.9994	531.791	0.9936	0.9928	
324	8'311.70	0.9823	0.9835	1'730.256	0.9877	0.9901	484.172	0.9738	0.9772	
325	6'362.56	0.9866	0.9876	957.391	0.9895	0.9893	384.005	0.9823	0.9817	
326	6'020.21	0.9856	0.9862	859.004	0.9910	0.9919	360.023	0.9702	0.9762	
327	3'359.87	1.0054	1.0064	623.667	1.0202	1.0206	107.840	1.0343	1.0335	
328	2'883.62	0.9981	0.9980	467.641	0.9945	0.9948	85.450	0.9908	0.9936	
329	1'595.15	0.9960	0.9968	174.761	1.0008	1.0006	36.763	1.0069	1.0060	
330	7'668.92	0.9895	0.9892	1'425.027	0.9860	0.9865	441.562	0.9633	0.9678	
331	4'754.91	1.0003	1.0006	667.355	1.0085	1.0088	275.863	1.0078	1.0059	
332	5'189.26	0.9699	0.9715	647.140	0.9672	0.9688	306.826	0.9614	0.9630	
333	3'973.01	0.9901	0.9905	488.520	0.9935	0.9927	220.191	0.9573	0.9627	
334	6'330.03	0.9815	0.9827	952.443	0.9844	0.9854	376.762	0.9638	0.9671	
335	3'871.75	0.9649	0.9656	474.196	0.9644	0.9644	214.532	0.9327	0.9384	
336	5'163.11	1.0162	1.0163	761.372	1.0170	1.0166	297.680	1.0101	1.0087	
337	4'963.61	0.9769	0.9778	732.449	0.9783	0.9802	281.993	0.9568	0.9628	
338	5'190.50	1.0216	1.0213	768.761	1.0268	1.0282	293.040	0.9943	0.9977	
339	5'597.75	0.9914	0.9914	910.356	0.9879	0.9902	305.555	0.9531	0.9609	
340	6'059.10	0.9920	0.9919	857.752	0.9895	0.9911	361.811	0.9751	0.9814	
341	4'969.77	0.9781	0.9783	732.178	0.9780	0.9788	282.914	0.9600	0.9641	
342	3'077.62	0.9933	0.9934	326.285	0.9964	0.9967	154.207	0.9967	0.9979	
343	6'208.79	1.0165	1.0164	885.976	1.0221	1.0221	374.874	1.0103	1.0113	
344	5'830.34	1.0095	1.0101	783.477	1.0157	1.0154	353.309	1.0114	1.0089	
345	4'972.13	0.9786	0.9795	735.676	0.9826	0.9835	285.689	0.9694	0.9708	
346	7'395.84	0.9989	0.9983	1'661.150	0.9959	0.9962	415.874	0.9918	0.9929	
347	3'388.45	0.9775	0.9781	388.017	0.9809	0.9821	177.966	0.9581	0.9621	
348	2'843.69	0.9843	0.9855	459.965	0.9782	0.9790	81.773	0.9481	0.9542	
349	4'559.21	0.9591	0.9594	626.010	0.9461	0.9492	252.955	0.9241	0.9277	
350	841.31	0.9967	0.9961	60.070	0.9963	0.9966	13.077	0.9910	0.9935	
351	1'147.76	0.9791	0.9824	102.477	0.9929	0.9940	22.219	1.0049	1.0122	
352	1'373.86	0.9995	0.9996	131.957	0.9939	0.9950	27.271	0.9692	0.9798	
353	1'387.14	1.0092	1.0095	134.779	1.0152	1.0157	28.141	1.0001	1.0032	
354	1'578.16	0.9854	0.9864	171.034	0.9794	0.9815	35.040	0.9597	0.9663	
355	1'581.49	0.9875	0.9883	170.781	0.9780	0.9812	34.235	0.9376	0.9465	
356	999.02	0.9953	0.9948	78.968	0.9859	0.9877	16.539	0.9713	0.9758	
357	2'482.66	0.9928	0.9973	364.317	0.9943	0.9966	71.631	0.9966	1.0020	
358	3'870.45	0.9980	0.9979	785.274	0.9980	0.9971	127.462	1.0030	1.0026	
359	3'895.67	1.0045	1.0059	798.185	1.0144	1.0141	128.263	1.0093	1.0113	
360	3'262.09	0.9762	0.9803	604.166	0.9883	0.9895	102.897	0.9869	0.9889	
361	2'833.25	0.9807	0.9836	463.611	0.9860	0.9869	83.057	0.9630	0.9673	
362	4'467.39	0.9938	0.9952	991.088	0.9907	0.9914	146.325	0.9617	0.9651	
363	5'151.91	0.9925	0.9952	1'257.630	0.9981	0.9981	178.901	0.9669	0.9670	
364	3'878.36	1.0001	1.0003	786.570	0.9997	0.9992	125.378	0.9866	0.9881	
365	2'441.30	0.9763	0.9772	352.892	0.9631	0.9644	67.802	0.9433	0.9516	
366	1'529.28	0.9549	0.9603	167.776	0.9608	0.9635	33.540	0.9186	0.9257	
367	2'258.60	0.9842	0.9843	201.399	0.9954	0.9962	94.777	0.9730	0.9769	
368	3'103.58	1.0017	1.0024	326.350	0.9966	0.9980	154.238	0.9969	1.0000	
369	3'117.11	1.0060	1.0067	326.419	0.9968	0.9982	154.137	0.9963	0.9991	
370	3'087.23	0.9964	0.9976	326.544	0.9972	0.9978	153.769	0.9939	0.9955	
371	4'112.91	1.0250	1.0249	504.978	1.0270	1.0265	231.431	1.0062	1.0077	
372	3'656.18	1.0547	1.0537	419.016	1.0593	1.0583	195.461	1.0524	1.0476	
373	4'048.22	1.0089	1.0086	494.243	1.0051	1.0047	224.377	0.9755	0.9797	
374	3'920.09	0.9769	0.9787	486.004	0.9884	0.9883	227.210	0.9879	0.9894	
375	4'961.89	0.9766	0.9783	741.595	0.9905	0.9904	285.299	0.9681	0.9704	
376	6'219.35	0.9874	0.9890	1'153.501	0.9946	0.9961	356.192	0.9909	0.9929	
377	4'478.58	1.0104	1.0108	595.590	1.0264	1.0257	260.822	1.0210	1.0190	
378	4'521.70	1.0201	1.0203	590.037	1.0168	1.0168	260.479	1.0196	1.0178	
379	4'964.35	0.9771	0.9773	732.056	0.9778	0.9802	275.467	0.9347	0.9448	
380	4'699.65	0.9886	0.9890	653.248	0.9872	0.9885	266.160	0.9724	0.9715	
381	7'372.00	0.9957	0.9956	1'659.358	0.9948	0.9949	416.146	0.9925	0.9935	
382	7'676.23	0.9777	0.9786	1'893.136	0.9814	0.9812	419.099	0.9565	0.9599	
383	5'671.17	1.0044	1.0043	926.246	1.0051	1.0057	324.052	1.0109	1.0133	
384	5'563.35	0.9853	0.9853	901.892	0.9787	0.9796	306.560	0.9563	0.9615	
385	5'582.42	0.9887	0.9890	908.239	0.9856	0.9876	305.828	0.9540	0.9608	
386	4'470.75	1.0086	1.0079	584.064	1.0065	1.0064	253.223	0.9912	0.9894	
387	1'927.40	1.0023	1.0009	152.569	0.9968	0.9956	69.900	0.9510	0.9554	
388	3'712.80	0.9722	0.9714	363.889	0.9633	0.9630	173.893	0.9345	0.9457	
389	3'762.91	0.9854	0.9848	370.294	0.9803	0.9786	173.654	0.9332	0.9423	
390	3'201.45	0.9751	0.9756	293.856	0.9906	0.9883	137.133	0.9351	0.9386	
391	4'712.03	0.9993	0.9986	546.722	0.9955	0.9946	254.630	0.9643	0.9666	
392	6'224.43	1.0190	1.0188	888.346	1.0248	1.0255	373.509	1.0066	1.0085	
393	6'182.64	1.0122	1.0118	878.788	1.0138	1.0143	370.145	0.9975	1.0007	
394	5'701.35	0.9872	0.9871	763.168	0.9894	0.9898	336.139	0.9622	0.9650	
395	5'824.59	1.0085	1.0090	788.318	1.0220	1.0219	348.786	0.9984	0.9990	
396	6'350.67	0.9847	0.9860	959.419	0.9916	0.9913	382.827	0.9793	0.9792	
397	8'220.81	0.9716	0.9732	1'709.564	0.9759	0.9796	484.958	0.9754	0.9805	
398	8'474.33	1.0016	1.0015	1'753.095	1.0007	1.0008	493.565	0.9927	0.9937	
399	8'294.43	0.9803	0.9814	1'723.233	0.9837	0.9859	480.812	0.9671	0.9704	
400	9'534.52	1.0046	1.0038	2'363.140	1.0105	1.0104	531.540	0.9932	0.9921	

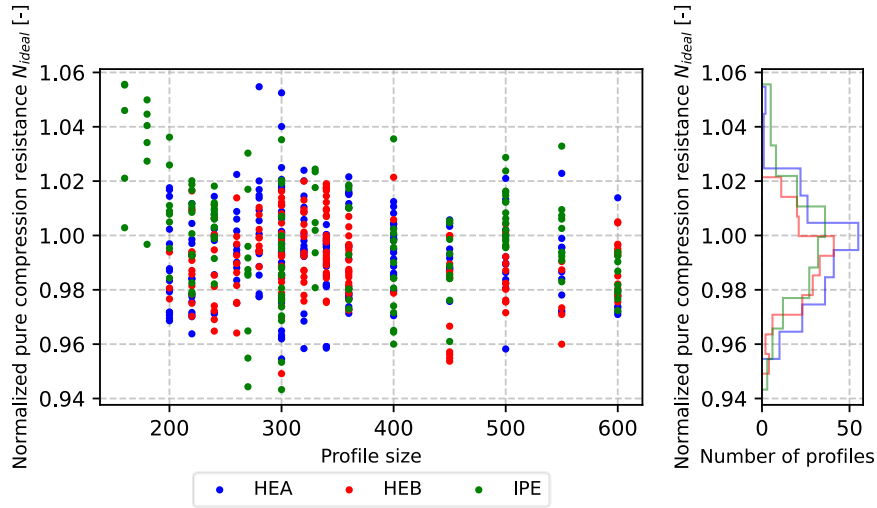
Profile Nr.	Pure Compression				Bending strong axis			Bending weak axis		
	N_ideal [kN]	N_ideal / N_nom [-]	A_ideal / A_nom [-]	My_ideal [kNm]	My_ideal / My_nom [-]	Wpl_y_ideal / Wpl_y_nom [-]	Mz_ideal [kNm]	Mz_ideal / Mz_nom [-]	Wpl_z_ideal / Wpl_z_nom [-]	
401	6'311.93	0.9787	0.9791	940.541	0.9721	0.9742	372.178	0.9520	0.9591	
402	6'041.84	0.9891	0.9895	861.828	0.9942	0.9949	361.891	0.9753	0.9790	
403	5'675.80	0.9828	0.9833	760.882	0.9864	0.9867	339.516	0.9719	0.9746	
404	4'230.20	0.9927	0.9980	468.110	1.0180	1.0171	229.670	1.0265	1.0146	
405	3'719.91	0.9741	0.9729	362.219	0.9589	0.9586	176.035	0.9460	0.9559	
406	3'902.17	1.0062	1.0068	788.299	1.0018	1.0024	125.059	0.9841	0.9893	
407	3'067.85	0.9901	0.9916	323.325	0.9874	0.9888	152.614	0.9865	0.9921	
408	5'635.12	0.9980	0.9989	925.059	1.0038	1.0032	320.434	0.9996	0.9969	
409	7'647.65	0.9868	0.9865	1'420.848	0.9831	0.9837	440.883	0.9618	0.9663	
410	6'415.21	0.9947	0.9959	969.349	1.0018	1.0021	385.583	0.9863	0.9871	
411	2'228.00	0.9709	0.9711	197.286	0.9751	0.9759	91.869	0.9431	0.9464	
412	3'865.47	0.9633	0.9640	475.385	0.9668	0.9668	214.825	0.9340	0.9392	
413	4'248.03	0.9584	0.9594	557.641	0.9610	0.9623	239.732	0.9384	0.9380	
414	5'531.22	0.9796	0.9817	901.644	0.9784	0.9822	310.561	0.9688	0.9771	
415	2'843.76	0.9843	0.9857	460.742	0.9799	0.9803	81.975	0.9505	0.9571	
416	6'223.01	1.0188	1.0188	887.803	1.0342	1.0244	376.601	1.0149	1.0150	
417	3'391.98	0.9785	0.9788	387.958	0.9808	0.9816	174.889	0.9417	0.9484	
418	4'943.47	0.9730	0.9740	730.707	0.9760	0.9772	283.456	0.9618	0.9653	
419	4'108.41	0.9641	0.9663	451.869	0.9827	0.9834	211.047	0.9432	0.9517	
420	5'692.64	1.0082	1.0079	930.985	1.0103	1.0093	322.726	1.0067	1.0064	
421	1'927.44	1.0352	1.0323	228.260	1.0104	1.0136	45.495	0.9723	0.9807	
422	4'556.58	0.9585	0.9588	625.067	0.9446	0.9477	252.719	0.9233	0.9261	
423	1'856.00	0.9969	0.9988	225.340	0.9975	1.0002	45.345	0.9691	0.9784	
424	1'372.91	0.9988	0.9979	130.148	0.9803	0.9840	27.510	0.9777	0.9867	
425	1'182.19	1.0085	1.0066	103.301	1.0009	1.0004	21.979	0.9940	0.9968	
426	1'164.01	0.9930	0.9918	101.743	0.9858	0.9864	21.768	0.9845	0.9877	
427	1'040.09	1.0362	1.0334	82.452	1.0294	1.0272	17.470	1.0260	1.0261	
428	725.51	1.0211	1.0206	45.446	1.0085	1.0098	9.919	0.9910	0.9964	
429	4'173.46	1.0401	1.0390	510.245	1.0377	1.0357	238.607	1.0374	1.0340	
430	4'037.57	1.0062	1.0059	492.565	1.0017	1.0017	226.694	0.9856	0.9896	
431	3'954.68	0.9856	0.9856	482.736	0.9817	0.9810	219.953	0.9563	0.9620	
432	5'095.96	0.9817	0.9862	1'246.887	0.9896	0.9904	181.120	0.9788	0.9802	
433	3'925.65	1.0123	1.0119	806.700	1.0252	1.0241	130.130	1.0240	1.0223	
434	2'876.45	0.9956	0.9971	471.760	1.0033	1.0028	85.820	0.9951	0.9960	
435	2'547.00	1.0186	1.0164	372.691	1.0172	1.0156	72.820	1.0131	1.0127	
436	1'812.88	0.9737	0.9757	216.973	0.9605	0.9638	43.037	0.9197	0.9317	
437	1'874.38	1.0067	1.0051	222.984	0.9871	0.9897	44.238	0.9454	0.9563	
438	3'886.05	1.0021	0.9994	785.085	0.9978	0.9965	126.300	0.9939	0.9937	
439	4'522.35	1.0060	1.0056	1'016.031	1.0156	1.0148	155.636	1.0229	1.0214	
440	2'860.37	0.9900	0.9903	465.679	0.9904	0.9899	84.780	0.9830	0.9861	
441	2'119.89	0.9808	0.9821	280.077	0.9675	0.9703	52.890	0.9177	0.9305	
442	1'840.09	0.9883	0.9884	220.399	0.9756	0.9781	44.254	0.9458	0.9551	
443	1'861.70	0.9999	1.0005	225.930	1.0001	1.0011	47.272	1.0103	1.0112	
444	3'989.01	0.9941	0.9946	488.929	0.9943	0.9937	228.358	0.9928	0.9930	
445	4'009.77	0.9993	0.9996	491.929	1.0004	0.9996	230.266	1.0011	1.0012	
446	5'716.77	1.0125	1.0128	942.555	1.0228	1.0217	330.089	1.0297	1.0266	
447	4'398.22	0.9923	0.9928	584.087	1.0066	1.0066	254.605	0.9967	0.9984	
448	4'739.14	0.9969	0.9969	656.718	0.9925	0.9935	268.851	0.9822	0.9808	
449	4'743.92	0.9980	0.9984	666.256	1.0069	1.0072	274.026	1.0011	1.0014	
450	4'755.40	1.0004	1.0000	659.422	0.9966	0.9969	273.118	0.9978	0.9941	
451	5'036.71	0.9913	0.9920	746.824	0.9975	0.9977	293.524	0.9960	0.9962	
452	5'638.92	0.9987	0.9990	922.846	1.0014	1.0018	322.488	1.0060	1.0061	
453	5'639.76	0.9988	0.9992	920.579	0.9990	0.9988	321.472	1.0028	1.0051	
454	5'479.66	0.9705	0.9719	897.104	0.9735	0.9751	306.948	0.9575	0.9593	
455	5'648.06	1.0003	1.0004	924.141	1.0028	1.0028	322.287	1.0053	1.0052	
456	7'642.99	0.9734	0.9746	1'891.409	0.9805	0.9796	417.655	0.9532	0.9551	
457	5'568.15	0.9861	0.9863	904.237	0.9812	0.9829	307.605	0.9595	0.9660	
458	6'334.67	1.0057	1.0054	1'170.340	1.0091	1.0100	352.142	0.9797	0.9830	
459	6'882.74	0.9894	0.9890	1'401.664	0.9834	0.9834	388.173	0.9706	0.9728	
460	6'885.96	0.9898	0.9904	1'409.617	0.9889	0.9896	389.937	0.9750	0.9806	
461	7'241.61	0.9781	0.9812	1'643.223	0.9851	0.9864	407.798	0.9726	0.9768	
462	4'084.16	1.0178	1.0175	497.618	1.0120	1.0114	228.490	0.9934	0.9957	
463	4'435.38	1.0006	1.0012	587.752	1.0129	1.0129	256.865	1.0055	1.0056	
464	4'664.15	0.9812	0.9813	651.153	0.9841	0.9837	267.501	0.9773	0.9755	
465	5'132.32	1.0101	1.0112	768.917	1.0270	1.0262	302.738	1.0272	1.0240	
466	3'873.36	0.9988	0.9988	786.269	0.9993	0.9991	126.759	0.9975	0.9975	
467	9'258.76	0.9756	0.9771	2'303.764	0.9851	0.9850	525.345	0.9816	0.9813	
468	8'861.80	0.9874	0.9876	2'006.805	0.9862	0.9866	504.537	0.9777	0.9784	
469	9'420.32	0.9926	0.9925	2'341.840	1.0014	1.0001	526.179	0.9832	0.9803	
470	8'259.93	0.9762	0.9775	1'726.185	0.9854	0.9854	495.277	0.9962	0.9942	
471	7'749.56	1.0000	0.9997	1'444.766	0.9997	1.0007	451.888	0.9858	0.9904	
472	7'417.86	0.9572	0.9584	1'384.296	0.9578	0.9610	433.832	0.9465	0.9530	
473	6'907.03	0.9788	0.9790	1'143.197	0.9768	0.9797	394.883	0.9473	0.9564	
474	6'093.53	0.9976	0.9976	863.643	0.9963	0.9974	370.776	0.9992	1.0026	
475	6'065.44	0.9930	0.9933	863.502	0.9962	0.9966	368.690	0.9936	0.9950	
476	6'097.64	0.9983	0.9983	868.241	1.0016	1.0019	370.204	0.9977	0.9991	
477	5'700.44	0.9870	0.9881	767.290	0.9947	0.9952	347.230	0.9940	0.9952	
478	4'320.41	1.0138	1.0143	471.304	1.0250	1.0241	226.376	1.0117	1.0174	
479	2'525.58	1.0100	1.0076	367.127	1.0020	1.0016	71.678	0.9972	0.9975	
480	5'390.71	1.0076	1.0067	674.760	1.0085	1.0082	319.816	1.0021	0.9983	
481	8'496.69	1.0042	1.0048	1'781.445	1.0169	1.0161	508.548	1.0228	1.0202	
482	4'981.71	0.9805	0.9814	740.695	0.9893	0.9900	287.930	0.9770	0.9795	
483	7'640.77	0.9859	0.9859	1'417.510	0.9808	0.9818	442.034	0.9643	0.9685	
484	6'108.21	1.0000	0.9998	867.135	1.0004	1.0007	366.912	0.9888	0.9908	
485	2'764.22	1.0078	1.0076	268.426	1.0122	1.0118	128.364	1.0132	1.0138	
486	7'285.42	0.9840	0.9846	1'638.461	0.9823	0.9827	403.299	0.9619	0.9652	
487	6'861.66	0.9863	0.9872	1'411.025	0.9899	0.9908	385.033	0.9627	0.9661	
488	6'145.60	0.9757	0.9766	1'133.059	0.9769	0.9793	341.902	0.9512	0.9547	
489	2'782.24	1.0144	1.0141	273.951	1.0330	1.0324	128.923	1.0176	1.0167	
490	2'291.45	0.9985	0.9970	202.854	1.0026	1.0012	95.982	0.9853	0.9871	
491	1'390.07	1.0113	1.0126	136.723	1.0298	1.0282	28.624	1.0173	1.0148	
492	2'321.87	1.0118	1.0103	206.079	1.0186	1.0171	98.222	1.0083	1.0075	
493	2'743.45	1.0002	1.0000	265.635	1.0016	1.0015	127.171	1.0038	1.0035	
494	5'610.97	0.9937	0.9938	912.207	0.9899	0.9913	309.141	0.9643	0.9706	
495	5'706.59	1.0107	1.0108	932.234	1.0116	1.0123	324.762	1.0131	1.0137	
496	3'388.45	0.9775	0.9781	388.017	0.9809	0.9821	177.946	0.9581	0.9621	
497	2'843.69	0.9843	0.9855	459.965	0.9782	0.9790	81.773	0.9481	0.9542	
498	4'559.21	0.9591	0.9594	626.010	0.9461	0.9492	252.955	0.9241	0.9272	
499	988.05	0.9843	0.9844	79.131	0.9880	0.9889	17.272	1.0143	1.0166	
500	1'011.65	1.0079	1.0072	81.106	1.0126	1.0128	17.513	1.0285	1.0288	

Profile Nr.	Pure Compression			Bending strong axis			Bending weak axis		
	N_ideal [kN]	N_ideal / N_nom [-]	A_ideal / A_nom [-]	My_ideal [kNm]	My_ideal / My_nom [-]	Wpl_y_ideal / Wpl_y_nom [-]	Mz_ideal [kNm]	Mz_ideal / Mz_nom [-]	Wpl_z_ideal / Wpl_z_nom [-]
501	1'029.79	1.0259	1.0250	82.823	1.0341	1.0332	17.827	1.0469	1.0463
502	2'665.38	0.9718	0.9703	255.783	0.9645	0.9634	116.499	0.9196	0.9259
503	1'146.96	0.9785	0.9806	103.209	1.0000	0.9997	21.445	0.9699	0.9719
504	2'305.03	1.0044	1.0048	203.376	1.0052	1.0062	98.140	1.0075	1.0097
505	1'955.33	1.0168	1.0165	155.937	1.0188	1.0188	75.773	1.0309	1.0321
506	1'891.00	0.9834	0.9826	151.921	0.9926	0.9920	68.889	0.9373	0.9435
507	3'700.60	0.9691	0.9685	365.127	0.9666	0.9660	172.474	0.9269	0.9373
508	3'798.54	0.9947	0.9951	380.366	1.0069	1.0072	185.153	0.9950	0.9969
509	3'314.48	1.0095	1.0091	301.759	1.0172	1.0163	147.541	1.0061	1.0018
510	3'263.00	0.9938	0.9945	296.651	1.0000	0.9997	147.022	1.0025	1.0001
511	3'313.96	1.0093	1.0103	303.148	1.0219	1.0221	150.670	1.0274	1.0239
512	2'763.95	0.9806	0.9808	225.500	0.9769	0.9777	112.310	0.9764	0.9810
513	1'378.73	1.0031	1.0056	135.971	1.0242	1.0240	29.300	1.0413	1.0396
514	1'388.05	1.0099	1.0119	136.940	1.0315	1.0307	29.463	1.0471	1.0445
515	2'278.27	0.9928	0.9925	200.407	0.9905	0.9908	94.250	0.9675	0.9701
516	1'862.63	0.9686	0.9680	148.825	0.9723	0.9721	67.833	0.9229	0.9304
517	3'258.44	0.9924	0.9919	291.884	0.9840	0.9836	143.837	0.9808	0.9828
518	2'526.49	1.0104	1.0083	367.308	1.0025	1.0023	71.019	0.9880	0.9927
519	1'816.97	0.9759	0.9785	220.393	0.9756	0.9776	44.744	0.9562	0.9641
520	2'214.23	1.0244	1.0211	294.803	1.0184	1.0177	59.087	1.0253	1.0258
521	4'751.29	1.0076	1.0083	561.035	1.0215	1.0210	266.187	1.0080	1.0115
522	3'081.89	0.9947	0.9955	323.519	0.9880	0.9896	151.861	0.9816	0.9847
523	3'498.70	1.0093	1.0088	397.774	1.0056	1.0052	182.279	0.9814	0.9857
524	4'079.79	1.0167	1.0169	501.792	1.0205	1.0200	237.391	1.0321	1.0296
525	5'308.81	0.9923	0.9928	659.132	0.9851	0.9860	316.217	0.9908	0.9909
526	4'404.46	0.9937	0.9936	569.865	0.9821	0.9823	247.660	0.9695	0.9707
527	4'292.76	0.9685	0.9682	558.050	0.9617	0.9623	241.470	0.9452	0.9453
528	2'991.87	1.0356	1.0312	488.897	1.0397	1.0375	90.016	1.0437	1.0400
529	1'875.00	1.0071	1.0086	229.434	1.0156	1.0175	47.269	1.0102	1.0138
530	3'357.44	1.0047	1.0041	616.360	1.0082	1.0078	101.640	0.9748	0.9775
531	5'122.68	0.9869	0.9901	1'254.266	0.9954	0.9961	184.652	0.9979	1.0001
532	6'821.87	0.9806	0.9813	1'388.720	0.9743	0.9756	381.156	0.9530	0.9597
533	8'254.04	0.9755	0.9768	1'714.378	0.9786	0.9806	486.923	0.9793	0.9814
534	4'183.00	0.9816	0.9839	456.102	0.9919	0.9929	218.462	0.9764	0.9851
535	4'458.50	1.0059	1.0056	578.109	0.9963	0.9961	251.902	0.9861	0.9880
536	3'443.18	0.9933	0.9931	391.221	0.9890	0.9890	182.050	0.9802	0.9810
537	3'468.42	1.0006	1.0001	394.868	0.9982	0.9976	182.905	0.9848	0.9858
538	4'095.32	1.0206	1.0207	501.563	1.0200	1.0196	239.328	1.0405	1.0387
539	7'102.78	1.0210	1.0194	1'450.564	1.0177	1.0160	408.068	1.0203	1.0178
540	4'689.67	0.9946	0.9940	547.254	0.9964	0.9959	257.357	0.9746	0.9755
541	4'687.83	0.9942	0.9942	546.457	0.9950	0.9943	257.065	0.9735	0.9743
542	4'687.50	0.9941	0.9942	546.331	0.9947	0.9940	257.045	0.9734	0.9744
543	4'733.11	0.9957	0.9953	657.172	0.9932	0.9932	271.716	0.9927	0.9913
544	2'773.60	0.9600	0.9650	454.090	0.9657	0.9670	82.136	0.9524	0.9579
545	2'788.21	0.9651	0.9684	454.157	0.9659	0.9666	82.023	0.9510	0.9566
546	4'725.84	1.0022	1.0026	557.117	1.0144	1.0139	263.799	0.9990	1.0020
547	5'635.73	0.9758	0.9768	751.497	0.9742	0.9751	331.492	0.9489	0.9582
548	4'401.03	0.9929	0.9937	578.033	0.9961	0.9961	252.411	0.9881	0.9883
549	4'687.60	0.9941	0.9937	546.753	0.9955	0.9950	262.198	0.9929	0.9933
550	5'354.41	1.0008	1.0006	673.375	1.0064	1.0065	314.245	0.9847	0.9840
551	3'954.63	0.9855	0.9858	478.751	0.9736	0.9730	225.865	0.9820	0.9840
552	3'913.25	0.9752	0.9759	479.343	0.9748	0.9746	223.175	0.9703	0.9725
553	7'208.00	1.0214	1.0208	1'192.731	1.0191	1.0193	427.543	1.0256	1.0245
554	4'248.08	0.9969	1.0013	473.338	1.0294	1.0279	229.866	1.0273	1.0171
555	5'222.58	0.9762	0.9788	660.475	0.9872	0.9884	312.324	0.9787	0.9793
556	4'057.80	1.0113	1.0107	495.615	1.0079	1.0072	227.772	0.9903	0.9925
557	3'288.60	0.9841	0.9865	605.984	0.9912	0.9925	100.845	0.9672	0.9706
558	3'021.32	0.9751	0.9756	320.037	0.9773	0.9783	143.824	0.9296	0.9355
559	4'661.09	0.9885	0.9881	542.762	0.9883	0.9879	254.502	0.9638	0.9670
560	4'506.88	1.0026	1.0022	1'007.958	1.0075	1.0074	152.391	1.0016	1.0023
561	7'049.15	1.0133	1.0126	1'440.558	1.0107	1.0096	406.706	1.0169	1.0149

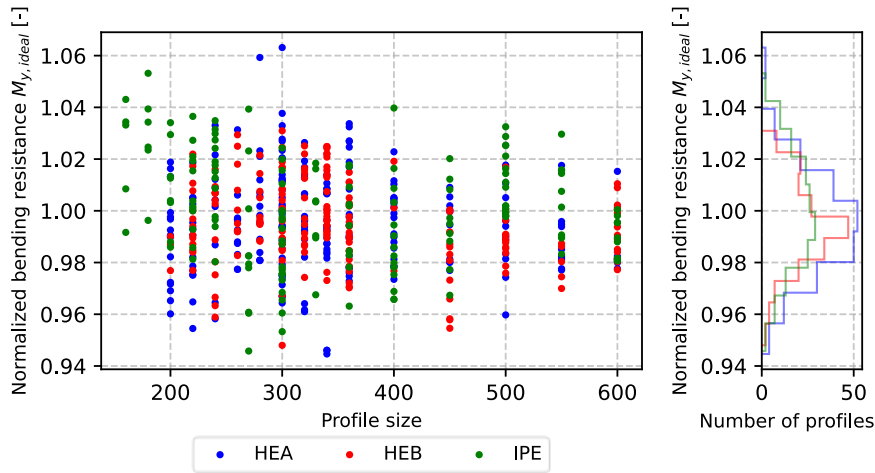
C.4.2 Visualization of the obtained cross-sectional resistances

The cross-sectional resistances are normalized with respect to the obtained nominal cross-sectional resistances.

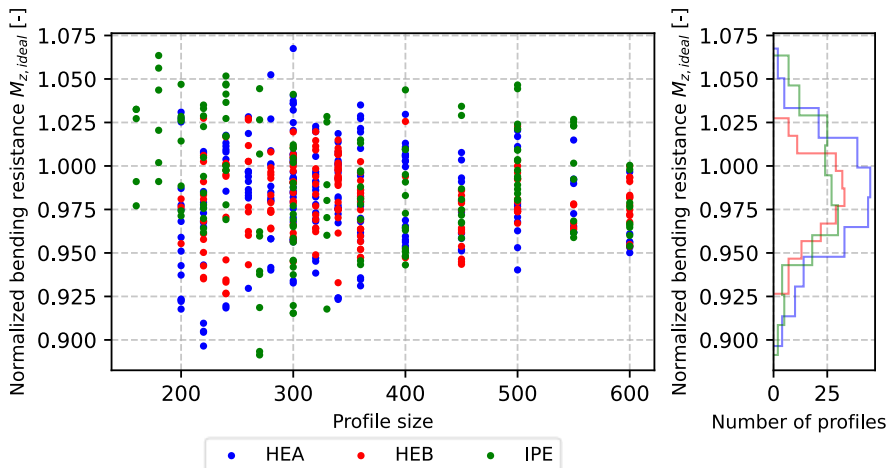
N_{ideal} :



$M_{y,ideal}$:



$M_{z,ideal}$:



C.4.3 Comparison real vs. ideal resistances

The following tables summarize the mean values and the coefficients of variation of the relation between the real and the ideal cross-sectional resistances for each category.

Mean values [-]:

cat.	$\frac{N_{real}}{N_{ideal}}$	$\frac{M_{y,real,pos}}{M_{y,ideal}}$	$\frac{M_{y,real,neg}}{M_{y,ideal}}$	$\frac{M_{z,real,pos}}{M_{z,ideal}}$	$\frac{M_{z,real,neg}}{M_{z,ideal}}$
Total	0.9993	0.9989	0.9990	0.9944	0.9927
Small	0.9987	0.9986	0.9988	0.9949	0.9923
Large	1.0004	0.9993	0.9993	0.9937	0.9933
HEA	0.9998	0.9989	0.9990	0.9945	0.9928
HEB	0.9979	0.9981	0.9983	0.9940	0.9908
IPE	1.0005	0.9998	0.9997	0.9948	0.9948

Coefficients of variation [%]:

cat.	$\frac{N_{real}}{N_{ideal}}$	$\frac{M_{y,real,pos}}{M_{y,ideal}}$	$\frac{M_{y,real,neg}}{M_{y,ideal}}$	$\frac{M_{z,real,pos}}{M_{z,ideal}}$	$\frac{M_{z,real,neg}}{M_{z,ideal}}$
Total	0.3419	0.2368	0.2361	0.4674	0.6024
Small	0.3622	0.2388	0.2457	0.4975	0.5893
Large	0.2774	0.2279	0.2168	0.4079	0.6184
HEA	0.2529	0.1827	0.1829	0.4517	0.5305
HEB	0.3071	0.1697	0.1621	0.5007	0.7007
IPE	0.4258	0.3272	0.3359	0.4444	0.4887

C.5 Further Abaqus investigations

Investigation of the influence of the web eccentricity and residual stresses to the bending resistance around the weak axis:

In the following, a short investigation is made concerning the influence of the web eccentricity to the positive and negative bending resistance around the weak axis. As only the influence of the web eccentricity is to be studied, six idealized cross-sections from chapter 4.3 are taken (two sections per profile type) and modified by introducing a positive web eccentricity of 3 mm. In this way, it is omitted to include other factors such as different flange thicknesses, such that the pure influence of the web eccentricity can be examined. The six fictive cross-sections are studied in Abaqus using the approaches defined in section 5.

The following table summarizes the inserted dimensions for the six profiles (being profiles Nr. 60, 75, 176, 209, 324 and 356 of Appendix B.2.1 with a fictive eccentricity):

	Type	h [mm]	b [mm]	t _w [mm]	t _f [mm]	r [mm]	e [mm]
CS 1	HEA 450	441.54	300.17	11.55	21.12	24.69	3.00
CS 2	HEB 320	321.85	297.76	11.84	20.15	24.91	3.00
CS 3	IPE 500	499.89	200.69	10.12	16.04	20.95	3.00
CS 4	HEA 240	230.23	241.12	7.47	11.97	21.30	3.00
CS 5	HEB 500	504.29	299.85	14.45	27.40	25.15	3.00
CS 6	IPE 200	200.13	100.78	5.78	8.12	12.49	3.00

In the following table, the resulting bending moment resistances around the weak axis are displayed:

	M _{z,pos} [kNm]	M _{z,neg} [kNm]	M _{z,pos} / M _{z,neg}
CS 1	363.950	359.146	1.01209
CS 2	339.631	334.182	1.01001
CS 3	129.096	127.393	1.01321
CS 4	128.570	126.604	1.01338
CS 5	486.502	482.194	1.01631
CS 6	16.754	16.376	1.01336

In the last column, the comparison between the positive and the negative bending resistance is shown. It is remarkable that there is a difference of approximately 1-2 % for all cross-sections due to the positive web eccentricity of 3 mm. A positive web eccentricity means that for a positive bending moment, the shorter flange part is under compression. This leads to a larger resistance due to the smaller slenderness of the flange under compression compared to the case of a negative bending moment where the flange part under compression is the longer flange part.

In addition to the influence of the different slendernesses due to the web eccentricity, the introduced residual stress model may also influence the discrepancy between the positive and the negative bending resistance. This can be shown by studying the same six cross-sections again but without considering any residual stress state. The results are as follows:

cat.	$M_{z, \text{pos}}$ [kNm]	$M_{z, \text{neg}}$ [kNm]	$M_{z, \text{pos}} / M_{z, \text{neg}}$
CS 1	361.311	360.456	1.00237
CS 2	336.695	333.589	1.00931
CS 3	129.111	127.899	1.00947
CS 4	127.423	126.777	1.00509
CS 5	486.933	483.684	1.00672
CS 6	16.689	16.482	1.01257

Comparing these results to the ones when considering the residual stresses, it is clearly observed that the difference between the positive and the negative bending resistance gets attenuated when neglecting the residual stress state. Therefore, it seems that the assumed residual stresses already induce some bending action. For some of the investigated profiles this effect seems to be large, while for other profiles, this effect occurs only slightly. For IPE sections, the effect of the residual stresses doesn't seem to be that pronounced compared to the other profile types, because the IPE sections have significant shorter flanges compared to the other profile types. Therefore, the bending action induced by the residual stresses in the flanges is not that pronounced.



Eigenständigkeitserklärung

Die unterzeichnete Eigenständigkeitserklärung ist Bestandteil jeder während des Studiums verfassten Semester-, Bachelor- und Master-Arbeit oder anderen Abschlussarbeit (auch der jeweils elektronischen Version).

Die Dozentinnen und Dozenten können auch für andere bei ihnen verfasste schriftliche Arbeiten eine Eigenständigkeitserklärung verlangen.

Ich bestätige, die vorliegende Arbeit selbständig und in eigenen Worten verfasst zu haben. Davon ausgenommen sind sprachliche und inhaltliche Korrekturvorschläge durch die Betreuer und Betreuerinnen der Arbeit.

Titel der Arbeit (in Druckschrift):

Verfasst von (in Druckschrift):

Bei Gruppenarbeiten sind die Namen aller Verfasserinnen und Verfasser erforderlich.

Name(n):

Vorname(n):


Ich bestätige mit meiner Unterschrift:

- Ich habe keine im Merkblatt [„Zitier-Knigge“](#) beschriebene Form des Plagiats begangen.
- Ich habe alle Methoden, Daten und Arbeitsabläufe wahrheitsgetreu dokumentiert.
- Ich habe keine Daten manipuliert.
- Ich habe alle Personen erwähnt, welche die Arbeit wesentlich unterstützt haben.

Ich nehme zur Kenntnis, dass die Arbeit mit elektronischen Hilfsmitteln auf Plagiate überprüft werden kann.

Ort, Datum

Unterschrift(en)

Bei Gruppenarbeiten sind die Namen aller Verfasserinnen und Verfasser erforderlich. Durch die Unterschriften bürgen sie gemeinsam für den gesamten Inhalt dieser schriftlichen Arbeit.